

1978

The interaction of eolian sand transport, vegetation, and dune geomorphology: Currituck Spit, Virginia-North Carolina

Andrew L. Gutman

College of William and Mary - Virginia Institute of Marine Science

Follow this and additional works at: <https://scholarworks.wm.edu/etd>



Part of the [Geomorphology Commons](#), [Oceanography Commons](#), and the [Physical and Environmental Geography Commons](#)

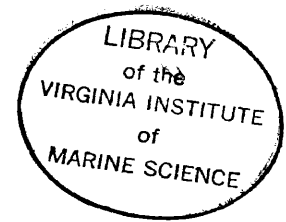
Recommended Citation

Gutman, Andrew L., "The interaction of eolian sand transport, vegetation, and dune geomorphology: Currituck Spit, Virginia-North Carolina" (1978). *Dissertations, Theses, and Masters Projects*. Paper 1539617483.

<https://dx.doi.org/doi:10.25773/v5-4qa6-1344>

This Thesis is brought to you for free and open access by the Theses, Dissertations, & Master Projects at W&M ScholarWorks. It has been accepted for inclusion in Dissertations, Theses, and Masters Projects by an authorized administrator of W&M ScholarWorks. For more information, please contact scholarworks@wm.edu.

THE INTERACTION OF EOLIAN SAND TRANSPORT,
VEGETATION, AND DUNE GEOMORPHOLOGY
CURRITUCK SPIT, VIRGINIA-NORTH CAROLINA



A Thesis

Presented to

The Faculty of the School of Marine Science
The College of William and Mary in Virginia

In Partial Fulfillment
Of the Requirements for the Degree of
Master of Arts

by

Andrew L. Gutman

1978

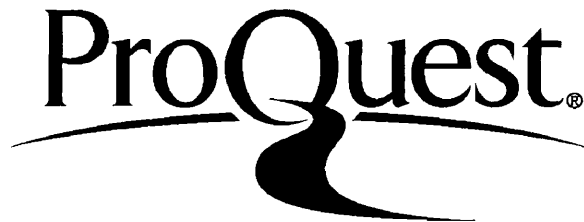
ProQuest Number: 10626197

All rights reserved

INFORMATION TO ALL USERS

The quality of this reproduction is dependent upon the quality of the copy submitted.

In the unlikely event that the author did not send a complete manuscript and there are missing pages, these will be noted. Also, if material had to be removed, a note will indicate the deletion.



ProQuest 10626197

Published by ProQuest LLC (2017). Copyright of the Dissertation is held by the Author.

All rights reserved.


This work is protected against unauthorized copying under Title 17, United States Code
Microform Edition © ProQuest LLC.

ProQuest LLC.
789 East Eisenhower Parkway
P.O. Box 1346
Ann Arbor, MI 48106 - 1346

APPROVAL SHEET

This thesis is submitted in partial fulfillment of
the requirements for the degree of

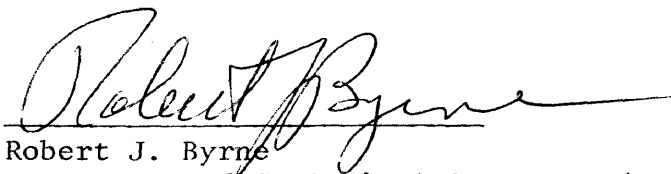
MASTER OF ARTS


Andrew L. Gutman

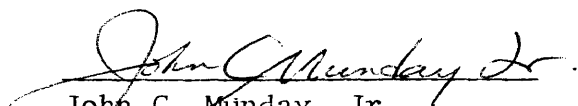
Approved,



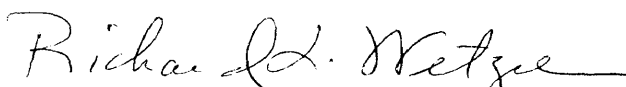
Victor Goldsmith, Chairman
Department of Geological Oceanography



Robert J. Byrne
Department of Geological Oceanography



John C. Munday, Jr.
Department of Geological Oceanography



Richard L. Wetzel
Department of Wetlands Research



Alan D. Howard
Department of Environmental Sciences
University of Virginia

TABLE OF CONTENTS

	Page
ACKNOWLEDGMENTS	vi
LIST OF TABLES	vii
LIST OF FIGURES	viii
ABSTRACT	xii
INTRODUCTION	2
Eolian Coastal Processes	2
Geologic and Geographic Setting	3
Present Geography and Management of Currituck Spit.	5
METHODS	10
Wind Regime	10
Migration Rate of Sand Hills	10
Orientation of Parabolic Dunes	12
Cross-Barrier Eolian Sand Grading	12
Sand Transport Model	13
WIND CLIMATE	14
Data Analysis and Reduction	15
Corolla Station Wind Climate	16
Monthly and Seasonal Wind Regime	18
Hatteras and Corolla Wind Data	25
Long Term Wind Regime	42
Conclusions	46

TABLE OF CONTENTS (Continued)

	Page
MOVEMENT OF LARGE SAND HILLS.	50
Migration Rates	51
Northern and Southern Differences in Migration Rates. .	58
Slipface Orientation and Movement Direction	61
Volume Discharge of Sand.	62
Conclusions	64
ORIENTATION OF COASTAL PARABOLIC DUNES.	66
Wind Vector Analyses.	69
Conclusions	79
EOLIAN GRADING OF SAND ACROSS TWO BARRIER ISLAND TRANSECTS. . . .	80
Field Procedure	82
Textural Analyses	85
False Cape Transect	87
Whalehead Hill Transect	91
Conclusions	94
DEVELOPMENT OF A MODEL TO PREDICT EOLIAN SAND TRANSPORT	96
Mechanism of Eolian Sand Transport.	97
Wind Data	103
Soil Moisture Variable.	104
Soil Moisture Equation.	108
Vegetation Effects.	113
Summary of Model.	117
Variables Not Included in Model	118
Verification of Model with Sand Transport Measurements. .	123
Verification of Model Using Migration Rate of Medanos .	132
Conclusions	136

TABLE OF CONTENTS (Continued)

	Page
APPLICATIONS OF SAND TRANSPORT MODEL.	137
Sand Fencing and Dune Growth.	137
Net Movement of Sand Across a Barrier Spit.	142
Conclusions	147
DISCUSSION AND MANAGEMENT IMPLICATIONS.	150
Wind.	150
Moisture.	151
Vegetation.	153
Interaction of Wind, Vegetation, and Parabolic Dunes.	154
North-South Differences	155
Management Implications	156
REFERENCES.	159
APPENDIX 1. COROLLA STATION WIND DATA.	163
APPENDIX 2. WIND ROSE DIAGRAM PROGRAM.	175
APPENDIX 3. WIND RESULTANT PROGRAM	180
APPENDIX 4. EOLIAN SAND TRANSPORT MODEL.	184
VITA.	190

ACKNOWLEDGMENTS

I wish to express my grateful appreciation to Dr. Victor Goldsmith and Dr. Robert J. Byrne for their guidance, encouragement and understanding. To Dr. Alan D. Howard, Dr. John C. Munday, Jr., and Dr. Richard L. Wetzel, I extend grateful appreciation for their careful review and constructive criticism.

I am especially grateful to NASA Wallops for the loan of the anemometer which was an integral part of this study. I would also like to thank the United States Coast Guard Fifth District for the use of the Currituck Beach Lighthouse.

Finally, a special thanks to Mrs. Linda Jenkins for typing this manuscript.

LIST OF TABLES

Table		Page
1	Corolla Station Wind Data Summary	24
2	Annual Rate of Coastal Sand Dune Movement of Various Locations Throughout the World.	54
3	Parabolic Dune Orientation From Aerial Photographs.	72
4	Wind Data Prior to Sediment Sampling.	84
5	Variables in Eolian Transport Process	101
6	Soil Moisture Data.	109
7	Output of Linear Least-Squares Curve Fitting Program.	111
8	Results of Sand Transport Calculations.	119
9	Sand Transport Measurements Near Corolla, N.C..	129
10	Sand Transport Measurements Near False Cape, Va..	130
11	Total Transport Calculated By Eolian Sand Transport Model (2/76-2/77) Assuming Z_o of 3.0 cm for All Offshore Wind Directions.	133
12	Total Transport Calculated By Eolian Sand Transport Model (2/76-2/77 Assuming Z_o of 6.0 cm for All Wind Directions	134
13	Total Transport Calculated By Eolian Sand Transport Model (2/76-2/77) Assuming Z_o of 1.0 cm for All Wind Directions	145
14	Total Transport Calculated By Eolian Sand Transport Model (2/76-2/77) Assuming Z_o of 6.0 cm for All Offshore Wind Directions.	146

LIST OF FIGURES

Figure		Page
1	Regional location map	4
2	Schematic diagram of typical cross-barrier transects. .	7
3	Currituck Light House	11
4	Corolla Station wind rose for all wind speeds	17
5	Corolla Station wind rose for wind speeds greater than 5.0 m/sec.	19
6	Corolla Station wind rose for wind speeds greater than 10.0 m/sec	20
7	Frequency occurrence of wind speeds greater than 5.0 and 10.0 m/sec.	22
8	Monthly mean wind speeds.	23
9	February wind rose diagrams	26
10	March wind rose diagrams.	27
11	April wind rose diagrams.	28
12	May wind rose diagrams.	29
13	June wind rose diagrams	30
14	July wind rose diagrams	31
15	August wind rose diagrams	32
16	September wind rose diagrams.	33
17	October wind rose diagrams.	34
18	November wind rose diagrams	35
19	December wind rose diagrams	36
20	January wind rose diagrams.	37
21	Hatteras Station wind rose for all wind speeds.	43

LIST OF FIGURES (Continued)

Figure		Page
22	Hatteras Station wind rose for wind speeds greater than 5.0 m/sec.	44
23	Hatteras Station wind rose for winds speeds greater than 10.0 m/sec	45
24	Hatteras Station wind rose 1953-1957.	47
25	Hatteras Station wind rose 1956-1970.	48
26	Distance travelled by Whalehead Hill 1961-1977.	52
27	Whalehead Hill looking southeast and southwest.	55
28	Aerial views of Barbours Hill looking northeast and southwest	56
29	Schematic illustration of the movement of two sand hills.	57
30	Eolian transport of sand off of Whalehead Hill covering paved road to the east	59
31	Slipface of Whalehead Hill advancing to the southwest covering dirt road.	59
32	Volume discharge of a large sand dune based on a known height and movement	63
33	High altitude photograph of parabolic dune field.	67
34	Diagrammatic representation of parabolic dune phases.	68
35	Low altitude aerial photographs of parabolic dunes	70
36	Corolla Station vector wind resultant	73
37	Mean orientation of parabolic dune field.	74
38	Corolla Station wind resultant excluding offshore winds.	77
39	Comparison of Corolla and Hatteras wind resultants.	78
40	Regional location map showing location of transects	81

LIST OF FIGURES (Continued)

Figure		Page
41	Profile of barrier island showing sample locations	83
42	Grain size moments after offshore winds at False Cape.	88
43	Grain size moments after onshore winds at False Cape.	89
44	Grain size moments after offshore winds at Corolla. . .	92
45	Grain size moments after onshore winds at Corolla . . .	93
46	Saltation	98
47	Vertical wind velocity distribution over sand surfaces.	105
48	Experimental data illustrating the effect of humidity and soil moisture on threshold shear velocity.	106
49	Computer plot of the distribution of residuals determined from soil moisture data.	114
50	Computer plot of residuals versus fitted Y.	115
51	The change of surface roughness parameter after grass plantings on an Indiana coastal dune.	116
52	Sand trap and anemometers used to measure sand transport	124
53	Measured and predicted sand transport rates	126
54	Typical "light" and "very light" density vegetation.	127
55	Typical "medium" and "heavy" density vegetation	128
56	Sand fence created foredunes along Currituck Spit.	138
57	Calculation of the volume of sand trapped by a single and double row sand fence.	140
58	Vertical aerial photograph sequence at False Cape.	143

LIST OF FIGURES (Continued)

Figure		Page
59	Vertical aerial photograph sequence at Corolla.	148
60	Lee side eddy	152

ABSTRACT

The three most important variables influencing eolian sand transport in the coastal zone are wind, vegetation, and moisture. Eolian sand transport, resulting from the interaction of these variables, is the dominant physical process responsible for the development, migration, and orientation of sand dunes along Currituck Spit, Virginia/North Carolina. Due to the present lack of overwash fans and inlets along the spit, eolian transport has also become the major source of cross-barrier sediment transport. The interaction of eolian sand transport, dune dynamics, and cross-barrier sediment transport was the subject of this study.

A detailed wind climate was compiled from one year (February 1, 1976-January 31, 1977) of local wind data acquired as part of this study, and 18 years of data (1953-1970) from Cape Hatteras, North Carolina 115 km to the south. The local wind regime along Currituck Spit is directionally polymodal, with prevailing winds from the north and southwest (20% and 32% of all observations, respectively) and dominant winds from the northeast, north, and northwest (mean wind speed approximately 8.0 m/sec). The strongest average wind speeds occur during December and the lowest in July. Rather than four distinct seasonal wind regimes, there is a long period of high velocity winds (October-June) and a shorter low velocity period (July-September). The comparison with Cape Hatteras wind data determined that the local record was typical of the long-term distant wind regime.

These wind data analyses support the assertion (Goldsmith, et al., 1977) that the Currituck Spit multidirectional wind regime is responsible for the development of medano sand hills, by gathering together sand spread out over a sand sheet or old overwash fan, resulting in a heightened and steepened dune.

An increase in the moisture content of sand increases the threshold shear velocity, thereby decreasing the eolian sand transport for a given wind speed. When the moisture effects are included, there was a good correlation between the measured migration rate (6 m/year) of a sand hill and the rate predicted by an eolian sand transport model. If the effect of moisture had been ignored, the predicted migration rate would have exceeded the measured by 30%.

Vegetation is the most important variable other than wind in the eolian transport process. An increase in the vegetation density and/or height increases the value of the surface roughness parameter, thus reducing the transport rate. Varying amounts of vegetation along Currituck Spit, along with the wind and precipitation, control the migration and development of dunes, and the cross-barrier flux of sand.

The mean orientation (North 8° East) of a parabolic dune field is hypothesized to have resulted from the interaction between local wind climate and maritime forest vegetation. A vector wind resultant, compiled by taking into account the effect of vegetation, and the location of the sand source, compared well (within 20°) with the mean orientation of the parabolic dunes. This resultant was dramatically different from a resultant (West 30° North) based on only wind climate.

An eolian sand transport empirical model was developed to calculate the net directional movement of sand, after careful consideration of the coastal eolian transport mechanisms. One year of precipitation, temperature, and wind data were input into the model consisting of eolian transport equations of Hsu (1971) and Bagnold (1941), threshold shear velocity equation of Kadib (1964), and an experimental relation between precipitation and soil moisture content developed from field measurements. After verification by comparison with field measurements of eolian sand transport, the model was run for varying levels of vegetation density reflecting both the north-south and past-present differences in vegetation cover.

Forty years ago Currituck Spit contained a completely unvegetated sand sheet. The model predicts only a very small (2,000 kg/m/year) net onshore sand transport (despite a large gross transport). For the vegetation characteristic of twenty years later in False Cape State Park and today near Corolla, North Carolina (i.e., mostly sparse dune grass) the model predicts a net onshore transport of 10,000 kg/m/year.

A continuous 40 year sand fencing program in False Cape State Park succeeded in creating a high (2-4 meters) multiple-ridge foredune. Vegetation has become very dense across the interior. The model predicts in this case a net onshore sand movement that will be mostly trapped by the vegetated foredune system.

The understanding of dune dynamics, cross-barrier sediment flux, and the interaction of wind, sand, moisture, vegetation, and dunes determined in this study are used to suggest certain coastal resource management techniques (e.g., the planning design and effects of a sand fencing program). These studies indicate that the protection and encouragement of vegetation for stabilizing shifting eolian flat sands and migrating sand hills should be a prime coastal resource management objective.

THE INTERACTION OF EOLIAN SAND TRANSPORT,
VEGETATION, AND DUNE GEOMORPHOLOGY
CURRITUCK SPIT, VIRGINIA-NORTH CAROLINA

INTRODUCTION

Eolian Coastal Processes

Wherever a large supply of sand is available to be transported by the wind in a temperate coastal zone, an interaction exists between wind energy, vegetation, and eolian sand transport and deposition. As sand is deposited on the beach by waves via longshore transport, onshore winds transport this material towards the interior sometimes winnowing out the fines. The net movement of this sand depends on the local wind regime and vegetation. With a unimodal onshore wind regime there will be a net movement of sand towards the interior regardless of vegetation. In coastal areas, such as the southeast coast of the United States, the wind regime consists of both onshore and offshore components. In a vegetation-free environment the net movement of sand will be in the direction of the dominant wind component. However, vegetation is an important factor determining the net movement of sand and the development of dunes.

Vegetation lowers the wind velocity both within, and downwind of, the vegetation as a function of both the vegetation height and density. Where vegetation is downwind of a source of sand, perhaps a beach, deposition will occur in and around this vegetation. The vegetation which thrives with some but not too much sand burial, will continue to grow upwards, resulting in dune development. However, if vegetation (especially shrub and maritime forest) is upwind of a sand supply it will act to decrease the sand transport by reducing

the downwind velocity. Therefore, the presence or absence of vegetation along with the local wind regime, will determine the net direction and amount of sand transport, either inland from the beach or seaward onto the beach, as well as the resulting development of dunes.

Moisture is another important variable in the eolian sand transport process. Soil moisture increases the wind velocity necessary to initiate sand transport. Since rain is often associated with maximum wind speeds, moisture can diminish the net movement of sand by wind during the time of maximum eolian sand transport. It is this interaction of sand transport, vegetation, moisture, and dunes which was investigated in this study.

Geologic and Geographic History

Currituck Spit, extending from Cape Henry, Virginia to Oregon Inlet, North Carolina (Figure 1) is part of a long barrier island system that extends along the Virginia-North Carolina Coast. It has been hypothesized that these barrier islands have been migrating landward since their formation (Field and Duane, 1977; discussed in Zellmer, 1977), in response to the rise in sea level of approximately 1 cm/year over the last 6,000 years (Milliman and Emery, 1969) and 0.1 cm/year over the last 40 years (Hicks, 1973). Sutton et al. (1977) have documented the historical shoreline changes since 1850 along Currituck Spit. At False Cape (Figure 1) there has been an anomalous accretion trend of less than 1 m/year, while near Corolla, North Carolina historical erosion has averaged 2 m/year. Maximum historical erosion along northern Currituck Spit is about 4 m/year at Dam Neck.

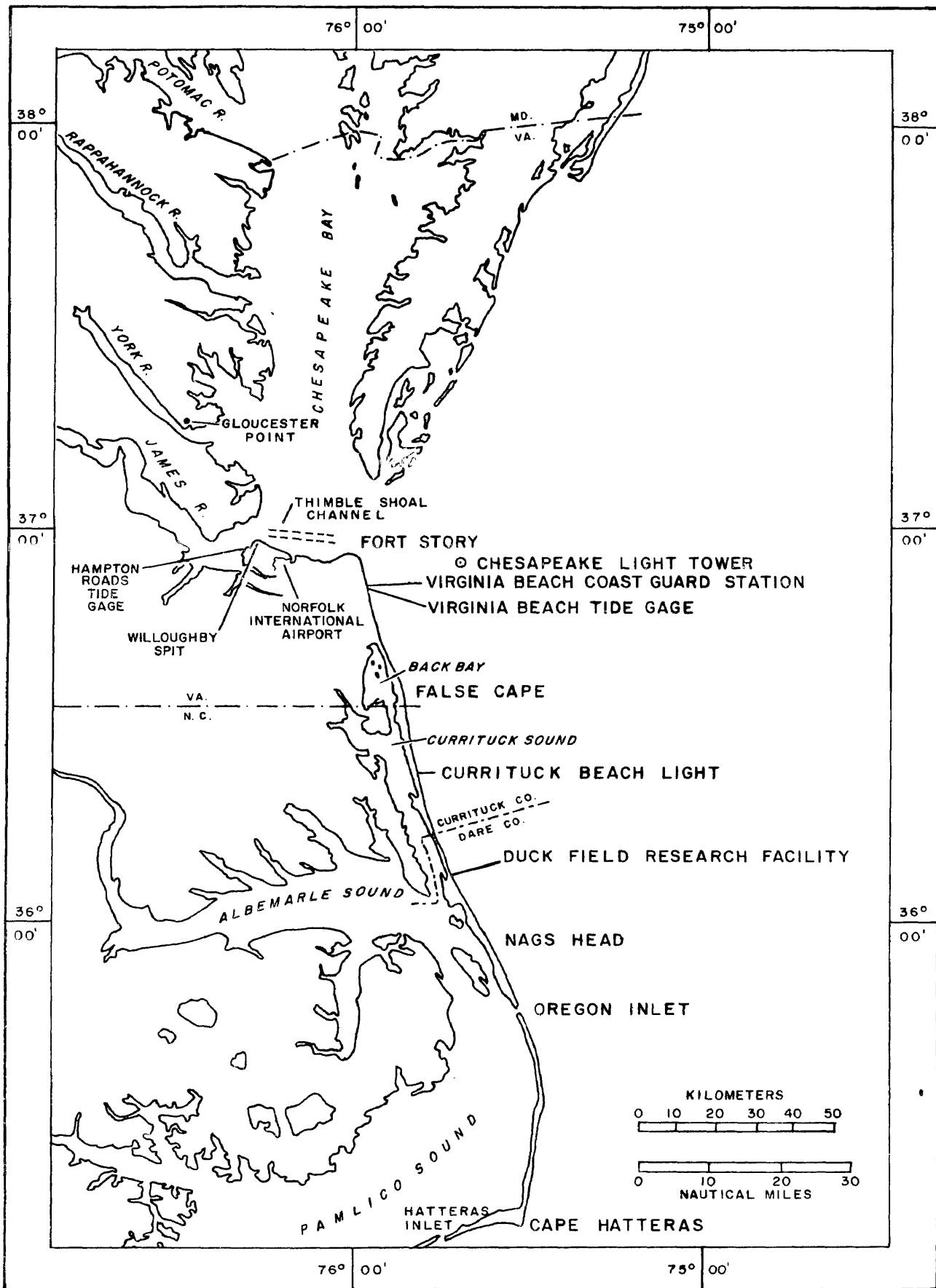


Figure 1. Regional location map.

The islands making up the Virginia-North Carolina barrier chain including Currituck Spit are generally narrow (0.5 km to 2 km) with elevations about 3 m except for the higher foredunes at False Cape (about 10 m) and the sand hills (up to 25 m). Washover channels and fans are presently rare and generally unimportant features due to the stabilization of foredunes by sand fencing and vegetation planting. However, over-washing was extensive in the past and as recently as 1962. Along Currituck Spit there are presently no inlets over a distance of 130 km. However, two inlets were present along Currituck Spit in the eighteenth and early nineteenth century (Hennigar, 1978): old Currituck Inlet, at the Virginia-North Carolina state line, which closed in 1729 and New Currituck Inlet near Corolla which closed in 1812. Therefore, although Currituck Spit is a dynamic ecosystem responding to wave and wind energy, vegetation, and a slowly rising sea level, it is (geographically) very different today than in the historical and recent past.

Present Geography and Management of Currituck Spit

Currituck Spit presents a complex picture of coastal land use. Previously undeveloped sections south of the North Carolina/Virginia border are undergoing development as residential subdivisions. To the north, False Cape State Park and Back Bay National Wildlife Refuge preserve the section of barrier island south of Sandbridge, Virginia, from development pressures by prohibiting development, and in the case of Back Bay, by limiting access. However, these areas are subject to increasing pressures from recreational users, and the entire area may undergo rapid and complex usage changes in the next decade. The barrier island represents a fragile balance between the physical processes that form and maintain it. The ability of such

a fragile ecosystem to withstand development pressures without major disruption is questionable.

To minimize the impact of development and recreational activities through coastal resource planning, an understanding is required of the interactive process and response system which determines the development, orientation and migration of sand dunes, the distribution of vegetation, the sediment dynamics, and the overall stability of the coastal ecosystem. Knowledge of coastal processes is required to evaluate coastal zone management problems and to initiate planning programs. The human and natural forces affecting the coastal zone, the present state of the ecosystem, and the effect of uses and prospective uses on coastal resources is important information for proper management of coastal ecosystems. This information can be best acquired through quantitative studies of the eolian processes in the area.

The most apparent and dominant geomorphic features in the study area are sand dunes. There are four basic dune types, discussed in detail by Goldsmith et al. (1977): (a) the medano sand hill or transverse dune ridge, (b) the parabolic or U-dune, and either the (c) artificially or (d) naturally created foredunes. These four dune types are unequally distributed along the Currituck Spit.

A cross barrier transect near Corolla traverses a very different environment than a transect at False Cape (see Figure 2A); the foredune system is lower (1-2 m) due to a lack of continual sand fencing (Hennigar, 1978), there is an absence of a shrub thicket and instead only sparse dune grass vegetation across the eolian flat, and large highly mobile medianos (10-25 m high) are presently invading the maritime forest. The nature of eolian sand transport is radically different in the two areas. The flux of sand across areas typified

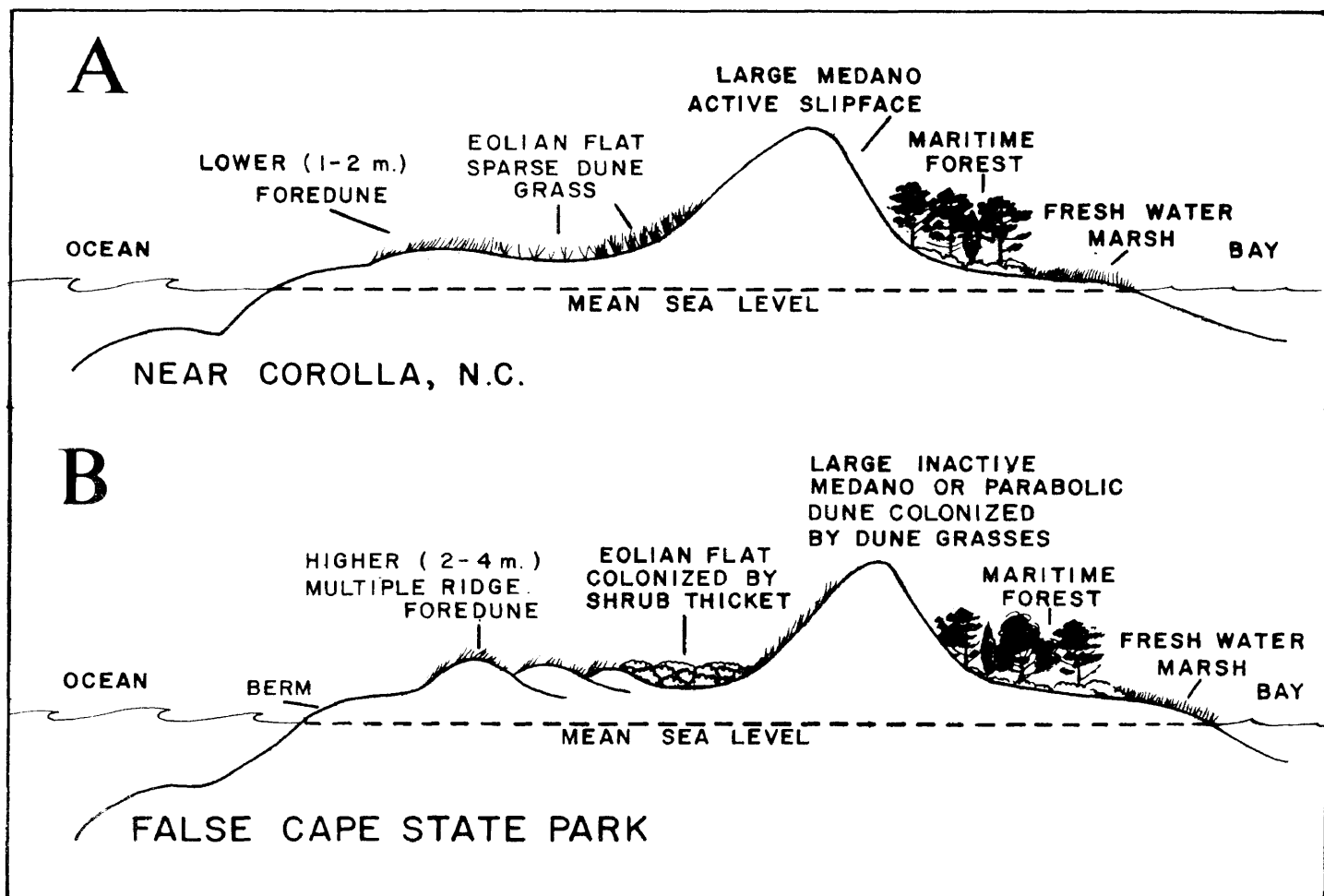


Figure 2. Schematic diagram of typical cross-barrier transects near Corolla, North Carolina (A) and False Cape State Park, Virginia (B). Notice the difference in the height of the foredunes and density of eolian flat vegetation.

by profile A (Figure 2) would be much greater than at areas similar to profile B due to the differences in vegetation cover.

A cross barrier transect in False Cape State Park (shown schematically in Figure 2B) first crosses a 2-4 meter high multiple ridge foredune system formed by 40 years of continuous sand fencing in the area (Hennigar, 1978). Landward along the transect, a 1-2 m high shrub thicket grows on the eolian flat. Then, depending on the location of the transect the next feature encountered is either a medano, or several parabolic dunes stabilized by dune grass vegetation. These dunes have been stabilized by dune grass at the edge of a maritime forest which grades into a freshwater marsh and then the Bay.

Pierce (1969), in constructing a sediment budget for a barrier island (Core Banks), concluded that not much of the eolian-transported sediment is permanently lost to the longshore system. A cursory look at Currituck Spit would show that millions of cubic meters of sand (Hennigar, 1978) are tied up in the many sand hills and parabolic dunes. Since these eolian deposits are eventually stabilized by vegetation and thus permanently lost to longshore system the conclusion drawn by Pierce for the Core Banks is not applicable to Currituck Spit. On the other hand, a Corps of Engineers report (New England Division, Corps of Engineers, 1968) estimated that over a period of twenty-five years, 1,000,000 m³ of sand were blown from Nauset Beach, a barrier-spit, landward into Pleasant Bay. Of interest here is the fact that both of these estimates were derived from the amount of sand trapped by sand fencing. The estimates by Pierce and the Corps of Engineers probably represent the extremes.

A reliable quantitative and qualitative understanding of the interaction of eolian sand transport, vegetation and dunes is necessary for the purpose of estimating coastal sand budgets, for protection of structures from mobile dunes, for understanding the cause and effect relationship of human activities, for understanding the development, orientation, and migration of sand dunes, and to intelligently manage and protect the coastal ecosystem. This study addresses these fundamental and broad issues using methods outlined in the following section.

METHODS

The specific details of the pertinent methods are included in each appropriate chapter. An overview of the methods used in this study is included here.

Wind Regime

The most important variable determining the rate of sand transport, and the development, orientation and migration of sand dunes is the wind. Therefore a comprehensive wind climate was compiled for Currituck Spit detailing and comparing the long term, yearly, seasonal and monthly wind characteristics. A continuously recording anemometer was installed at the top of Currituck Light House (Figures 1 and 3) 53 m above mean sea level (MSL) for a one year period (February 1, 1976 to January 31, 1977) to determine an accurate and detailed local wind record. The data were digitized at 3 hour intervals and compared with long term wind data from the closest national weather station at Cape Hatteras, North Carolina. The wind climate determined from these data became the data input for a model of sand transport, for help in understanding sand size grading across the barrier spit and for the orientation and migration of the parabolic and medano sand dunes.

Migration Rate of Sand Hills

The migration rate of large mendanos was determined by placing reference markers around the perimeter of two sand hills and then measuring the net movement of these dunes relative to the markers after



Figure 3. Views of Currituck Light House at Corolla, North Carolina, in February 12, 1977 (top) showing anemometer, and June 14, 1889 (bottom). The area that was pastureland for the light house keeper's fresh meat supply, was bare sand in the 1940's, is now being naturally revegetated.

a one year period. The migration rate thus determined was then compared with historical migration rates determined from aerial photographs, the wind climate over the same one year period, and the effects of vegetation.

Orientation of Parabolic Dunes

Vegetation was also important in the development and orientation of parabolic dunes in False Cape State Park. The development of parabolic dunes was traced with a series of aerial photographs between 1939 and 1975 (discussed in detail by Hennigar, 1978). The orientation of the axes of the parabolic dunes were determined from recent vertical aerial photographs. These orientations were then compared with the vector wind resultants from the local wind data, the vegetation distribution, and shoreline orientation.

Cross Barrier Eolian Sand Grading

Sand grading was investigated across two barrier spit transects, one in False Cape State Park, the other south of Corolla. Sand samples of the sand surface and the top 5.0 cm were collected at eight stations across each of the two transects, and then the grain distribution was analyzed using the Woods Hole Rapid Sediment Analyzer (Zeigler, 1960). The grain size statistics (expressed in sedimentation diameter) for these samples were plotted against distance across the transect. This eolian grading study was conducted in order to investigate the geologic processes responsible for the grain size differences in the subenvironments of the north and south transects, and to help clarify the role that eolian sand transport plays in the overall sediment dynamics of a barrier island.

Sand Transport Model

In order to quantitatively estimate the net movement of sand by wind across the spit in all directions an empirical eolian sand transport model was developed. This model utilizes equations developed by other investigators (Bagnold, 1941; Kadib, 1964; Hsu, 1973) as well as equations developed in this study. Field measurements of sand transport, wind profiles, and the relationship between soil moisture and threshold velocity were conducted for development and verification of the model, and for deriving an equation to predict soil moisture content using a canned computer linear least squares curve fitting program. Model output was utilized to aid in understanding the migration rate of sand dunes, the effects of moisture and vegetation on the transport process and for addressing the basic question of the role of eolian sand transport in the sediment dynamics of a barrier spit.

WIND CLIMATE

Wind is the most important environmental variable determining the rate and net movement direction of eolian and transport, and the orientation and movement of sand dunes. A continuously recording anemometer was installed in February, 1976, 35 m above MSL on top of the Corolla Lighthouse (Figure 3) to provide an accurate and detailed local wind climatology. Wind data from the closest existing weather station at Cape Hatteras, North Carolina (approximately 115 km to the south) could not be used for description of the local wind regime without comparisons of simultaneous data, due to the possibility of regional variations in wind characteristics.

An anemometer was installed on top of the lighthouse because of its height, availability of electricity, and security for the equipment. The top of the lighthouse provided relatively unobstructed wind flow from all directions to the anemometer, while at other possible locations the anemometer would have been subject to eddies of wind caused by high sand dunes or forests. Nevertheless, the wind characteristics recorded by the anemometer were influenced by the lighthouse. The wind velocity at the top of the lighthouse (Figure 3) would increase due to compression of streamlines over the obstruction. Even though the anemometer was about 3 m above the top of the lighthouse the anemometer records winds effected somewhat by the lighthouse. Other investigators using these wind data in the future should keep this effect in mind.

A Bendix Aerovane Transmitter (model 120) was mounted on top of a 9 m telescoping tower which was bolted to the lower iron catwalk of the lighthouse. The transmitter was oriented north-south using the position of solar noon and then raised to its permanent position above the lighthouse. The electric output of the transmitter magneto (speed) and synchro (direction) were transmitted through a 20 m cable to a Bendix Aerovane Wind Recorder (model 141) which is a two-element recorder that simultaneously records, in separate channels, inked traces of wind direction and speed values on a strip chart. The chart paper operating at 3.81 cm/hour (1.5 inches/hour) was changed every 14 days and then returned to VIMS for digitizing. The anemometer has operated continuously since it was installed in February 1976 except 22 days (Appendix 1) for recorder repairs, withstanding wind speeds greater than 45 m/sec.

Date Analysis and Reduction

The wind data on the strip charts, now in storage at VIMS, were digitized by visually picking a wind speed and direction which represented an average value for each three hour period beginning at 0100 Eastern Standard Time. For each day eight average wind speeds and directions, the maximum wind speed for the day, and the direction associated with this gust, were recorded on a standard form for key-punching. This data format was chosen to coincide with standard National Weather Service procedures, in order to facilitate comparison of Corolla and National Weather Service wind records.

The wind data were initially processed using a computer program which lists each data point and the vector average wind speed

and direction for each day. Appendix 1 is a listing of the twelve months of data processed using this program. To further aid in preparing a wind climate for Currituck Spit the digitized wind data were compiled into computer generated wind rose diagrams using the College of William and Mary Computer Center CALCOMP Model 665 digital plotter. The program which generates these plots is listed in Appendix 2. The average wind speed and duration for each direction in an eight point compass were computed according to the following relations:

$$A_i = s(\sum U_i / N_i)$$

and

$$B_i = s(N_i / \sum_{ni} \times 100)$$

where:

- A_i = average wind speed for each of eight wind directions
- B_i = average duration in percent for each wind direction
- U_i = wind speed for one three hour interval within each of eight class interval
- N_i = number of observations in each class interval
- \sum_{ni} = total number of observations for all eight wind directions
- s = scaling factor for plotting
- i = 1 to 8, for each wind direction class interval

Corolla Station Wind Climate

Figure 4 is a wind rose summarizing all data from the Corolla station anemometer for a one year period (February 1, 1976–January 31, 1977). The length and size of each arrow indicate the average wind speed and direction, while the shaded area indicates the duration of the wind from each direction. The highest average wind speed (8.0 m/sec) is associated with northerly winds, with both the northeast and southwest directions being within 0.5 m/sec of this average wind velocity. Thus, Figure 4 indicates at least three modes with respect to the highest average wind velocities (northeast, north, and southwest).

2/76-2/77
**COROLLA STATION
 WIND ROSE**

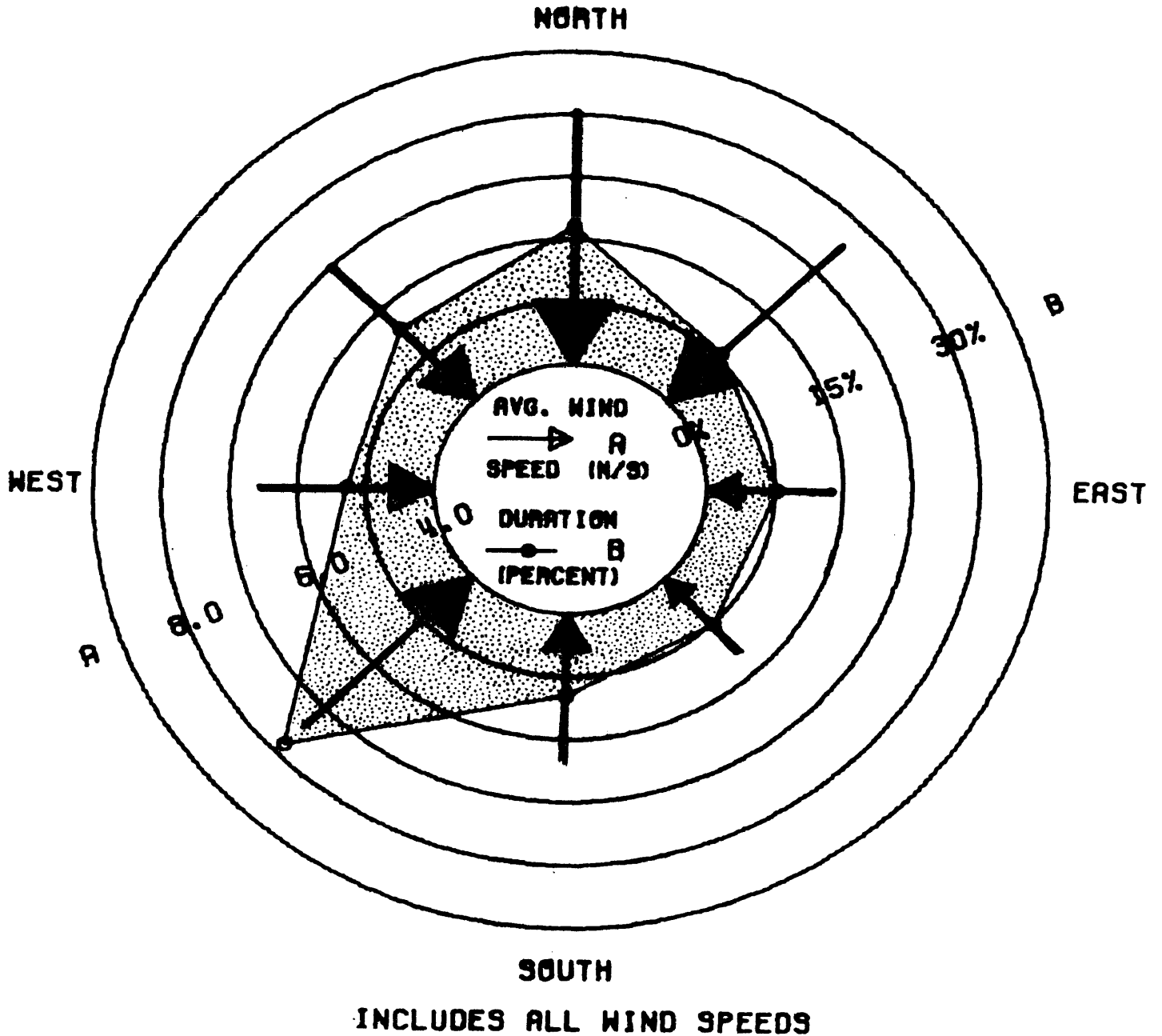


Figure 4. Corolla Station wind rose (February 1, 1976 to January 31, 1977) for all wind speeds. Average wind speed is indicated by arrows and scale A, while duration is indicated by shading and scale B.

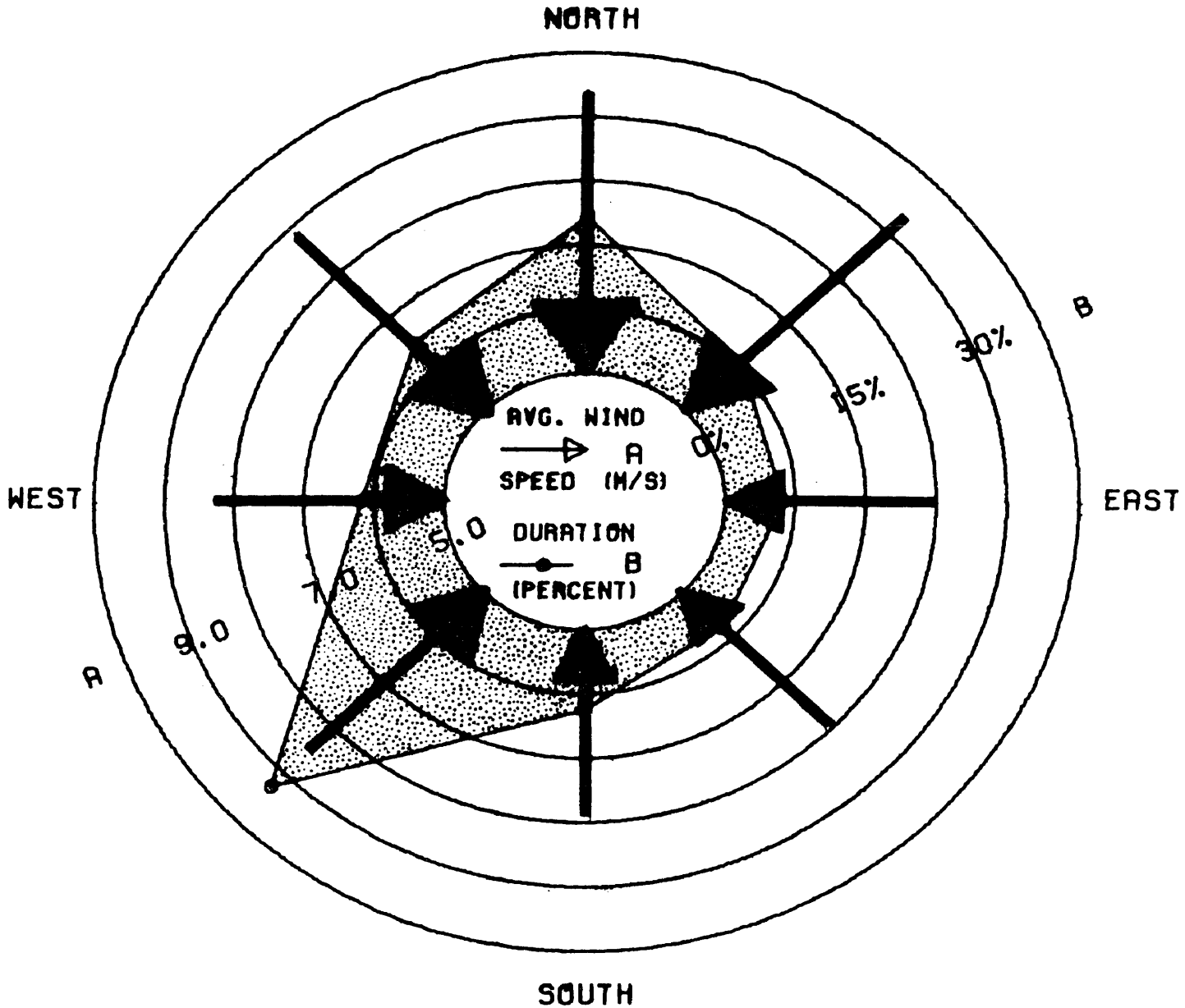
The threshold wind velocity necessary to initiate sand transport is approximately 5.0 m/sec (Bagnold, 1941 for 0.25 mm sand). Therefore to establish a dominant (direction or directions from which highest velocity winds occur) and prevailing (direction or directions from which the most frequent winds occur) wind regime for Currituck Spit, it is more important to concentrate on higher wind speeds. Figures 5 and 6 are wind rose diagrams compiled by excluding all wind speeds less than 5.0, and 10.0 m/sec, respectively. In Figure 5 the highest average wind speeds are from the north and northeast (9.5 m/sec); however, the northwest, west, and southwest average velocities are only slightly lower. In Figure 6 the northeast, northwest, and north, directions have the highest average wind velocity (all > 13.0 m/sec).

Although the dominant wind regime changes only slightly in plots of increasing wind speeds, these plots show significant changes in the prevailing wind regime. In Figure 4, which includes all wind speeds, the southwest is clearly the prevailing wind direction with a duration of 30%, although there is a secondary mode in the north (15%). However, at higher wind speeds the north becomes increasingly important. In Figure 6, which excludes all winds less than 10.0 m/sec, the northerly winds are equal in duration to the southwest. Therefore these plots indicate no single dominant or prevailing wind direction but instead a polymodal wind regime. This has a profound impact on the dunes and sediment dynamics of the spit, and will be discussed in detail later in this thesis.

Monthly and Seasonal Wind Regime

The Corolla station wind data summarized in Figures 4, 5, 6 and Appendix 1 were further broken down into monthly compilations to

2/76-2/77
COROLLA STATION
WIND ROSE



EXCLUDES WIND SPEEDS < 5.0 M/S

Figure 5. Corolla station wind rose (February 1, 1976 to January 31, 1977) for winds greater than 5.0 m/s.

2/76-2/77

COROLLA STATION WIND ROSE

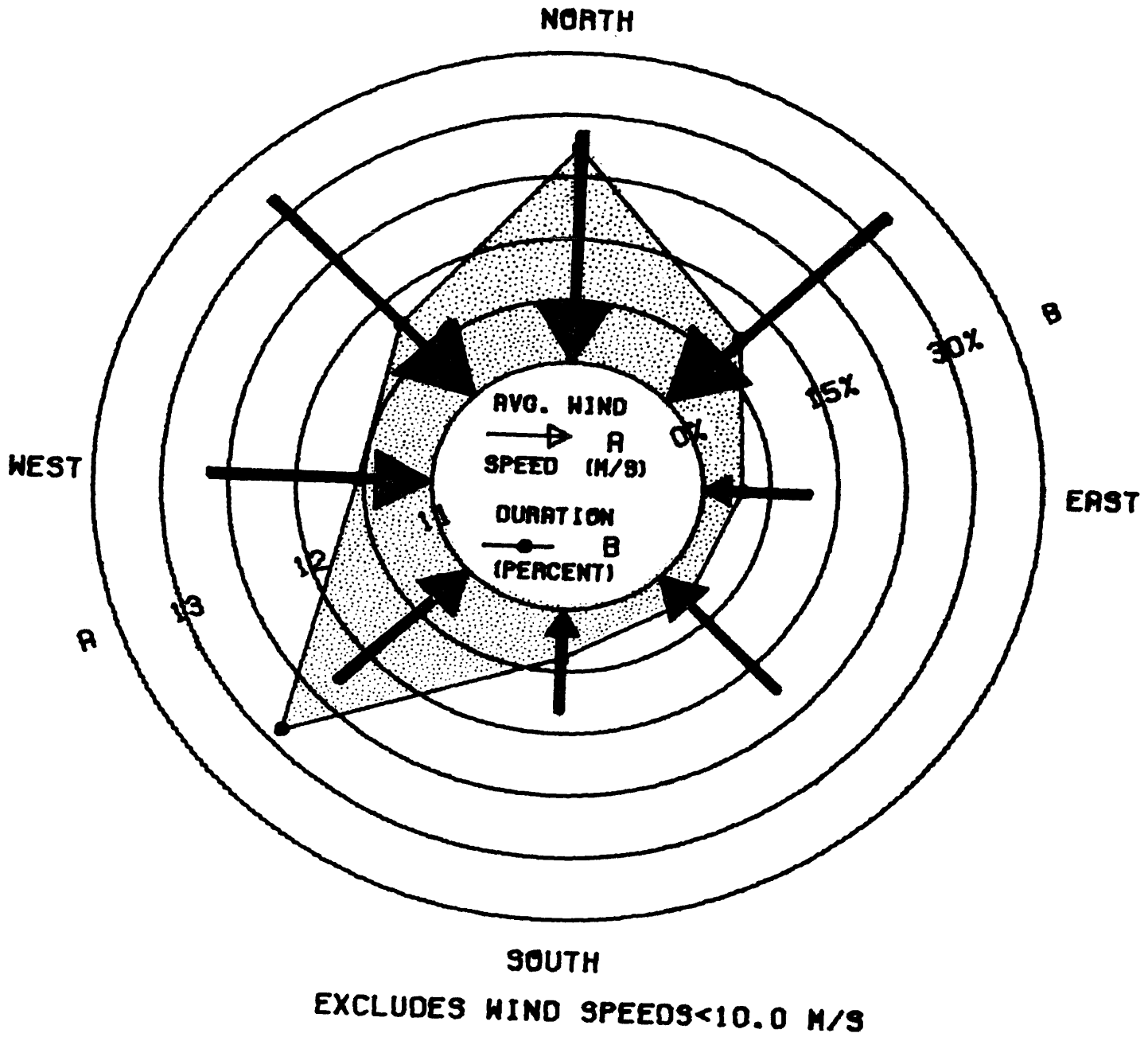


Figure 6. Corolla Station wind rose (February 1, 1976 to January 31, 1977) for winds greater than 10.0 m/s.

investigate the wind fluctuations on a shorter time scale.

Figure 7 shows the frequency of occurrence of wind speeds greater than both 5.0 and 10.0 m/sec on a monthly basis. Notice there is no obvious four-modal seasonality in this figure. Instead the lowest frequency occurrence of winds in both categories is during July, August, and September (55% > 5.0 m/sec, 10% > 10.0 m/sec) while between October and May over 65% of winds were greater than 5.0 m/sec and 20% were greater than 10.0 m/sec. Therefore rather than four distinct seasonal wind regimes there is only two indicated in this figure; a low velocity period during July-September and a higher velocity period during the rest of the year.

Figure 8 is a plot of the monthly mean wind speed. Table 1 lists the values plotted in this figure and the standard deviation associated with each monthly mean wind speed. The lower of the two lines in Figure 8 is a plot of the means computed from all wind speed data. Notice that this graph is very similar to Figure 7. Again there is no obvious seasonality but instead a period of low mean wind speeds (6 m/sec; July-September) and a longer period of higher mean wind speeds (7-8 m/sec; October-June).

The top of Figure 8 is a plot of the mean maximum wind speed for each month. During digitizing of the strip charts a maximum wind speed and direction (see Appendix 1) were recorded for each day. The mean and standard deviation associated with each of these monthly maximum wind speeds are listed in Table 1. This figure, unlike the others, does indicate some groupings which can be loosely related to four distinct seasons. The summer period (June-September) has the lowest mean (11-12 m/sec), the winter and fall period have the highest

Figure 7.

PERCENT FREQUENCY OCCURRENCE OF WIND SPEEDS
GREATER THAN 5.0 AND 10.0 METERS/SECOND

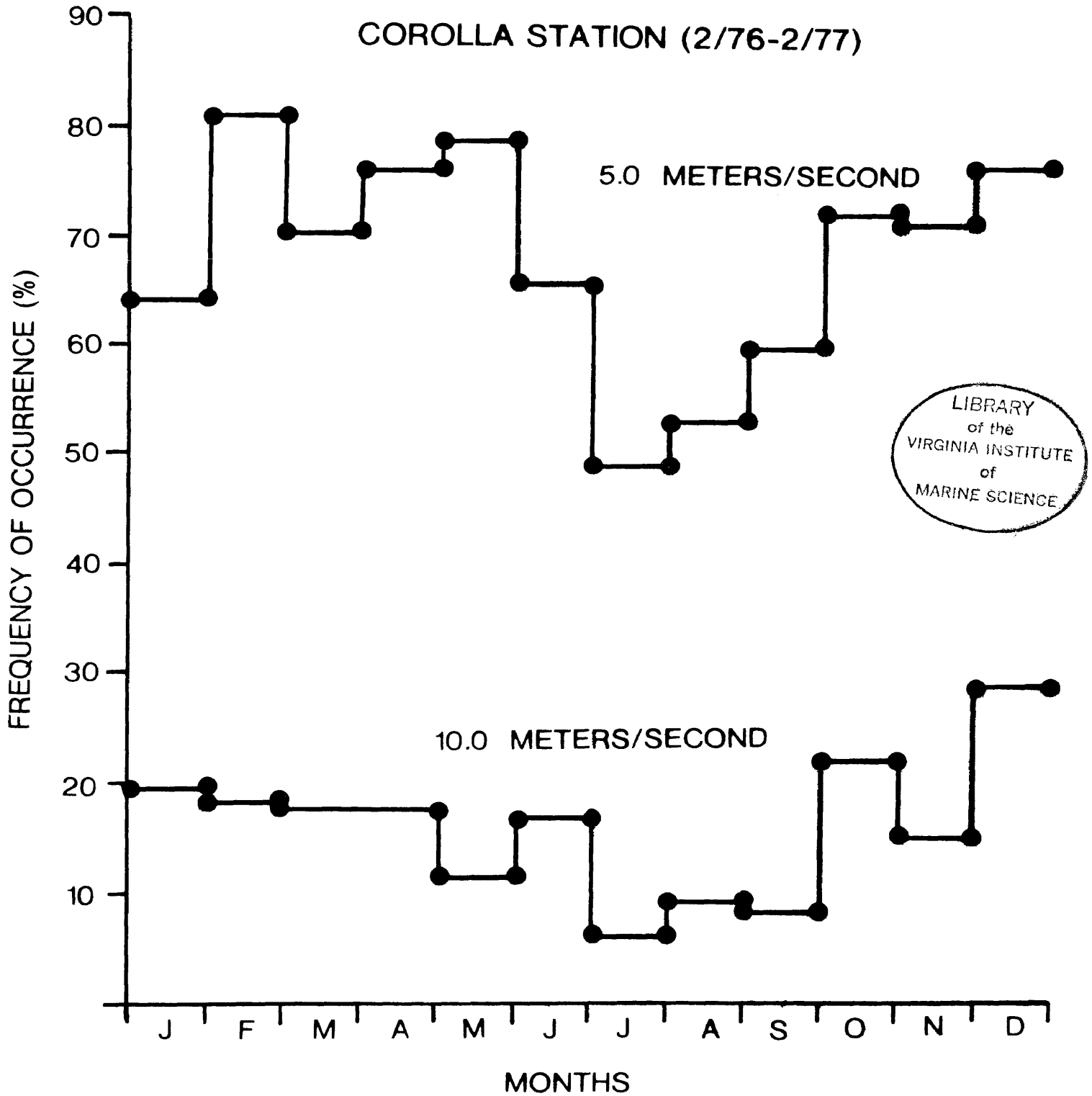


Figure 8.

MONTHLY MEAN WIND SPEED IN METERS/SECOND

COROLLA STATION (2/76-2/77)

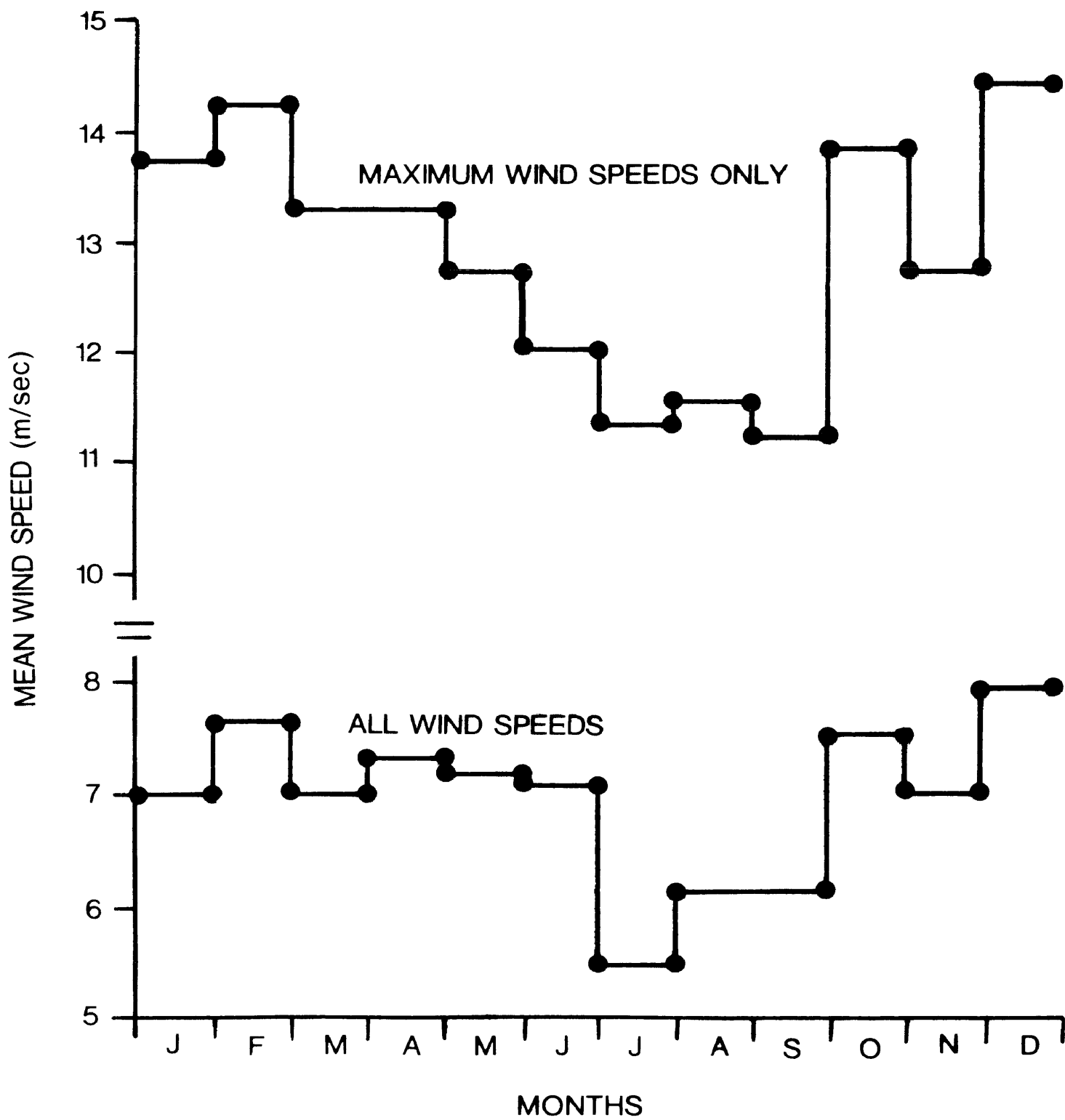


TABLE 1

COROLLA STATION WIND DATA SUMMARY, FEBRUARY 1976-FEBRUARY 1977

	<u>% \geq</u>	<u>% \geq</u>	<u>All Winds (m/sec)</u>		<u>Maximum Winds (m/sec)</u>	
	<u>5.0 m/sec</u>	<u>10.0 m/sec</u>	<u>Mean Wind</u>	<u>Standard</u>	<u>Mean Wind</u>	<u>Standard</u>
			<u>Speed</u>	<u>Deviation</u>	<u>Speed</u>	<u>Deviation</u>
January	63.5	19.3	7.0	3.7	13.7	4.3
February	80.1	18.1	7.6	3.2	14.2	5.5
March	70.2	17.3	7.0	3.5	13.3	4.3
April	75.9	17.3	7.3	3.2	13.3	4.0
May	78.3	10.8	7.2	2.7	12.7	3.9
June	65.0	19.5	7.1	4.4	12.0	3.7
July	49.6	3.6	5.4	2.3	11.3	4.3
August	52.6	9.9	6.1	3.5	11.5	4.0
September	59.6	8.3	6.1	3.2	11.2	3.9
October	72.9	22.9	7.5	3.7	13.8	7.4
November	71.7	16.7	7.0	3.3	12.7	3.6
December	76.9	27.5	7.9	3.7	14.3	4.0

mean maximum winds speeds (14 m/sec), while the spring (March-May) is a transition period (13 m/sec). As indicated in this Figure and in Figure 7 both the greatest frequency of occurrence and highest velocity winds occur during December.

Figures 9-20 are monthly wind rose diagrams compiled for one year (February 1976 to January 1977) in the same manner as Figures 4-6 for both Corolla and Cape Hatteras. Wind rose diagrams for the Cape Hatteras Weather Station will be discussed in the next section. These twelve figures can be used to determine the monthly and seasonal, directional wind regime.

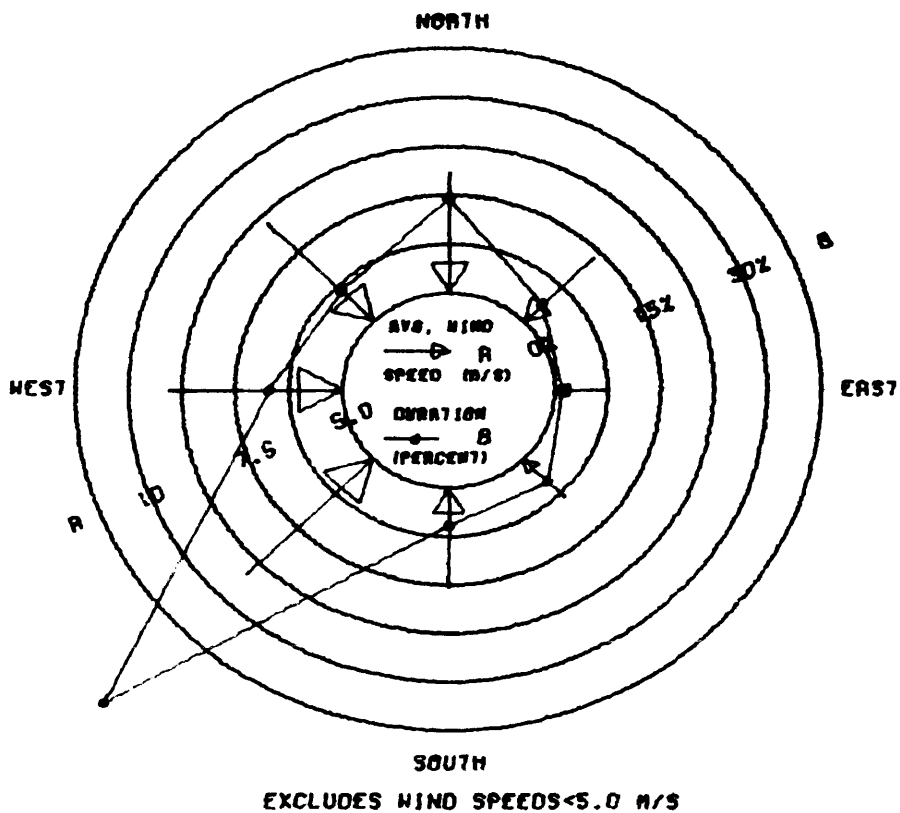
During October-January the northerly and northwesterly winds are clearly prevailing, accounting for about 55% of all wind observations. Beginning in February, and lasting until July, the southwest winds predominate (40%) while during August and September winds occur from all directions. Therefore, although the yearly summaries indicate a polymodal wind regime, monthly wind rose diagrams clearly indicate that these modes occur during separate times of the year. The northerly and northwesterly mode occurs between October and January while the southwesterly occurs between February and July.

Cape Hatteras and Corolla Station Wind Data

The mean, extreme, and directional wind regime has been compiled from one year of Corolla station wind data. However, the question remains whether this wind climate is actually representative of the average long term wind regime in the area.

An anemometer operating at the Cape Hatteras National Weather Station is the closest (115 km south of Corolla) available source of wind data covering a fairly long period of time (25 years). Before

COROLLA STATION FEBRUARY WIND ROSE



HATTERAS STATION FEBRUARY WIND ROSE

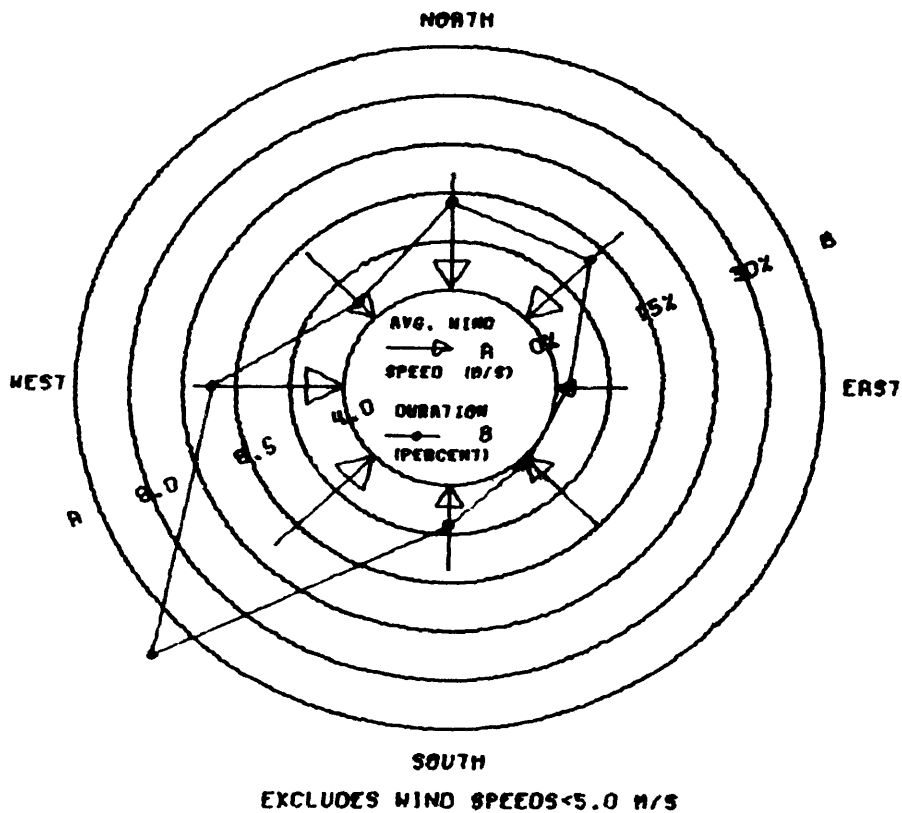
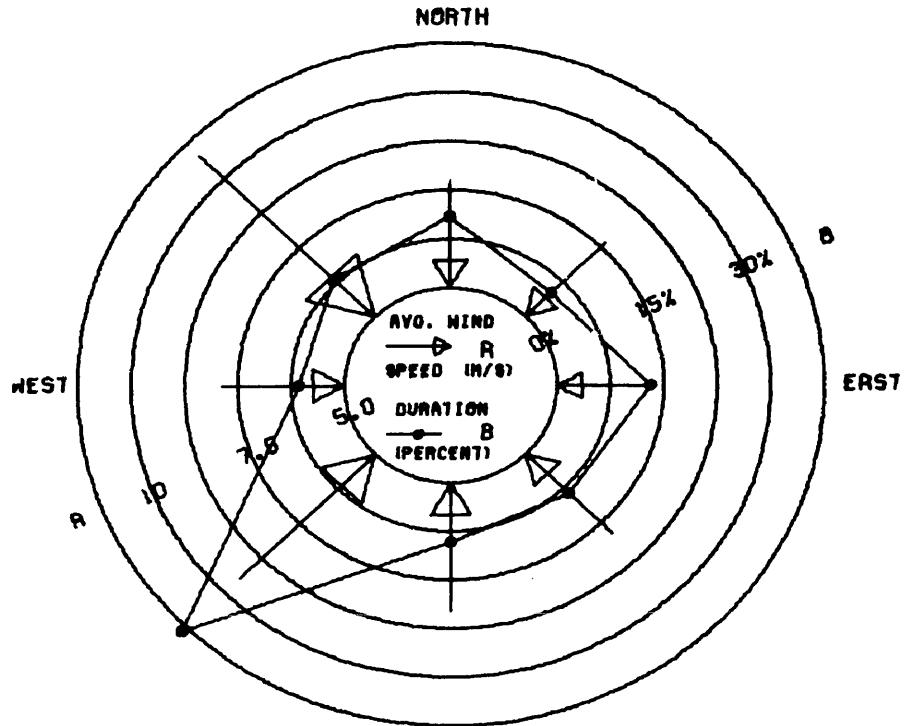


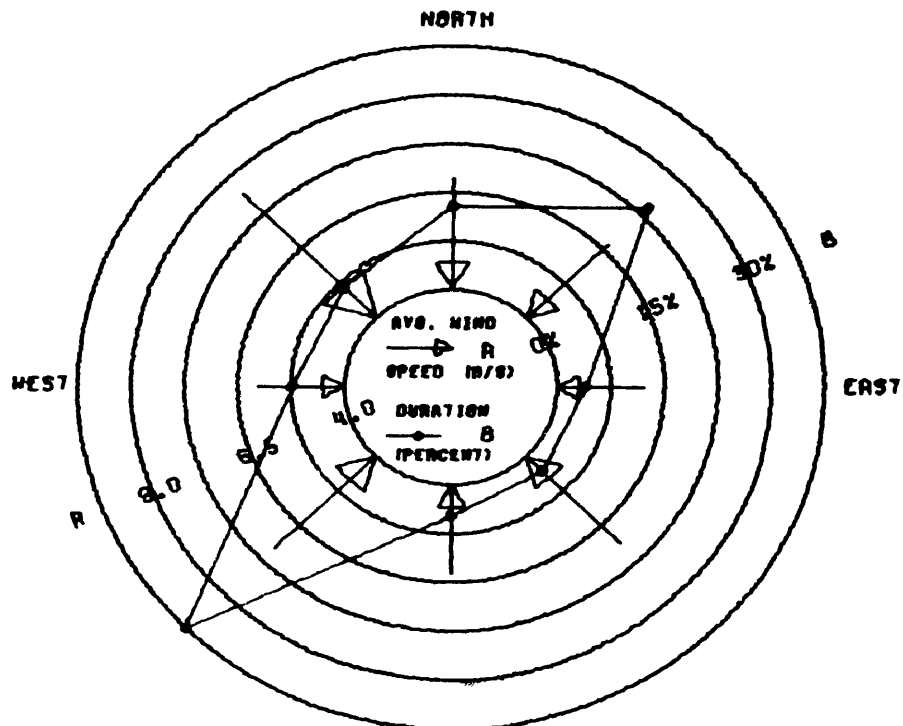
Figure 9. February 1976 wind rose diagrams.

COROLLA STATION
MARCH WIND ROSE



SOUTH
EXCLUDES WIND SPEEDS < 5.0 M/S

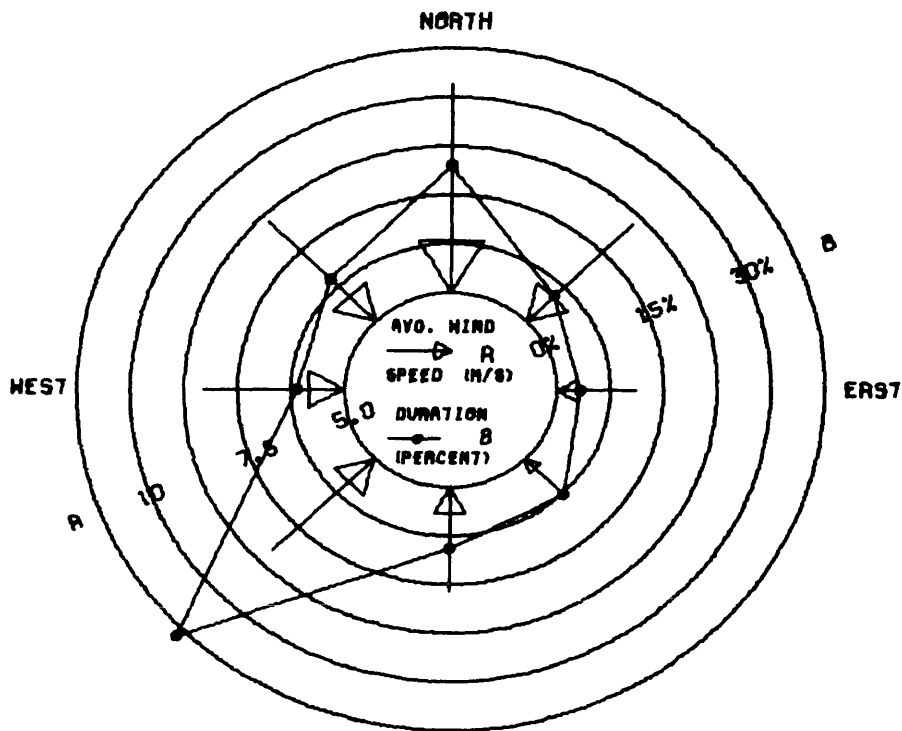
HATTERAS STATION
MARCH WIND ROSE



SOUTH
EXCLUDES WIND SPEEDS < 5.0 M/S

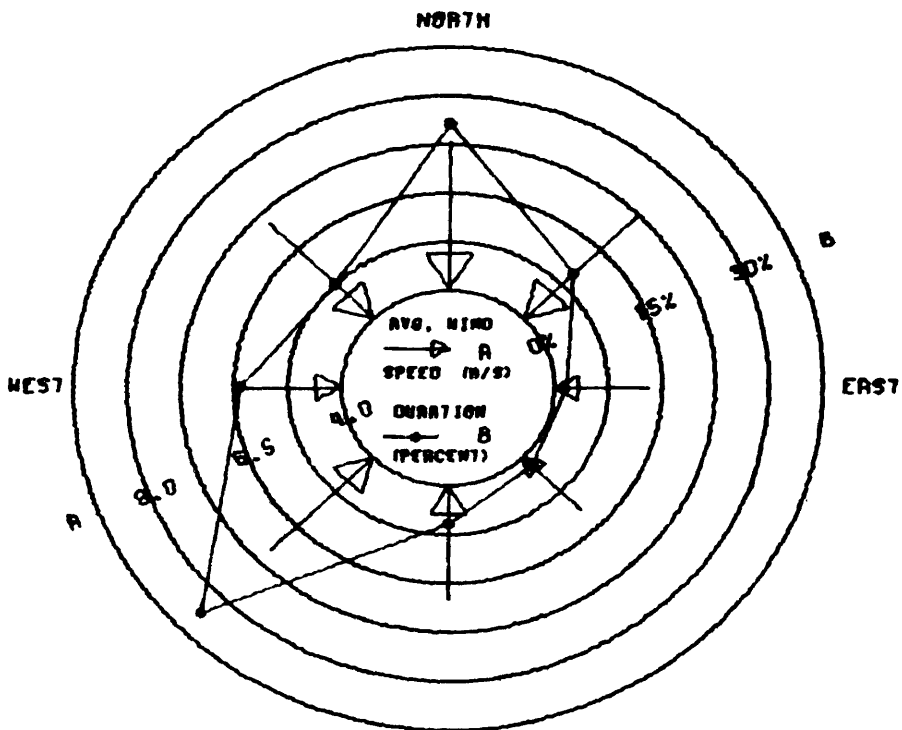
Figure 10. March 1976 wind rose diagrams.

COROLLA STATION
APRIL WIND ROSE



SOUTH
EXCLUDES WIND SPEEDS < 5.0 M/S

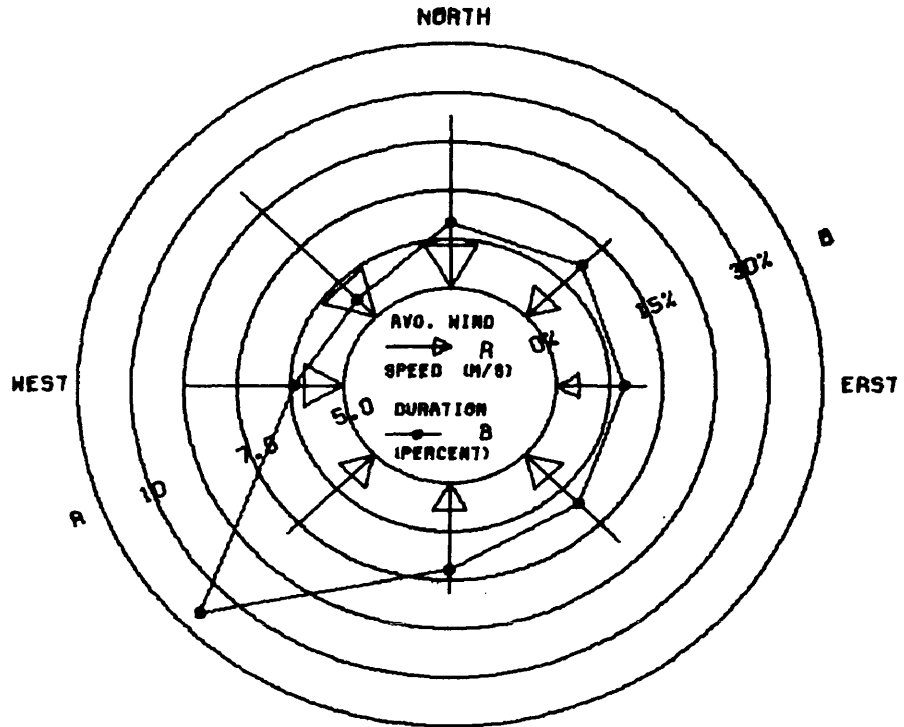
HATTERAS STATION
APRIL WIND ROSE



SOUTH
EXCLUDES WIND SPEEDS < 5.0 M/S

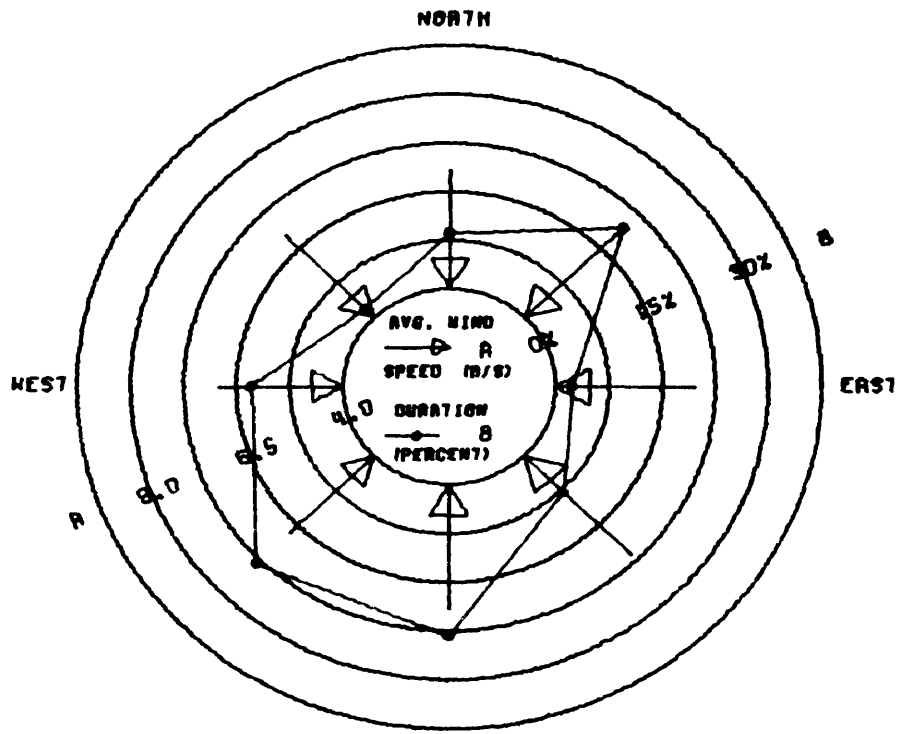
Figure 11. April 1976 wind rose diagrams.

COROLLA STATION MAY WIND ROSE



SOUTH
EXCLUDES WIND SPEEDS < 5.0 M/S

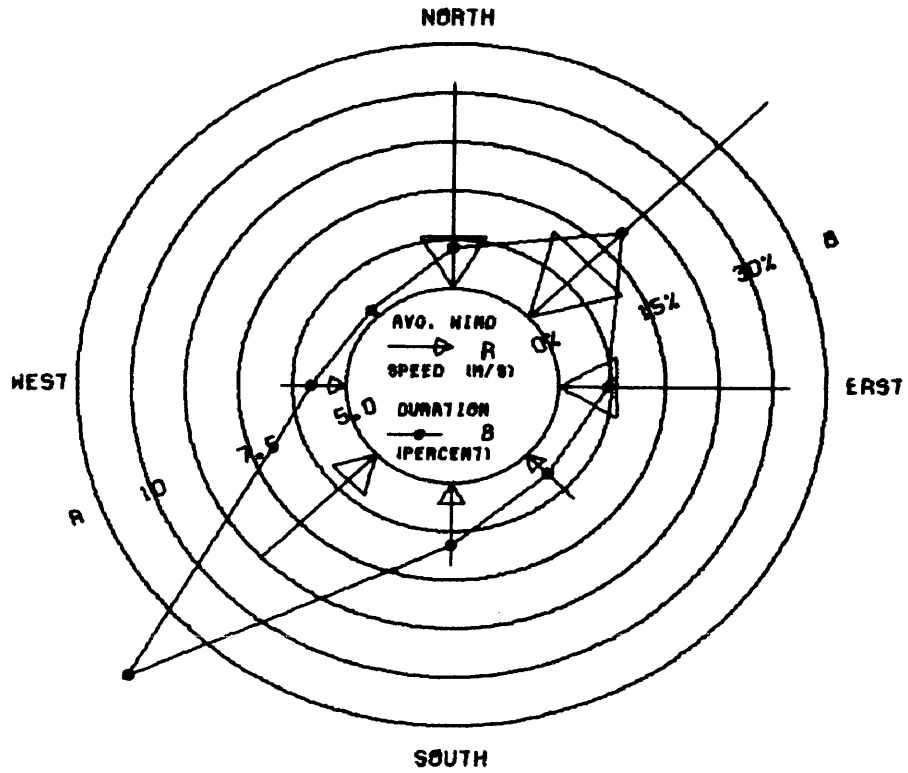
HATTERAS STATION MAY WIND ROSE



SOUTH
EXCLUDES WIND SPEEDS < 5.0 M/S

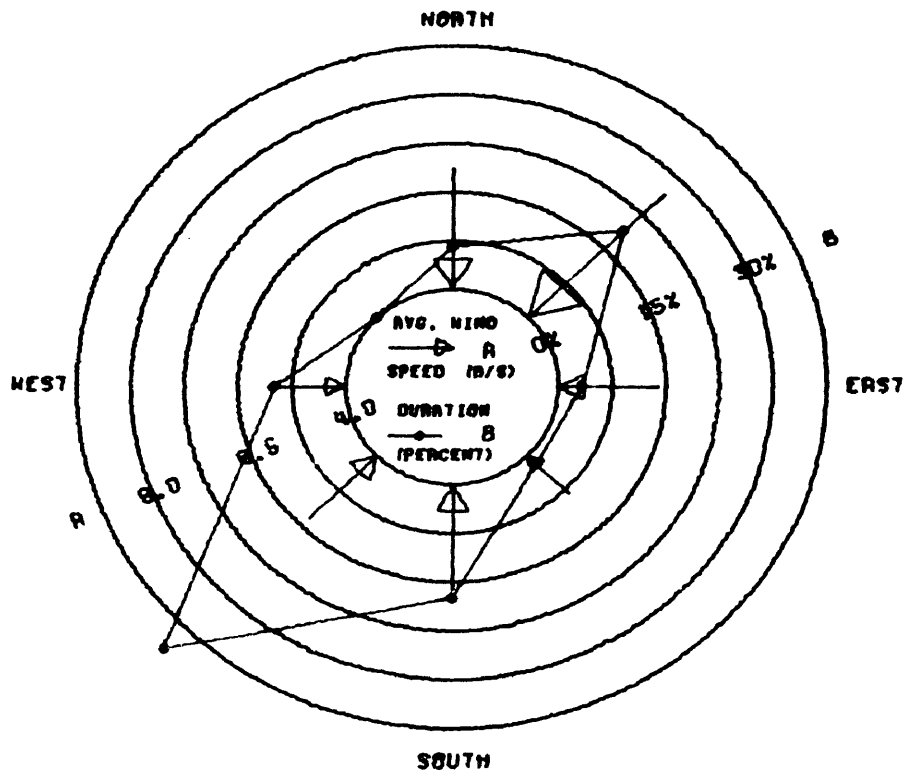
Figure 12. May 1976 wind rose diagrams.

COROLLA STATION JUNE WIND ROSE



EXCLUDES WIND SPEEDS < 5.0 M/S

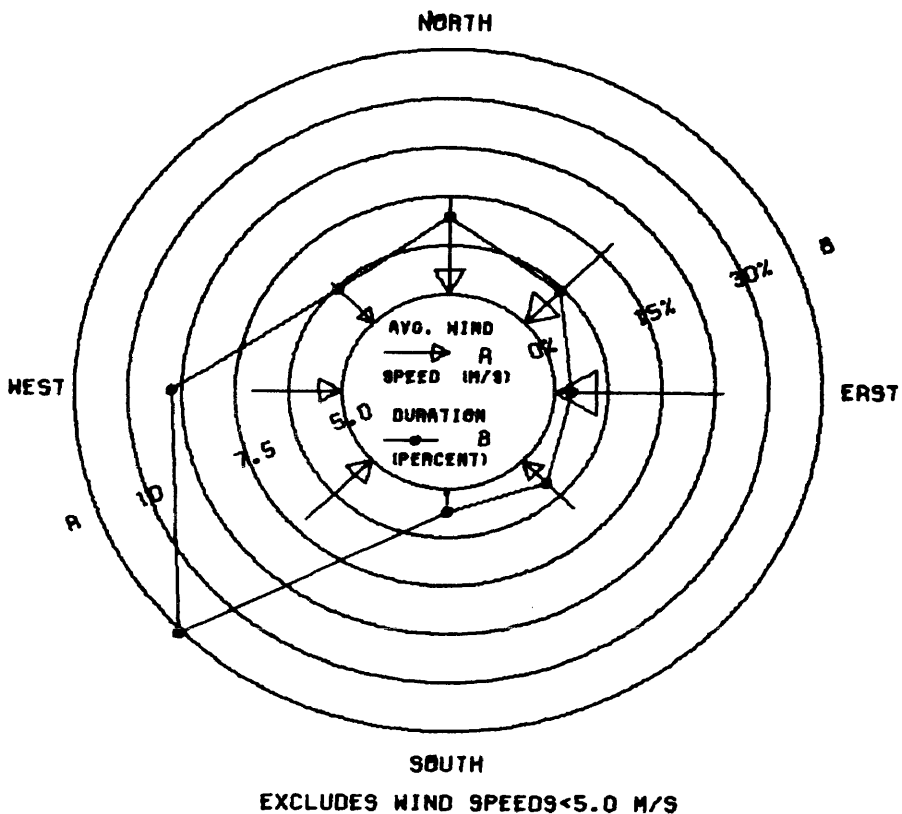
HATTERAS STATION JUNE WIND ROSE



EXCLUDES WIND SPEEDS < 5.0 M/S

Figure 13. June 1976 wind rose diagrams.

COROLLA STATION JULY WIND ROSE



HATTERAS STATION JULY WIND ROSE

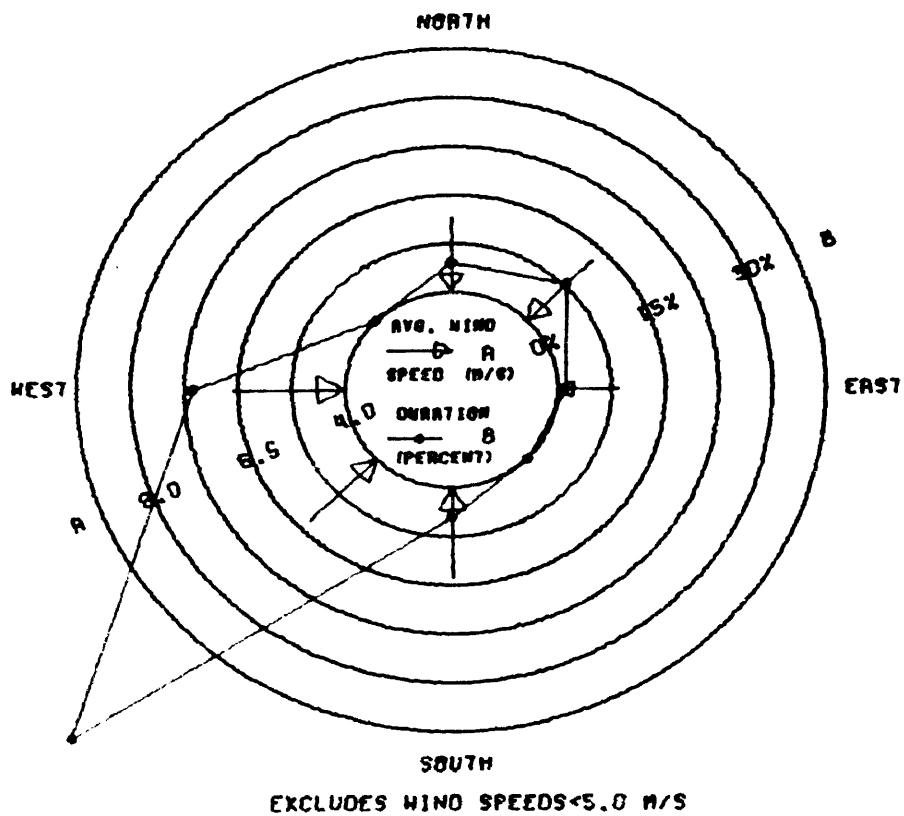
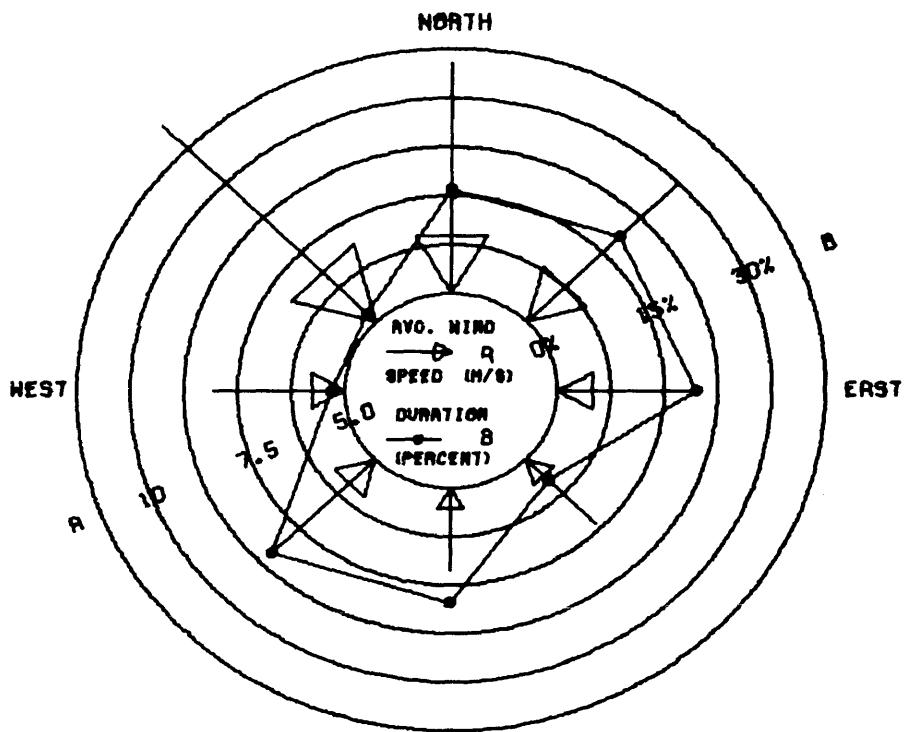


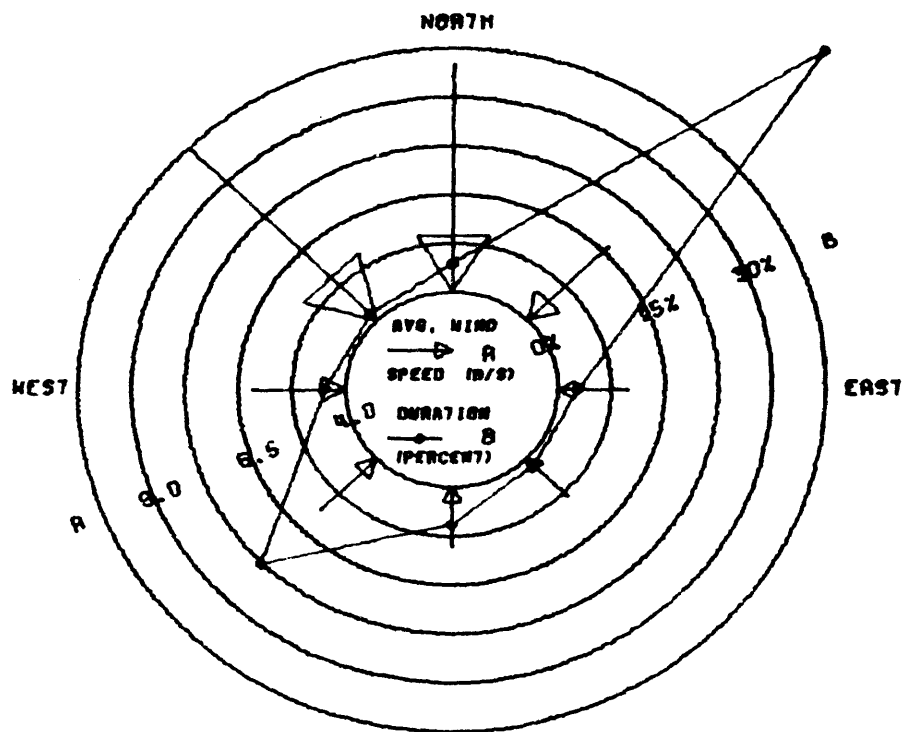
Figure 14. July 1976 wind rose diagrams.

COROLLA STATION AUGUST WIND ROSE



SOUTH
EXCLUDES WIND SPEEDS < 5.0 M/S

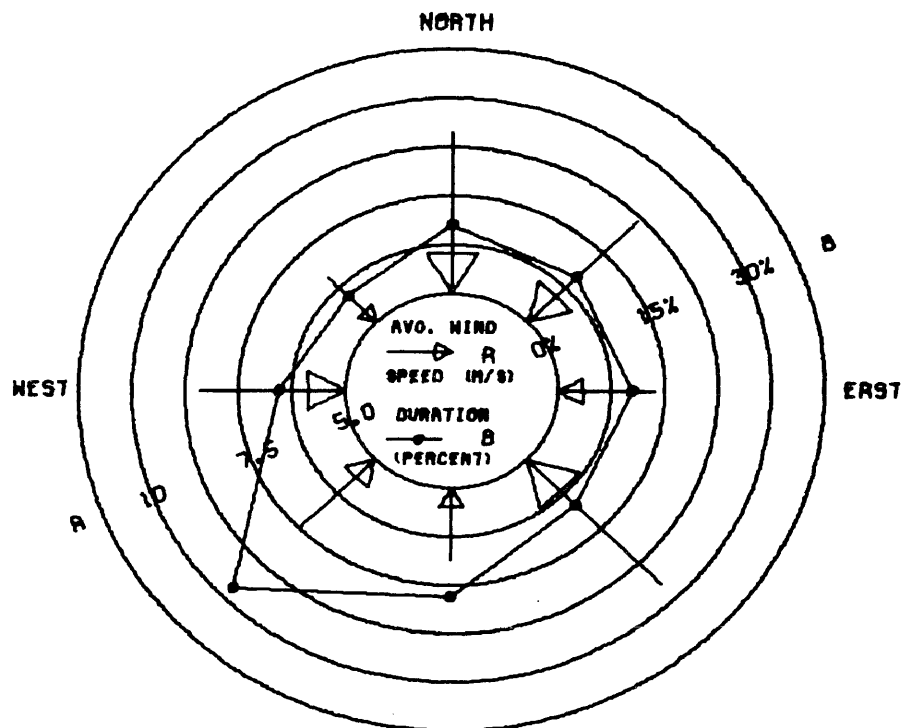
HATTERAS STATION AUGUST WIND ROSE



SOUTH
EXCLUDES WIND SPEEDS < 5.0 M/S

Figure 15. August 1976 wind rose diagrams.

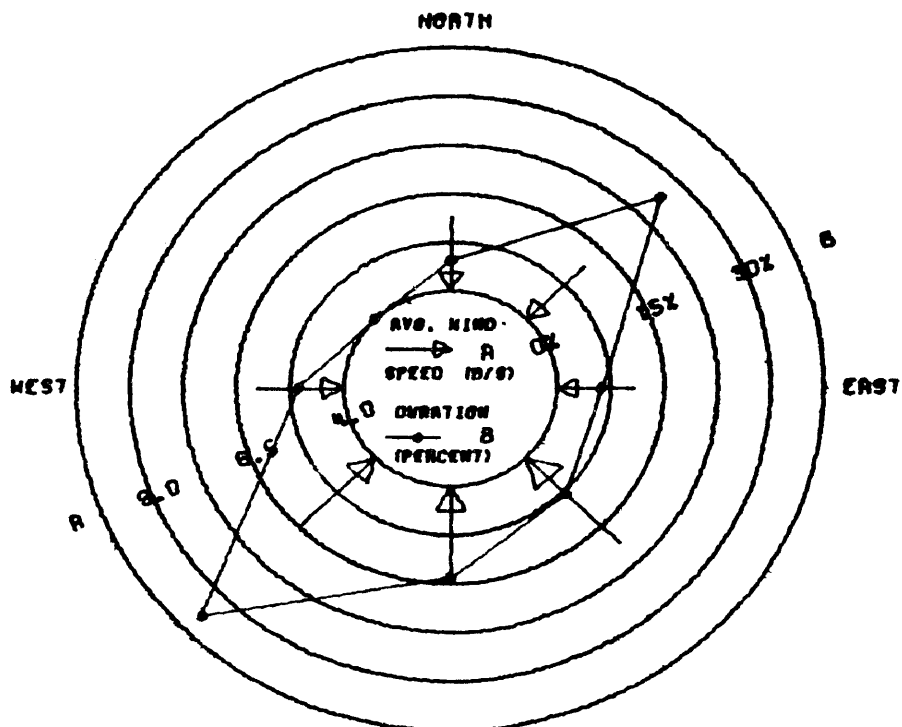
COROLLA STATION
SEPTEMBER WIND ROSE



SOUTH

EXCLUDES WIND SPEEDS < 5.0 M/S

HATTERAS STATION
SEPTEMBER WIND ROSE

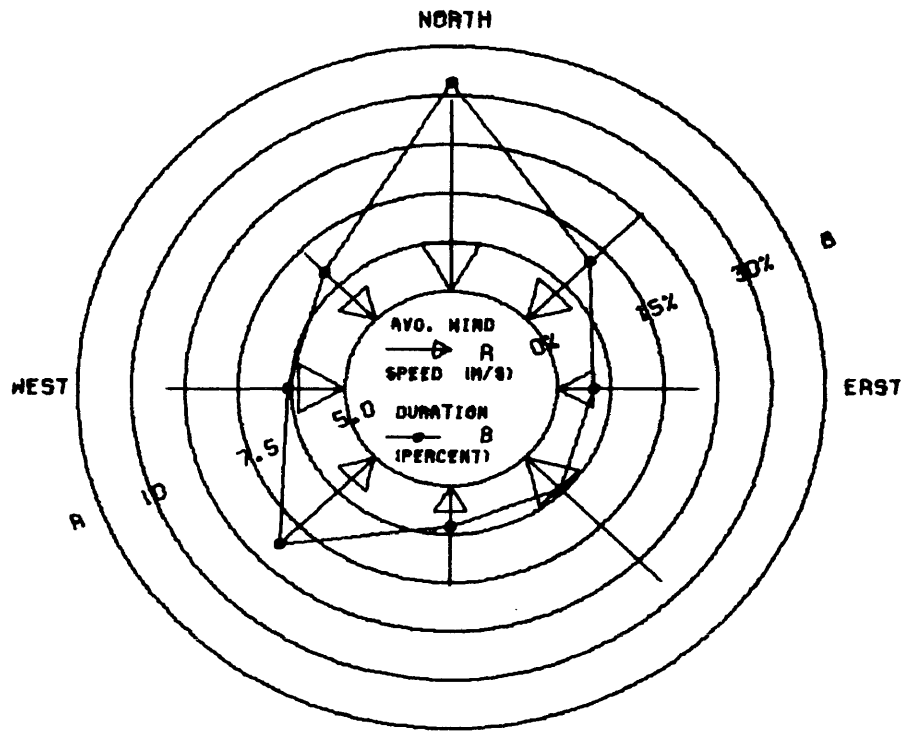


SOUTH

EXCLUDES WIND SPEEDS < 5.0 M/S

Figure 16. September 1976 wind rose diagrams.

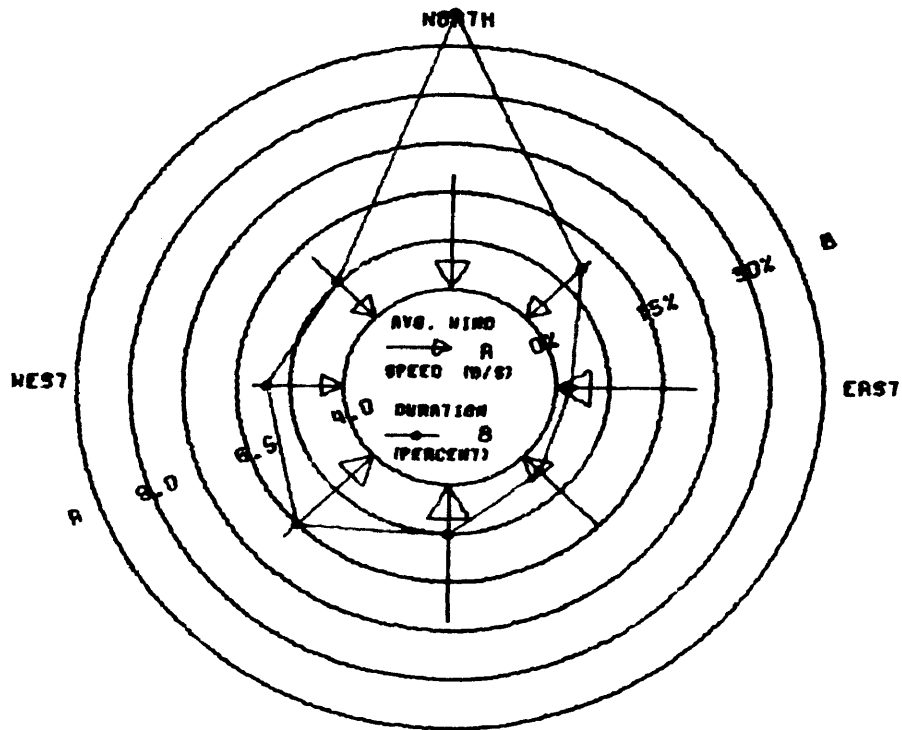
COROLLA STATION OCTOBER WIND ROSE



SOUTH

EXCLUDES WIND SPEEDS < 5.0 M/S

HATTERAS STATION OCTOBER WIND ROSE

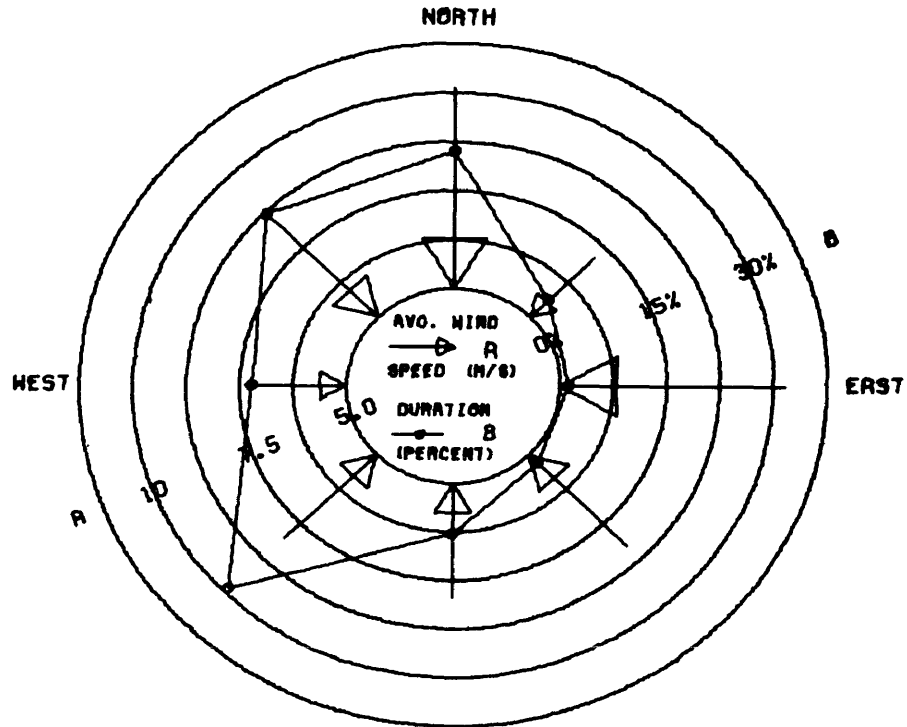


SOUTH

EXCLUDES WIND SPEEDS < 5.0 M/S

Figure 17. October 1976 wind rose diagrams.

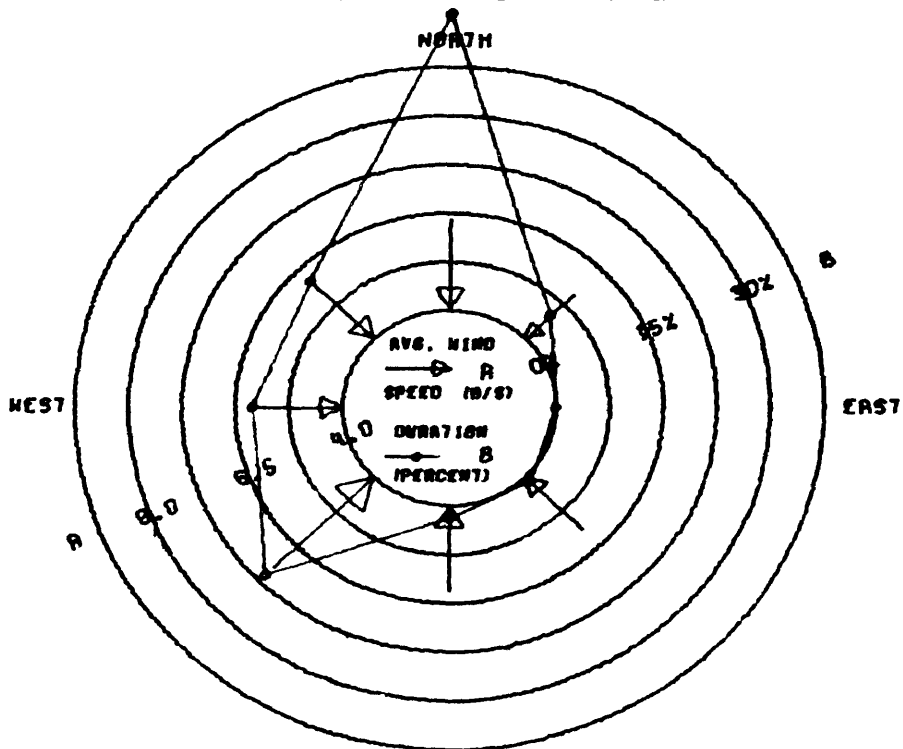
COROLLA STATION NOVEMBER WIND ROSE



SOUTH

EXCLUDES WIND SPEEDS < 5.0 M/S

HATTERAS STATION NOVEMBER WIND ROSE

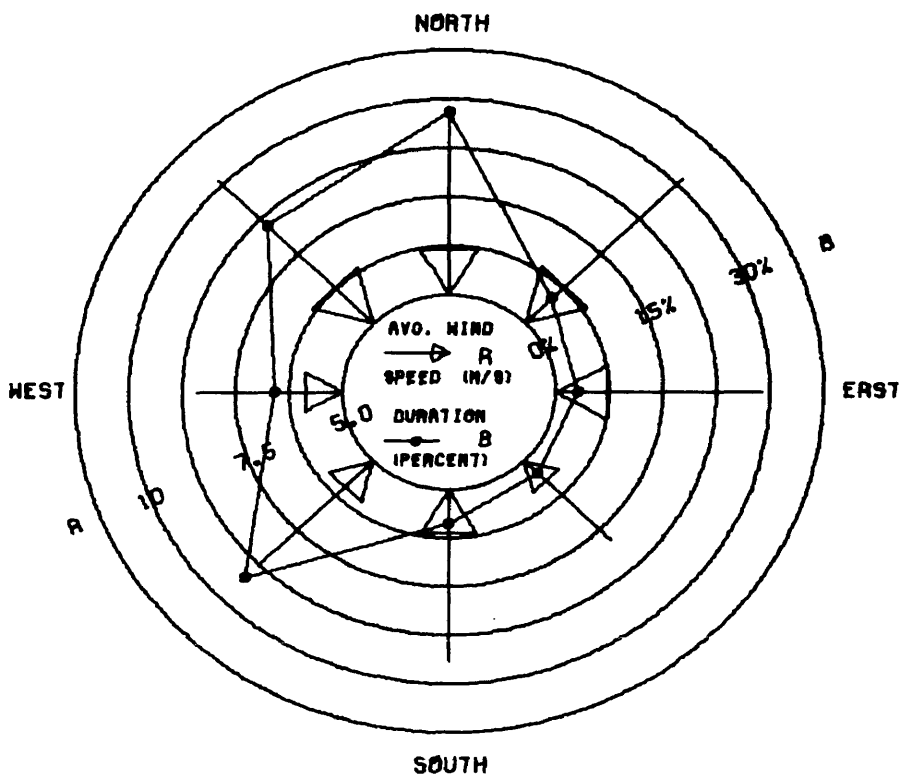


SOUTH

EXCLUDES WIND SPEEDS < 5.0 M/S

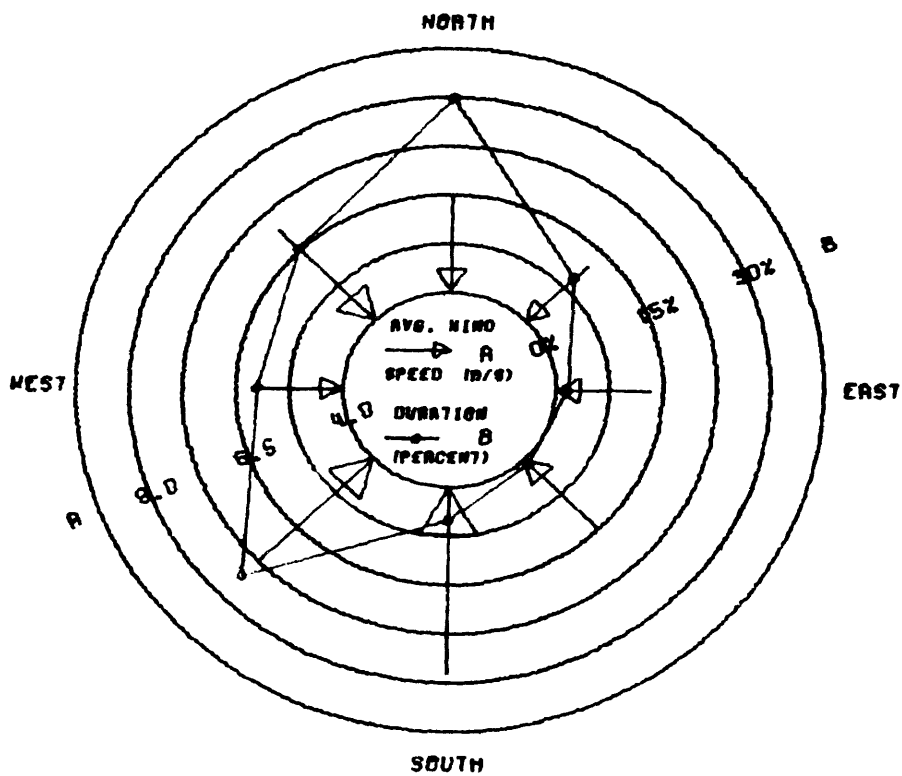
Figure 18. November 1976 wind rose diagrams.

COROLLA STATION
DECEMBER WIND ROSE



EXCLUDES WIND SPEEDS < 5.0 M/S

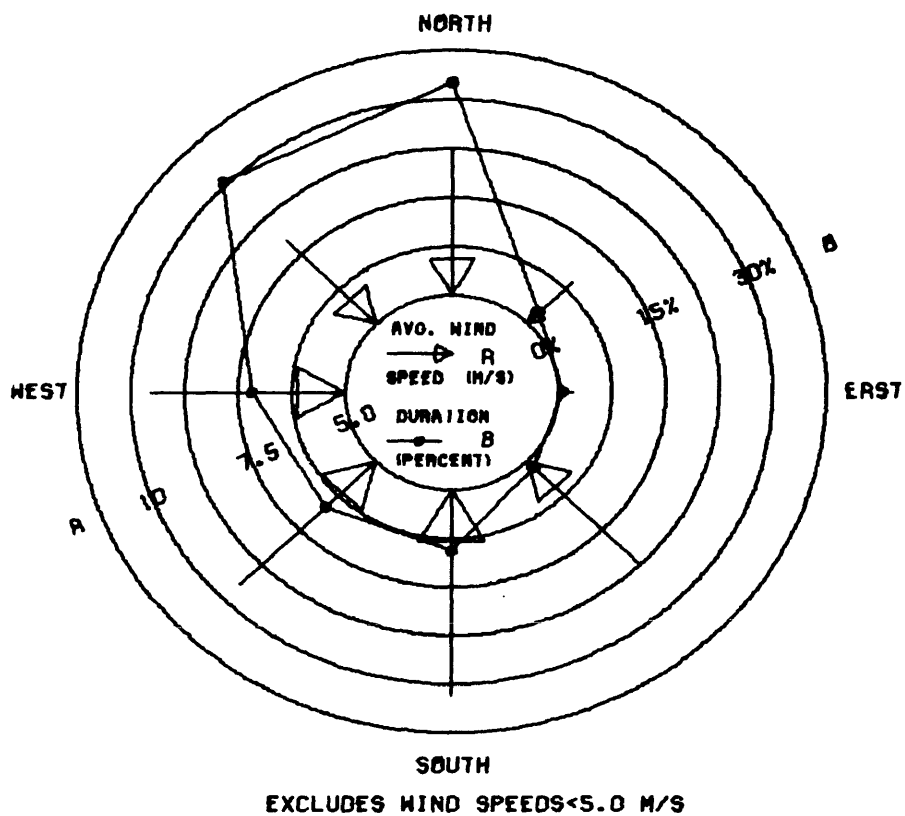
HATTERAS STATION
DECEMBER WIND ROSE



EXCLUDES WIND SPEEDS < 5.0 M/S

Figure 19. December 1976 wind rose diagrams.

COROLLA STATION
JANUARY WIND ROSE



HATTERAS STATION
JANUARY WIND ROSE

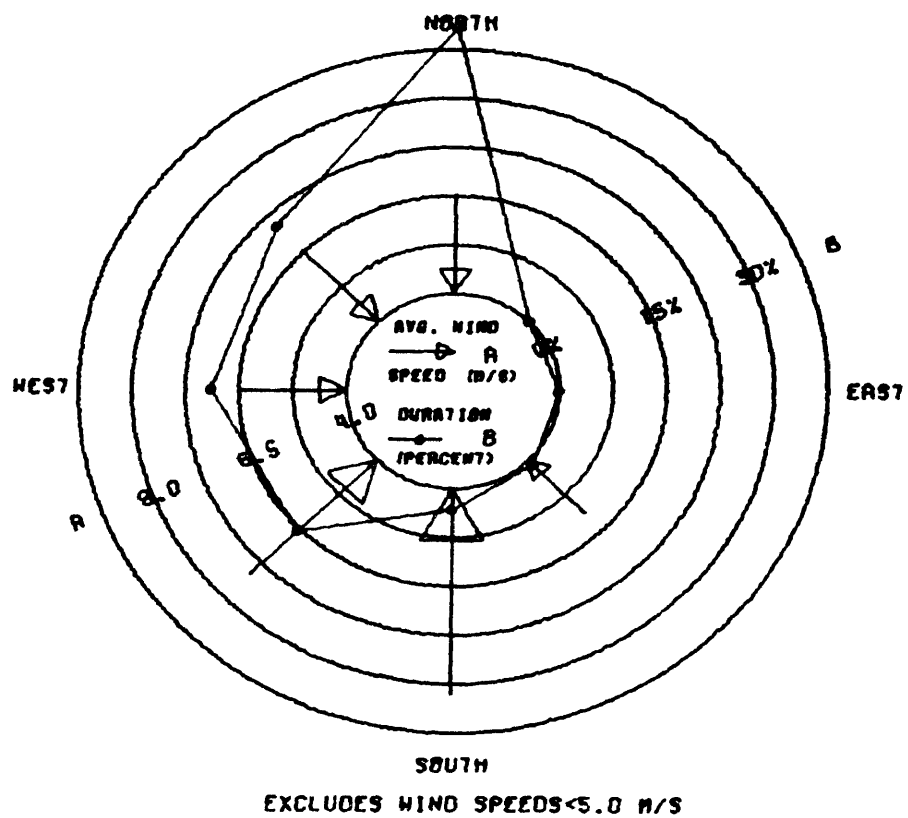


Figure 20. January 1977 wind rose diagrams.

application of these data it was necessary to investigate regional variation in wind characteristics to determine if the long-term Hatteras data were applicable to the local wind regime along Currituck Spit.

In order to determine if the wind regime measured at Hatteras and Corolla for an identical time period (2/76-2/77) was similar, an analysis of variance for paired comparisons using the t-test (Sokal and Rohlf, 1969) was conducted for the entire data sets from both stations. The t-test was chosen over others such as typical ANOVA tests because it allows for comparison of two time series of paired observations. The data from the two anemometers consists of a paired set of wind velocity and direction observations for each three hour interval throughout the one year period. The paired t-test compares each of these 2920 pairs (8/day for one year) while other tests compare one entire data set against the other.

In the paired t-test the difference between each pair of observations is compared with a hypothetical mean difference. The null hypothesis is that the mean difference between the two data sets is equal to zero.

Since the wind data consist of both wind velocity and direction observations, two tests were run on the data sets. The first comparison investigates if the wind speed measured at the two stations at each three hour interval for a one year period is similar. However, due to the difference in height of the two anemometers (53 m at Corolla and 6 m at Hatteras) a certain difference in the wind velocity measured at the two stations at the same time is expected. Since wind velocity theoretically varies as a function of the logarithm of elevation above

the surface the two data sets were compared after compensating for the theoretical effects of anemometer elevation.

To compensate for the expected difference in wind speed measured at two elevations a series of profile curves of wind speed vs. logarithm of height were plotted. A maximum wind velocity was arbitrarily selected (5,10,15,20,25 m/sec) for each profile at the 53 m level. A surface roughness (Z_0) of 5 cm was chosen. Since Z_0 is the elevation above the surface of zero wind velocity each profile was plotted to intersect the log height axis at 5 cm. From each profile could be read the expected wind velocity at 6 m based on an original velocity at 53 m. Then, the wind velocities at 6 m and 53 m were plotted on log-log paper. A graphical curve fitting method (Spiegel, 1961) was used to determine the equation of this line:

$$U_2 = .70 \times U_1^{.95}$$

where: U_2 = wind velocity at 53 m
 U_1 = theoretical wind velocity at 6 m based on a logarithmic relation of wind speed and height

Using this derived equation the theoretical wind velocity at 6 m for each three hour interval was calculated from the observed at 53 m (Corolla Station). This calculated wind speed was compared with the corresponding observation at Hatteras to examine if there exists a significant difference in wind velocity measured by the two anemometers due to factors other than that accounted for by elevations of the two anemometers.

The mean difference (\bar{D}) in wind velocity measured at 6 m (Hatteras) and calculated from an observed at 53 m (Corolla) was .17 m/sec. The standard error $S_{\bar{D}}$ of this mean difference was .28 m/sec.

The t-test to determine the significance of this mean difference yields:

$$t = \frac{.17}{.28}$$

$$= .61$$

For degrees of freedom greater than 120 the probability of a t value larger than .61 is greater than .50. This means that a t of .61 is exceeded more than 50% of the time in sampling from a population with a mean difference of zero. This test then provides no evidence to reject the null hypothesis. It is concluded then that apart from differences due to sampling heights of the two anemometers the wind velocity measured at Corolla for the one year period (2/76-2/77) is similar to that measured at Hatteras.

A paired sample t-test was also applied to the wind direction data. However, in this case there was no relationship assumed between wind direction and elevation above the surface. Therefore, for each three hour interval the wind direction (expressed from 0-360 degrees) at Corolla was subtracted from the wind direction at Hatteras. The mean difference (\bar{D}) in wind direction for the entire one year record was 10.6° with a standard error of 9.4°. Therefore, the t-test yields:

$$t = \frac{10.6^\circ}{9.4^\circ}$$

$$= 1.13^\circ$$

The t-tables indicate a probability of around .30 for this value. In most cases the null hypothesis that the difference is nonsignificant, would not be rejected for $p > .20$.

A qualitative analysis of the data also supports the conclusion that the mean difference between the wind direction at Hatteras and

Corolla is not significant. Close examination of the data showed no constant clockwise or counter-clockwise pattern to the wind direction difference. Subtracting one direction from the other gave 908 positive and 1026 negative differences out of the total of 2920 pairs (the remainder were zero, calm conditions, or missing data points). This tends to support the conclusion indicated by the statistical test because no pattern is evident. If most of the observations at Hatteras, for example, were 20° clockwise of those at Corolla a different conclusion might have been indicated.

It should also be noted that a mean difference of 10.6° is small considering the fluctuations during each three hour interval. Each data point represents an 'eyeballed' mean value for the interval. However the direction at any one moment can be 5-10 degrees different from this mean value.

Finally, remember that wind data are generally reduced by dividing the 360° into eight or twelve intervals (northeast, east, etc.). In many cases a difference of 10.6° would not cause the pair of data points to be grouped into different directions. Qualitatively these two data points separated by 10.6° would be equivalent wind directions.

In conclusion, the statistical and qualitative analyses of wind speed and direction data from the Hatteras and Corolla stations indicate that the two records are very similar although certainly not identical. There was variability in both the wind speeds and directions measured at the two stations but most of the difference in wind speed was accounted for by the elevation of the two anemometers. There was considerably more variation between wind direction pairs than with

wind speed, but the analysis supports the conclusion that the wind regimes monitored at the two stations are similar.

Comparison of yearly wind diagrams for the same 1976-1977 period for both stations indicate again a very similar wind regime. Figures 21, 22 and 23 are wind rose diagrams which were plotted for comparison with the corresponding Corolla diagrams (4, 5 and 6). Comparison of these plots for each station indicate only one important discrepancy. Notice in Figure 4 the northerly winds have the highest average wind speed while the Hatteras wind rose (Figure 21) indicates the lowest average wind speed for this direction. This discrepancy is also evident in comparisons of the wind rose diagrams for winds greater than 5.0 m/sec (Figures 5 and 22). However, Hatteras wind rose diagrams (Figures 24 and 25) compiled from 25 years of data indicate that the annual Corolla anemometer does reflect the true average velocity of these northerly winds. Figures 24 and 25 both indicate that one of the highest average velocities is associated with northerly winds.

Long Term Wind Regime

One year of wind data from the Corolla station anemometer was compiled into a detailed monthly, seasonal, and yearly wind climate for Currituck Spit. This wind climate, as discussed in the following section, became the basis for investigation of the development, orientation, and migration of sand dunes, and the net flux of sand across the barrier spit due to wind transport. From comparisons of the Hatteras and Corolla wind data for the same one year period it was concluded that the long term Cape Hatteras wind climate compiled from 13 years of data could be compared directly with the Corolla wind climate determined from only one year of data. Unfortunately

2/76-2/77
 HATTERAS STATION
 WIND ROSE

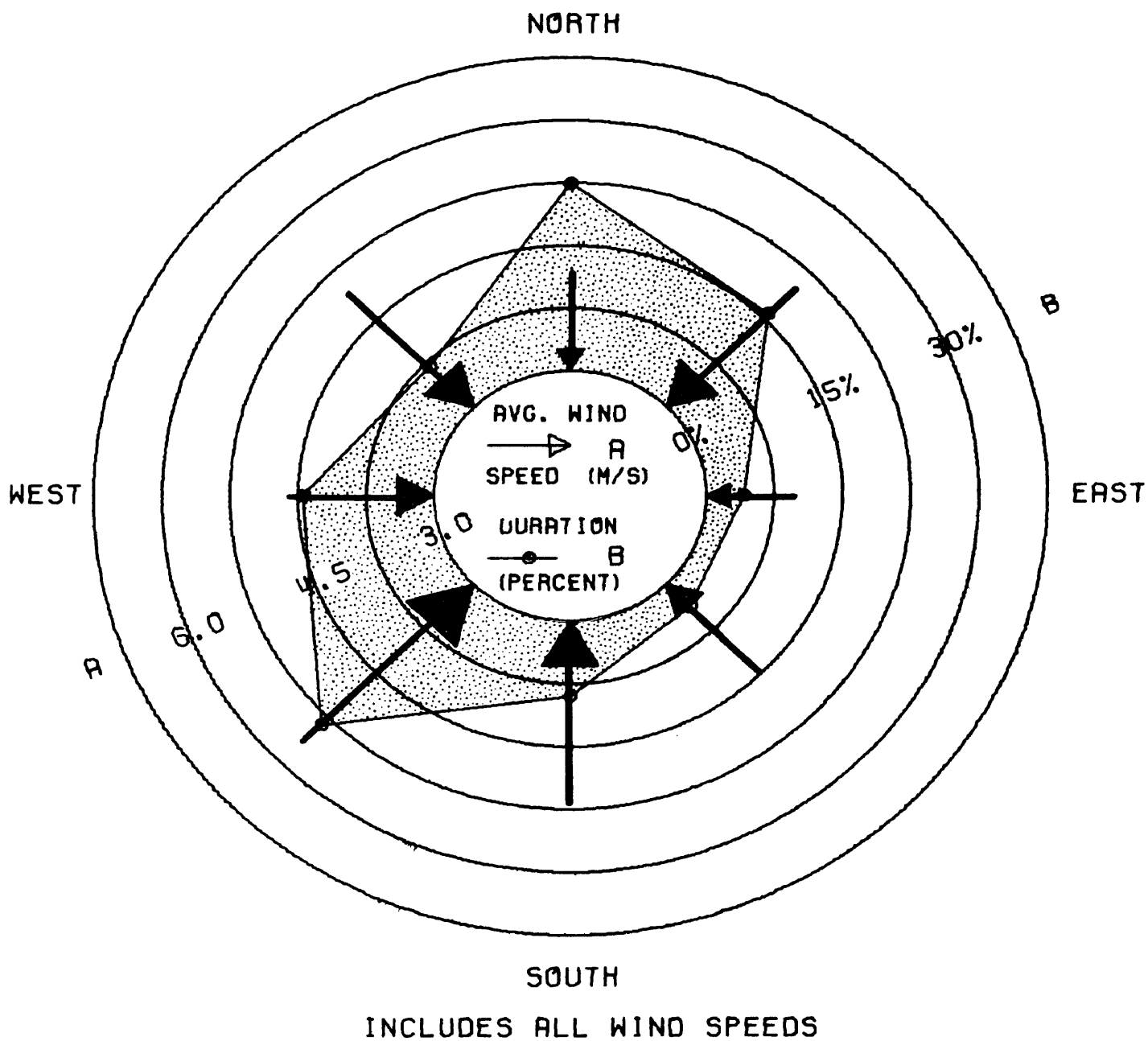


Figure 21. Hatteras station wind rose (February 1, 1976 to January 31, 1977) for all wind speeds.

2/76-2/77 HATTERAS STATION WIND ROSE

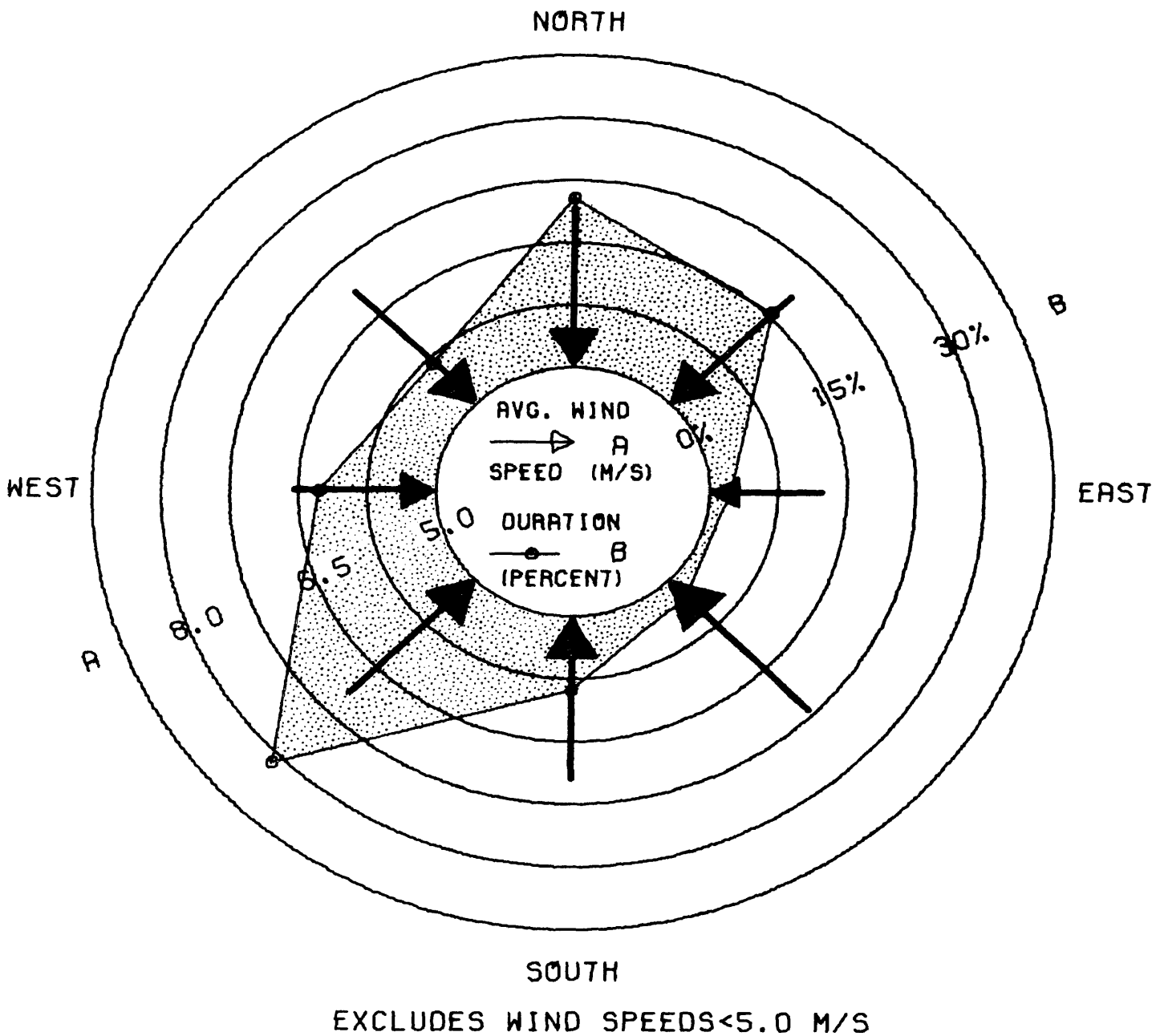


Figure 22. Hatteras station wind rose (February 1, 1976 to January 31, 1977) for all wind speeds greater than 5.0 m/s.

2/76-2/77 HATTERAS STATION WIND ROSE

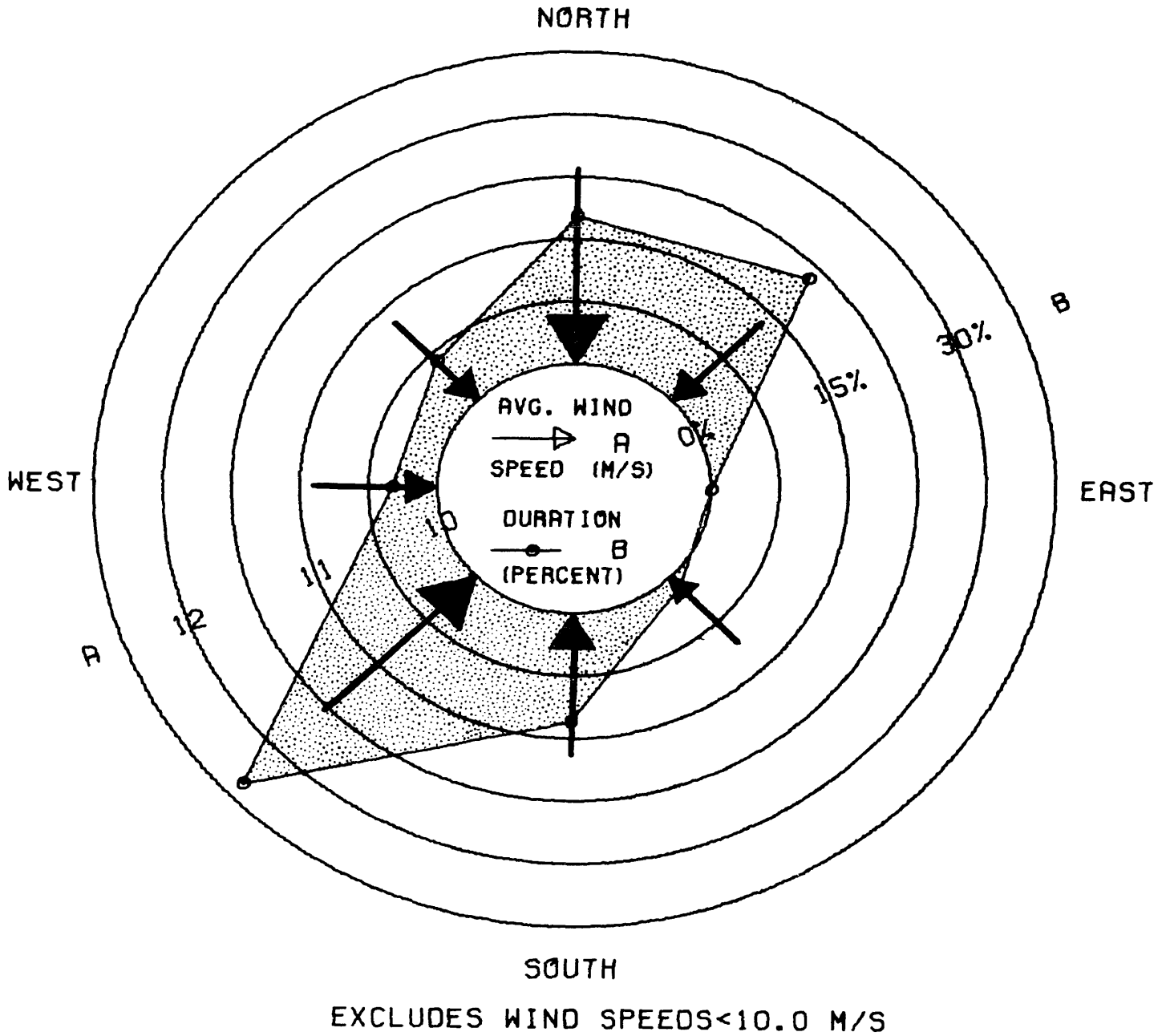


Figure 23. Hatteras station wind rose (February 1, 1976 to January 31, 1977) for all wind speeds greater than 10.0 m/s.

only a visual qualitative comparison was possible since the 18 years of data from Cape Hatteras were unavailable for statistical tests of similarity.

Figures 24 and 25 cover the period 1953-1957 and 1956-1970, respectively. These figures show again a polymodal wind regime with modes in the northeast, north, northwest, and southwest with the highest average velocities from the northerly directions and the south. This appears to be essentially the same wind climate determined from the one year of Corolla data, and the local one year wind climate determined from a limited amount of data should represent a typical year. Therefore the conclusions, based upon this local one year record are applicable to the typical long term dune and sediment dynamics of the spit.

Conclusions

1. A detailed wind climate was determined for Currituck Spit from compilations of monthly, seasonal, and yearly wind data from a local source (one year of data) and a nearby source (18 years of data).
2. The wind regime at Currituck Spit is polymodal, with prevailing winds from the north and southwest, and dominant winds from the northeast, north, and northwest.
3. The highest frequency occurrence of winds (including all winds) is from the southwest (32%) while the northerly winds had the highest average velocity (8.0 m/sec).
4. There was no obvious seasonality with regard to the mean wind speed or frequency of occurrence of winds greater than 5.0 and

1953-1957 HATTERAS STATION WIND ROSE

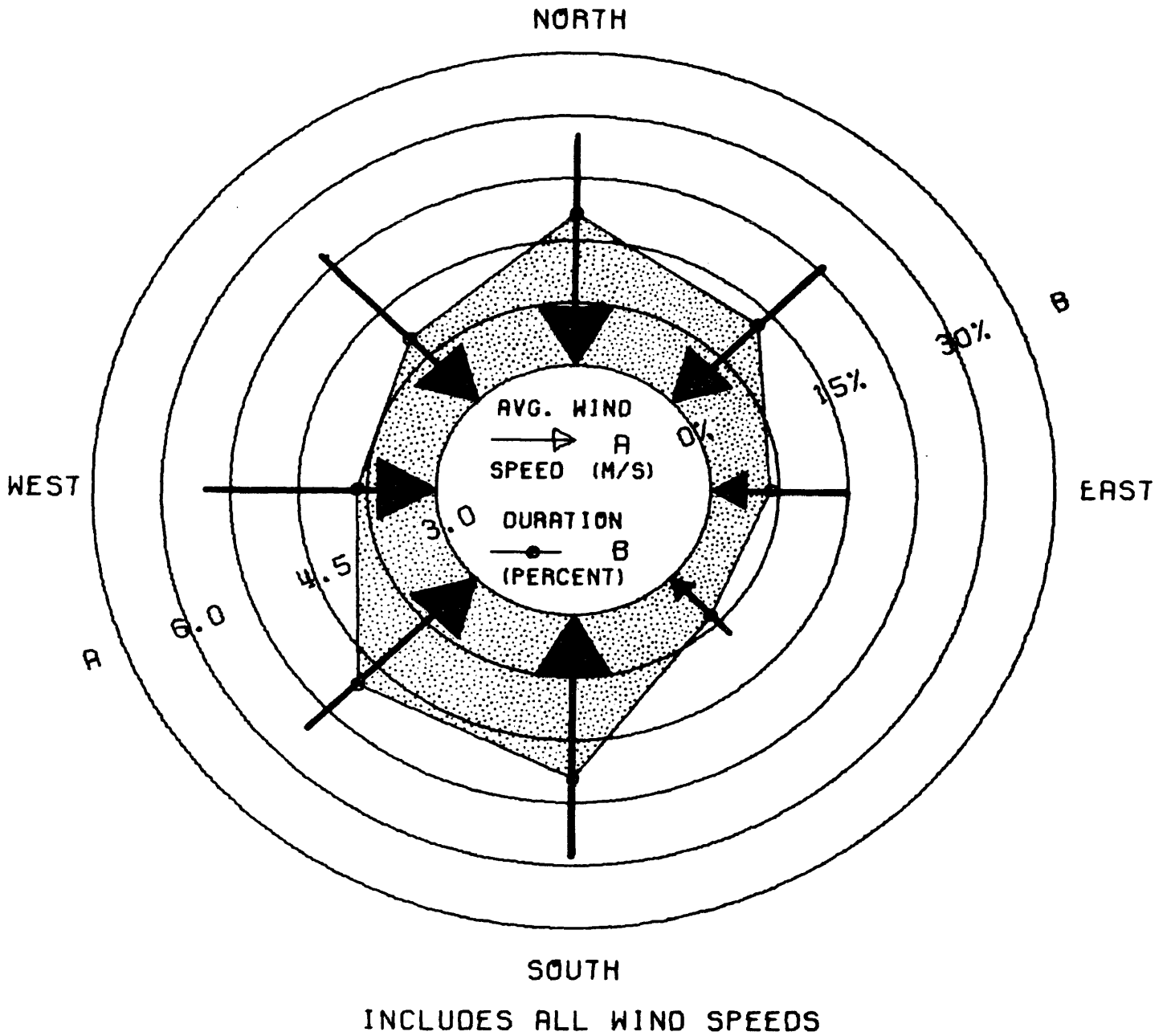
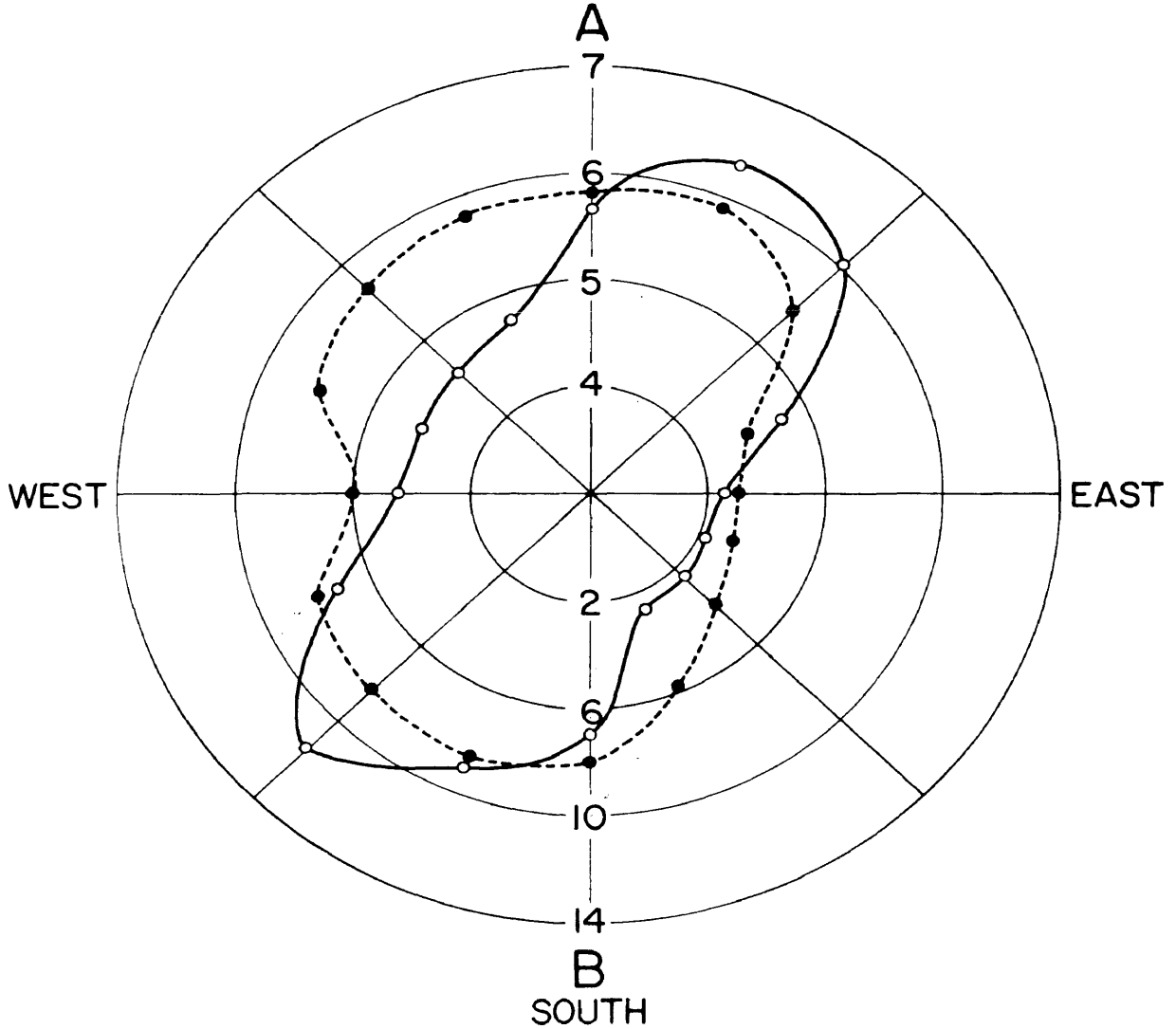


Figure 24. Hatteras station wind rose compiled from five years of Corps of Engineers wind data (1953-1957).

WIND DIAGRAM CAPE HATTERAS, N. C. [1956-1970] NORTH



A ---◆--- AVERAGE VELOCITY (METERS PER SECOND)

B —○— DURATION
(PERCENTAGE OF TIME BLOWING FROM)

Figure 25. Hatteras Station wind rose compiled by NOAA Environmental Data Service from fifteen years of data (1956-1970).

10.0 m/sec. Instead there was a long period of high velocity winds (October-June) and a shorter low velocity period (July-September).

5. Statistical comparison of the one year Corolla Station wind data with data for the same period from the Cape Hatteras Weather Station indicates very little variation in wind regime between the two stations separated by 115 km.

6. The long term wind regime compiled from 18 years of Cape Hatteras data was found to be very similar to the wind regime determined from one year of Corolla wind data. Therefore this detailed monthly, seasonal, and yearly wind climate is representative of the local long term wind regime. This conclusion lends credence to the following sections which relate this one year local wind climate and concomitant field data, to the long-term interaction of eolian sand transport, vegetation, and sand dunes, as evidenced by the flux of sand across the barrier spit and the development, orientation and migration of large sand dunes.

MOVEMENT OF LARGE SAND HILLS

Large sand dunes, or medianos (10-25 high), represent a significant amount of sand removed from the longshore transport system. Such dunes are found along Currituck Spit between False Cape, Virginia and the Duck Research Facility, North Carolina (Figure 1). Many of these large dunes are migrating landward towards the southwest, obliquely across the barrier island. These dunes are significant in terms of the sediment budget of the spit and also due to their effects on development in the area.

Mobile dunes in the area are notorious for interfering with and often destroying towns, roads and forests. Henry Lathrobe, Esq. (1814), referring to the Cape Henry area, warned that these mobile dunes would eventually "swallow up the whole swamp, and render the coast a desert indeed, for not a blade of grass finds nutriment on this sand". Though the mobile dunes are still a problem 163 years after Lathrobe wrote these words, the coast of Virginia-North Carolina is not a desert. Aerial photographs have, in fact, shown a trend of increasing vegetation since the 1930's, with a concomitant decrease in the amount of shifting sands. The largest increase in vegetation seems to have occurred in False Cape, the northern part of the study area.

False Cape State Park is characterized by a large variety of eolian features including relatively high (2-4 m), continuous, multiple foredune ridges, thick shrub vegetation across the eolian flat, stabilized parabolic dunes (5-10 m high) with axis' uniformly

oriented to the north, several large (15-20 m) mobile dunes or sand hills (i.e., medianos), and a maritime forest which is presently being invaded by the mobile dunes.

The area near Corolla, North Carolina is quite different than False Cape approximately 30-40 km to the north. Here there is a lower (1-3 m), non-continuous foredune ridge, only sparse dune vegetation across the eolian flat, and large medianos (10-25 m) which are highly mobile and temporally varying in orientation. These dunes are also invading a maritime forest on the bay side.

Migration Rates

The migration rates of large dunes on Currituck Spit are useful data for evaluating the role of dunes in the sediment dynamics of the spit, the effect of the differences between the northern and southern regions, and for predicting the problems which will occur after development in the terrain surrounding these mobile dunes. Dune migration rates can be determined from studies of aerial photographs, maps and ground measurements. Air photos provide a longer record of migration rates than field measurements, though the rates from air photos may represent an average for a number of years rather than an actual rate for each of the years. Given the increase in vegetation over the last thirty years a rate determined from old photographs should represent a faster mean rate than expected today. Figure 26 shows a typical large dune in Currituck Spit and its migration since 1961. Over 16 years, the dune has moved south-southwest obliquely toward the bay at about $8 \text{ m} \pm 0.6 \text{ m}$ per year (accuracy of these measurements is discussed in detail by Hennigar, 1978). Accuracy depends on the photo-



Figure 26. Distance travelled by Whalehead Hill (1:6000 scale).
1961-1977

scale, and suffers in comparing dune movements in this area because it is free of landmarks. Table 2 lists migration rates determined by other investigators for coastal dunes throughout the world. To determine the actual present yearly migration rate, measurements must be made in the field.

In February of 1976, reference markers were placed around the perimeters of Whalehead Hill (Figure 27) located just south of Corolla, and Barbours Hill (Figure 28) located at False Cape, Virginia. Both sand hills are approximately 15-20 m high with active slipfaces (5.5 m in height) oriented approximately west-northwest - east-southeast, and advancing to the south-southwest. Nine other sand hills south of Whalehead Hill show an approximate uniformity in height and spacing, therefore, suggesting that the migration rate measured for Whalehead Hill is typical of the sand hill field to the south.

Figure 29 shows a schematic illustration (not to scale) of the net 12 month movement of the two dunes between February 1976 and February 1977, as measured by the difference to the control points. This distance can be determined accurately only at the slipface, for only there does the sand hill show a line of demarkation between the dune and the surrounding terrain. On all other flanks the dunes grade slowly into hummocks and small dunes, making measurement difficult. In addition, only the slipface movement indicates a migration of the entire dune. Extensions along the other flanks reflect sand being blown off the dune and onto the surrounding eolian flat. Cross movements of the dune occur in all directions. However along the slipface there is a steady (determined from aerial photos and field measurements) net movement.

TABLE 2
 ANNUAL RATE OF COASTAL SAND DUNE MOVEMENT
 AT VARIOUS LOCATIONS THROUGHOUT WORLD

from Pickard (1968)

Location	Rate (m/year)	Source
Coast of France	9.1	Salisbury, 1952
Lancashire, U.K.	5.5-7.3	Salisbury, 1952
Newborough, Warren, U.K.	1.5-3.1	Ranwell, 1958
Lake Michigan, U.S.A.	2.0-4.0	Ranwell, 1958
Cronulla, Australia	8.0-9.0	Pickard, 1968

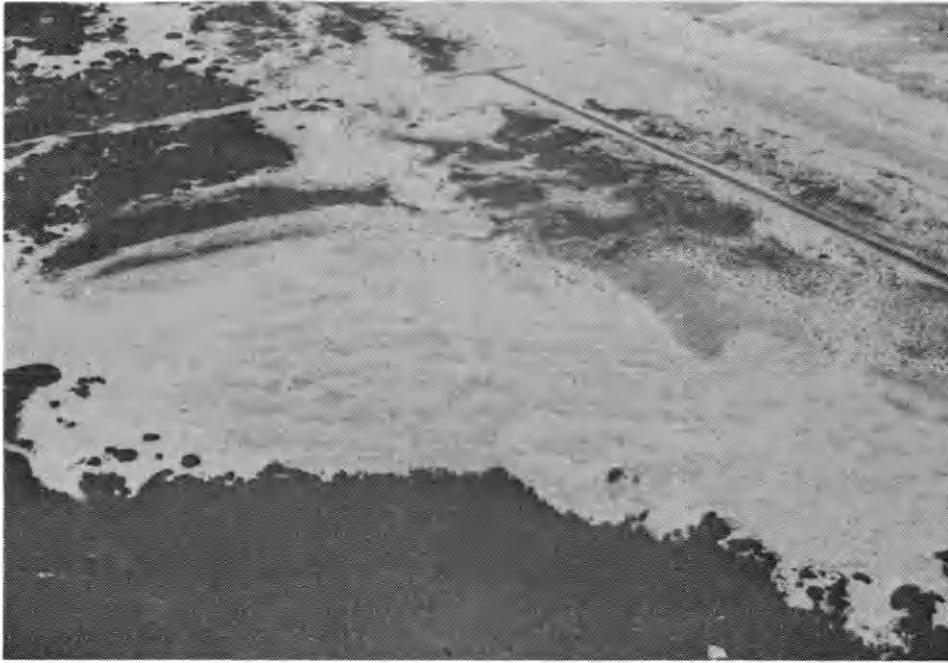


Figure 27. Whalehead Hill Medano looking southwest (top, October, 1976) and southeast (bottom, March 1977). The slipface, 5.5 m high, has migrated 6 m/year to the south-southwest (1976-1977)

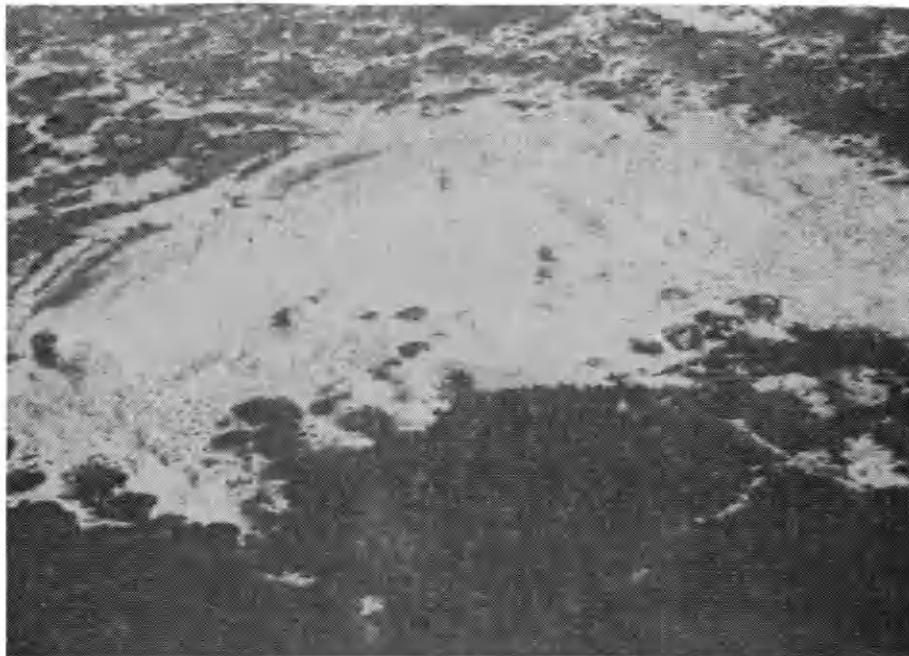


Figure 28. Aerial views of Barbour Hill looking northeast (top, January, 1975) and southwest (bottom, April, 1976). Note extensive vegetation surrounding sand hill.

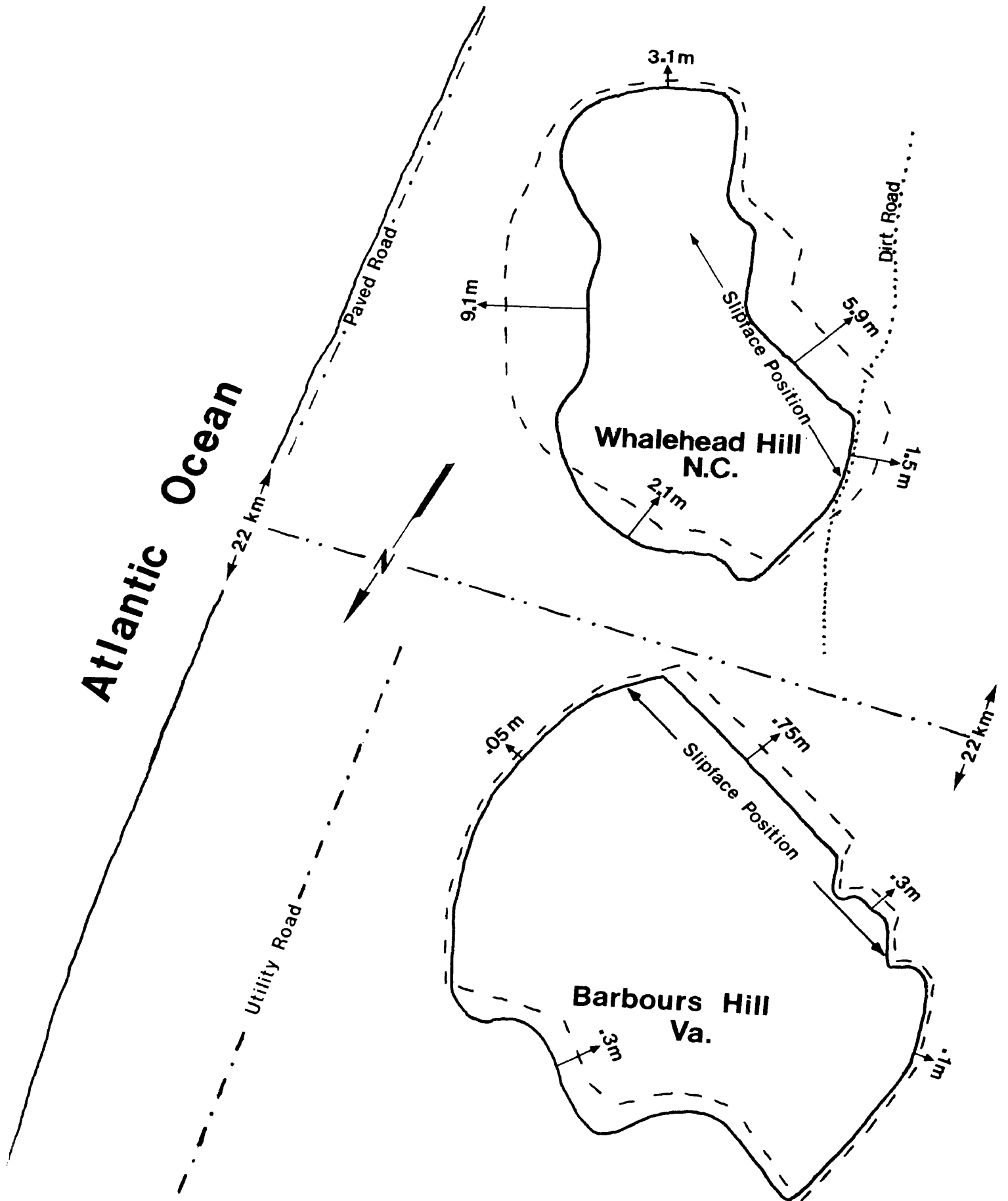


Figure 29. Schematic illustration of the movement of two large sand hills (Feb. 1, 1976 to Jan. 31, 1977). Dashed line indicates new dune position.

Figure 29 shows that the south-southwest movement of Whalehead Hill, as measured at the slipface, was eight times greater than the Barbours Hill rate (6 m as opposed to 0.75 m). At Whalehead, a lobe with a low (2 m) slipface marched about 1.5 m across an old unpaved road. This movement was particularly evident since travel past the dune along the road, which at the start of this study in 1976 was possible, is now no longer possible (Figure 30). Notice also that the largest net change occurred on the east flank of Whalehead Hill, which showed a movement of some 9 m over one year.

As evident in Figure 4, the highest wind duration was from the southwest. It is not surprising then that the east flank of Whalehead Hill showed a net lateral accretion of 9 m derived from sand blowing off the dune onto the adjacent flat. This movement of Whalehead Hill is particularly significant considering that the new paved road leading to Corolla is located only 100 m farther to the east of the dune. On many occasions this new (1975) road has been covered by sand blowing off the large medianos during strong westerly winds (Figure 31).

Northern and Southern Differences in Migration Rate

The present rate of south-southwest migration of Whalehead Hill is approximately 6 m/year while at Barbours Hill this rate is less than 1 m/year. Old aerial photographs (Figure 26) indicate that the migration rate of Whalehead Hill, which has averaged 8 m per year over the last 16 years, was considerably greater in the past. These past-present and north-south differences are evident even though the dunes are very similar in size (approximately 17 m high and 200 m across), the height of the slipface in both cases is about 5.5 m,



Figure 30. Eolian transport of sand off of Whalehead Hill covering paved road to the east (top).



Figure 31. Slipface of Whalehead Hill advancing to the southwest covering dirt road (bottom).

and these dimensions have not changed much in the past 16 years. Therefore other factors must account for the large differences in migration rate.

The migration rate of large dunes is controlled by sand transport, anchoring vegetation, and the wind regime. Sixteen years ago (Figure 26) there was only scarce vegetation to the east and north of Whalehead Hill to impede sand transport. Therefore, the dune moved at the maximum rate possible under the existing wind regime of the area.

However, when vegetation colonizes the eolian flat and a foredune system is formed, the surface roughness upwind of the dune increases and the wind velocity over the dune crest decreases. This will cause the dunes to decrease their rates of migration. Vegetation colonization has proceeded farther at False Cape than at Corolla (Figure 28). A stable multiple-ridge foredune system has effectively cut off sand transport to the interior allowing thick shrub vegetation to colonize the eolian flat. Dune grasses have colonized much of Barbours Hill, further slowing its advance.

Sand transport measurements (detailed and discussed in a later section) illustrate this effect of vegetation colonization. During 15 m/sec onshore winds a zero transport rate was measured across the eolian flat to the east of Barbours Hill. During the same 15 m/sec onshore wind conditions the transport rate across the eolian flat at Whalehead Hill was 0.2-.3 g/cm·sec. In the Whalehead Hill region there are only low, discontinuous foredunes, little eolian flat vegetation, and therefore a greater flux of sand between the beach and the sand hill (compare Figures 27 and 28). No vegetation has colonized

Whalehead Hill and the upwind surface roughness is much less at Whalehead Hill than Barbours Hill. Therefore, Whalehead Hill shows a much faster migration rate than Barbours Hill, though still less than the migration rate of Whalehead Hill 16 years ago.

Slipface Orientation and Movement Direction

Examination of the Corolla station wind diagrams (Figures 4-6) leads to the obvious question as to why there is no persistent slipface oriented normal to the southwest winds. Indeed, slipfaces were seen throughout the period on the easterly flanks of Whalehead Hill. However, these were only temporal features lasting until a change of wind direction occurred. On the contrary, the slipface on the south flank of Whalehead Hill is persistent, being evident in all old aerial photographs.

Notice in Figure 4 that the strongest average wind speeds were for the north and northeast directions. The northerly winds (20%) were second in duration only to the southwest winds (32%). However, the effectiveness of the southwest winds are greatly diminished by the presence of a thick forest with trees 15 m high, to the west of all the sand hills. Due to the blockage of the southwest winds, the northerly winds can be considered dominant. This explains the orientation of the slipface which is approximately normal to, and downwind of, these northerly winds. Once established, this high slipface (6 m) acts as a sink for any sand blowing over the crest, because the winds blowing over the forest can not develop the sheer velocity necessary to carry sand up the steeply sloping (32°) slipface. Therefore, all of the sand hills show a net movement to the

south-southwest in response to the northerly winds, but only temporary movements in other directions in response to the multi-directional wind regime.

Volume Discharge of Sand

The volume discharge of sand across the slipface of both Barbours and Whalehead Hills can be estimated if the size and rate of advance of the dune is known. Figure 32 shows a schematic of a slipface for a large dune such as Barbours or Whalehead Hill. The volume discharge is the area of the shaded portion times a unit width which is calculated according to the relation:

$$V = BB' * H * W$$

where:

$$\begin{aligned} V &= \text{volume discharge/year/meter of slipface} \\ BB' &= \text{distance dune travelled in one year} \\ H &= \text{height at brink of slipface} \\ W &= \text{length of slipface crest (here set at 1 meter)} \end{aligned}$$

Similarly, the equivalent weight of sand discharged:

$$Q = V * \gamma$$

where

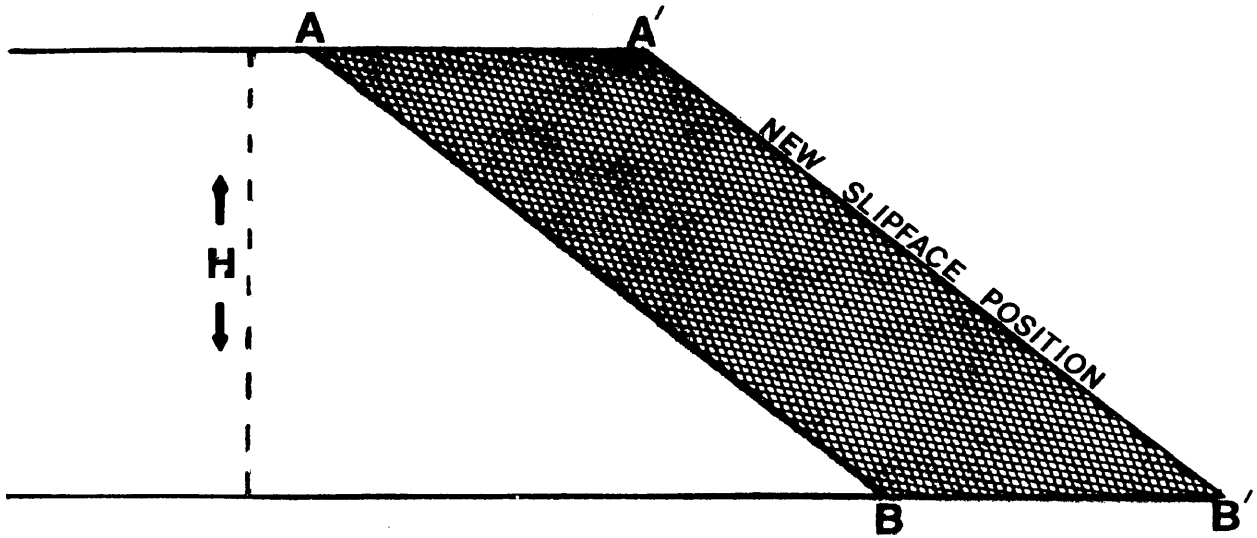
$$\begin{aligned} Q &= \text{discharge in g/unit width} \\ V &= \text{volume discharge} \\ \gamma &= \text{bulk density of loosely packed sand which} \\ &\quad \text{is about } 1.4 \text{ g/cm}^3 \text{ (Inman, 1966)} \end{aligned}$$

Therefore the discharge of sand for Barbours Hill is:

$$\begin{aligned} V &= 0.75 * 5.5 \\ &= 4.1 \text{ m}^3/\text{year/meter width} \\ Q &= 1.3 * 10^{-3} \text{ cm}^3/\text{cm}\cdot\text{sec} * 1.4 \text{ g/cm}^3 \\ &= 1.8 * 10^{-3} \text{ g/cm}\cdot\text{sec} \\ &= 5.7 * 10^3 \text{ kg/m}\cdot\text{year} \end{aligned}$$

and for Whalehead Hill is:

$$\begin{aligned} V &= 6.1 * 5.5 \\ &= 33.5 \text{ m}^3/\text{year/meter width} \end{aligned}$$



VOLUME DISCHARGE (SHADED AREA) OF A LARGE SAND DUNE
BASED ON A KNOWN HEIGHT (H) AND MOVEMENT (BB').

WHERE:

$$V = BB' \times H \times W$$

V = VOLUME DISCHARGE/YEAR/METER OF
SLIPFACE

BB' = DISTANCE DUNE TRAVELLED IN ONE
YEAR

H = HEIGHT AT BRINK OF SLIPFACE

W = LENGTH OF SLIPFACE CREST (HERE
SET AT 1 METER)

Figure 32. Volume discharge (shaded area) of a large sand dune based on a known height (h) and movement (BB').

$$\begin{aligned}
 Q &= 1.1 * 10^{-2} \text{ cm}^3/8 \text{ m}\cdot\text{sec} * 1.4 \text{ g/cm}^3 \\
 &= 1.54 * 10^{-2} \text{ g/cm}\cdot\text{sec} \\
 &= 4.9 * 10^4 \text{ kg/m}\cdot\text{year}
 \end{aligned}$$

Over 33 m (49,000 kg) of sand at Whalehead Hill, while only 4.1 m³ (5,700 kg) of sand at Barbours Hill, was transported across one meter of slipface crest between March 1976 and March 1977.

Therefore the transport of sand across the slipface at Whalehead Hill was about nine times greater than at Barbours Hill due to vegetation colonizing the eolian flat to the east of Barbours Hill.

Conclusions

1. Aerial photographs indicate that the migration rate of the large sand hills, Whalehead Hill, south of Corolla, North Carolina has averaged about 8 meters/year towards the south-southwest over the last 16 years.

2. Barbours Hill in False Cape State Park, Virginia has been nearly stabilized by vegetation and is now migrating at 0.75 m/year to the south-southwest. The volume discharged across the slipface was calculated to about 4 m³/m·year.

3. Whalehead Hill has not been stabilized as much by vegetation, and is now migrating to the south-southwest at about 6 m/year, corresponding to a calculated volume discharge of about 33 m³/m·year. In addition, the eastern flank of this dune has undergone 9 m of horizontal accretion in one year towards the new paved road leading to Corolla.

4. The persistent south-southwest slipface is attributed to the dominance of the north and northwest winds because of the adverse effect of the maritime forest to the southwest on the equally frequent and speedy southwest winds.

5. Apart from the wind, vegetation is the most crucial environmental variable in determining the migration rate and slipface orientation of large sand hills. As will be shown in the next section, vegetation is also very important in determining the development and orientation of coastal parabolic dunes.

ORIENTATION OF COASTAL PARABOLIC DUNES AND
REALTION TO WIND VECTOR ANALYSIS

One of the more striking features along Currituck Spit (Figure 1) is a field of parabolic (or U) dunes ranging from 3 to 10 m in height and extending south in False Cape State Park to the state line (Figure 33). Orientation of U dunes is a result of the interaction of many environmental variables including wind, vegetation, topography, standing water, and the location of the sand source. Landsberg (1956) and Jennings (1957) assumed wind was the dominant factor and therefore ignored the remaining environmental variables in their studies of the orientation of parabolic dunes in Denmark and Tasmania, respectively.

Landsberg (1956) first described the evolution of parabolic dunes. Figure 34 shows a four phase sequence which leads to the characteristic U shaped dunes found along many coasts of the world, including Currituck Spit. A large mobile sand mass (Phase 1) becomes increasingly stabilized by vegetation along the flanks which lag behind an advancing slip face and lead to the U shaped dune (Phase 2). Eventually the parabolic dune becomes completely stabilized (Phase 3) and the downwind end may even completely erode (Phase 4). This complete hypothetical evolutionary sequence of parabolic dunes is presently exhibited in Currituck Spit. Old aerial photos (1937) show a massive sand sheet in this area which eventually developed into the parabolic dune field according to the sequence shown in Figure 34 with the



Figure 33. High altitude aerial photograph (April, 1975) of parabolic dune field in False Cape State Park, Virginia, looking south.

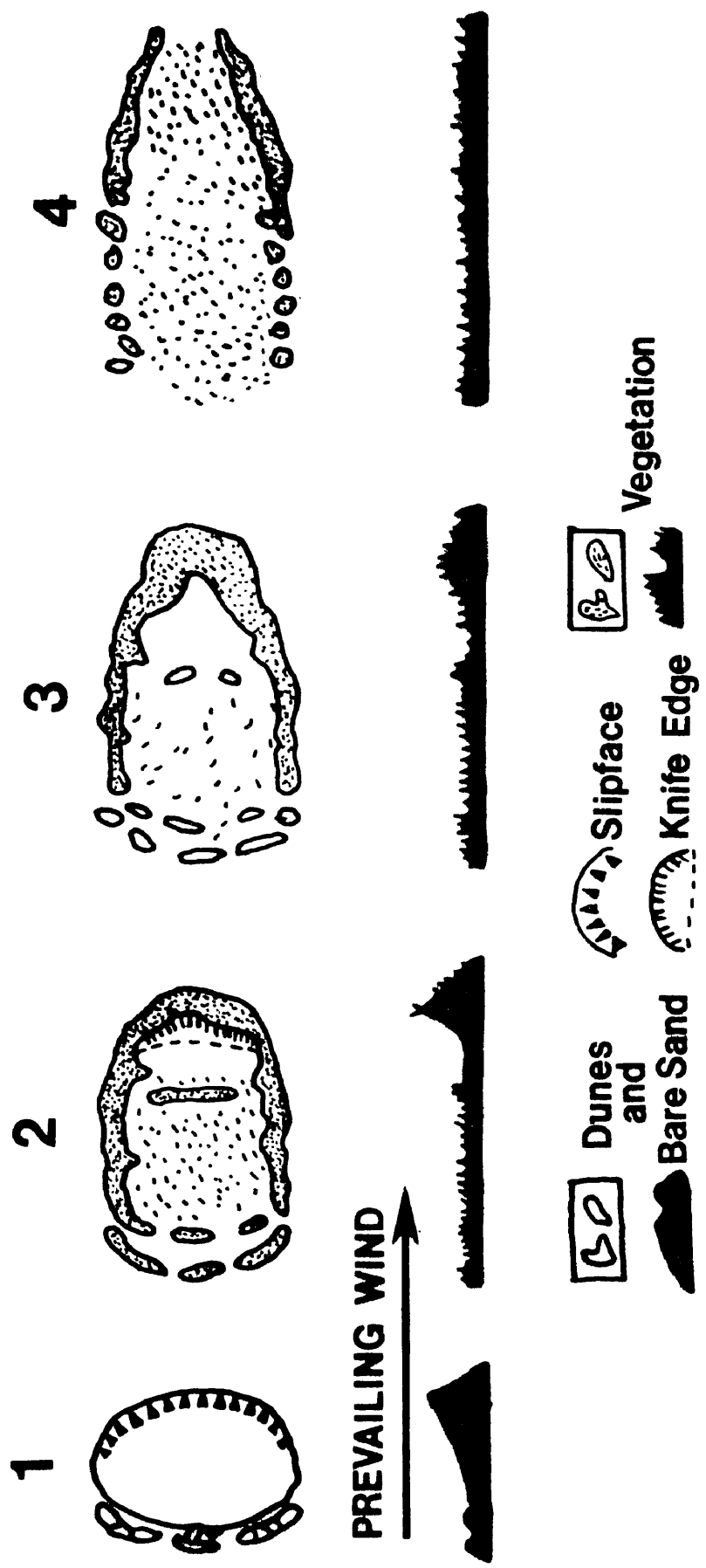


Figure 34. Diagrammatic representation of parabolic dune phases (after Landsberg, 1956). See text for discussion.

exception that phase four has not been reached (Henningar, 1978).

Barbour Hill (Figure 28), discussed at length in the previous section, represents the first phase of U-dune development. A small number of Phase 2 active parabolic dunes (6 m in height) are evident to the south of Barbours Hill. However, most of these parabolic dunes are lower (three meters) and completely stabilized Phase 3 dunes. Figure 35 contains low altitude photographs of parabolic dunes in False Cape State Park.

It is clear that the wind regime and vegetation are both critical in determining the orientation of parabolic dunes. The remaining environmental factor which was considered in this study is the orientation of the beach relative to the dunes. Since the beach is the initial source of sand for dunes, it follows that the orientation of the beach relative to the prevailing and dominant wind regime, and the parabolic dune field will also play a role in determining the orientation of U-dunes.

Wind Vector Analyses

If a clear relation exists between the sand transporting capabilities of wind and parabolic dune orientation, the vector mean of the Corolla Station wind data should correlate with the orientation. As will be shown, this is not necessarily true for coastal dunes. Bagnold (1941) showed experimentally that eolian sand transport is proportional to the cube of the wind velocity above a threshold level. Therefore, to accurately evaluate the wind field in relation to eolian transport a method originally proposed by Landsberg (1956) was used to determine the magnitude of individual vectors for each direction on

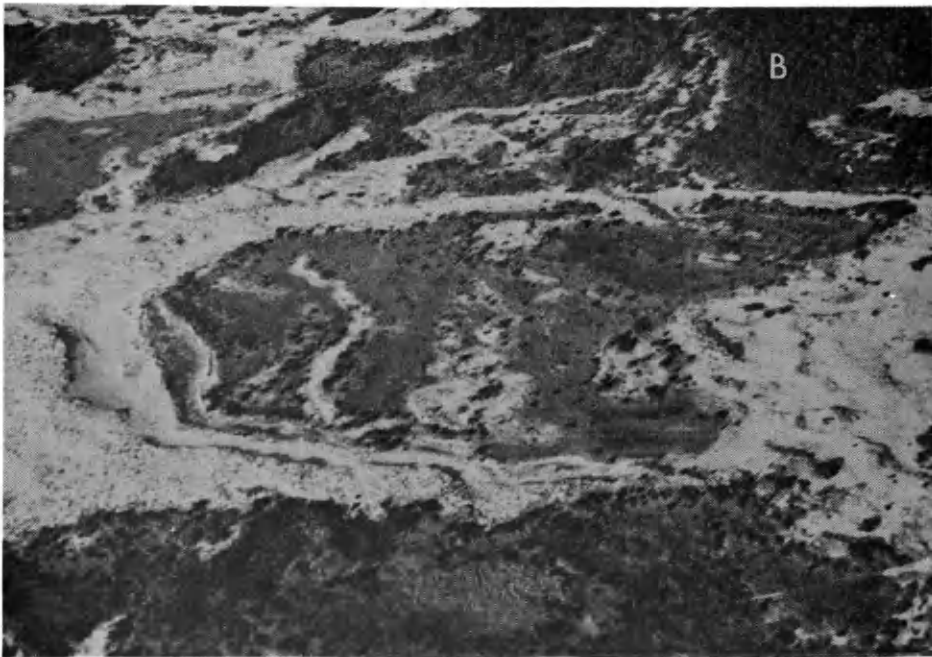
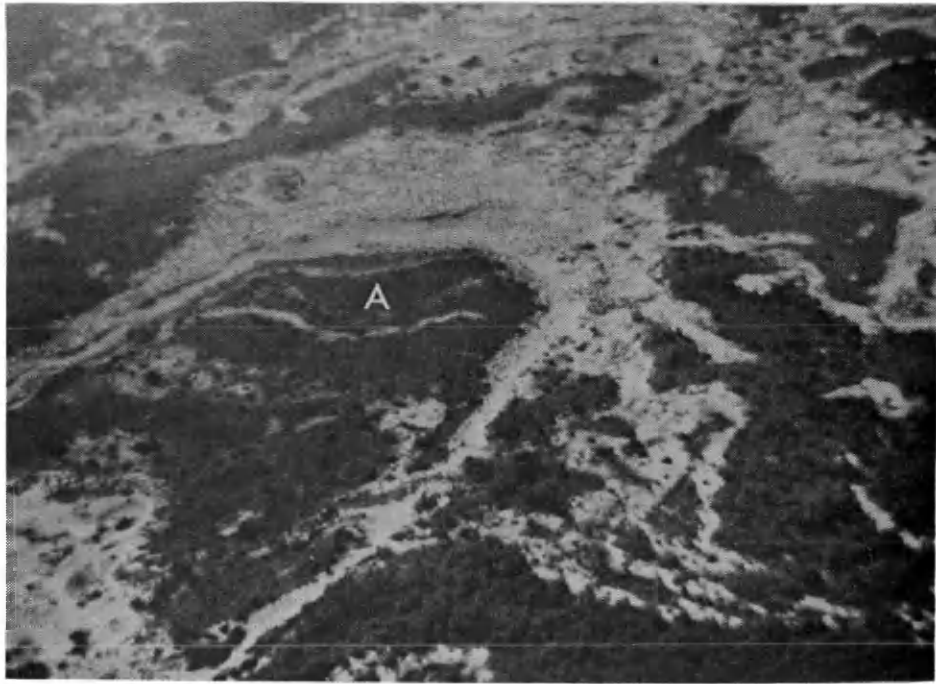


Figure 35. Parabolic Dunes
A. View toward south, note heavily vegetated blowout
B. View toward west of same dune

an eight point compass according to the relation:

$$b = s \sum_{i=1}^{i=n} (v - v_t)^3$$

where:

b = magnitude of individual vector, for each
of eight directions
s = scaling factor for plotting
n = number of observations in class interval
v = wind speed in meters per second
v_t = threshold velocity (5.0 m/sec)

After computing each value of b, the eight vectors were graphically added to determine a wind resultant. These calculations and the plots were generated by the computer program listed in Appendix 3.

The Corolla Station annual wind resultant (Figure 36) is oriented from the northwest to southwest. However, this resultant has no obvious relation with the average parabolic dune orientation.

Figure 37 shows the orientation of the field of parabolic dunes (Figure 33). The orientation was determined by bisecting the angle formed by lines tangent to the two arms of the U-dunes, and then measuring the angle of the bisector relative to north. Table 3 lists the orientation of all the dunes measured from vertical aerial photography along with calculations of the mean standard deviation and standard error of the mean. Several sets of imagery (ERTS frames) were utilized to determine orientation due to the difficulty of defining the actual location of flanks and slipfaces for certain dunes. The first column on the left in Table 3 lists the orientation of the 11 parabolic dunes shown in Figure 33 and additional dune measurements. The mean orientation of the 30 parabolic dunes is N 8°E. Notice the wind resultant (Figure 36) deviates by about 70° from the mean

TABLE 3

PARABOLIC DUNE ORIENTATION FROM AERIAL PHOTOGRAPHS

Orientation determined from bisector of two arms
(arranged by dates of aerial photo data sources)

<u>Dec., 1974</u>		<u>April, 1965</u>		<u>Dec., 1973</u>	
Dune No.	Compass Orientation of Bisectors	Dune No.	Compass Orientation of Bisectors	Dune No.	Compass Orientation of Bisectors
1	6°	12	2°	22	16°
2	8°	13	359°	23	10°
3	8°	(April, 1975)		(November, 1976)	
4	14°	14	14°	24	8°
5	352°	15	11°	25	12°
6	12°	16	7°	26	0°
7	13°	(June, 1973)		27	14°
8	11°	17	9°	28	3°
9	10°	18	6°	29	9°
10	9°	19	3°	30	9°
11	9°	20	357°		
		21	3°		

Mean Parabolic Dune Orientation = 7.9°

Standard Deviation = 5.5°

Standard Error of Mean = 1.04°

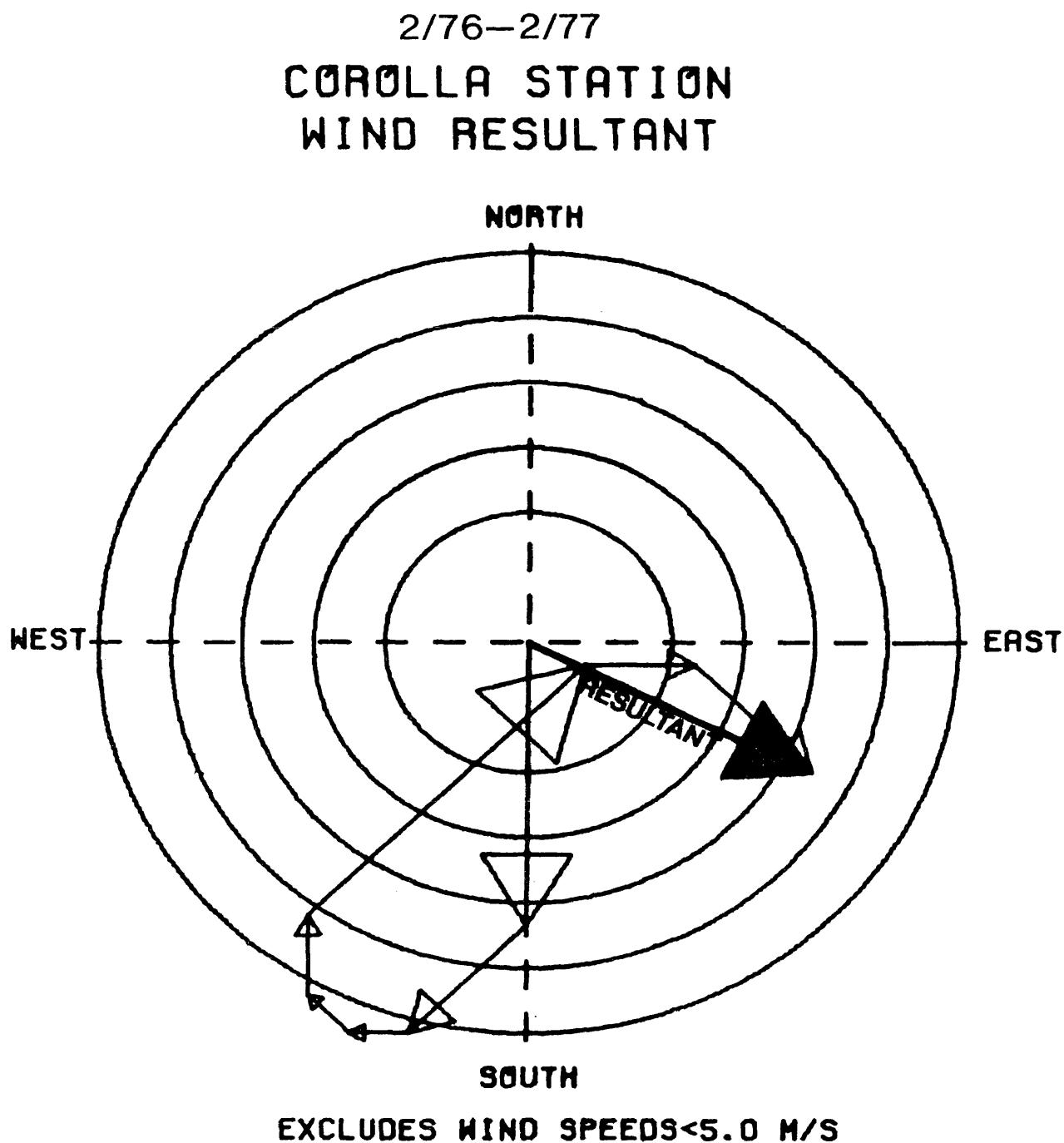


Figure 36. Corolla station annual vector mean wind resultant (February 1, 1976 to January 31, 1977).

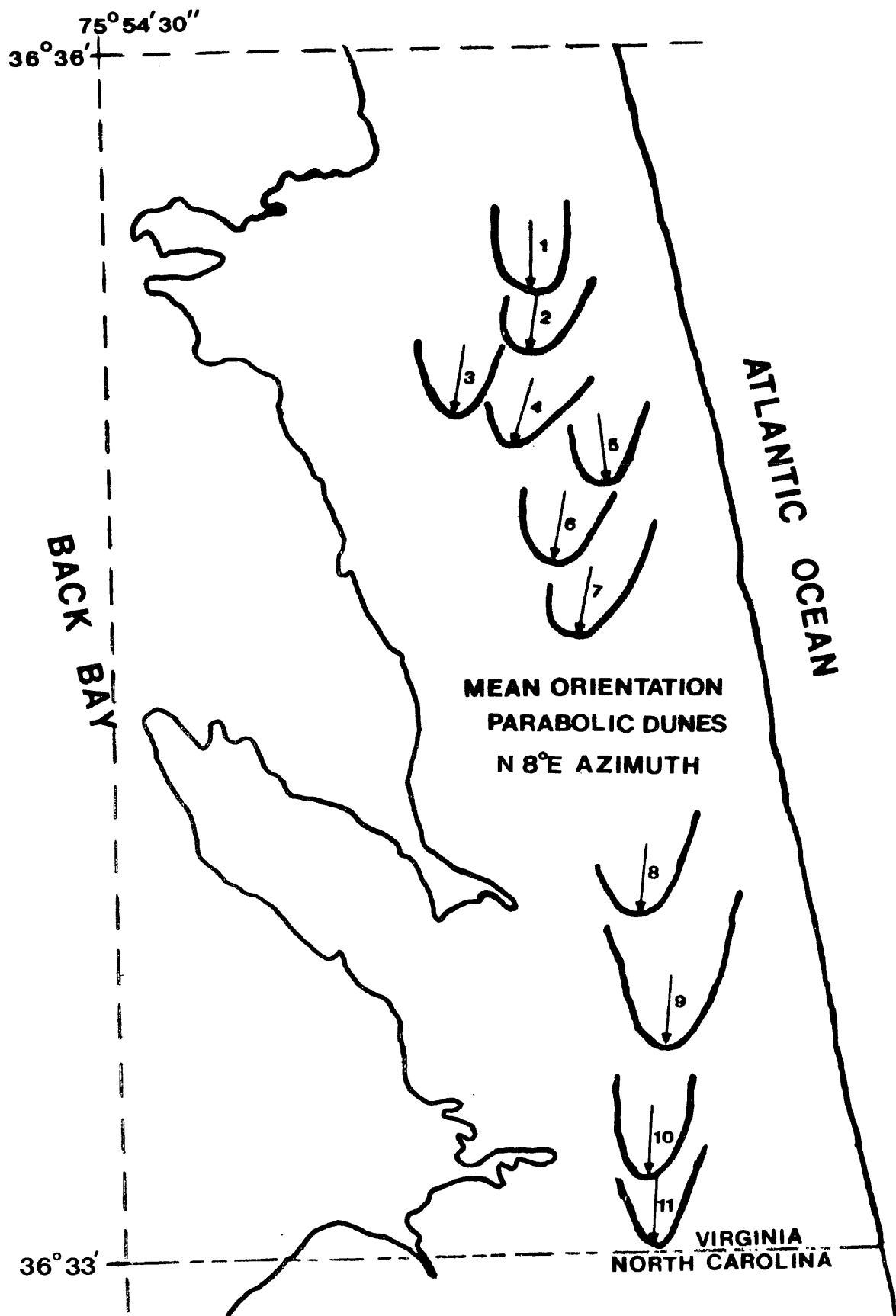


Figure 37. Parabolic dune field of False Cape, Virginia, illustrating location, plane view, and orientation of the dunes. The dunes are numbered and keyed to Table 3.

orientation. Therefore in using the simple vector mean of all cubed wind speeds there is no apparent correlation between wind regime and dune orientation. Jennings (1957) also found little correlation using this method in studies of King Island (Tasmania) parabolic dunes.

When two or more modes occur in a circular frequency distribution the vector mean is often not a useful measure (Potter and Pettijohn, 1963). Examination of the Corolla station wind rose for winds greater than or equal to 5.0 m/sec (Figure 5) show four general modes; northeast, north, northwest, and southwest. Figure 5, though it shows a northwest resultant, actually indicates the largest magnitude vectors are from the north and southwest. If, instead of examining just the vector resultant, we concentrate on the effects of vegetation on the individual vectors and the orientation of the shoreline, a much better relation emerges between the orientation of parabolic dunes and the important environmental variables.

Aerial photographs (Figure 33) show the parabolic dunes developed with a 15 meter high forest to the west of the dunes, which is higher than the height of the developing dunes. The wind velocity at the surface, and therefore the transporting capability of the wind, is dependent on the roughness characteristics of the surface. Vegetation, a surface roughness element, diminishes the wind velocity at the surface and downwind of the vegetation as a function of the density and height of vegetation (Bressolier and Thomas, 1977). Thus, the very thick and high forest of scrub pine and live oak, to the west of the parabolic dune field, greatly reduced the effectiveness of the westerly winds.

To the east of the parabolic dunes, at the time of their formation, was a sand flat with sparse dune grass vegetation. Easterly winds (i.e., northeast winds in this area) were thus unimpeded by

vegetation in the transport of sand. The onshore winds should also be considered the important winds for they blow over the primary source of sand for deposition as parabolic dunes. Therefore, given the effects of vegetation in greatly diminishing the sand transporting capability of the westerly winds, and the location of the source of sand relative to the dune field, it was concluded that the onshore winds were dominant in determining the orientation of parabolic dunes.

Since the initiation of the parabolic dunes, a high foredune with abundant vegetation has formed upwind of the parabolics. Thus, the same situation may not be present now; i.e., the vegetation is now blocking sand transport from onshore winds, as well as the offshore winds.

Figure 38 is a wind resultant diagram constructed in the same manner as Figure 36 except all offshore winds are excluded. Notice this resultant is much closer to the mean orientation of the parabolic dunes than the resultant in Figure 36. The resultant is within about 20 degrees of the mean orientation and much closer for a number of the U-dunes listed in Table 3.

The Corolla wind data, from which these wind resultants were determined, covers only one year of data even though the orientation of these parabolic dunes was determined over a twenty year period. The question which naturally arises is if these one year wind resultants are actually representative of the long term wind regime. In a previous section of this thesis, it was shown that the one year of Corolla and Hatteras Station wind data were similar. Figure 39, a comparison of wind resultants (within 20°) from the two stations, supports this conclusion. It was also shown in the wind climate section

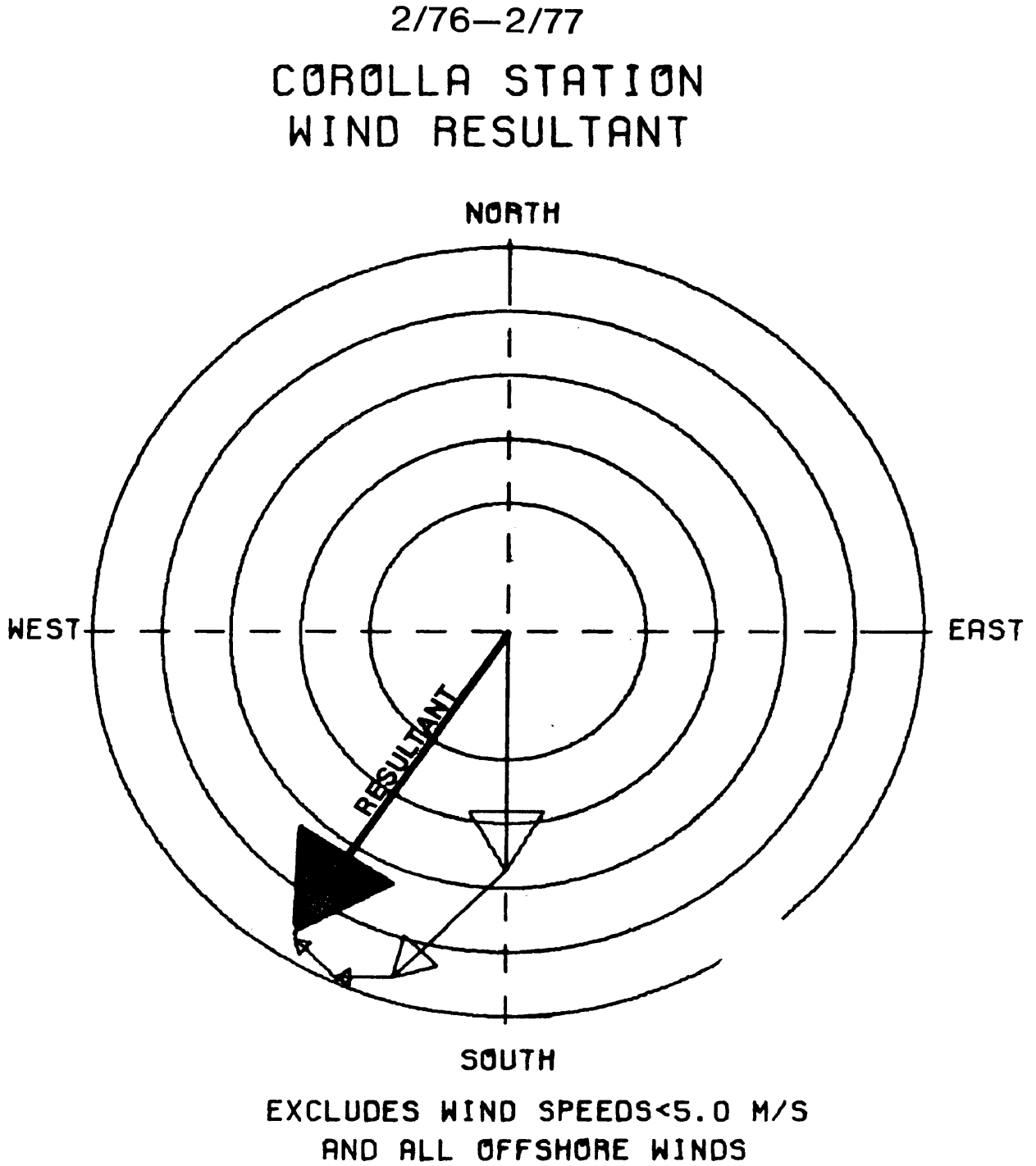
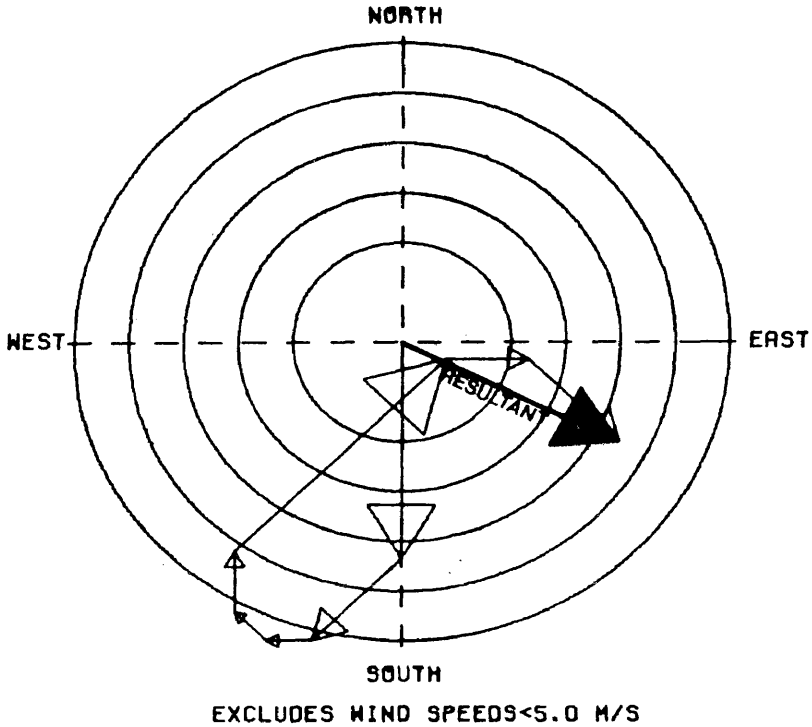


Figure 38. Corolla station wind resultant (February 1, 1976 to January 31, 1977) excluding all offshore winds.

2/76-2/77
COROLLA STATION
WIND RESULTANT



2/76-2/77
HATTERAS STATION
WIND RESULTANT

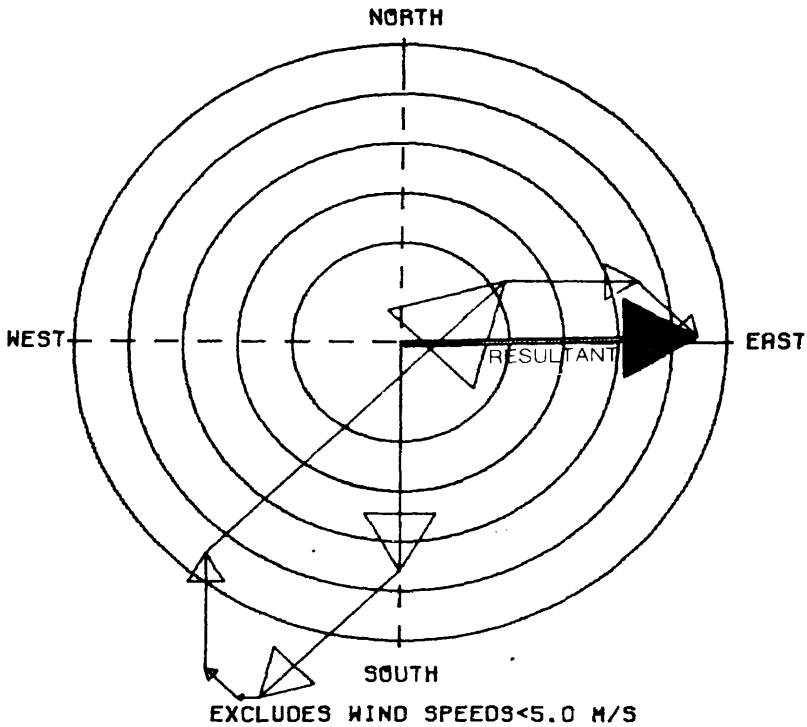


Figure 39. Comparison of Corolla and Hatteras Wind Resultants.

that the one year of Corolla wind data (February 1, 1976-January 31, 1977) from which these wind resultants were determined, was a fairly typical year relative to the long-term wind regime. Therefore, the Corolla wind resultants which were compared with the orientation of parabolic dunes should be similar to a wind resultant determined from long term data, if such data were available.

Conclusions

1. A relatively uniformly oriented field of parabolic dunes located in False Cape, Virginia, with a mean orientation of N 8° E, shows an evolutionary sequence similar to that detailed by Landsberg (1956).
2. It was concluded that a local one year (February 1, 1976 to January 31, 1977) wind resultant should be similar to a wind resultant determined from long term wind data for the area.
3. The vector mean wind resultant determined by cubing wind speeds above 5.0 m/sec showed no correlation with the mean orientation of the parabolic dunes.
4. Vegetation has an important effect in determining the development and orientation of parabolic dunes by stabilizing the arms of the developing U-dune and reducing the effective transporting capability of offshore winds.
5. It was assumed that the offshore winds were dominant in determining the orientation of the parabolic dunes because of a lack of vegetation seaward of the dune field (at the time of formation), and a high, dense maritime forest landward of the dune field. By making this assumption, the Corolla Station wind resultant was within 20° of the mean orientation of the False Cape parabolic dune field.

EOLIAN GRADING OF SAND ACROSS TWO BARRIER
ISLAND TRANSECTS

Textural studies of sands have been conducted in order to understand the environments of deposition of ancient geologic formations in connection with the search for stratigraphic oil traps (Friedman, 1961; Mason and Folk, 1958). Ahlbrandt (1974), however, concluded that the structures of deposits are more definitive of an ancient eolian environment than are the textures. Both Ahlbrandt (1974) and Sharp (1965) found that textural analyses of sand were useful in detailed analyses of known depositional environments.

Two very different depositional environments are evident on Currituck Spit (Transects A and C in Figure 40). A cross-barrier transect near Corolla, North Carolina includes a low, sparsely vegetated foredune ridge, shifting sands on the eolian flat and a large unvegetated medano (i.e., sand hill, Figure 27). To the north, in False Cape State Park a second transect crosses subenvironments quite different from those to the south. Here there are high multiple-ridge foredunes, dense eolian flat shrub thickets, and large vegetated parabolic dunes (Figure 28). Since textural parameters may be able to differentiate environments of deposition, a detailed sampling and analysis of sediment deposits across two transects was conducted with the hope that the textural parameters might indicate the geologic processes responsible for the differences in the subenvironments of the north and south transects, and help clarify the role that eolian sand transport plays in the overall sediment dynamics of a barrier island.

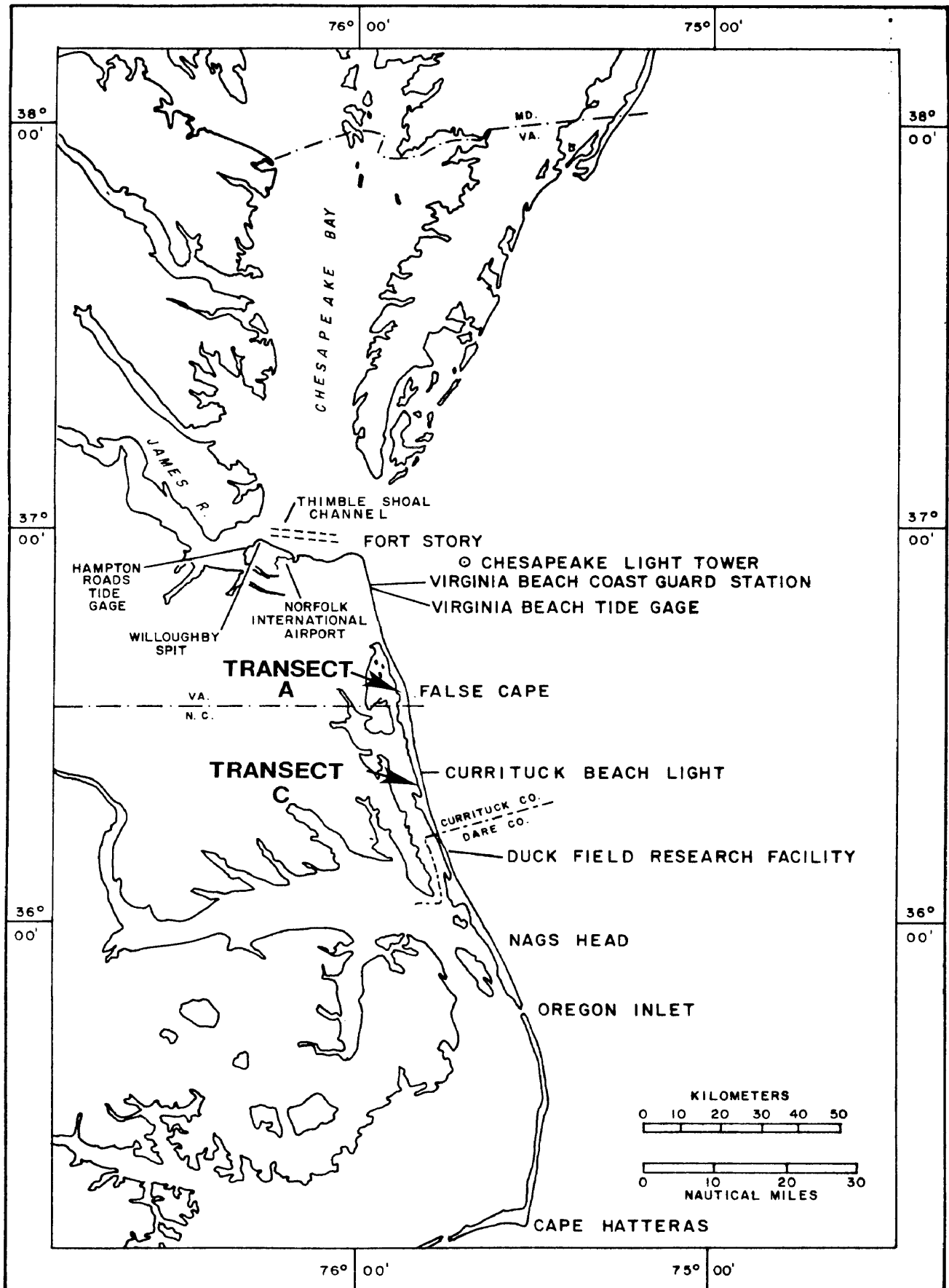


Figure 40. Regional location map showing two transects sampled.

Field Procedure

Field work for this study was conducted between January 1976 and January 1977. The field work consisted of sampling along two cross-barrier transects (Figure 40); one in False Cape State Park, Virginia, and the other just south of Corolla, North Carolina. The two transects were always sampled on the same day, as close to the time of low tide as possible.

Starting at the low water mark samples were collected across the transect at irregular intervals. In general the same number of samples were collected across the two transects. However, the distance between samples varied according to the width of the subenvironments that the transects crossed. The northern transect was 0.6 kilometers long with a wider and higher foredune system and a wider eolian flat, than the southern transect which was 0.45 kilometers long.

At each sampling site (Figure 41) on the transect two samples were collected. A surface sample was collected by scraping a thin layer of sand onto a sheet of cardboard and then storing it in a sample bag. This sample was supposed to represent the most recent response of the sediment to the wind regime. The sampling was conducted after a fairly long period (~72 hours) of winds above the threshold velocity for sand movement from a constant direction. Table 4 lists the wind data from the Currituck Light Station for the six day period prior to each of the two sampling periods. Notice that one sampling was conducted after a period of offshore winds while the other sampling was after a period of onshore winds. After collection of the surface sample a 2.54 cm diameter 5.0 cm deep core was taken at the same site and stored in a coded sample bag. This sample was supposed to represent many sedimentation

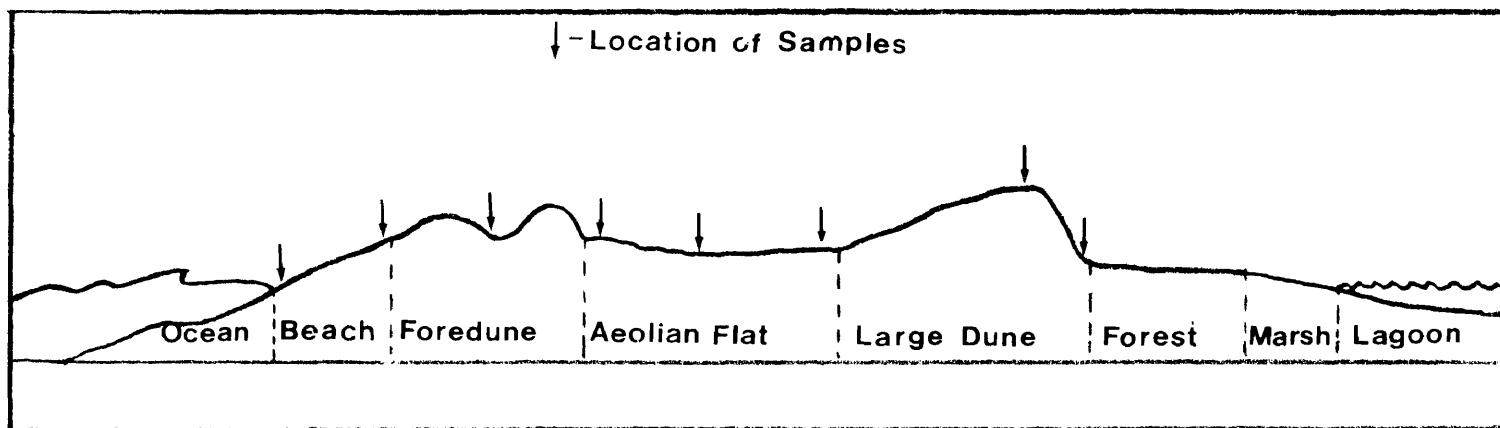


Figure 41. Profile of barrier island showing location of samples on transect.

TABLE 4

WIND DATA PRIOR TO SEDIMENT SAMPLING FOR SAND GRADING STUDY.

WIND DIRECTION AND SPEED DATA
 DIRECTIONS 0-360 DEG. FROM TRUE NORTH, SPEEDS MPH (Multiply By .44704 to get m/sec)

STATION-COROLLA LIGHT

DATE/HOUR	1		4		7		10		13		16		19		22		MAX.		VECTOR AV.	
	S	D	S	D	S	D	S	D	S	D	S	D	S	D	S	D	S	D	S	D
1/6/76	16	255	14	245	14	255	8	255	18	235	20	225	22	215	24	235	30	215	16	236
2/6/76	22	245	12	235	12	235	4	275	16	65	24	65	26	75	24	65	32	55	5	74
3/6/78	20	65	26	75	24	65	24	75	20	65	26	55	26	55	26	55	28	75	30	64
4/6/76	26	65	26	65	32	55	32	55	32	45	32	55	32	55	34	55	42	45	31	55
5/6/76	36	55	36	55	32	55	36	45	38	55	30	45	32	35	38	35	42	55	34	47
6/6/76	24	35	20	35	20	35	20	35	8	65	8	65	6	85	8	165	10	165	28	35

Sampling Conducted June 6, 1976 Following Period of Onshore Winds.

15/2/76	12	95	16	85	12	115	6	145	12	185	20	215	26	215	24	235	34	215	9	183
16/2/76	28	235	26	245	22	245	20	255	16	245	18	235	18	215	26	225	24	215	21	237
17/2/76	26	235	22	235	30	235	26	235	22	245	20	235	16	185	18	225	34	235	21	231
18/2/76	16	220	18	225	18	225	20	215	22	215	32	205	34	215	36	235	46	215	24	219
19/2/76	18	265	16	265	16	275	20	305	10	285	18	255	14	235	18	235	26	295	14	264
20/2/76	20	265	14	355	7	345	6	55	8	75	8	125	8	160	8	178	23	255	0	358

Sampling Conducted February 20, 1976 Following Period of Offshore Winds.

units though in many cases it may not have, due to the long duration of the unidirectional winds prior to sampling.

At each transect, samples were gathered at the low water mark, berm, beach dune interface, foredune crest, midway down the landward foredune slope, and across the eolian flat (Figure 41). Then samples were collected along the slope, at the crest, and at the base of the slipface, of a large dune. After completion of both transects the samples were taken back to the laboratory for analyses.

Textural Analyses

Grain size distributions for all samples were determined with the Rapid Sediment Analyser at the Virginia Institute of Marine Science. After oven drying, splits of samples were obtained using a Otte splitter. Several splits were necessary to get an optimum 5-15 gram sample size for the settling tube.

The Virginia Institute of Marine Science Rapid Sediment Analyser (RSA) is modelled after the unit designed by Zeigler et al. (1960) at Woods Hole. The falling velocity of particles over a one meter drop is measured by a differential pressure transducer which sends a voltage signal to a recording unit. Templates prepared from the tables of Zeigler and Gill (1959) are then used with a Gerber variable scale to determine from the record, sizes in sedimentation diameter (i.e., hydraulic radius) of ten percentiles along the curve. For simplicity and because the most important aspect of the study was detecting relative changes of texture, the grain size parameters from the settling tube were determined from the hydraulic radius.

The data from the settling tube analyses were input into a computer program for calculation of mean, standard deviation, skewness

and kurtosis. Many different methods for calculating these four moments have been proposed. The graphic method of Folk and Ward (1957) was chosen for all calculations. McCammon (1962) found that the mean derived by this method had an accuracy of 88% relative to the result of the moment method, while the standard deviation had an accuracy of 79%. The graphic method is also much simpler and the ability to discriminate environments of deposition by the graphic method of Folk and Ward (1957) has been shown by many authors (Friedman, 1961; Mason and Folk, 1958; Ahlbrandt, 1975; Anan, 1971).

Graphic Mean: A measure of the average size of the sand particles was determined according to the relation:

$$\bar{x} = \frac{\phi 16 + \phi 50 + \phi 84}{3}$$

where:

ϕ = phi unit corresponding to some percent level on the cumulative frequency curve.

Graphic Standard Deviation: A measure of the sorting of the sediment, was calculated according to the relation:

$$\sigma = \frac{\phi 84 - \phi 16}{4} + \frac{\phi 95 - \phi 5}{6.6}$$

A low value of σ indicates well sorted, while a high value indicates poorly sorted sediment.

Graphic Skewness: A measure of the symmetry of the grain size distribution about the mean, was determined according to the formula:

$$sk = \frac{\phi 16 + \phi 84 + 2 \phi 50}{2 (\phi 84 - \phi 16)} + \frac{\phi 5 + \phi 95 - 2 \phi 50}{2 (\phi 95 - \phi 5)}$$

Symmetrical curves have $sk = 0.0$; those with an excess of coarse sediment are negatively skewed, while those positively skewed indicate an excess of fine sediment.

Graphic Kurtosis: Is a quantitative measure of the departure from normality of the grain size distribution. Kurtosis measures the ratio between the sorting of the tails and the central portion of the probability curve. Kurtosis was calculated according to the formula:

$$k_g = \frac{\phi_{95} - \phi_5}{2.44 (\phi_{75} - \phi_{25})}$$

A normal curve has a k_g of 1.0. Curves with kurtosis greater than 1.0 are said to be leptokurtotic, that is the central portion is better sorted than the tails. A k_g less than 1.0 indicates a platykurtotic curve where the tails are better sorted than the central portion.

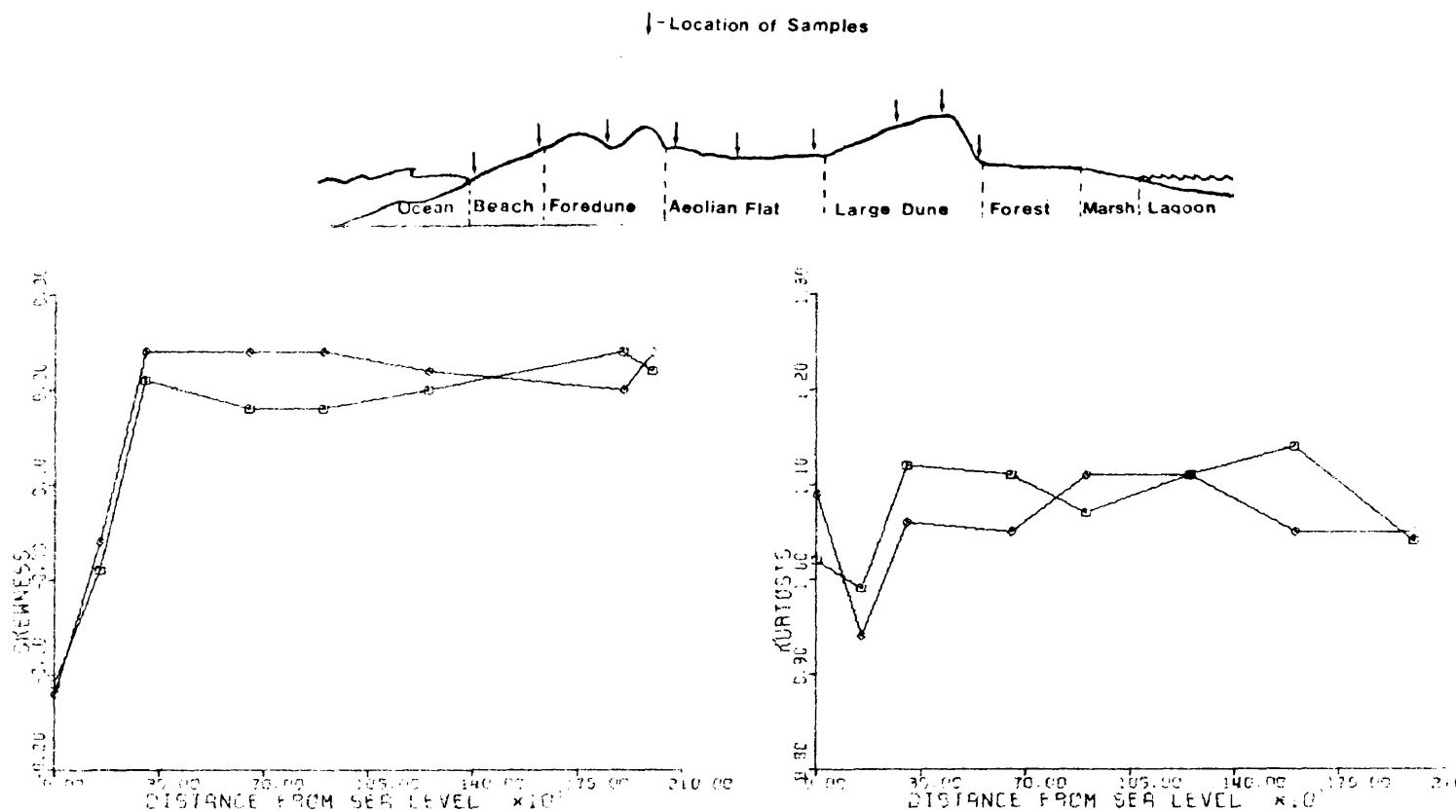
After computer calculation (DeAlteris, 1974) of the grain size parameters, plots of the moments (Figures 42-45) versus distance across transect were generated on a Calcomp plotter.

False Cape Transect

Figures 42 and 43 are plots of the four grain size moments versus distance across the barrier at False Cape for a set of samples taken after period of intense southwest (Figure 42) and northeast winds (Figure 43). Notice that neither figure indicates any clear cross-barrier changes in the grain size moments. Only samples gathered in the foreshore where deposition is primarily by waves is there any marked change in the grain size characteristics. In this area the beach sand showed a coarser (about 1.0 phi), more poorly sorted (standard deviation about 0.49) sediment with a skewness indicating a tail of coarse sand (-0.1).

Landward of the zone of wave activity where eolian processes are dominant the sand becomes very uniform in grain size characteristics across the barrier. This eolian sand has a mean size of about 1.8 phi,

A TRANSECT (FALSE CAPE, Va.) FOLLOWING OFFSHORE WINDS



◆ SURFACE SAMPLES

MOMENTS IN HYDRAULIC EQUIVALENTS (PHI UNITS)

■ CORE SAMPLES

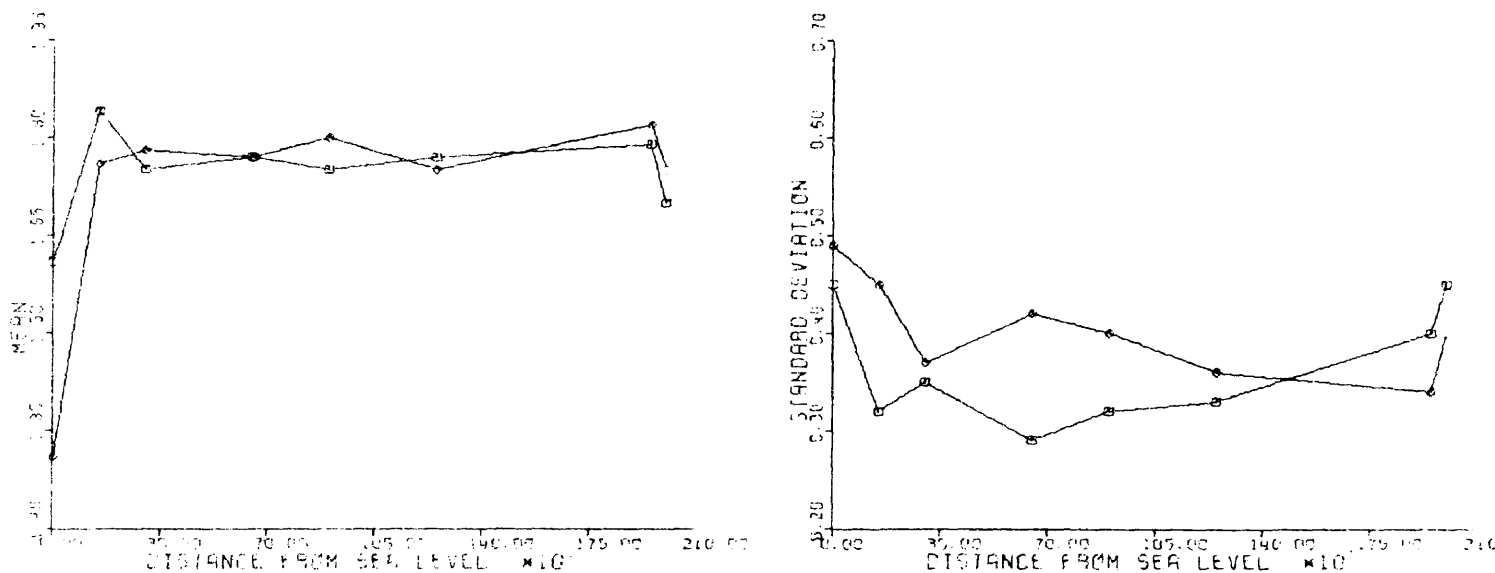


Figure 42. Grain-size moments across Transect A in False Cape State Park, Virginia (Barbours Hill).

A TRANSECT (FALSE CAPE; Va.) FOLLOWING ONSHORE WINDS

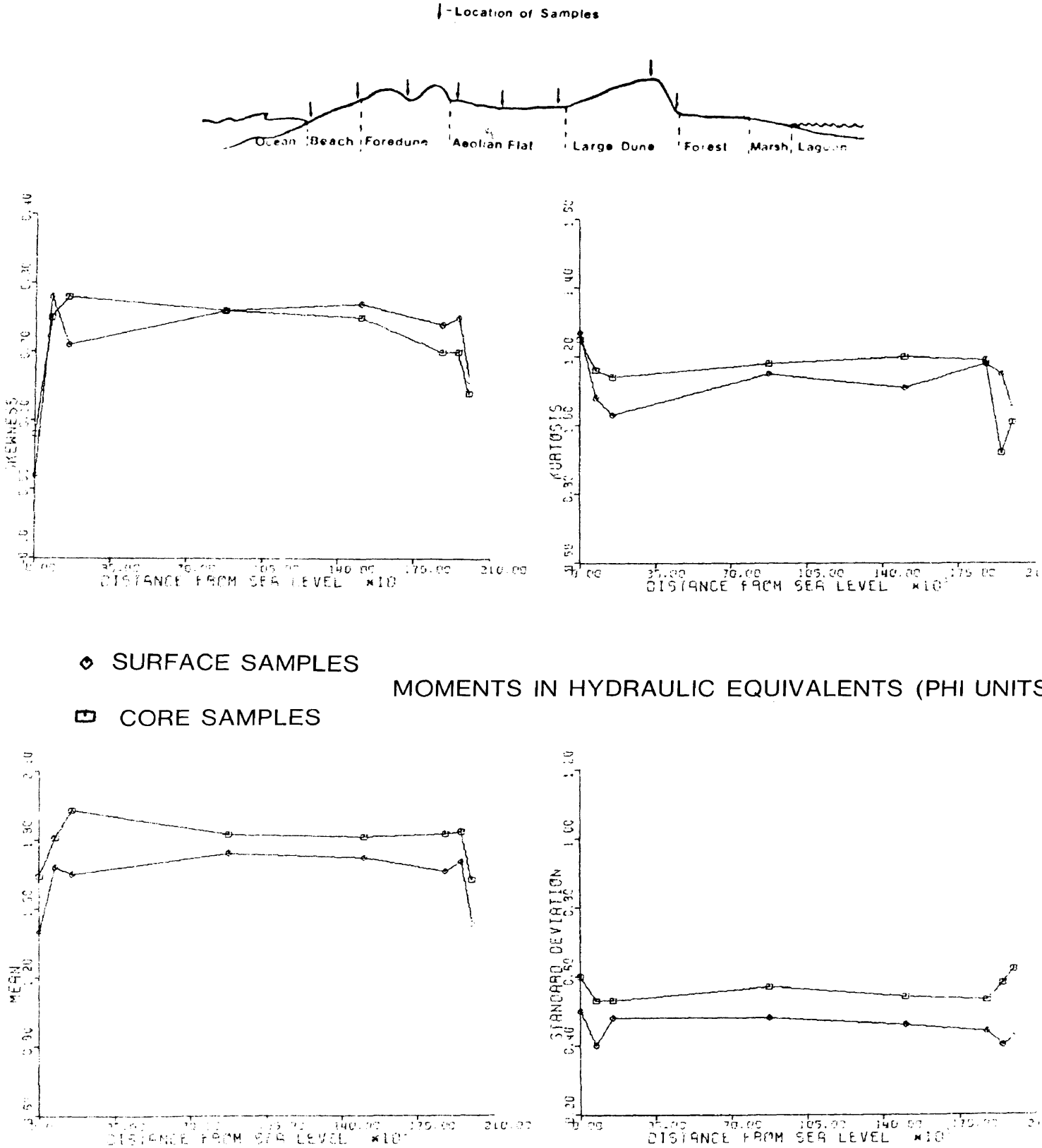


Figure 43. Grain-size moments across Transect A in False Cape State Park, Virginia (Barbours Hill).

is well sorted (standard deviation $\sim .3$) and a positive skewness ($\sim .3$) indicating a tail of fine material. These general grain size characteristics are to be expected for eolian deposited sand. What is surprising however is the apparent lack of any clear grading of sand across the transect. If we assume that the beach is the source of sand for eolian deposition then it would follow that samples gathered at increasing distances from the source should show the following:

1. Mean grain size should decrease (ϕ increase) because finer sand should be differentially transported farther inland.
2. Standard deviation should decrease as sand becomes finer and more uniform in size.
3. Skewness should become increasingly positive as normal curve becomes skewed towards the fines.
4. Kurtosis may become leptokurtotic as the central part of the curve becomes better sorted.

Examination of Figures 42 and 43 indicate no such changes at the False Cape transect for either onshore or offshore winds.

It is especially surprising that after a period of onshore winds (Figure 43) none of these grading characteristics were evident.

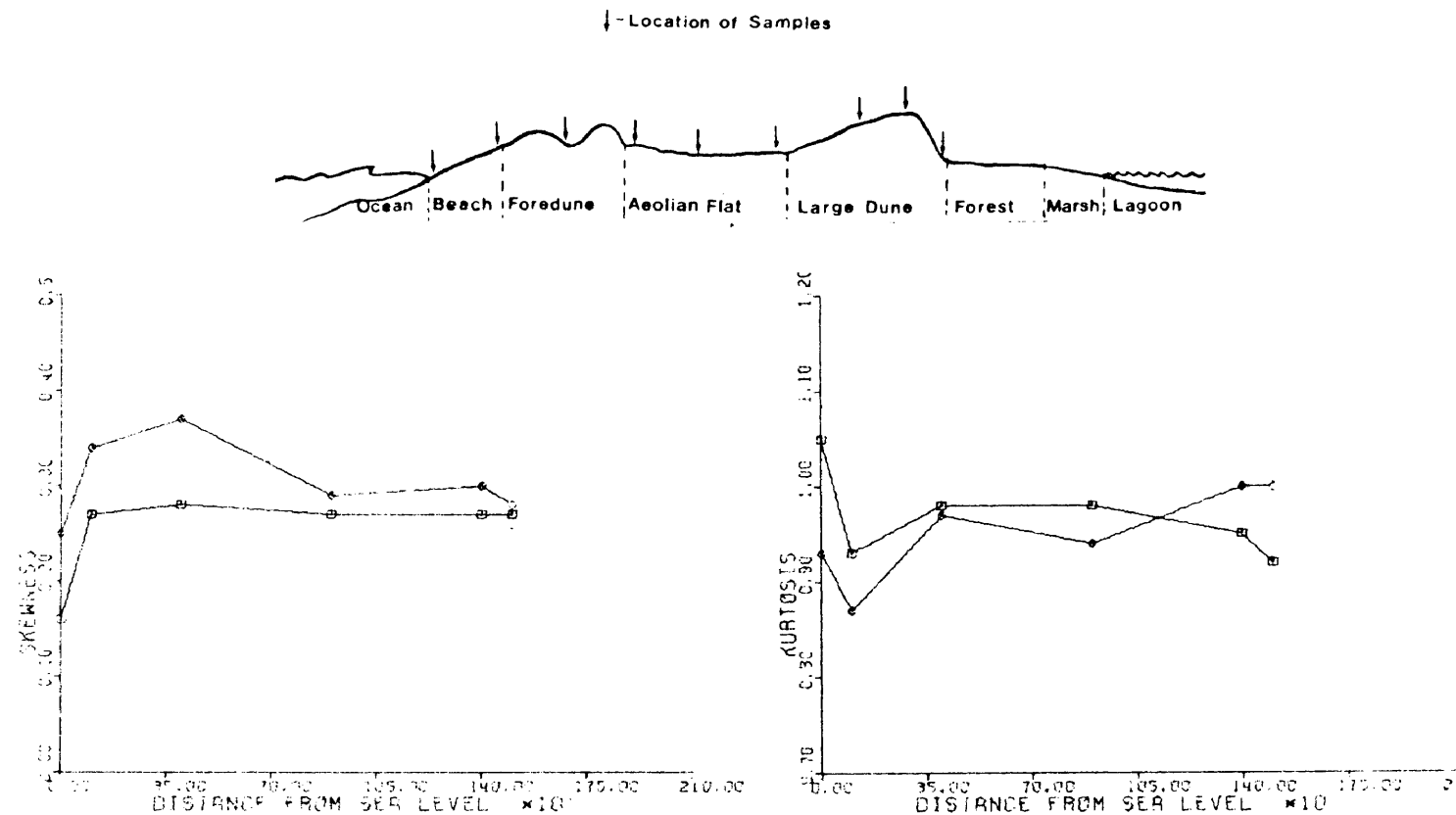
A field examination of the transect reveals a high (3-5 meters) multiple ridge foredune system with a thick growth of dune grasses, impeding most, if not all, transport to the interior. Further downwind from the sand source a very thick shrub thicket growing across the entire eolian flat is effectively eliminating any flux of sand between the beach and the interior, or across the barrier island. Figure 28 is an aerial photograph of this area showing the general distribution of vegetation. Field measurements of sand transport

(discussed in a later section) during 15 m/sec (35 miles/hour) onshore winds indicated a zero transport rate across the dunes and eolian flat. There is little cross-barrier sand transport in the False Cape region due to the presence of vegetation, so there could be no grading of sand. Therefore, it is suggested that this accounts for the lack of a change in trend in Figures 42 and 43.

Whalehead Hill Transect, South of Corolla

Figures 44 and 45 are plots of the four grain size moments versus distance across the Whalehead Hill transect south of Corolla (Figure 40), for the same dates as Figures 42 and 43, respectively. Figure 44 (following offshore winds) shows a slight seaward decrease from the large dune to the beach in mean size, and in skewness towards a fine tail in surface samples, relative to the Barbour's Hill transect. A greater difference is that there is no great change in the moments at Whalehead Hill after offshore winds for the foreshore surface samples, even though the core sample at the foreshore does show typical wave-deposited sand characteristics. It is suggested that the relatively small mean grain size of the surface sample is a result of eolian sand blowing off the dunes and eolian flat onto the beach. The core sample in the foreshore zone may have penetrated through the recent layers of eolian deposition into typical wave deposited sand, therefore giving a somewhat coarser grain size. The deposition of eolian sand in the foreshore zone is not indicated by the Barbour's Hill grading diagram (Figure 42) even though the sampling was conducted for Figures 42 and 44 on the same day. This is due to the large differences in the amount of sand carried onto the beach in the two areas. Sand transport measurements of sand blowing from the foredune and eolian flat onto

C TRANSECT (COROLLA,N.C.) FOLLOWING OFFSHORE WINDS



◆ SURFACE SAMPLES

MOMENTS IN HYDRAULIC EQUIVALENTS (PHI UNITS)

□ CORE SAMPLES

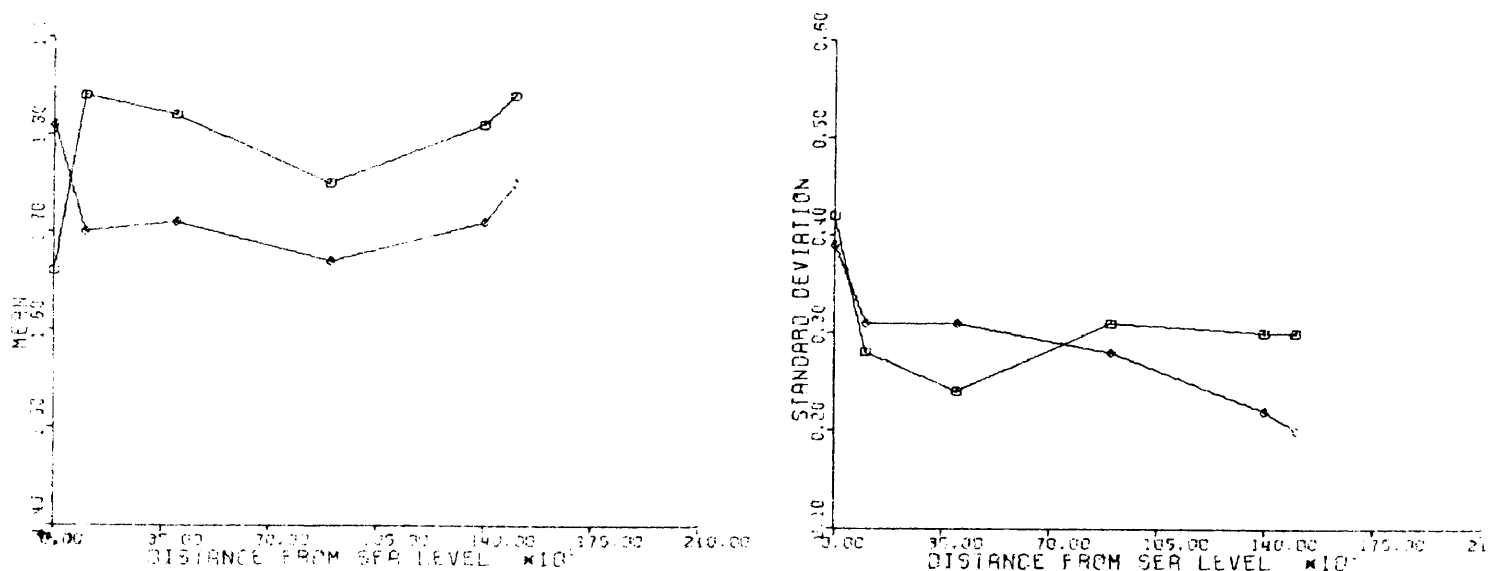
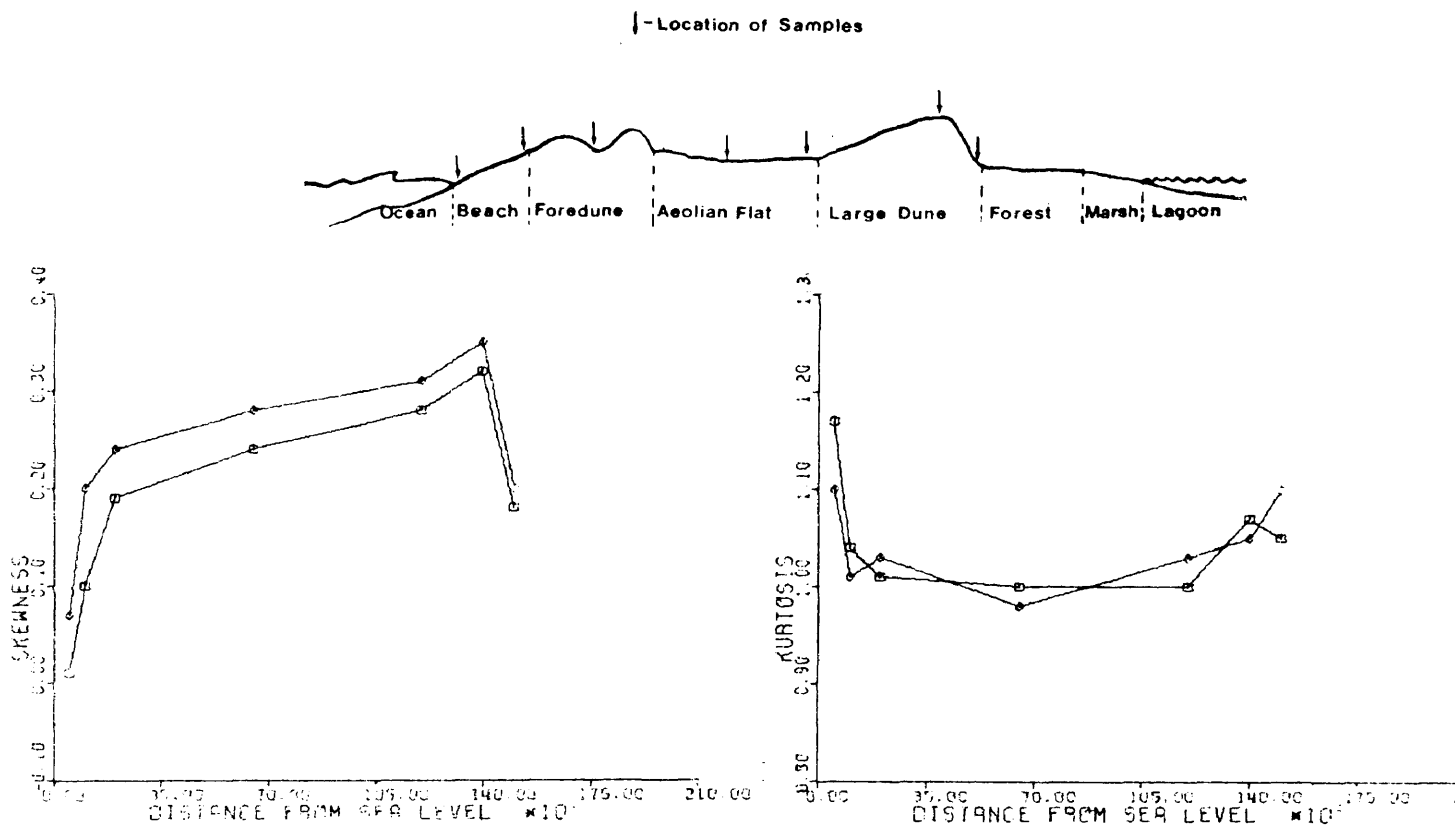


Figure 44. Grain size moments across Transect B south of Corolla, North Carolina (Whalehead Hill).

C TRANSECT (COROLLA, N.C.) FOLLOWING ONSHORE WINDS



◆ SURFACE SAMPLES

□ CORE SAMPLES

MOMENTS IN HYDRAULIC EQUIVALENTS (PHI UNIT)

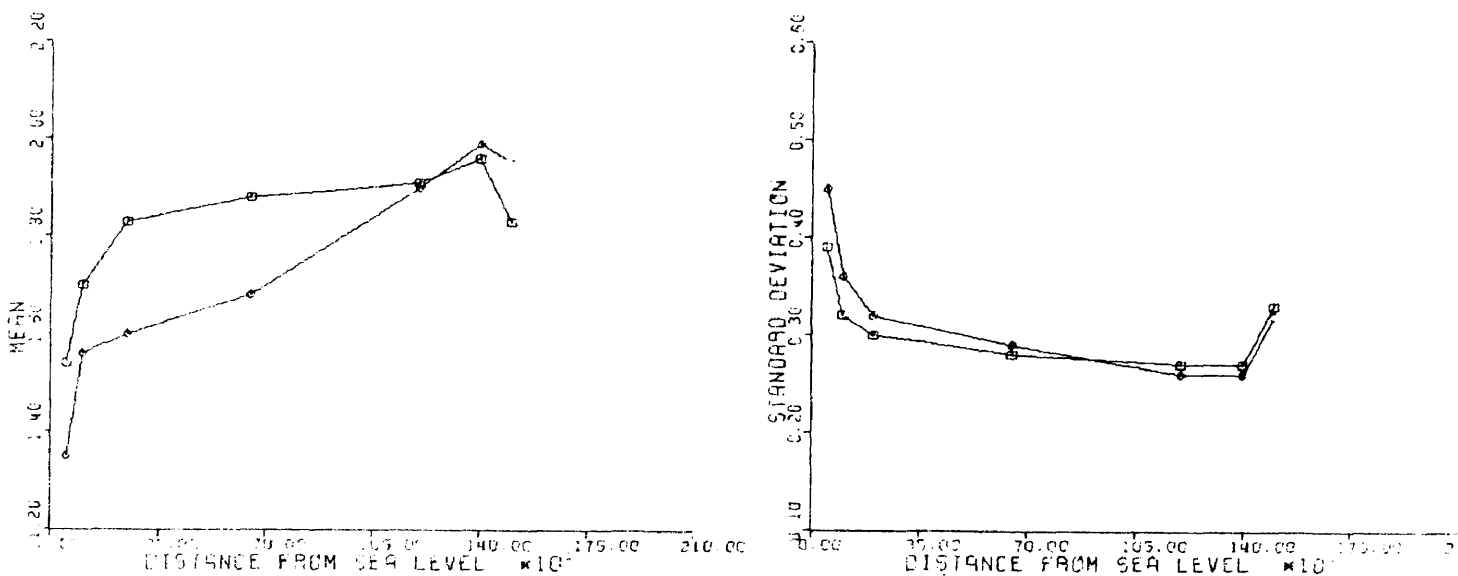


Figure 45. Grain-size moments across Transect B south of Corolla, North Carolina (Whalehead Hill).

the beach during 11 m/sec (24 miles/hour) winds (see Table 8) from the southwest were conducted at both areas. At the Whalehead Hill transect the transport rate was about 0.07 g/cm·sec while at the Barbours Hill transect it was only 0.01 g/cm·sec. For a one hour period and a one meter width, this is equivalent to a difference of over 20 kg of sand. The explanation for this large difference in transport rate is the lack of thick eolian flat and foredune vegetation in the Whalehead region which does not inhibit the flux of sand as it does in the Barbours Hill region.

Figure 45 contains plots of the four moments after a period of onshore winds (Table 4). Notice that in the first three moments there is a slight trend of increasing phi values (fining) across the barrier from the ocean beach, indicating some of the expected changes in grain size characteristics as the sediment is carried across the barrier under the influence of the onshore winds. The mean grain size decreases slightly, the sorting improves, and the skewness increases towards the fine tail as would be expected. Kurtosis does not indicate any clear trend. The cross-barrier trends in Figure 45 are not pronounced, but they do correlate with known transport measurements and vegetation characteristics. As indicated in Figure 27, the extent of vegetation and height of foredunes south of Corolla is much less than in False Cape. Due to this lack of vegetation there was a flux of sand, which extended a distance of approximately 0.5 km in response to both onshore and offshore winds, resulting in eolian grading of sand.

Conclusions

1. No pronounced cross-barrier eolian grading of sand between the beach and dune was observed with the exception of surface samples

gathered on the transect south of Corolla at Whalehead Hill after onshore winds and after offshore winds.

2. The complete lack of grading in the Barbours Hill region is attributed to the effects of a thick vegetation cover which has effectively stabilized the interior of the barrier spit, thus precluding eolian grading of sand.

3. In the Whalehead Hill region, diagrams of the four moments indicate a greater flux of sand in response to onshore and offshore winds than is evident in the False Cape region. This greater flux is attributed to a lower foredune system and less extensive vegetation.

4. These grading characteristics corroborate field measurements of sand transport which indicate that there is a much greater sand transport rate during both onshore and offshore winds in the Whalehead Hill region than to the north in False Cape State Park.

5. The only pronounced changes across the transect were at the foreshore where wave activity resulted in a coarser sand in contrast with eolian deposition further inland. The ability to discriminate beach and dune depositional environments by grain size analysis confirms the studies of Mason and Folk (1958), Friedman (1961) and Ahlbrandt (1975).

DEVELOPMENT OF A MODEL TO
PREDICT EOLIAN SAND TRANSPORT

A quantitative estimate of the rate and amount of sand movement over a fairly long period is necessary to accurately evaluate the role of eolian sand transport with respect to:

- 1) Sediment dynamics of a barrier spit
- 2) Migration of large sand dunes
- 3) Orientation of parabolic dunes
- 4) Effect of northern and southern cross-barrier transect differences
- 5) Effect of sand fencing.

Field measurements of eolian sand transport can provide instantaneous transport rates for a particular set of environmental conditions but there is no instrument developed which will measure and record continuously the eolian sand transport. Therefore an empirical computer model was developed to compute directional eolian sand transport from one year (2/76-2/77) of wind and precipitation data. Unlike sand transport these environmental variables are easily measured and recorded by available instrumentation. The model was developed after careful consideration of the coastal mechanisms of eolian sand transport to determine the important variables in the transport process, the best equations of transport available, and what equations if any must be developed to compute eolian sand transport in the coastal zone. The

model was then verified using field measurements of eolian sand transport.

Mechanism of Eolian Sand Transport

Atmospheric winds blowing over a surface will, depending on the wind velocity, particle weight, and other environmental variables, initiate three different types of motion; suspension, surface creep, and saltation. For a particle to travel in suspension its settling velocity must be less than the upward eddy diffusion currents. During eolian transport, suspension is rarely the method of travel. Bagnold (1941) and Horikawa and Shen (1960) showed that for sand transported by wind, less than 5% of the material travels in suspension while some 20% travels as surface creep and 70% travels by a mechanism known as saltation. During saltation, as shown in Figure 46, individual grains are ejected from the surface and follow trajectories under the influence of gravity and shear stress. In reality the particles do not follow such distinct paths as in Figure 46. Instead observations suggest a more random trajectory which is reasonable considering the turbulence of the air and the randomness of impact of the particles. If the particles do not enter suspension they will travel with the wind a certain distance and then gradually descend to the surface when the particles may either rebound back into the so-called saltation layer, or eject other particles by the transfer of momentum and remain behind. The grains moving along the immediate surface, the surface creep, receive their momentum from grains returning to the surface. Surface winds are generally turbulent for any velocities that exceed 1.0 m/sec (Binder, 1973). Turbulence is indicated by irregular velocity fluctuations generally known as gusts. For the case of eolian sand transport, wind movement can be described as a turbulent boundary layer above an aero-

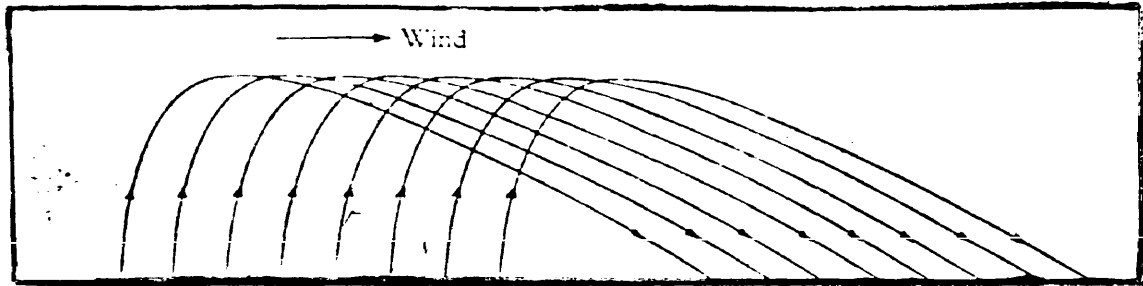


Figure 46. Saltation

dynamically rough surface.

As the wind flows over the surface of a particle, movement is initiated if the upward directed pressures exerted on the grain overcome the forces of gravity. The air as it flows over the surface of the particle, exerts a resultant force. One component, along the line of the wind velocity, is the resistance or drag. At right angles to the drag is the lift force. The total drag on a particle immersed in a fluid is dependent on the viscous and inertial forces. Therefore the drag is proportional to the Reynolds number. The drag component itself may be divided into components; skin friction and pressure drag. The skin friction component is due to the formation of the boundary layer on the surface of the particle. Pressure drag is caused by pressure differences upstream and downstream from the particle (Binder, 1973).

The velocity above the surface of a particle resting on a bed is greater than below the particle. It follows then, by the Bernoulli equation, that the pressure on the lower side of the particle will be greater than the pressure on the surface above. This pressure difference represents the lift component of the resultant force on a particle immersed in a flowing fluid.

Kadib (1966) described lift (\bar{L}) by the equation:

$$\bar{L} = C_p \frac{U^2 A}{2} D^2$$

where:

C = lift coefficient

U = instantaneous velocity acting as a distance y from the surface

p = density of air

D = diameter of particle

A = shape factor for grain area

Chepil (1959) has shown that the equilibrium between the lift and drag, and velocity is influenced by the diameter, shape, and density of the grains, the angle of the repose of the grains with respect to the mean drag level of the wind, the closeness of packing of the top grains on the sediment bed, and the lift and drag impulses of turbulence. Chepil (1961) also showed that the ratio of lift to drag is greatest at the surface. The near vertical liftoff of a grain during saltation is a result of lift, the effect of rebounding, and the shear stress. However, it is the shear force which is critical in dislocating the particle from the surface. The observed low angle of descent of a saltating grain (Bagnold, 1941) is due to the acceleration induced by drag as the particle falls under gravity.

The nature of eolian transport is made very complex by the effects of turbulence, degree of hiding in the laminar sublayer, height of the saltation layer, and by many environmental variables which are listed in Table 5. Because of the complexity of the transport process, equations used to predict the quantity of sand transported have been largely empirically derived.

From wind tunnel and field data, Bagnold (1941) developed the following equation which is still the most widely used;

$$Q = C \frac{d}{D} \frac{p}{g} U_*^3$$

where:

- Q = amount of sand transported (g/cm·sec)
- U_* = shear velocity
- C = an empirical coefficient which varies with the uniformity of the sand
- d = diameter of the sand
- D = standard diameter of 0.25 mm sand
- p = specific weight of air
- g = gravity

TABLE 5
 VARIABLES IN EOLIAN SAND TRANSPORT PROCESS

Wind	Surface	Topography	Soil	Surface Effects
Speed	Roughness	Flat	Texture	Removal
Direction	Obstructions	Undulating	Structure	Deposition
		Broken	Organic content	Surface markings
Temperature	Temperatures		Moisture content	Dune formations
Humidity	Vegetation Cover		Soil binders	

Kawamura (1951) developed the equation:

$$Q = k \frac{\rho}{g} (U_* - U_{*t}) (U_* + U_{*t})$$

where:

k = constant determined by the experiment
 U_{*t} = threshold shear velocity which depends on the cohesive properties of the soil, such as moisture or organic binders

O'Brien and Rindlaub (1936) developed from field observations the expression;

$$Q = 0.036 U^3$$

where

U = wind velocity

Hsu (1971) recently developed the expression for transport over a beach

$$Q = k F^3 = k \frac{(U_*)^3}{(gd)^{\frac{1}{2}}}$$

where

F = a special froude number
 k = constant

Here Q is proportional to the shear stress and inversely proportional to the product of gravitational acceleration (g) and mean grain size (d).

Yves-Belly (1964) tested the accuracy of the Kawamura, Bagnold, and O'Brien formulas and found the O'Brien equation to be inadequate and the Bagnold equation to be the best. These empirical equations of Bagnold and Hsu were used in development of a computer model. Unfortunately these equations were determined for conditions where the effects of vegetation, soil moisture and soil freezing were ignored. Obviously in the temperate coastal zone these factors cannot be ignored if an accurate model of eolian sand transport is to emerge.

Wind Data

The most important environmental factors (Table 5) in the transport process are the speed, direction, and structure of the wind. In this model the local Corolla station digitized wind data (see discussion of wind climate and Appendix 1) were input into the Bagnold and Hsu transport equations. However, first these wind data from 53 m above mean sea level had to be related to the shear velocity at the surface.

The standard profile of wind flowing over a surface can be expressed as (Binder, 1973):

$$U = \frac{2.3}{k} U_* \log \frac{z}{z_0}$$

where

- U = velocity at height z
- k = Von Karman constant (approximately = 0.40)
- z₀ = aerodynamic roughness height defined under the boundary condition that U_z = 0 at z = z₀. The value of z₀ depends on the underlying surface.

The velocity profile and therefore the value of U_{*} is also influenced by the thermal stability of the wind profile. In general the profile will fit the theory under neutral conditions. However, when the air is thermally stratified such as during the night, the wind profile may be distinctly nonlogarithmic (Horikawa, 1960). Hsu (1971) has shown that a sea breeze can often exhibit a non-logarithmic velocity profile.

However, as an approximation Hsu (1973) used the logarithmic law, to compute shear velocity at the surface from routine wind data at standard heights, obtaining the expression:

$$U - U_t = \frac{U_*}{k} \ln \frac{z}{z_{0t}}$$

where

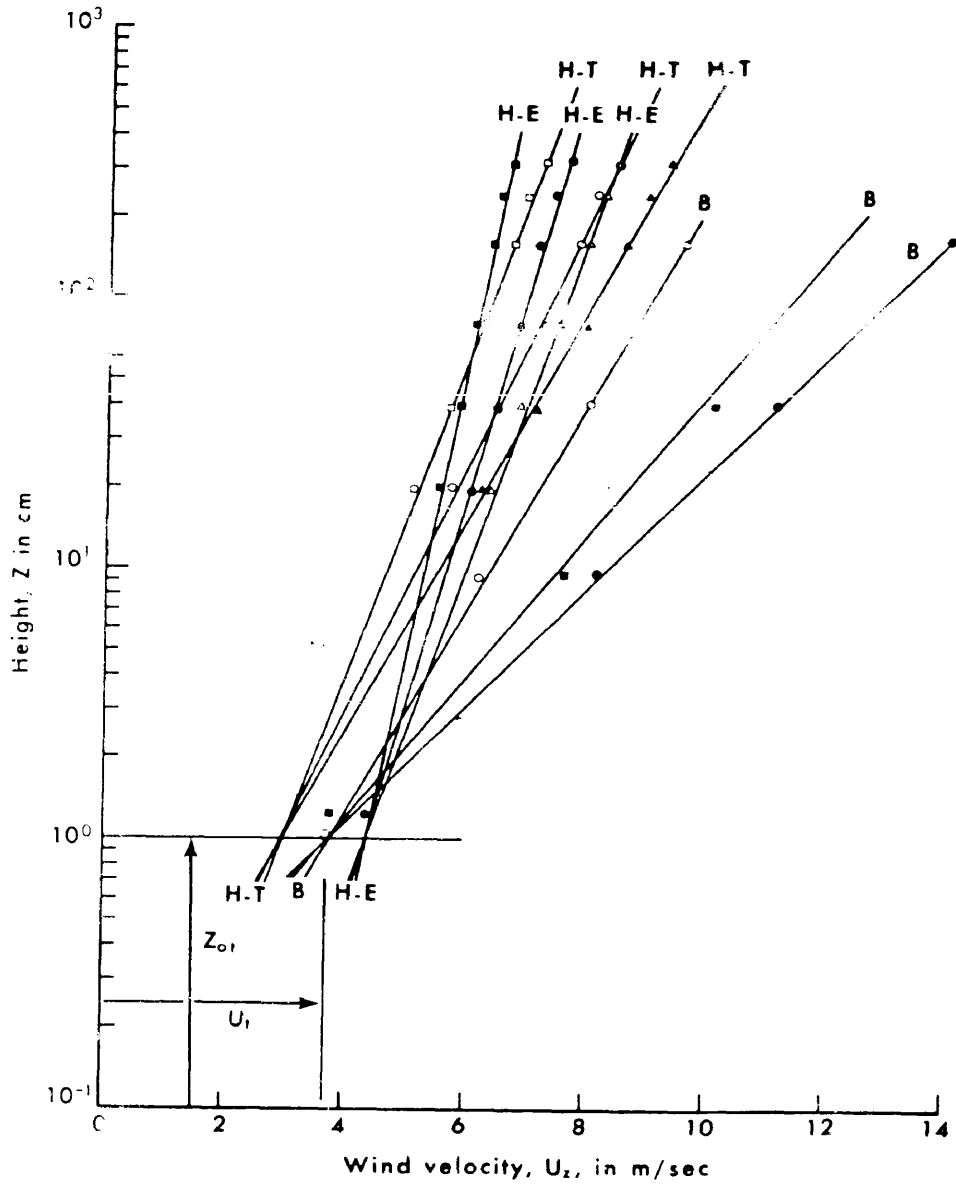
U = wind velocity at anemometer
 U_t = threshold wind velocity
 U_* = shear velocity
 k = Von Karman constant (= .4)
 z = height of anemometer
 z_{ot} = roughness length defined under boundary
 condition that $U=U_t$ at $z=z_{ot}$

Figure 47 shows the data from which this equation was determined. This shear velocity equation was used in the eolian sand transport model to calculate the shear velocity from the recorded wind data (see subroutine SHRVL, Appendix 4).

In desert regions the use of shear velocity and transport equations would be sufficient for an eolian sand transport model. However, in the temperate coastal zone, precipitation, freezing of the sand, and vegetation must also be accounted for, because these environmental variables greatly influence the rate of sand transported. Kadib (1964) chose to ignore these variables in an overly simplistic calculation of sand transport by wind on natural beaches. As will be shown, ignoring these variables can lead to overestimates of eolian sand transport ranging from 20-40%.

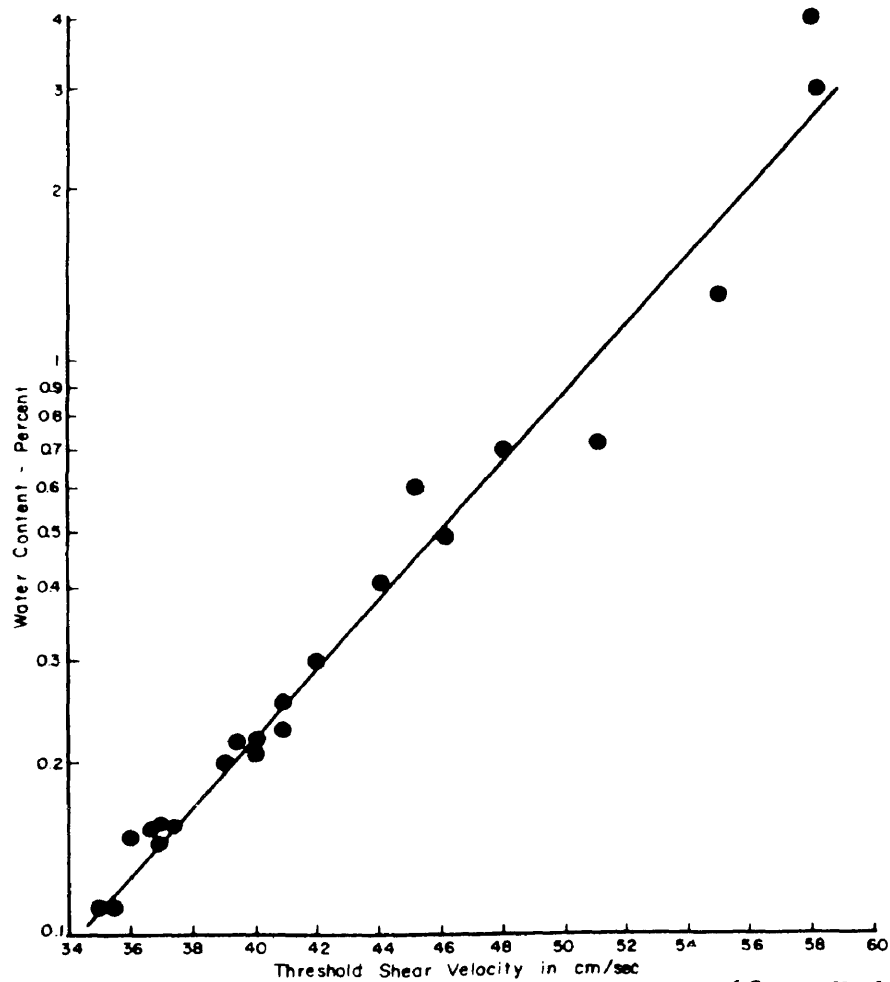
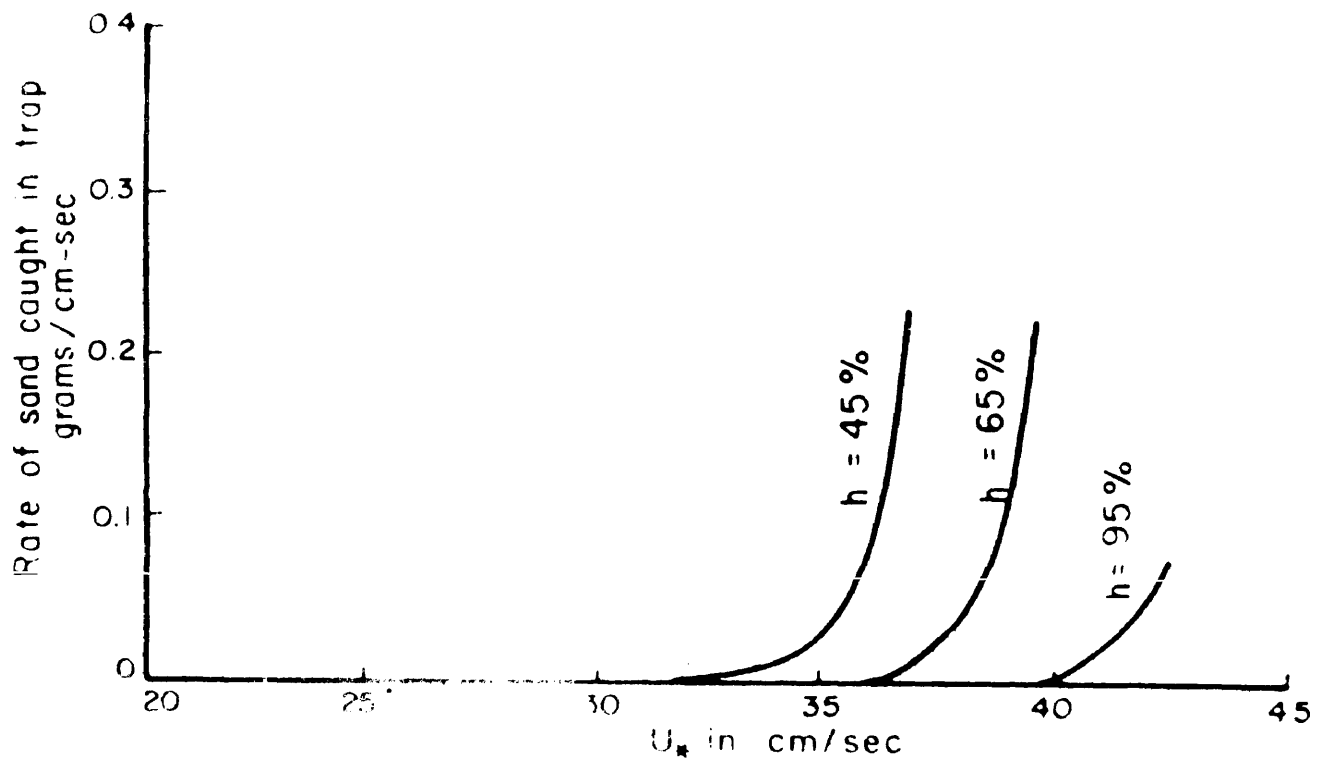
Soil Moisture Variable

Chepil (1956) and Johnson (1963) have investigated the effect of soil moisture on the erodibility of the soil. It was found that air humidity has only a small effect on the threshold shear velocity (U_{*t}) while water content of the soil greatly increases the strength of the wind necessary to initiate movement (Figure 48). Kadib (1964) suggested use of an equation to solve for U_{*t} which takes the effect of moisture into account.



(from Hsu, 1971)

Figure 47. Observed wind velocity vertical distribution over sand surfaces when sand was in motion. The data lines are indicated by H-E, H-T, and B for measurements made by Hsu over an Ecuador and Texas beach, and by Bagnold for measurements made in the Libyan Desert.



(from Kadib, 1964)

Figure 48. Experimental data illustrating the effect of humidity (top) and soil water content (bottom) on the threshold shear velocity.

$$U_{*t} = A(1 + \frac{1}{2}(\frac{h}{100})) \frac{\sigma - p}{p} \text{ gd} \quad \text{for the effect of air moisture}$$

$$U_{*t} = A(1.8 + 0.6 \log w) \frac{\sigma - p}{p} \text{ gd} \quad \text{for the effect of soil moisture}$$

where

w = soil moisture (%)
 h = relative humidity
 p = density of air
 σ = density of the sand grains
 A = fluid threshold value approximately = .1
 g = gravitational acceleration

Chepil (1956) showed that the effect of the moisture was due to the cohesive force of adsorbed water films which surround the soil particles. The second equation listed above for the effect of soil moisture on the threshold shear velocity was including in this model (see subroutine THRSH, Appendix 4). In the model, if the calculated shear velocity for a three hour period does not exceed the calculated threshold shear velocity, due to either a large amount of rain or a low wind velocity, then no transport is calculated.

The problem in utilizing the above soil moisture equation was to develop a relationship between precipitation and actual soil moisture content because the threshold equation requires the input of this variable (w). Unfortunately calculation of soil moisture is very difficult because it is dependent on (Chang, 1968):

- 1) Precipitation
- 2) Amount of sunlight
- 3) Wind profile near ground
- 4) Vapor pressure profile near ground
- 5) Temperature
- 6) Amount of transpiration
- 7) Soil texture
- 8) Vegetation density

To calculate soil moisture from theoretical considerations, one must be able to predict the amount of moisture imparted to the soil by a given amount of precipitation and then calculate an evapotranspiration rate using all the environmental variables listed above. This type of data was not available for the one year period from local climatological monthly summaries and no equipment was available to measure evapotranspiration (lysimeters and evaporimeters) in the field. Therefore an empirical moisture equation, using the available data (wind velocity, temperature, and precipitation), was developed from field measurements of sand moisture content.

Fifteen sand samples were gathered during and after rain events on bare sand along Currituck Spit. In addition, 20 samples were collected for soil moisture determination after applying known amounts of water to a box filled with Currituck Spit beach sand. In both sets of samples the wind velocity, temperature, and precipitation during the sampling were recorded. The samples were returned to the lab and then weighed before and after drying. The moisture content was calculated according to the relation:

$$\% \text{ water} = \frac{\text{Wet Weight} - \text{Dry Weight}}{\text{Dry Weight}}(100)$$

Table 6 lists all the data collected for determination of a soil moisture equation.

Soil Moisture Equation

The soil moisture measurements, as a function of wind velocity, temperature and precipitation, were input into a Computer Linear Least-Squares Curve Fitting Program which was on file at the College of William and Mary Computer Center. A detailed description of the program and

TABLE 6

LISTING OF SOIL MOISTURE DATA INPUT INTO LINEAR LEAST-SQUARES CURVE
FITTING PROGRAM. SOIL MOISTURE WAS MEASURED AS A FUNCTION OF
PRECIPITATION, TEMPERATURE AND WIND SPEED.

Obsv.	Precipitation mm x 10 ⁻¹		Temperature °C		Wind Speed m/sec		Moisture % by weight	
1	8.63	01	1.11	01	1.23	01	6.50	00
2	8.63	01	1.60	01	1.23	01	3.00	00
3	1.14	02	8.94	00	2.40	01	1.23	01
4	1.01	02	1.78	01	2.12	01	2.00	00
5	3.81	01	8.94	00	1.28	01	1.00	00
6	2.54	01	1.56	01	1.00	01	5.00	-01
7	8.89	01	1.56	01	2.40	01	1.40	00
8	1.01	02	1.78	01	2.96	01	1.00	-01
9	6.35	01	8.94	00	1.56	01	3.40	00
10	5.08	01	1.34	01	7.28	00	1.50	00
11	7.62	01	1.11	01	2.12	01	3.00	00
12	7.62	01	1.11	01	1.00	01	5.40	00
13	7.87	01	1.34	01	1.00	01	5.00	00
14	6.35	01	1.56	01	2.40	01	4.00	-01
15	2.54	01	2.23	00	1.79	01	7.00	00
16	5.08	01	2.23	00	1.79	01	1.20	01
17	7.62	01	2.23	00	1.79	01	1.60	01
18	1.01	02	2.23	00	1.79	01	2.00	01
19	1.27	01	2.23	00	1.79	01	4.20	00
20	3.81	01	2.23	00	1.79	01	7.20	00
21	1.27	01	4.02	00	2.40	01	1.00	00
22	2.54	01	4.02	00	2.40	01	3.00	00
23	3.81	01	4.02	00	2.40	01	5.00	00
24	5.08	01	4.02	00	2.40	01	8.20	00
25	7.62	01	4.02	00	2.40	01	1.40	01
26	1.01	02	4.02	00	2.40	01	1.90	01
27	2.54	00	4.02	00	2.40	01	2.00	-01
28	1.27	01	6.70	00	2.40	01	1.00	-01
29	3.81	01	1.11	01	2.40	01	5.00	-01
30	1.27	01	7.15	00	1.73	01	4.00	-01
31	2.54	01	7.15	00	1.73	01	3.00	00
32	3.81	01	7.15	00	1.73	01	3.50	00
33	5.08	01	7.15	00	1.73	01	6.50	00
34	7.62	01	7.15	00	1.73	01	1.25	01
35	1.01	02	7.15	00	1.73	01	1.70	01

the least-squares method can be found in the book by Daniel and Wood (1971) which accompanies the program. Simply stated the least-squares method finds the values of constants in a chosen equation which minimize the sum of the squared deviations of the observed values from those predicted by the equation. The form of the equation predicted by this program is

$$Y = b_0 + b_1x_1 + b_2x_2 + b_3x_3$$

where

Y = dependent variable (soil moisture)
 x_1, x_2, x_3 = dependent variables
 b_0, b_1, b_2, b_3 = constants calculated from the data

Table 6 is a listing of the input data. The first independent variable is precipitation in tenths of mm. The second independent variable is temperature in degrees centigrade while the third variable is wind speed in m/sec. The one dependent variable is the measured moisture content in percent.

Table 7 lists the statistics, coefficients, and ordered residuals for the data set listed in Table 6. The fitted linear least-squares equation has the form:

$$\begin{aligned} \% \text{ moisture} = & 8.4 + (.159 \times \text{Precipitation}) + (-1.02 \times \text{Temperature}) \\ & + (-1.73 \times \text{wind velocity}) \end{aligned}$$

Since the standard error of the coefficients is about 0.03, the values of the coefficients, might well be written as $b \pm 0.03$.

The F-value can be compared with tabulated values to give a joint test of the hypothesis that all coefficients are zero against the alternative that the equation as a whole produced a significant reduction in the total sum of squares (Daniel and Wood, 1971). The tabular value for F (99.5, 31, 3) is about 42.3 therefore there is a highly significant (greater than 99.5%) fit. The multiple correlation coefficient squared

TABLE 7

OUTPUT OF LINEAR LEAST-SQUARES CURVE FITTING PROGRAM

ORDERED BY RESIDUALS

Obsv.	Obs. Y	Fitted Y	Ordered Resid.	Seq.
6	0.500	-5.278	5.778	1
35	17.000	14.242	2.758	2
26	19.000	16.273	2.727	3
34	12.500	10.207	2.293	4
14	0.400	-1.652	2.052	5
25	14.000	12.237	1.763	6
29	0.500	-1.122	1.622	7
16	12.000	11.097	0.903	8
17	16.000	15.132	0.868	9
31	3.000	2.136	0.864	10
18	20.000	19.168	0.832	11
28	0.100	-0.591	0.691	12
33	6.500	6.171	0.329	13
30	0.400	0.118	0.282	14
24	8.200	8.202	-0.002	15
10	1.500	1.527	-0.027	16
15	7.000	7.061	-0.061	17
27	0.200	0.534	-0.334	18
13	5.000	5.480	-0.480	19
2	3.000	3.563	-0.563	20
4	2.000	2.603	-0.603	21
32	3.500	4.153	-0.653	22
19	4.200	5.044	-0.844	23
3	12.300	13.268	-0.968	24
7	1.400	2.383	-0.983	25
8	0.100	1.146	-1.046	26
21	1.000	2.149	-1.149	27
22	3.000	4.166	-1.166	28
23	5.000	6.184	-1.184	29
20	7.200	9.079	-1.879	30
12	5.400	7.360	-1.960	31
1	6.500	8.585	-2.085	32
5	1.000	3.104	-2.104	33
11	3.000	5.417	-2.417	34
9	3.400	6.654	-3.254	35

Ind. Var (I)	Name	Coef. B(I)	S.E. Coef.	T-Value	R(I)SQRD
0		8.41702D 00			
1	PRECIP	1.58879D-01	1.09D-02	14.6	0.1575
2	WIND	-1.02152D 00	7.11D-02	14.4	0.1834
3		-1.73447D-01	6.15D-02	2.8	0.0402

TABLE 7 (Continued).

No. of Observations	35
No. of Ind. Variables	3
Residual Degrees of Freedom	31
F-Value	99.9
Residual Root Mean Square	1.87622951
Residual Mean Square	3.52023719
Residual Sum of Squares	109.12735287
Total Sum of Squares	1163.71600000
Mult. Correl. Coef. Squared	.9062

is .9062. This indicates that 91 percent of the total sum of squares of y is accounted for by the fitted equation.

Figure 49 is a plot generated by the computer program of the empirical distribution of residuals. The residuals fall, as they should, approximately on a straight line. There are no outliers (wild data points). Figure 50 is a plot of the residuals versus the fitted values of y . The points fall, as they should on both sides of the zero line.

The linear equation derived from soil moisture data has a highly significant F value, a high multiple correlation coefficient, and a normal distribution of residuals. Therefore this equation represents a very good fit of the data. The moisture equation was used in the empirical model to predict the soil moisture content every three hours from precipitation, wind velocity and temperature data (see subroutine moist, Appendix 4).

Vegetation Effects

As indicated in Table 5, vegetation is another variable influencing the transport of sand by wind. Vegetation, as shown in Figure 51, increases the value of the surface roughness parameter (Z_0) and thus reduces the sand transport rate. Bressolier and Thomas (1977) have shown that the increase in Z_0 is a function of the height and density of the vegetation. For a typical dune grass (*Ammophilla* sp.) they suggest a Z_0 ranging from 0.29-6.30 centimeters. A bare sand surface has a Z_0 of approximately 0.1 cm (Yves-Belly, 1964). Along Currituck Spit vegetation cover varies widely. Therefore, a range of Z_0 values (1.0, 3.0, 6.0, 9.0 and 12.0 cm) were input into the model to reflect differing vegetation distributions.

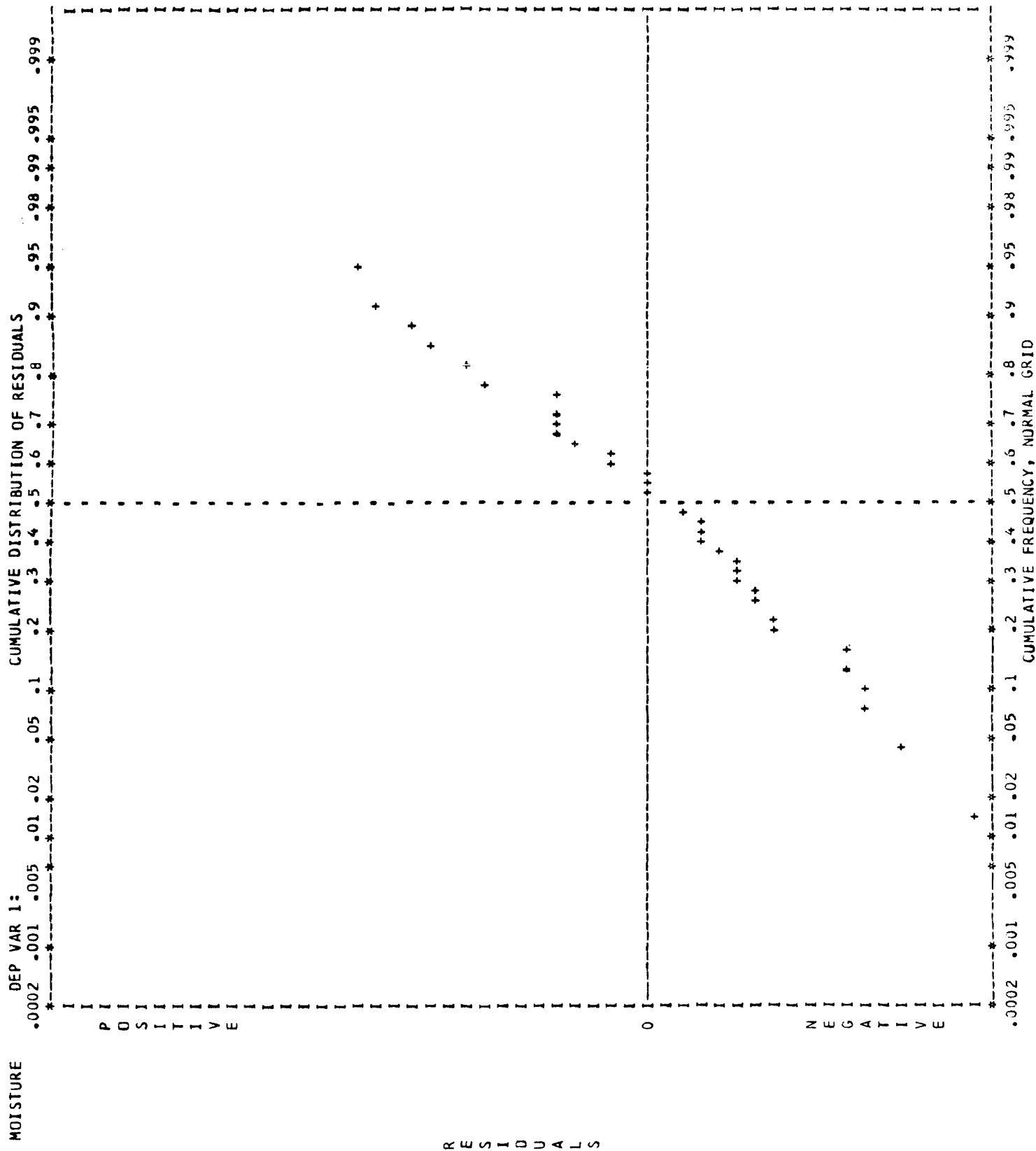


Figure 49. Computer generated plot of the empirical distribution of residuals determined from sand moisture data.

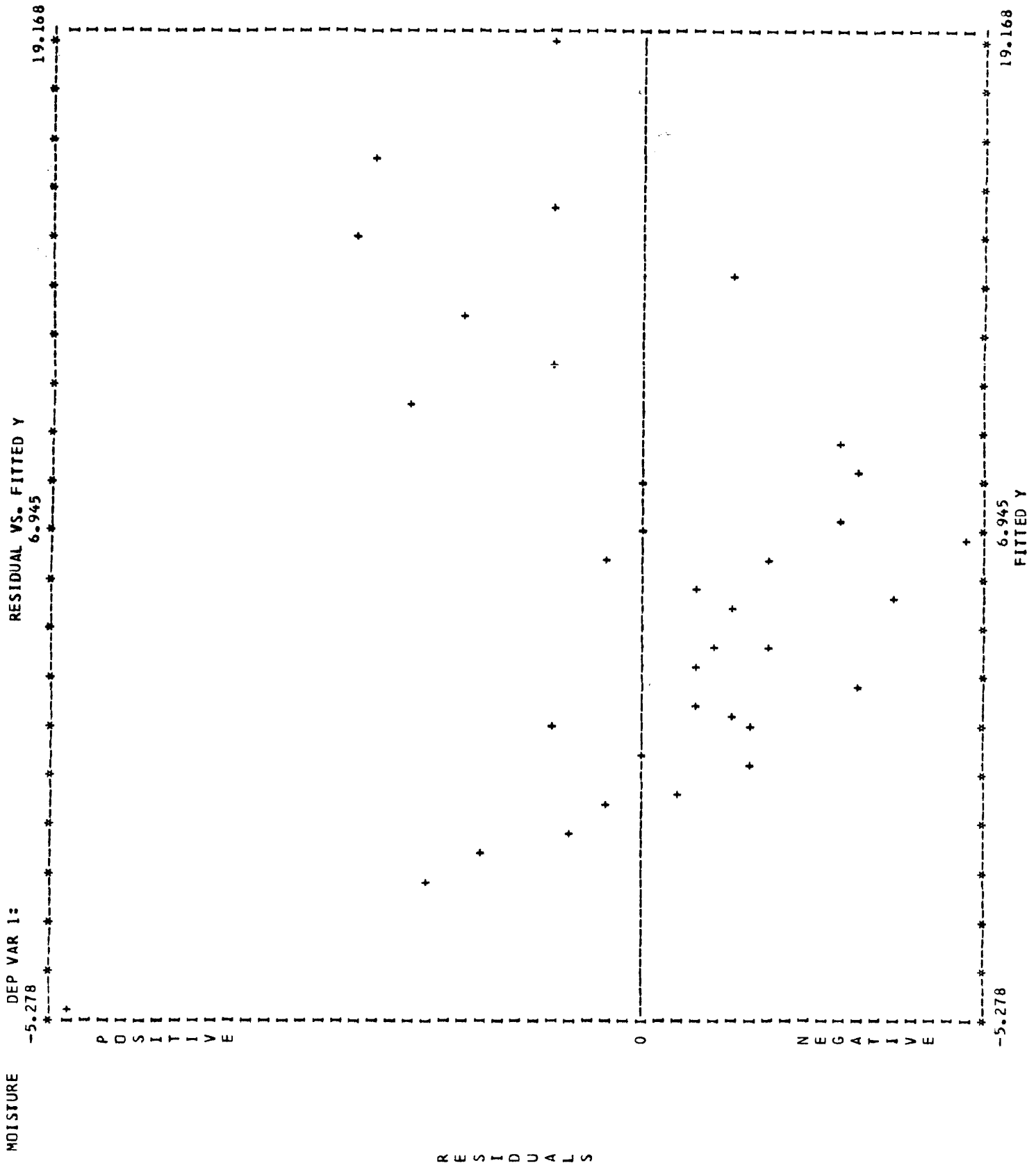


Figure 50. Computer generated plot of the residuals versus the fitted value of y (sand moisture content).

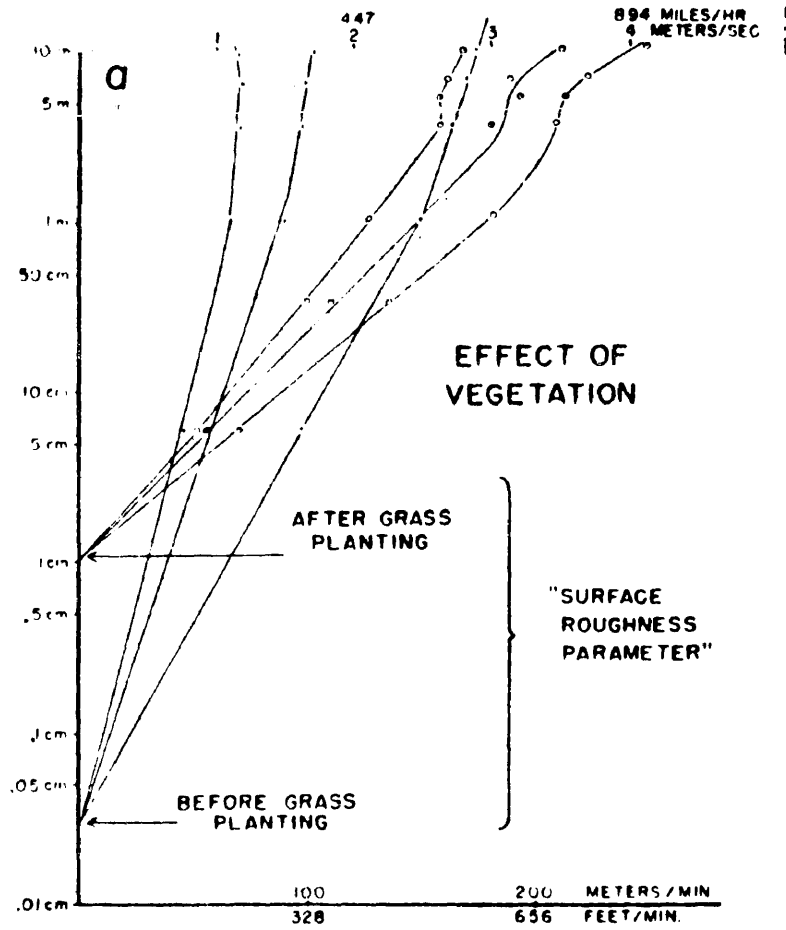


Figure 51. The change in surface roughness parameter and dune wind profiles before and after grass planting on an Indiana coastal sand dune. (after Olson, 1958)

Vegetation, by reducing the wind velocity at the surface, also increases the soil moisture content relative to a bare sand surface. The equation which computes soil moisture content was developed for bare sand conditions. Chang (1968) estimated that under identical environmental conditions the moisture content of a vegetated surface will be 20 percent greater than a bare surface. Therefore, in the MOIST subroutine (Appendix 4), the computed moisture content is multiplied by 1.2 for transport across vegetated surfaces.

Summary of Model

From considerations of the mechanism of eolian sand transport and development of an empirical moisture equation, a model was developed which computes the transport of sand by wind for an entire year of record. During each three hour period (8 per day) the wind velocity, temperature, and precipitation data is read into the model. If the temperature is less than -1.0°C the model skips to the next three hour period because field observations indicated that the soil was frozen below this temperature and therefore no transport could occur. Comparison of the model run with and without the inclusion of the freezing variable indicate that the sand freezing decreases total transport by only three percent (offshore transport) or nine percent (onshore transport). However, at low temperatures the evaporation rate is slow and therefore, given a certain amount of precipitation the soil moisture content will be greater than at higher temperatures, as shown in the derived soil moisture equation.

The next step in the model is calculation of a soil moisture content as a function of the temperature, wind velocity, precipitation, and soil moisture content of the previous three hour interval. Then

the model calculates a threshold shear velocity for this soil moisture content. For a soil moisture of 0.0 percent the threshold shear velocity was determined by Kadib (1964) to be about 30.0 cm/sec and his value was adopted for this model. The wind velocity from the Corolla Station anemometer for the three hour period is then used to calculate a shear velocity at the surface. If this shear velocity is not greater than the calculated threshold shear velocity, no transport is computed and the model moves to the next three hour interval. However, if the shear exceeds the threshold a sand transport rate ($\text{g/cm}\cdot\text{sec}^{-1}$) is calculated using the equations of Bagnold (1941) and Hsu (1973). The model was then run for differing vegetation densities by changing the value of the surface roughness parameter (20). Table 8 is a sample of the output from the model.

Variables Not Included in Model

Eolian sand transport is a very complex process. This transport model includes only wind speed and direction, temperature, moisture, vegetation and grain size as variables. However, other important variables (Table 5) were not included in development of the model. The shear velocity equation assumes a neutral atmosphere with a logarithmic wind profile although Hsu (1971), who developed the equation, has shown that this assumption may not always be valid. In addition the effects of topographic and surface obstructions were not considered. Instead the model calculates transport across a flat surface assuming that surface formations (ripples, dunes etc.,) affect all directions of transport equally. Binding of the sand by salt, which would increase the threshold shear velocity, was also not a variable included in the model. Studies by Svasek and Terwindt (1974)

TABLE 8
RESULTS OF SAND TRANSPORT CALCULATIONS

Date	Wind Direction	Wind Speed m/sec	Thresh Velocity cm/sec	Sheer Velocity cm/sec	Hsu Transport g/cm/sec	Bagnold Transport g/cm/sec	Rain cm	% Water
2/02/76	215.	15.	28.00	44.42	0.14	0.20	0.0	0.00
2/02/76	275.	16.	28.00	47.96	0.18	0.25	0.0	0.00
2/02/76	295.	16.	28.00	47.96	0.18	0.25	0.0	0.00
2/02/76	285.	16.	28.00	47.96	0.18	0.25	0.0	0.00
2/02/76	305.	13.	28.00	33.78	0.06	0.09	0.0	0.00
6/02/76	5.	10.	28.00	29.15	0.04	0.07	0.01	0.00
6/02/76	15.	11.	28.00	33.62	0.06	0.11	0.0	0.00
7/02/76	5.	10.	28.00	29.15	0.04	0.07	0.0	0.00
7/02/76	5.	10.	28.00	29.15	0.04	0.07	0.0	0.00
8/02/76	255.	13.	28.00	33.78	0.06	0.09	0.0	0.00
10/02/76	215.	13.	28.00	33.78	0.06	0.09	0.0	0.00
10/02/76	235.	13.	28.00	37.32	0.09	0.12	0.0	0.00
11/02/76	235.	13.	28.00	35.55	0.07	0.10	0.0	0.00
11/02/76	245.	11.	28.00	28.46	0.04	0.05	0.0	0.00
13/02/76	245.	11.	28.00	28.46	0.04	0.05	0.0	0.00
14/02/76	25.	12.	28.00	38.08	0.09	0.16	0.0	0.00
15/02/76	215.	12.	28.00	30.23	0.05	0.06	0.0	0.00
16/02/76	235.	13.	28.00	33.78	0.06	0.09	0.0	0.00
16/02/76	245.	12.	28.00	30.23	0.05	0.06	0.0	0.00
16/02/76	225.	12.	28.00	30.23	0.05	0.06	0.0	0.00
17/02/76	235.	12.	28.00	30.23	0.05	0.06	0.0	0.00
17/02/76	235.	13.	28.00	37.32	0.09	0.12	0.0	0.00
17/02/76	235.	12.	28.00	30.23	0.05	0.06	0.0	0.00
18/02/76	205.	14.	28.00	40.87	0.11	0.15	0.0	0.00
18/02/76	215.	15.	28.00	44.42	0.14	0.20	0.0	0.00
18/02/76	235.	16.	28.00	47.96	0.18	0.25	0.0	0.00

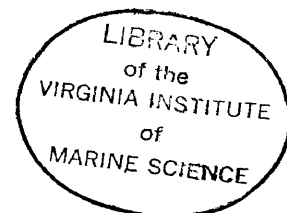


TABLE 8 (Continued).

Date	Wind Direction	Wind Speed m/sec	Thresh Velocity cm/sec	Sheer Velocity cm/sec	Hsu Transport g/cm/sec	Bagnold Transport g/cm/sec	Rain cm	% Water
22/02/76	215.	18.	28.00	33.78	0.06	0.09	0.0	0.00
22/02/76	215.	15.	28.00	44.42	0.14	0.20	0.0	0.00
22/02/76	215.	15.	28.00	44.42	0.14	0.20	0.0	0.00
22/02/76	225.	12.	28.00	30.23	0.05	0.06	0.0	0.00
22/02/76	215.	13.	28.00	33.78	0.06	0.09	0.0	0.00
22/02/76	245.	16.	28.00	47.96	0.18	0.25	0.0	0.00
22/02/76	5.	12.	28.00	38.08	0.09	0.16	0.0	0.00
23/02/76	355.	11.	28.00	33.62	0.06	0.11	0.0	0.00
29/02/76	215.	12.	28.00	30.23	0.05	0.06	0.0	0.00
5/03/76	245.	12.	28.00	30.23	0.05	0.06	0.0	0.00
5/03/76	245.	13.	28.00	37.32	0.09	0.12	0.0	0.00
5/03/76	245.	12.	28.00	30.23	0.05	0.06	0.0	0.00
5/03/76	215.	12.	28.00	30.23	0.05	0.06	0.0	0.00
6/03/76	245.	12.	28.00	30.23	0.05	0.06	0.0	0.00
9/03/76	95.	13.	28.00	47.02	0.17	0.30	0.05	0.00
9/03/76	105.	13.	28.00	47.02	0.17	0.30	0.10	0.00
9/03/76	335.	12.	28.00	30.23	0.05	0.06	0.0	0.00
9/03/76	5.	11.	28.00	33.62	0.06	0.11	0.0	0.00
12/03/76	140.	11.	28.00	33.62	0.06	0.11	0.0	0.00
12/03/76	195.	13.	28.00	37.32	0.09	0.12	0.06	0.00
13/03/76	225.	13.	28.00	37.32	0.09	0.12	0.0	0.00
13/03/76	225.	16.	28.00	47.96	0.18	0.25	0.0	0.00
13/03/76	225.	14.	28.00	40.87	0.11	0.15	0.0	0.00
13/03/76	235.	16.	28.00	47.96	0.18	0.25	0.0	0.00
13/03/76	245.	14.	28.00	40.87	0.11	0.15	0.0	0.00
13/03/76	315.	16.	28.00	47.96	0.18	0.25	0.0	0.00
13/03/76	325.	13.	28.00	37.32	0.09	0.12	0.0	0.00

TABLE 8 (Continued).

Date	Wind Direction	Wind Speed m/sec	Thresh Velocity cm/sec	Sheer Velocity cm/sec	Hsu Transport g/cm/sec	Bagnold Transport g/cm/sec	Rain cm	% Water
16/03/76	235.	13.	28.00	33.78	0.06	0.09	0.01	0.00
16/03/76	315.	18.	28.00	55.05	0.28	0.38	0.01	0.00
17/03/76	315.	12.	28.00	30.23	0.05	0.06	0.0	0.00
19/03/76	245.	12.	28.00	30.23	0.05	0.06	0.0	0.00
21/03/76	215.	12.	28.00	30.23	0.05	0.06	0.0	0.00
21/03/76	225.	12.	28.00	30.23	0.05	0.06	0.0	0.00
21/03/76	225.	16.	28.00	47.96	0.18	0.25	0.0	0.00
21/03/76	245.	13.	28.00	33.78	0.06	0.09	0.0	0.00
25/03/76	275.	13.	28.00	37.32	0.09	0.12	0.0	0.00
27/03/76	215.	14.	28.00	40.87	0.11	0.15	0.04	0.00
28/03/76	25.	10.	28.00	29.15	0.04	0.07	0.0	0.00
28/03/76	25.	11.	28.00	33.62	0.06	0.11	0.0	0.00
31/03/76	135.	10.	28.00	29.15	0.04	0.07	0.0	0.00
31/03/76	165.	10.	28.00	29.15	0.04	0.07	0.0	0.00
31/03/76	145.	11.	28.00	33.62	0.06	0.11	0.01	0.00
1/04/76	185.	12.	28.00	30.23	0.05	0.06	0.0	0.00
2/04/76	285.	12.	28.00	30.23	0.05	0.06	0.0	0.00
2/04/76	315.	15.	28.00	44.42	0.14	0.20	0.0	0.00
2/04/76	345.	14.	28.00	40.87	0.11	0.15	0.0	0.00
3/04/76	345.	12.	28.00	30.23	0.05	0.06	0.0	0.00
4/04/76	265.	14.	28.00	40.87	0.11	0.15	0.0	0.00
4/04/76	25.	13.	28.00	47.02	0.17	0.30	0.0	0.00
5/04/76	5.	12.	28.00	38.08	0.09	0.16	0.0	0.00
8/04/76	55.	12.	28.00	38.08	0.09	0.16	0.01	0.00
8/04/76	55.	11.	28.00	33.62	0.06	0.11	0.0	0.00
9/04/76	45.	13.	28.00	47.02	0.17	0.30	0.0	0.00
9/04/76	35.	13.	28.00	47.02	0.17	0.30	0.0	0.00
9/04/76	25.	16.	28.00	60.42	0.36	0.63	0.0	0.00
9/04/76	25.	15.	28.00	55.95	0.29	0.50	0.0	0.00
9/04/76	25.	16.	28.00	60.42	0.36	0.63	0.0	0.00
9/04/76	15.	12.	28.00	38.08	0.09	0.16	0.0	0.00

TABLE 8 (Continued).

Date	Wind Direction	Wind Speed m/sec	Thresh Velocity cm/sec	Sheer Velocity cm/sec	Hsu Transport g/cm/sec	Bagnold Transport g/cm/sec	Rain cm	% Water
10/04/76	355.	10.	28.00	29.15	0.04	0.07	0.0	0.00
11/04/76	305.	16.	28.00	47.96	0.18	0.25	0.0	0.00
11/04/76	5.	13.	28.00	47.02	0.17	0.30	0.0	0.00
12/04/76	5.	12.	28.00	38.08	0.09	0.16	0.0	0.00
12/04/76	25.	13.	28.00	47.02	0.17	0.30	0.0	0.00
12/04/76	15.	13.	28.00	47.02	0.17	0.30	0.0	0.00
12/04/76	5.	12.	28.00	38.08	0.09	0.16	0.0	0.00
21/04/76	215.	12.	28.00	30.23	0.05	0.06	0.0	0.00
25/04/76	235.	13.	28.00	33.78	0.06	0.09	0.0	0.00
25/04/76	235.	12.	28.00	30.23	0.05	0.06	0.0	0.00
25/04/76	225.	13.	28.00	33.78	0.06	0.09	0.0	0.00
25/04/76	225.	13.	28.00	37.32	0.09	0.12	0.0	0.00
25/04/76	215.	12.	28.00	30.23	0.05	0.06	0.0	0.00
25/04/76	255.	13.	28.00	37.32	0.09	0.12	0.0	0.00
25/04/76	225.	13.	28.00	33.78	0.06	0.09	0.0	0.00
26/04/76	25.	12.	28.00	38.08	0.09	0.16	0.0	0.00
26/04/76	5.	11.	28.00	33.62	0.06	0.11	0.0	0.00

indicate that the effect of a surface crust formed from salt is small because the crust is easily broken by saltating grains coming from areas where no crust is present.

The exclusion of these variables from the model is not the only source of potential error in calculating eolian sand transport. Although the mechanism by which vegetation affects sand transport is understood, quantifying this effect is very difficult. The density and height of the vegetative cover on the dunes and eolian flat along Currituck Spit is very variable. Therefore, the transport rates calculated by the model represent average values assuming a uniform vegetation cover instead of being specific to a particular geographic location. Another problem is the transport equations which were derived for a bare sand surface. Therefore, the computed transport rates taken as estimates only.

Verification of Model with Sand Transport Measurements

In order to evaluate the accuracy of the calculations the model was compared with field measurements of sand transport. Tables 9 and 10 are lists of sand transport measurements along Currituck Spit conducted under a variety of wind, moisture and vegetation conditions. The rate of sand transport was measured with a vertical, mechanical sand trap. The sand trap (Figure 52) was modeled after a design described by Horikawa and Shen (1960). They determined an efficiency, which is the ratio of trapped sand to total sand in transport, of about 80 percent for this particular design.

On days when the wind velocity was sufficient to initiate sand transport, the sand trap and portable anemometers were set up at a number of locations along Currituck Spit to measure the transport



Figure 52. Sand trap and portable anemometers used to measure eolian sand transport. Section of PVC pipe (bottom) was used to dig a hole for placement of sand trap.

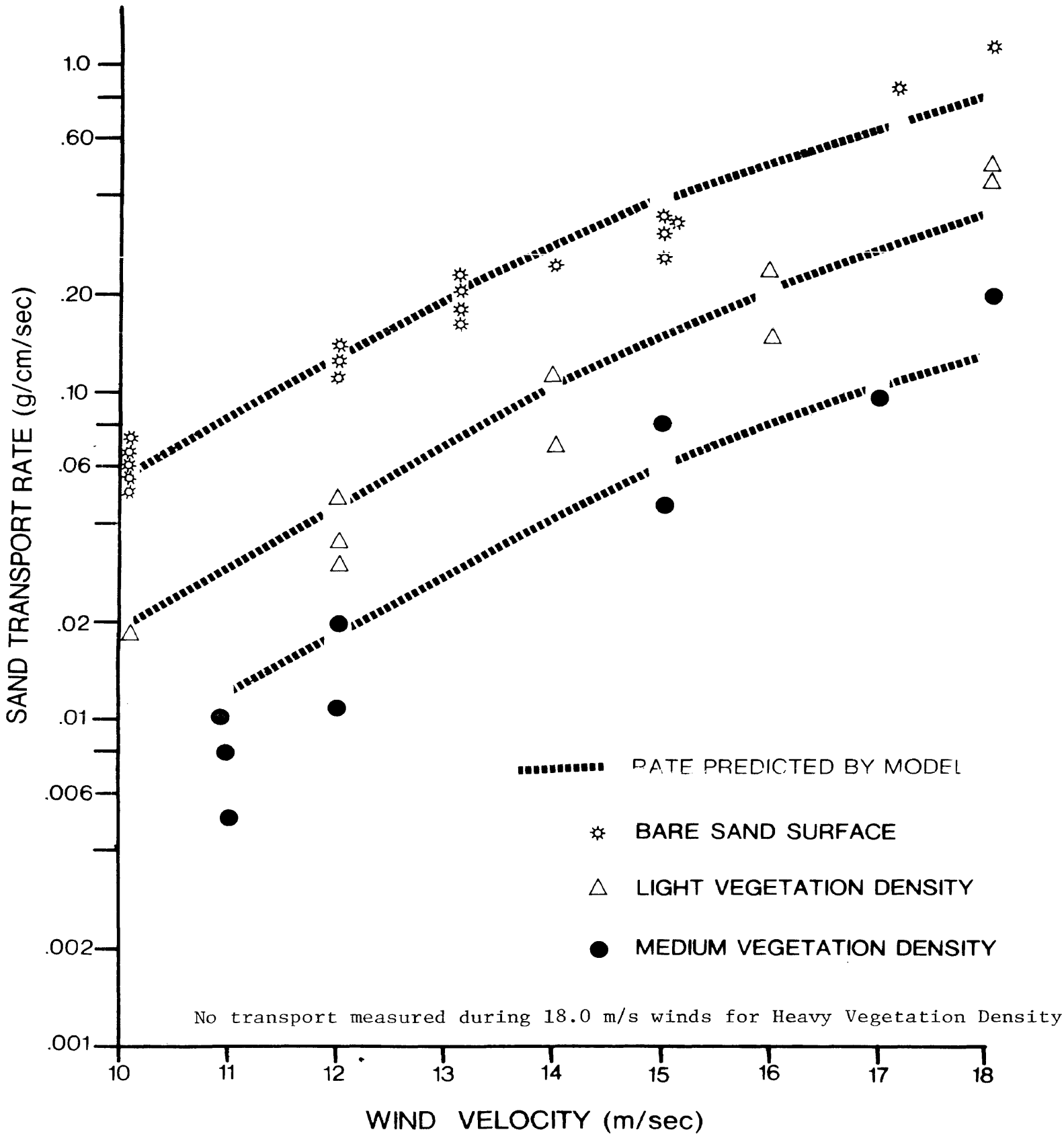
rate. The sand trap was installed by digging a hole with a cylinder of a slightly larger inside diameter than the base of the sand trap. This procedure caused only minimal disturbance of the sand surface. The sand transport was measured for a period of time ranging from 1-30 minutes depending on the wind velocity and vegetation cover. Measurements during offshore winds were taken in areas with very light, light, medium and high density vegetation cover (see Table 9). The wind velocity at the surface was measured and then compared with the wind velocity measured at the Corolla station anemometer. The trapped sand was returned to the laboratory, dried and then weighed. The sand transport rate, expressed in $\text{g}/\text{cm}\cdot\text{sec}$, could then be computed using an assumed sand trap efficiency of 80%.

Comparison of the measured and computed transport rate was very simple because both sets of data were expressed in terms of the wind velocity and direction as measured at the Corolla Station anemometer.

Figure 53 is a comparison of measured transport rates (data listed in Tables 9 and 10) with the rate predicted by the eolian transport model. The predicted lines are the average of the rate computed by the Bagnold and Hsu equations for three different vegetation densities. The vegetation density was a subjective measure of the vegetative cover upwind of the sampling site. "None" refers to bare sand; "very light" to sparse dune grass (Figure 54); "light" to typical dune grass (Figure 54); "medium" refers to dense dune grass and other herbaceous vegetation (Figure 55); and "heavy" to a shrub thicket (Figure 55). The sand trap was positioned on the beach just seaward of the dunes to measure the transport from the beach to the dunes,

Figure 53.

SAND TRANSPORT RATE (g/cm/sec) AS A FUNCTION OF WIND VELOCITY (m/sec) AND VEGETATION DENSITY.



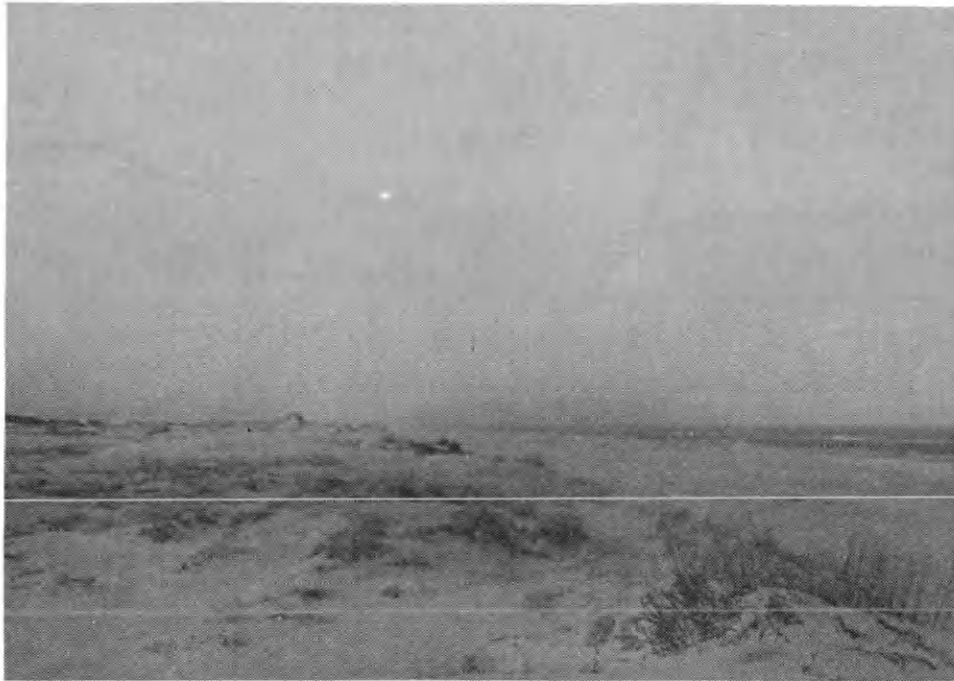


Figure 54. Typical "very light" density (top) and "light" density (bottom) vegetation along Currituck Spit.

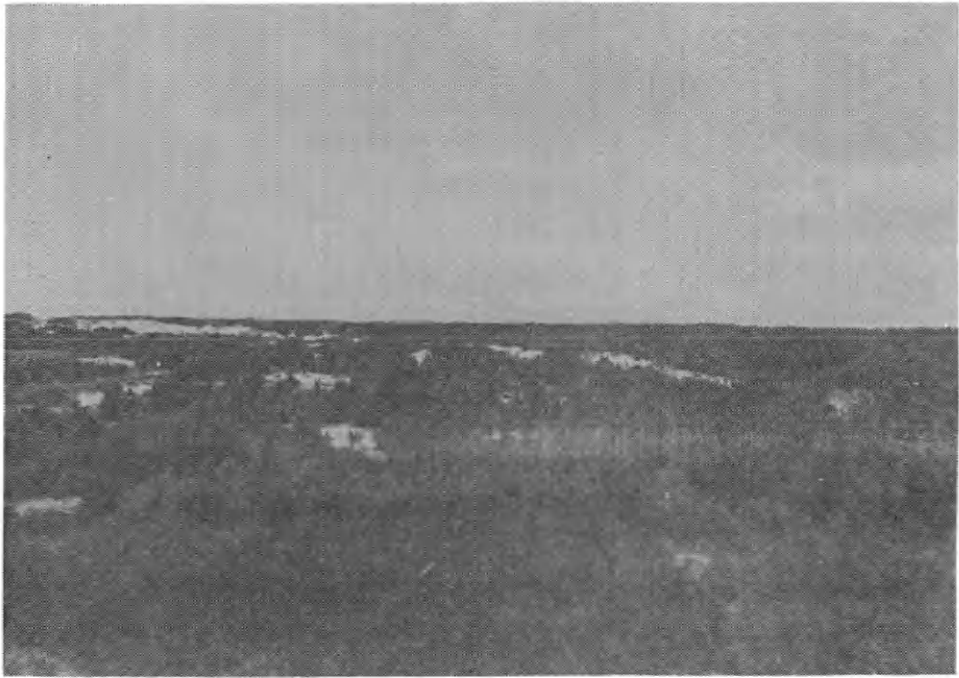


Figure 55. Typical "medium" density (top) and "heavy" density (bottom) vegetation along Currituck Spit.

TABLE 9

SAND TRANSPORT MEASUREMENTS NEAR FALSE CAPE, VIRGINIA (F)
AND COROLLA, NORTH CAROLINA (C) WITH NO VEGETATION COVER

Wind Velocity m/sec		Wind Direction	Transport Rate g/cm/sec	Location
<u>1 meter</u>	<u>53 meters</u>			
8	10	E	.06	Across Beach (F)
8	10	E	.06	Across Beach (F)
8	10	E	.07	Across Beach (F)
8	10	E	.05	Across Beach (C)
8	10	E	.06	Across Beach (C)
8	10	E	.05	Across Beach (C)
9	12	S	.11	Across Beach (C)
9	12	NE	.12	Across Beach (C)
9	12	NE	.10	Across Beach (C)
10	13	NE	.18	Across Beach (F)
10	13	NE	.15	Across Beach (F)
10	13	NE	.20	Across Beach (C)
10	13	NE	.19	Across Beach (C)
11	14	NE	.25	Across Beach (C)
12	15	NE	.30	Across Beach (F)
12	15	NE	.32	Across Beach (F)
12	15	NE	.34	Across Beach (C)
13	15	NE	.35	Across Beach (C)
14	17	W	.6	Across Foredune (C)
14	18	W	.9	Across Foredune (C)

TABLE 10

SAND TRANSPORT MEASUREMENTS NEAR FALSE CAPE, VIRGINIA (F) AND COROLLA, NORTH CAROLINA (C) WITH VARYING VEGETATION COVER

Wind Speed m/sec	Wind Direction	Transport Rate g/cm/sec	Location	Upwind Vegetation Density
7	SW	.06	Across Eolian Flat (C)	Very Light
7	SW	.04	Across Eolian Flat (C)	Very Light
12	SW	.2	Across Eolian Flat (C)	Very Light
6	SW	.02	Across Foredune (C)	Light
7	SW	.03	Across Foredune (C)	Light
7	SW	.04	Across Eolian Flat (C)	Light
11	W	.07	Across Foredune (C)	Light
11	W	.08	Across Foredune (C)	Light
13	W	.15	Across Foredune (C)	Light
13	W	.20	Across Foredune (C)	Light
13	W	.5	Across Foredune (C)	Light
13	W	.4	Across Foredune (C)	Light
6	SW	.009	Across Foredune (F)	Medium
6	SW	.007	Across Foredune (F)	Medium
5	SW	.004	Across Foredune (F)	Medium
7	SW	.02	Across Foredune (F)	Medium
8	SW	.01	Across Foredune (F)	Medium
10	W	.04	Across Foredune (F)	Medium
11	W	.08	Across Foredune (F)	Medium
12	W	.09	Across Foredune (F)	Medium
13	W	.2	Across Foredune (F)	Medium
12	W	0.0	Across Eolian Flat (F)	Heavy
12	W	0.0	Across Eolian Flat (F)	Heavy

and back to the beach during both onshore and offshore winds. Transport was also measured across the eolian flat to monitor cross-barrier flux of sand.

Comparison of measured and predicted transport rates indicate that the model is fairly accurate for onshore wind conditions. For example, the measured transport rate during 13 m/sec onshore winds was 0.18-.20 g/cm·sec (samples T-14, T-15, T-34, and T-35). The model predicted (Table 8, March 9, 1976) a transport rate of 0.17-.30 g/cm/sec for identical conditions. Similarly during 15 m/sec onshore winds the measured transport rate was .30-.35 g/cm·sec (samples T-17, T-36, T-37, and T-38) while the model predicted (Table 8, April 9, 1976) a transport rate of .29-.50 g/cm·sec. Therefore the model predicted onshore transport rates which compare well with measured values.

Calculation of sand transport during offshore wind conditions using the same surface roughness parameter (Z_0) as during onshore winds, would greatly exceed the measured values. Table 8, however, is a listing from computations with a $Z_0 = 6.0$ cm input for all offshore winds. There is a very good correlation between the observed and predicted transport rate for offshore winds blowing over a lightly vegetated surface. For example the measured transport rate for samples T-3, T-4 and T-5 compares well with the calculated values in Table 8. However, for the medium vegetated surfaces, comparisons of observed and predicted indicate a poor correlation. For these medium density vegetation conditions a Z_0 of 9.0 cm, was used and as shown in Figure 53 there is a fairly good correspondence between the measured and predicted transport rate. Therefore it was concluded that good estimate of the sand transport rates during both onshore and offshore wind conditions

is possible with a reasonable value of Z_0 , and that the Z_0 can be chosen which correlates with vegetation density.

Verification of Sand Transport Using Migration Rate of Medanos

In a previous section the transport of sand, across the slipface of two large sand hills was determined from the migration rate of the dunes (see Figure 32). The sand transport across the Whalehead Hill slipface was about 49,000 kg/meter slipface/year while across Barbours Hill the sand transport was 5,700 kg/m/year.

Inman et al. (1966) and Tsoar (1974) have compared the measured rate of dune movement with that calculated from empirical equations of eolian sand transport. Both found that the calculated rate exceeded the measured amount by some constant amount. Inman attributed the discrepancies to calibration of the anemometer or problems associated with the equations. Tsoar attributed the differences to reduction of the transport by soil moisture.

Table 11 lists the output of the model using wind, temperature, and precipitation data covering the period of measured dune movement. Notice that the northeast and southwest are by far the dominant directions with respect to eolian sand transport. Table 11 also indicates the discharge calculated across a slipface oriented approximately west-northwest to east-southeast. This total was determined by adding together each three hour interval sand transport rate for wind directions between 300° and 100° azimuth. It was assumed that this 160° arc would include all wind directions contributing to sand transport across the slipface.

The total value for calculated sand transport across the slipface (35,000 and 59,000 kg/m/year for Bagnold and Hsu equations)

TABLE 11

TOTAL TRANSPORT CALCULATED BY EOLIAN SAND TRANSPORT MODEL

(2/76-2/77) ASSUMING A Z_0 OF 3.0 CM FOR ALL OFFSHORE

WIND DIRECTIONS

Direction	(Bagnold Equation) Total Transport of Sand for Year kg/m/year	(Hsu Equation) Total Transport of Sand for Year kg/m/year
North	22488.	13193.
Northeast	27198.	15575.
East	4420.	2531.
Southeast	3758.	2152.
South	2105.	1493.
Southwest	12493.	9157.
West	2875.	2107.
Northwest	6758.	4953.
Onshore Transport (180-340 Degrees AZ)	49463.	28325.
Offshore Transport (0-160 Degrees AZ)	32632.	22837.
Transport Across Slipface (300-100 Degrees AZ)	35002.	59030.

TABLE 12

TOTAL TRANSPORT CALCULATE BY EOLIAN SAND TRANSPORT MODEL

(2/76-2/77) ASSUMING A Z_0 OF 6.0 CM FOR ALL

WIND DIRECTIONS

Direction	(Bagnold Equation) Total Transport of Sand for Year kg/m/year	(Hsu Equation) Total Transport of Sand for Year kg/m/year
North	10413.	6236.
Northeast	11810.	6763.
East	1556.	891.
Southeast	1225.	701.
South	1592.	1148.
Southwest	10747.	7877.
West	2492.	1826.
Northwest	5856.	4293.
Onshore Transport (180-340 Degrees AZ)	20466.	11720.
Offshore Transport (0-160 Degrees AZ)	25223.	18015.
Transport Across Slipface (300-100 Degrees AZ)	17300.	28396.

agrees well with the measured value for Whalehead Hill (49,000 kg/m/year). Notice that the total predicted by the Bagnold equation and Hsu equation straddle the measured discharge. This comparison of measured and computed discharge correlates better than the studies of Inman (1966) and Tsoar (1974). Tsoar attributed a discrepancy of 10-40% between the measured and computed advance of barchan dunes to precipitation effects. Without considering the effects of precipitation the model would have indicated 20-30% greater sand transport rates than the computed discharge for a large unvegetated sand hill.

Notice however, that a comparison of the transport across the Barbours Hill slipface (5,700 kg/m/year) with the predicted amount (Table 11) using a Z_0 of 3.0 shows a very poor correlation. This is attributed to the effects of vegetation. At Barbours Hill, all wind directions which contribute to the movement of the sand hill blow over a light to medium density vegetation cover. Table 12 is output from model which was run with a larger Z_0 input of 6.0 cm for all wind directions. In this case we see a much better correlation between the observed (5,700 kg/m/year) and predicted transport rates (20,000 kg/m/year).

Therefore, there seems to be a good correlation between the eolian sand transport predicted by the model and the transport determined from the migration of large sand hills. The best fit between observed and predicted is for bare sand surface conditions (Whalehead Hill). However, with use of an appropriate surface roughness parameter, (calibrated with vegetation density) the model predicts a fairly reliable transport for vegetated surfaces.

Conclusions

1. After a detailed investigation of the local coastal mechanisms of eolian sand transport an empirical model was developed to predict sand transport from routine wind, precipitation and temperature data.
2. Equations in the model included those by Kadib (1964) (to calculate the threshold shear velocity including the effects of moisture), Hsu (1973) (to calculate shear velocity and transport), and Bagnold (1941) (to calculate transport).
3. An equation was developed, using field measurements of soil moisture content and a multiple linear least-squares curve fitting program, to predict percent moisture content of sand from routine climatological data.
4. Values of the surface roughness parameter (Z_0) were chosen from studies by Bressolier and Thomas (1977) to represent in the model the effects of varying levels of upwind vegetation density.
5. The accuracy of the model was checked with field measurements of sand transport, and total transport determined from the migration of large sand dunes. The model predicts the transport rate best for bare sand surfaces. However, the model was also fairly accurate for winds blowing over vegetated surfaces when the surface roughness parameter was chosen to reflect the density and/or height of the upwind vegetation.

APPLICATIONS OF SAND TRANSPORT MODEL

The eolian sand transport model developed in this thesis predicts the rate and quantity of sand transport from routine meteorological data. The model could be used in many areas of the world where suitable meteorological data are available after only limited field measurements of soil moisture/grain size relations, vegetation effects, and threshold shear velocity to check the calculations. For example, in central and east Africa eolian transport of sand both inland from the coast and south from the Sahara Desert often endangers productive agricultural land, housing developments, oil rigs and other structures. A sand transport model which could predict the net quantity and direction of sand movement could greatly aid in the design of sand stabilization projects to protect these developments. Along Currituck Spit and other east coast barrier islands two major applications of the model are immediately evident.

Sand Fencing and Dune Growth

Sand fencing and vegetation planting (Figure 56) have been and continue to be used extensively along Currituck Spit and other east and Gulf Coast barrier islands for the formation and stabilization of foredunes (Hawk and Sharp, 1967; Savage, 1969; Dahl et al., 1975). These foredunes are created, at great expense (Gibbs, 1961), to protect inland structures from damage during storms. The planning and execution of a sand fencing and vegetation planting program would be greatly



Figure 56. Sand fence created foredunes north of Corolla, N.C.

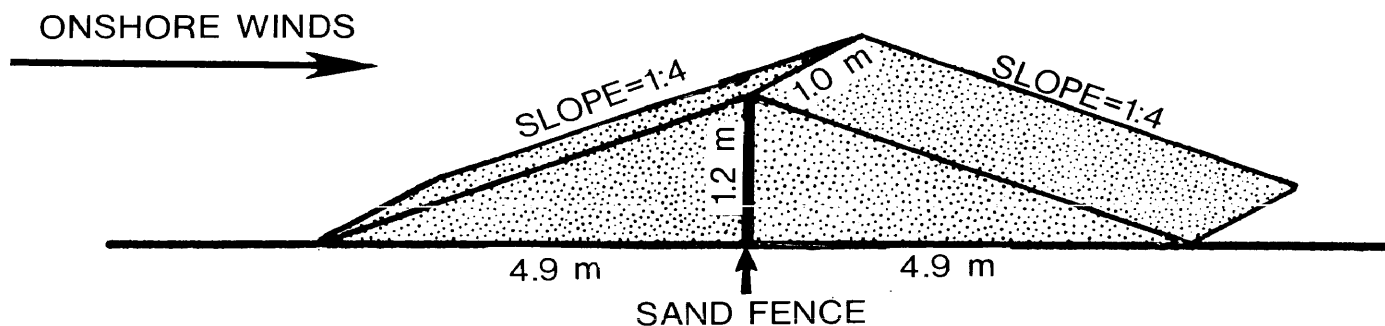
facilitated by a detailed knowledge of the local wind regime and eolian sand transport. For example, the use of either a single or double-row sand fence depends on the expected average wind speeds because a double row fence is much more efficient at trapping sand at high wind velocities (Manohar, 1970).

The amount of sand fencing material necessary for continual buildup of a foredune is determined by the rate of deposition caused by the sand fence. Generally, when one set of sand fences become covered by sand, another set is placed over the old ones to continue dune construction. The eolian sand transport model could be used to roughly estimate the rate of dune formation and therefore the amount of sand fencing material needed on a yearly basis.

A typical double-row sand fence is constructed with two rows of 1.2 m high (4 feet) sand fencing spaced 4.9 m (16 feet) apart (Manohar, 1971) while the single-row sand fence has only one line of sand fencing. If a 1:4 slope (Manohar, 1971; Goldsmith et al., 1977) of both the onshore and offshore sides of the artificially constructed foredune is assumed, then the volume of sand trapped by a completely buried single and double row fence (see Figure 57) is about 6 m^3 per linear meter of foredune (single-row) and 12 m^3 per linear meter (double-row). This volume of sand trapped by the sand fence could then be compared with the annual transport rates calculated with the model to determine the rate at which the dune will grow and the number of additional rows of sand fencing needed in a given period of time.

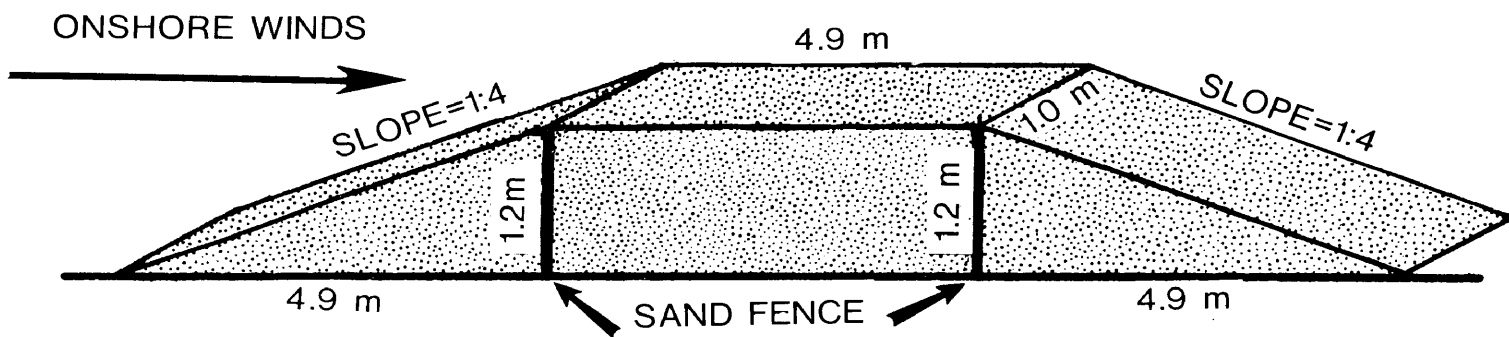
Table 11 lists the output of the transport model for one year of Corolla wind data. The onshore and offshore transport rates were computed by converting each calculated transport rate ($\text{g}/\text{cm}\cdot\text{sec}$)

SINGLE ROW SAND FENCE



$$\begin{aligned}
 \text{VOLUME} &= 0.5 \times \text{BASE} \times \text{HEIGHT} \times \text{WIDTH} \\
 \text{(of a Triangle)} & \\
 &= .5 \times 9.8\text{m} \times 1.2\text{m} \times 1.0\text{m} \\
 &= 5.9 \text{ m}^3
 \end{aligned}$$

DOUBLE ROW SAND FENCE



$$\begin{aligned}
 \text{VOLUME} &= .5 \times (\text{BASE}_1 + \text{BASE}_2) \times \text{HEIGHT} \times \text{WIDTH} \\
 &= .5 \times (14.7 + 4.9) \times 1.2\text{m} \times 1.0\text{m} \\
 &= 11.8 \text{ m}^3
 \end{aligned}$$

Figure 57. Calculation of the volume of sand trapped by a single row (top) and double row (bottom) sand fence with a 1:4 onshore and offshore slope.

to a transport rate expressed in kg/meter/3 hours. Then the entire year of transport rates (eight/day) were added together for all directions which contribute to onshore (0° - 160° AZ) and offshore (180° - 340° AZ) transport. This 160° arc normal to the orientation of the shoreline was assumed to contain all directions which contribute to onshore and offshore transport.

If it is assumed that only onshore winds supply sand for growth of a foredune (either due to dense vegetation or development across the interior of the barrier island) then the model predicts between 28,000 and 49,000 kg/m/year would be transported from the beach inland for dune growth. Sand transport measurements indicate that the mid point of this range (about 38,000 kg/m/year) would be a reliable estimate of the total transport. Assuming a bulk density for the sand of 1.4 g/cm^3 , then the predicted transport of 38,000 kg/m/year of sand is approximately equivalent to $27 \text{ m}^3/\text{m}/\text{year}$.

A typical double row sand fence has an efficiency (ratio of sand trapped to total sand transport) of about 40% (Manohar, 1970) although the efficiency varies with the wind speed. Single row sand fencing has a lower efficiency (approximately 20%) and at high wind speeds (greater than 17 m/sec) traps no sand. Using these efficiency ratios, the model predicts that a double row sand fence installed along Currituck Spit would trap about $11 \text{ m}^3/\text{m}/\text{year}$ while the single row would trap about $8 \text{ m}^3/\text{m}/\text{year}$. Since a double row sand fence can accommodate only 12 m^3 (Figure 56) of sand per meter of dune then the model predicts that this sand fence would fill in a little over a year. The single row sand fence would accumulate the limit of sand in about 9 months. Of course if a sand supply was available in the interior

for transport by onshore winds to the growing foredune, then the sand fencing would fill more rapidly. Observations of eolian deposition on sand fencing at Cape Hatteras, N.C. (Gibbs, 1961) indicate that the one year estimate is reasonable for the amount of time necessary to create a 1.2 meter high foredune. Observations by Goldsmith (personal communication, 1977) indicate that a single-row sand fence at Back Bay Wildlife Refuge in "light" vegetation density became $3/4$ filled in one year (1973-1974). Therefore an immediate application of the eolian sand transport model would be for aiding in the planning and design of sand fencing programs.

Net Movement of Sand Across a Barrier Spit; Historically and Presently

Forty years ago the False Cape area (Figure 1) was covered by an unvegetated sand sheet extending uninterrupted from the ocean to the bay (Figure 58-A). Today dense vegetation covers most of the area (Figure 58-D). Hennigar (1978) attributes this vegetation colonization over the last forty years to continual sand fencing which has succeeded in creating a high (3-4 meters) multiple ridge foredune system. This foredune system reduced sand transport from the beach to the interior. Shrub vegetation, which cannot tolerate continual sand burial, colonized the interior stabilizing the shifting sands of the eolian flat. Sand transport measurements (Table 8) during strong offshore winds indicate a zero transport rate across the eolian flat near False Cape.

The net movement of sand across Currituck Spit during periods of low density vegetation cover (1930's) and high density cover (1970's) was estimated by computing the transport model with different values of the surface roughness parameter.

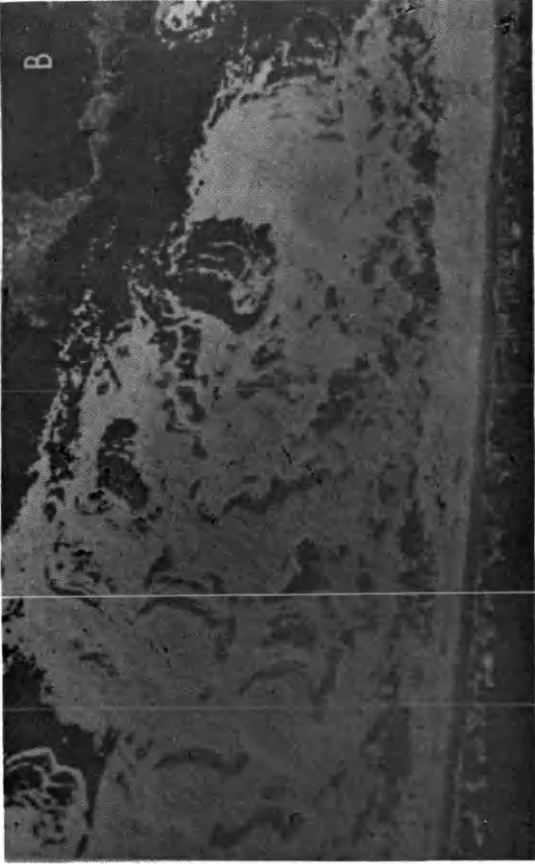
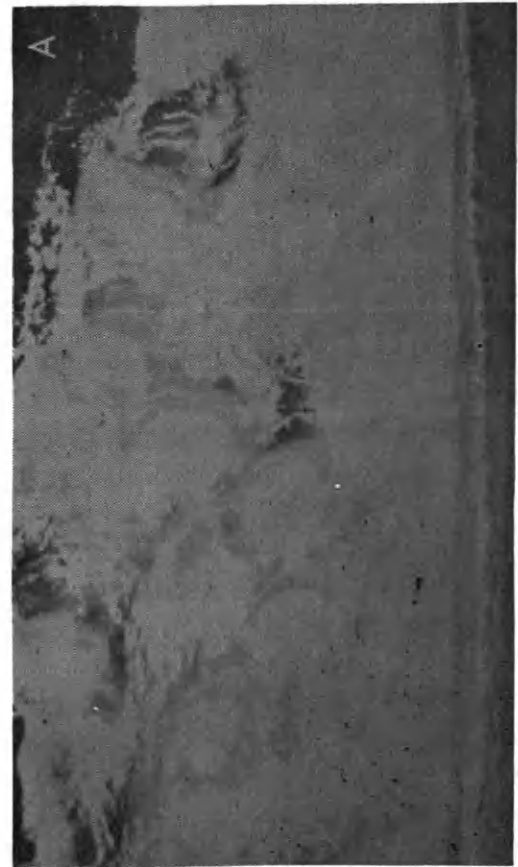


Figure 58. False Cape State Park
A-1947; B-1955; C-1963; D-1975

Table 13 is the output of the model with an input of $Z_0=1.0$ (bare sand) for all wind directions. Notice that the onshore transport exceeds the offshore by only a small amount. The net transport of sand would be only slightly onshore. Assuming the wind climate 40 years ago is similar to today (this is supported by long term wind records), this predicted small net direction of transport should apply to the transport conditions in False Cape 40 years ago. Therefore when the barrier spit was covered by a sand sheet (Figure 58), the net movement of eolian sand was only slightly onshore. Most of the sand which blew inland probably was blown by offshore winds back onto the beach. However, it is more than likely that significant amounts of sand were blown all the way across the island during storm wind conditions and then permanently deposited in the bay. This permanent loss of sand to the longshore driftsystem may have been offset by new beach sand supplied on the seaward side.

Table 14 is the output of the model assuming a high vegetation density ($Z_0 = 6.0$) across the barrier island. In this case there is a very pronounced net movement of sand onshore. However, field measurements of sand transport in False Cape State Park indicated that very little sand was carried beyond the foredunes into the eolian flat, even during strong onshore winds. Instead most of the onshore transport was trapped in the multiple ridge foredune system. The model indicates that most sand transport across a barrier spit with a dense vegetation cover would be onshore, however, this sand would be trapped by the foredune system. Thus, once vegetation begins to be effective via a small foredune for example, the processes are such as to cause the maximum accumulation in the foredune.

TABLE 13

TOTAL TRANSPORT CALCULATED BY EOLIAN SAND TRANSPORT

MODEL (2/76-2/77) ASSUMING A Z_0 OF 1.0 CM

Direction	(Bagnold Equation) Total Transport of Sand for Year kg/m/year	(Hsu Equation) Total Transport of Sand for Year kg/m/year
North	22933.	13537.
Northeast	27198.	15575.
East	4420.	2531.
Southeast	3758.	2152.
South	3175.	2277.
Southwest	18177.	13324.
West	4399.	3224.
Northwest	9058.	6640.
Onshore Transport (180-340 Degrees AZ)	49463.	28325.
Offshore Transport (0-160 Degrees AZ)	43654.	30935.

TABLE 14

TOTAL TRANSPORT CALCULATED BY EOLIAN SAND TRANSPORT

MODEL (2/76-2/77) ASSUMING A Z_0 OF 6.0 CM FOR ALL

OFFSHORE WIND DIRECTIONS

Direction	(Bagnold Equation) Total Transport of Sand for Year kg/m/year	(Hsu Equation) Total Transport of Sand for Year kg/m/year
North	22109.	12934.
Northeast	27198.	15575.
East	4420.	2531.
Southeast	3758.	2152.
South	1786.	1259.
Southwest	10747.	7877.
West	2492.	1826.
Northwest	5856.	4293.
Onshore Transport (180-340 Degrees AZ)	49463.	28325.
Offshore Transport (0-160 Degrees AZ)	28903.	20122.

Eolian sand transport seems to be most important in carrying sand from the beach to the interior when the barrier island is covered by only light density vegetation. False Cape State Park twenty years ago (Figure 58-B) and south of Corolla today (Figure 59-C) are characterized by such a vegetation distribution. Table 11 is the output of the model for a Z_0 input of 3.0 cm (light vegetation). Notice that in this case there is a net movement of a large amount of sand onshore. In this case the foredunes do not trap the transport. Strong onshore winds (19 m/sec) were observed to transport sand from the beach across the low, sparsely vegetated foredunes near Corolla, and onto the eolian flat. Therefore, field observations and the model indicate that there is a net movement of sand onshore in areas with a low density vegetation cover. The Corolla region today and False Cape 20 years ago are typical of such a vegetation distribution.

Therefore the eolian transport model can be applied to predicting the net movement of sand across a barrier spit covered by varying densities of vegetation. The transport regime can be estimated for coastal ecosystems typical of today and those typical twenty and forty years ago as determined from old aerial photographs.

Conclusions

1. The eolian sand transport model, though developed for Currituck Spit, could conceivably be used to evaluate sand drifting problems along other barrier islands and other parts of the world.

2. The transport model can be used to compute the rate of deposition of sand on typical single and double row sand fences.

According to the model it would take about 9 months with a single row

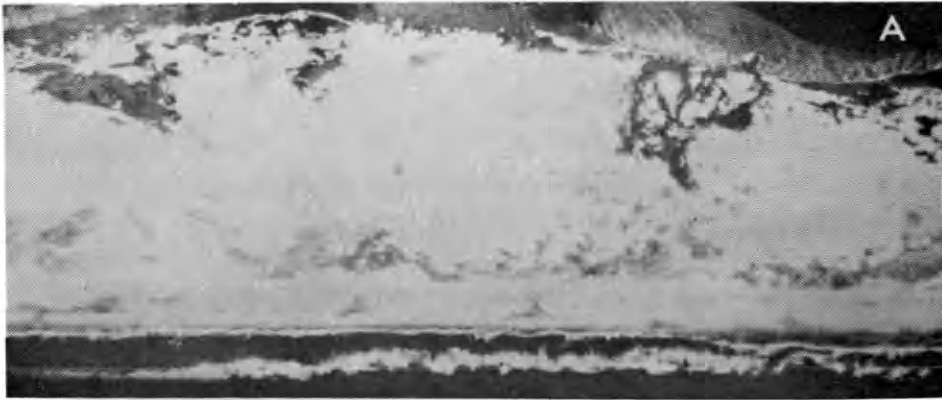


Figure 59. Corolla, North Carolina
A-1940; B-1955; C-1975

and about 13 months with a double row sand fence to create a 1.2 meter high foredune with a 1:4 onshore and offshore slope, assuming no vegetation. This information could be very valuable for planning, design and execution of sand fencing programs.

3. The model could also be very useful for estimating the net movement of sand across the barrier spit under varying levels of vegetation density. The model predicted only a small net onshore movement of sand across a barrier spit completely covered by bare sand. If the interior of the spit is covered by dense vegetation (Figure 58), according to the model there would be a strong net movement onshore. However, most of this sand would be trapped by the high, multiple ridge foredune system. Finally, according to the model if the spit is covered by sparse vegetation (Figure 58) there would be a significant net movement of sand onshore from the beach to the interior of the spit.

DISCUSSION AND MANAGEMENT IMPLICATIONS

Eolian sand transport is the dominant physical process along Currituck Spit responsible for the development, orientation, and migration of sand dunes. Due to the present lack of overwash fans and inlets along the spit, eolian transport has also become the major source of cross-barrier sediment transport. Unfortunately, development of a quantitative relationship between eolian sand transport, coastal dune dynamics, and cross-barrier sand flux is very difficult due to the complexity of the transport process. No instrumentation exists which can monitor sand transport over a long time period (e.g., months or years) and indirect calculations of sand transport are very difficult due to the large number of environmental variables which influence the transport process (wind speed, direction, and profile, soil texture and moisture content, surface obstructions, vegetation, and topography). In this study the interaction of eolian sand transport, dune dynamics and cross barrier sediment transport was investigated as a function of the three most important environmental variables influencing the transport process in the coastal zone; wind, vegetation, and moisture.

Wind

A detailed wind climate was compiled from one year (2/76-2/77) of data from a local source (Corolla, North Carolina) and 18 years of data from a nearby source (Cape Hatteras, North Carolina). The local wind regime along Currituck Spit is directionally polymodal, with

prevailing winds from the north and southwest (20% and 32%, respectively) and dominant winds from the northeast, north, and northwest (mean wind speed ~ 8 m/sec). This polymodal wind regime has profound implications for the development, orientation and migration of sand dunes and in the movement of sand across the spit. The effect of the wind regime is most apparent with the dynamics of the unvegetated sand hills or medianos.

Over a dozen large medianos (Figure 27) extend along Currituck Spit from north of Corolla to the south. The local polymodal wind regime may be responsible for the formation of these large sand hills (discussed at length in Goldsmith et al., 1977 and Hennigar, 1978). The dunes developed where a large supply of sand was available, such as on old overwash fans or areas recently denuded of vegetation. The high frequency and high velocity winds, which occur along Currituck Spit from several directions, would tend to gather this available sand together forming a heightened, steepened dune. Once formed a sand hill would continue to grow and maintain its form, due to the effect of a lee side eddy (Figure 60). Winds transporting sand from any direction would deposit sand on the lee side of the dune due to the zone of lower wind velocity. In this manner the local polymodal wind climate alone may be responsible for the development of medianos along Currituck Spit. However, the migration of these medianos, the development of parabolic dunes, and the cross barrier flux of sand are also influenced by the effects of vegetation and moisture.

Moisture

The threshold shear velocity (shear velocity necessary to initiate sand transport) increases as the moisture content of the

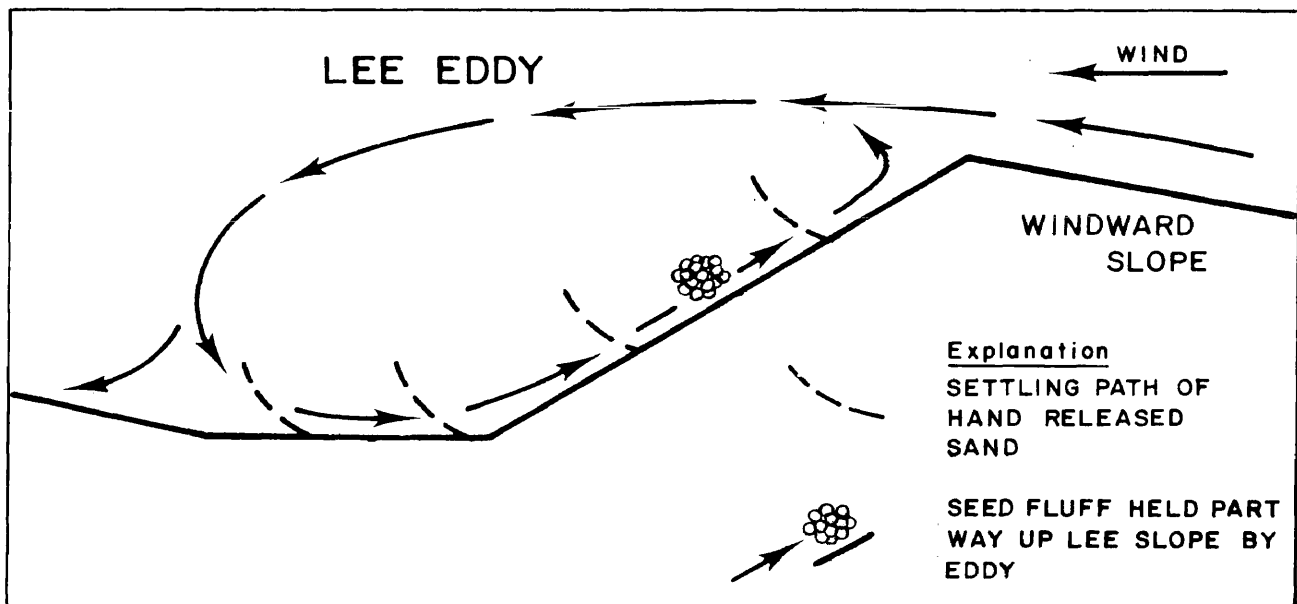


Figure 60. Lee side eddy (from Sharp, 1965)

sand increases (Figure 48). Therefore, precipitation will decrease the total amount of sand transport. In desert regions, the effect of moisture on sand transport rates has been largely ignored for obvious reasons. However, in a temperate coastal zone this variable can become very important. The measured migration rate (six m/year) of a large sand hill (Whalehead Hill) was compared with the rate predicted by the eolian transport model. It was determined that the model could predict the migration rate of these large medanos. However, if the effect of soil moisture had been ignored in the model, the predicted migration rate would have exceeded the measured by 30%. As an environmental variable influencing sand transport, moisture content of the sand is secondary in importance to the wind where vegetation is absent (e.g., sand sheet 40 years ago, Figure 58; or sand hills of 16 years ago, Figure 26). However, where present, vegetation is secondary only to the wind in determining the development, orientation, and migration of sand dunes and the flux of sand across a barrier spit.

Vegetation

Vegetation increases the value of the surface roughness parameter (Z_0) in the transport equations as a function of the height and density of the vegetation (see Figure 51). Therefore, increasing vegetation cover will decrease the rate of sand transport by wind. Forty years ago (Figure 58) vegetation was totally absent along the entire spit. However vegetation has colonized the area in varying degrees, aided by foredunes formed by sand fencing. These foredunes which reduced the sand transport from the beach to the interior allowed vegetation to survive. Vegetation colonization has proceeded the farthest near False Cape, due to continual sand fencing,

and least near Corolla, where sand fencing has not been continually maintained (Hennigar, 1978). Vegetation colonization has, in part, determined the development and orientation of parabolic dunes in False Cape State Park. The north-south differences in vegetation cover also account for differences in sand hill migration rates, and cross-barrier sand flux between the two regions of Currituck Spit (Corolla and False Cape).

Interaction of Wind, Vegetation and Parabolic Dunes

A series of vertical aerial photographs (Figure 58) indicate a development sequence beginning with a completely unvegetated sand sheet and culminating in a parabolic dune field. The key to this development sequence (Figure 34) is vegetation which colonizes the flanks of a sand hill. As the slipface migrates downwind the anchored flanks lag behind forming a U-shaped dune.

However, the orientation of the parabolic dune axis is not simply a function of the local prevailing or dominant wind regime. The Corolla vector wind resultant is oriented approximately west-northwest (Figure 35) while the parabolic dunes are oriented to the north-northeast. Instead the orientation of parabolic dunes is a result of both the local wind regime and the effect of vegetation on the wind. Due to the presence of a tall (15 m high) maritime forest to the west of the developing parabolic dunes (Figure 58) and an unvegetated sand sheet to the east of the dunes, the offshore winds were of minimal importance in determining the orientation of the parabolic dunes. A north-northeast oriented vector wind resultant compiled by excluding offshore winds correlates very well with the orientation of the parabolic dunes. Therefore this interaction of

wind regime and vegetation was responsible for the development and orientation of the parabolic dune field in False Cape State Park. This interactive process is also responsible for the present north-south differences in both sand hill migration rate and in cross barrier sand flux along Currituck Spit.

North-South Differences: Migration Rates and Cross Barrier Sediment Transport

The migration rate of a large sand hill near Corolla (Whalehead Hill, Figure 27) was six meters/year while a dune in False Cape State Park (Barbours Hill, Figure 28) migrated only .75 m/year. The difference in the migration rate of these two sand hills cannot be related to differences in dune dimensions, wind regime or precipitation. The density of the vegetation cover surrounding the two dunes accounts for the discrepancy.

Whalehead Hill (Figure 27) is surrounded on the east by only sparse dune grass vegetation, and is therefore attached to its source of sand, the beach. At Barbours Hill (Figure 28) however, there is a 2-3 meter shrub thicket to the east of the dune which has effectively isolated this sand hill from its source of sand. Due to these differences in vegetation cover, Whalehead Hill migrated eight times faster to the south-southwest than Barbours Hill.

The amount of vegetation cover in the two areas is also responsible for differences in the amount of cross-barrier sand flux. A cross-barrier sand grading study indicated no transport across a transect in False Cape State Park (Figures 42 and 43). However, the plots of grain size moments against distance across the barrier spit transect near Corolla indicated some grading (Figures 44 and 45) of

sediments and thus a cross-barrier flux of sand. This conclusion is also supported by sand transport measurements (Tables 8 and 9) and the transport model.

For a cross-barrier transect with a low foredune system and low-density vegetation across the eolian flat (typical of Corolla, in 1977) the model predicts a net onshore sand transport of approximately 10,000 kg/m/year (Table 11), but with large amounts of sand moving both onshore and offshore. If the barrier spit is covered by a dense growth of vegetation (False Cape State Park, in 1977) then the model predicts very little onshore-offshore transport across the interior. Instead there is a net movement of sand onshore from the ocean beach which would almost all be trapped by the high, multiple-ridge foredune system.

Management Implications

During the next few decades Currituck Spit will be undergoing rapid and complex changes due to increased development pressures. Back Bay National Wildlife Refuge and False Cape State Park will be subject to increased pressures as public recreational facilities while the section of the spit in North Carolina will see the development of private coastal recreational communities. In each of these areas the question now is how to efficiently and intelligently manage this coastal resource to minimize the environmental impact of increased development activities. The interactive process-mechanisms which relate eolian sand transport, vegetation, moisture, and dune dynamics, detailed in this thesis, has immediate management and planning implications. The control of large sand hills which can and do migrate over forests and towns is one such implication.

A source of sand and a polymodal wind regime is necessary for the formation of a medano. Therefore the most logical approach to avoiding the formation of medianos would be the elimination of the sand supply. Primarily, this could be accomplished by limiting the use of recreational vehicles, grazing animals, and foot traffic across the dunes and eolian flat. This would protect the vegetation so that no source of sand would become available for dune formation.

Protection of the vegetation and foredune is not only important for avoiding the development of medianos, but also for limiting their migration rate. The migration rate of a sand hill (Whalehead Hill) located in an area of low vegetation density migrated eight times further to the southwest over a one year period than a sand hill (Barbours Hill) located in an area with a high density vegetation cover. In fact both Barbours Hill and the previously mobile parabolic dunes in False Cape State Park have become stabilized by vegetation. Therefore the protection and encouragement of vegetation should be a prime coastal resource management objective.

The varying levels of net cross-barrier transport predicted by the eolian sand transport model also has important coastal resource management implications. The model indicates that sand fencing can have both beneficial and detrimental effects on the coastal ecosystem. The aim of most sand fencing programs is creation of a high (3-4 meters) multiple ridge foredune system. The model, field measurements, and old aerial photographs indicate that this high foredune system reduces sand transport from the beach to the interior. This reduction in sand transport allows colonization of the eolian flat by vegetation and stabilization of shifting sand. However, this reduction in transport can be considered detrimental because the interior of the barrier spit

will no longer buildup vertically by sand deposition. This would allow more inundation of low lying areas during storm surges than there might be otherwise. The decision to initiate a sand fencing program must be made by weighing the positive and negative effects relative to management objectives. The model, however, can aid in reaching an intelligent decision.

If it is decided to launch a sand fencing program, then the model can greatly aid in the design, planning and execution of the program. In particular, the location, orientation and amount of the sand fencing material needed can be determined from the eolian sand transport model.

This study has concentrated on determining the overall role of eolian sand transport in the coastal zone, by delineating the development, orientation and migration of sand dunes, and the net flux of sand across a barrier spit. Sand transport by wind is a complex, interactive process resulting from the combined effects of the local wind climate, vegetation, moisture and surface dune morphology.

REFERENCES

- Ahlbrandt, T. S. 1975. Comparison of textures and structures to distinguish eolian environments, Killpecker dune field, Wyoming. *The Mountain Geologist*, V. 12, p. 61-73.
- Anan, F. S. 1971. Provenance and statistical parameters of sediments of the Merrimack embayment, Gulf of Maine. Unpublished Ph.D. Thesis, University of Massachusetts, Amherst, Massachusetts, 377 p.
- Bagnold, R. A. 1941. *The Physics of Blown Sand and Desert Dunes*: William Morrow and Co., New York, 265 p.
- Binder, R. C. 1973. *Fluid Mechanics*: Prentice-Hall Inc., Englewood Cliffs, New Jersey, 401 p.
- Bressolier, C. and Y. Thomas. 1977. Studies on wind and plant interactions on French Atlantic coastal dunes: *Journ. Sed. Petrology*, v. 47, p. 331-338.
- Chang, J. H. 1968. *Climate and Agriculture, An Ecological Survey*: Aldine Publishing Company, Chicago, 249 p.
- Chepil, W. S. 1939. Comparative study of soil drifting in the field and in a wind tunnel: *Scientific Agriculture*, v. 19, p. 249-257.
- _____. 1956. Influence of moisture on erodibility of soil: *Proceedings of Soil Science Society*, v. 20, p. 288-291.
- _____. 1959. Equilibrium of soil grains at the threshold of movement of wind: *Proceedings of Soil Science Society*, v. 23, p. 422-428.
- _____. 1961. The use of spheres to measure lift and drag on wind eroded surfaces: *Proceedings of Soil Science Society*, v. 25, p. 343-345.
- Corps of Engineers, Department of the Army, New England Division. 1968. *Pleasant Bay Survey Report*.
- Dahl, B. E., B. A. Fall, A. Lolse and S. G. Appan. 1975. Construction and stabilization of coastal foredunes with vegetation: *Misc. Paper No. 9-75*, U.S. Army Coastal Engin. Res. Center, C.E., Washington, D. C.
- Daniel, C. and F. S. Wood. 1971. *Fitting Equations to Data*: Wiley-Interscience, New York, 342 p.

- DeAlteris, J. T. 1973. The Recent History of Wachapreague Inlet, School of Marine Science, College of William and Mary, Williamsburg, Va., Unpublished M.S. Thesis, 86 pp.
- Folk, R. L. and W. C. Ward. 1957. Brazo River Bar: A study in the significance of grain size parameters. Jour. of Sed. Petrology, v. 27, p. 3-26.
- Friedman, G. M. 1961. Distinction between dune, beach and river sands from their textural characteristics. Jour. of Sed. Petrology, v. 31, p. 514-529.
- Gibbs, R. F. and E. Nash. 1961. Beach and sand dune erosion control: Amer. Soc. Agr. Eng. Trans., v. 4, p. 122-127.
- Goldsmith, V. 1973. Eolian sedimentation in coastal areas. VIMS Contribution No. 533, 138 p.
- Goldsmith, V., H. F. Hennigar and A. L. Gutman. 1977. The VAMP coastal dune classification: in Goldsmith, V., (ed.) Coastal Processes and Resulting Forms of Sediment Accumulation, VIMS SRAMSOE No. 143, p. 26-1 - 26-20.
- Hawk, V. B. and W. C. Sharp. 1967. Sand dune stabilization along the North Atlantic Coast. Journ. Soil and Water Cons., v. 22, p. 143-146.
- Hennigar, H. F. 1978. Historical evolution of coastal sand dunes, Currituck Spit, Virginia-North Carolina: M.S. Thesis, VIMS, Gloucester Point, Virginia, in prep.
- Horikawa, K. and H. W. Shen. 1960. Sand movement by wind action: U.S. Army Corps of Eng., Tech. Memo No. 119.
- Hsu, S. 1971a. Wind stress criteria in eolian sand transport: Journ. Geophys. Res. v. 76, p. 8684-8686.
- _____. 1971b. Measurement of shear stress and roughness length on a beach: Journ. Geophys. Res. v. 76, p. 2880-2885.
- _____. 1973. Computing eolian sand transport from shear velocity measurements: Journ. Geology, v. 81, p. 739-743.
- Inman, D. L., et al. 1966. Coastal sand dunes of Guerrero Negro, Baja California, Mexico: G.S.A. Bull., v. 77, p. 787-802.
- Jennings, J. N. 1957. On the orientation of parabolic or u dunes: Geog. J., v. 123, p. 474-480.
- Johnson, J. W. 1963. Sand movement on coastal dunes: U.S.D.A. Misc. Publ. No. 970, p. 747-755.
- Kadib, A. 1963. Calculation procedure for sand transport by wind on natural beaches: U.S. Army Coastal Eng. Res. Center, Misc. Paper No. 2-64.

- Kadib, A. 1964. Sand movement by wind: U.S. Army Corps of Engineers, Tech. Memo., No. 1.
- Kawamura, R. 1951. Study of sand movement by wind: Report of the Institute of Science and Technology, v. 5, n. 3/4.
- Landsberg, S. Y. 1956. The orientation of dunes in Britain and Denmark in relation to wind: Geog. J., v. 122, pp. 176-189.
- Lathrobe, H. B., Esq. 1814. On the sand hills of Cape Henry in Virginia: Trans. Amer. Phil. Soc., v. 4, p. 439.
- Manohar, M. 1970. Mechanics of dune growth by sand fences: Dock and Harbour Authority, v. 51, p. 243-252.
- Mason, C. S. and R. L. Folk. 1958. Differentiation of beach, dune and aeolian flat environments by size analysis, Mustang Island, Texas. Jour. of Sed. Petrology, v. 28, p. 211-226.
- McCammon, R. B. 1962. Efficiency of percentile measures for describing the mean size and sorting of sedimentary particles. Journ. of Geology, v. 70, p. 453-465.
- O'Brien, M. P. and B. D. Rindlaub. 1936. The transportation of sand by wind: Civil Eng., May, 1936.
- Olson, J. S. 1958. Lake Michigan dune development, 1-2-3: Journ. Geol., v. 56, p. 254-263, p. 345-351, p. 413-483.
- Pickard, J. 1970. Rate of movement of transgressive sand dunes at Cronulla, New South Wales: Journ. of Geol. Soc. Australia, v. 19, p. 213-216.
- Pierce, J. W. 1969. Sediment budget along a barrier island chain: Sed. Geol., v. 3, p. 5-16.
- Potter, P. E. and F. J. Pettijohn. 1963. Paleocurrents and Basin Analysis, Academic Press, Inc., New York, 296 pp.
- Ranwell, D. 1958. Movement of vegetated sand dunes at Newborough Warren, Anglesey: Journ. Ecology. v. 46, p. 83-100.
- Savage, R. P. and W. W. Woodhouse. 1968. Creation and Stabilization of Coastal Barrier Dunes: U.S. Army Corps of Eng. CERC Reprint 3-69.
- Sharp, R. P. 1965. Kelso dunes, Mojave Desert, California. Geological Society of America Bulletin, no. 77, p. 1046-1073.
- Sokal, R. R. and F. J. Rohlf. 1969. Biometry. W. H. Freeman and Company, San Francisco, 776 p.
- Spiegel, M. R. 1961. Theory and Problems of Statistics. Schaum Publishing Company, New York, 359 p.

- Svaskek, J. N. and J. H. Terwindt. 1974. Measurements of sand transport by wind on a natural beach: *Sedimentology*, v. 21, p. 311-322.
- Tsoar, H. 1974. Desert dunes morphology and dynamics, El Arish (Northern Sinai), *Z. Geomorph. N.S. Suppl.* 3d. 20, pp. 41-61.
- Woodruff, N. P., et al. 1965. Sediment transportation mechanics: Wind erosion and transportation: *J. Hydraulics Div. Proc. Amer. Soc. Civil Engrn.* v. 91, p. 267-287.
- Yves-Belly, P. 1964. Sand movement by wind: U.S. Army Corps of Engrs. Tech. Memo. No. 1.
- Zeigler, J. M. and B. Gill. 1959. Tables and graphs for the settling velocity of quartz in water, above the stoke's law. References No. 59-36, Woods Hole Oceanographic Institution, Woods Hole, Mass., 13 p.
- Zeigler, J. M., G. G. Whitney and C. R. Hayes. 1960. Woods Hole rapid sediment analyser. *Journ. of Sed. Petrology*, v. 30, p. 490-495.

APPENDIX 1.

COROLLA STATION WIND DATA

Appendix 1 contains a monthly listing of the entire wind record from the anemometer operating on the Corolla Lighthouse (2/76-2/77).

Wind speeds are in miles/hour. To convert to m/sec multiply by .44704.

WIND DIRECTION AND SPEED DATA
DIRECTIONS 0-360 DEG.FROM TRUE NORTH, SPEEDS MPH

STATION- COROLLA LIGHT

DATE/ HOUR	1		4		7		10		13		16		19		22		MAX.		VECTOR AV.	
	S	D	S	D	S	D	S	D	S	D	S	D	S	D	S	D	S	D	S	D
1/ 2/76	12	195	8	205	16	185	10	195	16	205	14	185	22	175	24	175	42	175	14	186
2/ 2/76	34	215	36	275	36	295	36	285	28	305	14	305	4	295	4	295	81	305	21	279
3/ 2/76	2	145	12	205	12	145	14	155	10	125	10	125	4	25	8	335	25	145	5	146
4/ 2/76	4	318	4	225	12	225	14	230	14	245	16	235	12	245	12	245	20	245	10	239
5/ 2/76	12	245	17	55	19	45	18	35	14	15	13	35	12	15	6	135	24	15	9	35
6/ 2/76	22	225	24	235	20	265	18	5	12	15	20	5	22	5	24	15	32	5	9	327
7/ 2/76	22	5	22	5	16	5	11	355	18	335	14	335	10	355	6	275	35	355	13	351
8/ 2/76	10	245	16	235	24	235	24	245	28	255	18	285	11	325	14	304	34	245	16	259
9/ 2/76	11	315	11	315	16	335	19	355	14	355	12	35	12	25	7	5	34	355	11	352
10/ 2/76	0	35	9	235	8	215	14	225	19	215	24	214	28	215	30	235	37	215	16	221
11/ 2/76	29	235	22	245	25	245	21	235	20	256	21	315	10	37	3	355	28	305	14	256
12/ 2/76	6	85	3	85	12	55	8	45	8	65	8	145	12	155	16	155	12	155	6	107
13/ 2/76	18	185	10	235	14	235	25	245	18	255	18	255	20	245	15	240	25	245	16	238
14/ 2/76	22	255	16	285	20	5	20	25	26	25	20	35	18	65	18	65	36	25	12	17
15/ 2/76	12	95	16	85	12	115	6	145	12	185	20	215	26	215	24	235	34	215	9	183
16/ 2/76	28	235	26	245	22	245	20	255	16	245	18	235	18	215	26	225	24	215	21	237
17/ 2/76	26	235	22	235	30	235	26	235	22	245	20	235	16	185	18	225	34	235	21	231
18/ 2/76	16	220	18	225	18	225	20	215	22	215	32	205	34	215	36	235	46	215	24	219
19/ 2/76	18	265	16	265	16	275	20	305	10	285	18	255	14	235	18	235	26	295	14	264
20/ 2/76	20	265	14	355	7	345	6	55	8	75	8	125	10	160	8	178	23	255	0	358
21/ 2/76	14	155	12	155	16	140	20	145	16	185	20	195	16	195	22	205	32	195	15	174
22/ 2/76	28	215	34	215	34	215	26	225	28	215	36	245	10	325	26	5	50	235	20	231
23/ 2/76	16	5	24	355	16	5	16	335	20	335	16	45	10	35	2	115	28	335	13	2
24/ 2/76	10	175	14	225	16	245	18	245	20	235	20	215	22	235	24	235	24	235	17	229
25/ 2/76	18	235	18	235	14	255	14	245	16	235	18	215	24	215	18	225	28	215	17	230
26/ 2/76	16	225	12	225	14	225	14	235	14	215	14	225	16	235	20	225	22	205	14	226
27/ 2/76	14	265	11	285	12	315	8	335	16	25	20	25	14	45	10	185	26	15	6	346
28/ 2/76	14	225	19	230	18	235	20	245	18	255	24	235	16	225	18	235	28	245	18	236
29/ 2/76	16	235	14	225	16	225	16	225	20	235	26	215	24	215	20	225	30	215	18	224

***- DATA MISSING

WIND DIRECTION AND SPEED DATA
DIRECTIONS 0-360 DEG. FROM TRUE NORTH, SPEEDS MPH

STATION- COROLLA LIGHT

DATE/ HOUR	1		4		7		10		13		16		19		22		MAX.		VECTOR AV.	
	S	D	S	D	S	D	S	D	S	D	S	D	S	D	S	D	S	D	S	D
1/ 3/76	18	225	18	225	14	235	14	265	14	235	14	175	16	205	16	215	20	225	14	222
2/ 3/76	12	225	10	235	10	245	6	245	20	175	16	175	16	215	20	235	24	175	12	213
3/ 3/76	18	230	14	245	6	35	2	35	10	45	18	45	14	75	10	95	20	55	3	61
4/ 3/76	8	145	4	155	10	25	0	125	8	155	12	135	18	215	20	215	26	215	5	179
5/ 3/76	22	235	20	235	24	245	26	245	30	245	26	245	26	215	22	235	38	245	24	237
6/ 3/76	26	245	24	255	22	255	14	275	20	35	6	75	10	85	12	105	38	245	5	262
7/ 3/76	8	105	2	140	14	335	10	355	8	335	10	205	14	245	14	275	20	235	4	291
8/ 3/76	16	245	18	305	10	315	8	325	4	65	4	125	12	25	6	45	20	305	5	322
9/ 3/76	6	105	16	75	30	95	30	105	20	65	2	195	26	335	24	5	44	335	12	62
10/ 3/76	20	345	20	25	20	15	16	5	10	15	12	35	4	95	6	355	36	355	12	13
11/ 3/76	2	275	10	275	10	255	10	295	20	25	10	65	12	85	12	85	24	25	3	21
12/ 3/76	18	85	16	105	14	95	20	95	18	125	24	140	20	175	30	195	38	215	15	132
13/ 3/76	16	225	30	225	36	225	32	225	36	235	32	245	36	315	30	325	47	315	24	250
14/ 3/76	20	315	16	355	10	335	16	15	8	80	12	225	12	225	14	255	30	325	6	312
15/ 3/76	12	255	14	275	8	295	6	95	6	145	10	155	12	215	16	215	24	235	6	224
16/ 3/76	2	125	4	155	6	125	10	185	20	245	28	215	28	235	40	315	53	345	10	244
17/ 3/76	26	315	24	305	22	285	20	325	20	305	20	295	20	315	24	335	32	305	21	310
18/ 3/76	14	5	14	5	4	45	6	5	16	155	24	195	22	205	18	215	32	215	4	200
19/ 3/76	20	230	24	235	22	235	26	245	22	245	24	215	28	215	20	230	34	235	22	230
20/ 3/76	18	235	14	235	12	235	14	255	16	215	16	195	20	205	22	215	30	215	15	221
21/ 3/76	24	225	24	225	26	215	26	225	36	225	28	245	10	55	6	125	42	205	18	224
22/ 3/76	12	185	12	5	20	45	20	35	20	55	16	75	18	75	12	95	30	45	12	60
23/ 3/76	18	95	18	95	18	65	14	55	12	55	12	105	13	115	10	135	18	55	12	90
24/ 3/76	10	155	6	155	2	155	6	145	14	155	20	155	20	185	20	185	22	165	11	166
25/ 3/76	12	185	13	185	10	205	12	215	30	275	20	245	6	285	4	285	30	255	10	236
26/ 3/76	0	165	8	105	6	55	8	75	6	85	12	115	17	145	16	145	18	155	7	116
27/ 3/76	20	145	14	185	12	205	12	205	24	195	32	215	22	215	24	225	38	215	18	201
28/ 3/76	21	245	22	25	24	25	16	25	14	55	18	55	2	185	2	165	30	15	8	28
29/ 3/76	4	195	6	275	***	***	12	35	12	75	4	105	4	175	6	165	12	35	***	***
30/ 3/76	6	285	6	85	14	75	16	85	10	115	10	125	16	105	10	105	18	85	9	97
31/ 3/76	12	95	18	105	18	115	18	125	22	135	22	165	24	145	20	185	34	185	17	136

***- DATA MISSING

WIND DIRECTION AND SPEED DATA
DIRECTIONS 0-360 DEG. FROM TRUE NORTH, SPEEDS MPH

STATION- COROLLA LIGHT

DATE/ HOUR	1		4		7		10		13		16		19		22		MAX.		VECTOR AV.	
	S	D	S	D	S	D	S	D	S	D	S	D	S	D	S	D	S	D	S	D
1/ 4/76	26	185	20	205	24	215	24	345	8	65	14	135	16	165	14	185	38	205	9	187
2/ 4/76	14	245	14	275	14	285	12	295	26	285	16	315	34	315	32	345	39	315	17	302
3/ 4/76	26	345	20	335	20	345	12	355	8	65	10	125	0	125	10	215	30	345	8	349
4/ 4/76	18	225	20	235	24	245	20	245	20	225	32	265	12	95	30	25	42	15	12	249
5/ 4/76	26	5	22	345	14	345	20	25	10	55	10	145	18	185	18	215	36	5	5	4
6/ 4/76	16	235	16	235	16	235	14	255	12	245	20	45	16	75	12	135	22	35	4	224
7/ 4/76	8	215	12	275	18	25	16	35	16	55	12	105	14	135	14	125	24	35	5	75
8/ 4/76	12	115	10	115	16	95	20	95	10	15	20	65	26	55	24	55	34	55	15	73
9/ 4/76	30	45	30	35	36	25	34	25	36	25	26	15	20	5	20	5	42	35	28	24
10/ 4/76	20	325	20	335	20	335	22	355	12	35	8	55	12	195	10	205	38	355	9	340
11/ 4/76	18	245	20	245	20	245	22	245	14	225	24	275	36	305	30	5	44	25	16	273
12/ 4/76	26	5	30	25	30	15	26	5	20	35	16	45	2	15	4	185	38	15	17	19
13/ 4/76	14	215	10	255	6	275	4	285	14	145	20	155	12	215	20	235	26	155	9	208
14/ 4/76	14	245	12	235	12	275	4	305	14	55	10	55	10	155	12	155	18	235	2	209
15/ 4/76	***	***	***	***	***	***	14	155	14	155	18	185	20	185	18	215	24	235	***	***
16/ 4/76	20	225	16	235	18	245	18	245	16	245	16	225	20	215	20	245	24	255	17	234
17/ 4/76	18	265	12	275	12	305	8	335	10	55	16	85	10	115	8	185	16	305	1	308
18/ 4/76	4	155	0	145	8	135	8	125	4	115	8	145	12	155	12	185	16	165	6	149
19/ 4/76	12	195	6	265	4	205	10	215	14	165	18	155	18	195	16	215	26	175	10	192
20/ 4/76	16	235	14	245	10	255	14	235	14	215	20	175	20	205	20	215	22	235	14	218
21/ 4/76	18	235	14	235	14	245	14	225	16	155	16	185	24	195	26	215	30	215	15	210
22/ 4/76	18	215	16	215	18	225	16	215	22	215	24	205	16	235	12	235	28	225	17	218
23/ 4/76	14	275	10	305	10	15	12	45	6	105	10	175	20	195	10	215	22	25	2	227
24/ 4/76	12	145	16	165	6	215	6	205	12	215	20	235	22	215	24	235	28	235	12	209
25/ 4/76	28	235	26	235	28	225	30	225	26	215	30	255	24	225	28	225	52	305	26	230
26/ 4/76	22	245	20	245	18	15	18	305	12	205	12	55	26	25	24	5	34	25	7	330
27/ 4/76	20	5	16	5	10	345	10	335	12	35	8	85	8	95	18	5	28	35	10	14
28/ 4/76	20	335	20	335	18	335	14	335	10	65	10	95	6	215	8	315	26	335	9	343
29/ 4/76	16	345	14	335	12	325	8	335	10	55	6	145	8	165	8	195	20	35	3	344
30/ 4/76	16	169	8	215	6	235	10	215	16	205	24	215	22	215	16	215	26	215	14	208

***- DATA MISSING

WIND DIRECTION AND SPEED DATA
DIRECTIONS 0-360 DEG.FROM TRUE NORTH, SPEEDS MPH

STATION- COROLLA LIGHT

DATE/	HOUR 1		4		7		10		13		16		19		22		MAX.		VECTOR AV.	
	S	D	S	D	S	D	S	D	S	D	S	D	S	D	S	D	S	D	S	D
1/ 5/76	12	215	16	195	20	185	20	165	32	185	30	185	***	***	***	***	***	***	***	***
2/ 5/76	***	***	***	***	***	***	***	***	10	45	10	115	10	155	20	155	20	165	***	***
3/ 5/76	12	225	12	235	16	275	12	265	20	305	16	335	16	55	14	95	44	25	5	294
4/ 5/76	12	95	10	35	18	35	20	25	16	35	12	75	10	125	16	185	34	45	9	61
5/ 5/76	12	195	18	215	16	235	18	245	18	225	23	215	18	215	26	215	30	215	18	220
6/ 5/76	20	225	22	225	12	235	18	225	14	245	18	215	28	215	24	215	32	215	19	223
7/ 5/76	22	225	24	225	22	225	20	215	24	265	10	155	18	215	18	235	40	245	18	226
8/ 5/76	10	255	22	15	14	25	26	25	18	45	12	45	12	35	6	65	36	15	12	27
9/ 5/76	4	35	6	45	10	355	8	35	10	55	10	105	10	225	10	155	10	125	3	66
10/ 5/76	12	195	10	185	2	205	2	215	12	155	14	155	14	165	16	185	18	185	9	174
11/ 5/76	14	215	10	215	12	205	10	185	16	205	20	195	14	215	18	205	28	195	14	204
12/ 5/76	14	235	12	245	10	305	26	15	26	35	14	75	12	95	12	85	32	15	6	33
13/ 5/76	12	125	14	105	18	95	24	105	18	105	14	155	26	155	18	155	26	105	16	125
14/ 5/76	20	185	12	175	16	185	12	185	16	185	20	175	20	195	20	215	24	185	16	188
15/ 5/76	14	215	14	215	10	195	8	185	10	185	20	185	16	205	20	205	28	185	13	199
16/ 5/76	14	195	18	205	16	205	14	215	22	185	16	185	***	***	20	205	28	205	***	***
17/ 5/76	20	225	16	155	16	215	18	215	16	195	16	205	20	215	16	215	28	215	16	206
18/ 5/76	20	235	18	245	18	245	10	225	20	225	28	215	30	305	38	345	50	225	15	262
19/ 5/76	30	315	22	315	22	285	24	285	30	275	24	285	20	275	12	85	34	295	19	292
20/ 5/76	12	175	16	245	16	295	16	285	8	305	14	275	20	245	18	235	24	305	12	257
21/ 5/76	20	245	18	255	16	255	10	245	12	215	22	245	22	245	18	245	30	245	16	244
22/ 5/76	18	265	14	325	18	15	10	35	12	65	10	105	10	125	12	135	24	15	4	42
23/ 5/76	16	145	14	185	14	235	0	325	18	35	14	45	22	45	14	65	24	45	5	76
24/ 5/76	18	45	20	65	22	55	30	75	32	65	24	35	28	35	20	35	40	65	23	52
25/ 5/76	18	35	18	25	24	35	20	45	18	55	18	55	18	55	20	55	24	35	18	44
26/ 5/76	16	65	16	65	16	65	12	55	12	65	14	35	14	75	14	85	20	65	13	64
27/ 5/76	10	95	8	105	8	65	6	75	10	55	10	95	6	125	8	155	12	95	7	93
28/ 5/76	10	145	8	125	12	95	16	95	18	105	20	95	16	135	18	145	22	95	13	115
29/ 5/76	22	145	18	135	22	125	32	145	22	135	22	145	22	135	12	145	34	135	21	138
30/ 5/76	6	225	4	215	10	215	6	305	10	215	10	185	18	225	10	215	22	175	8	219
31/ 5/76	14	225	10	245	6	255	2	245	14	215	***	***	14	215	20	235	36	285	***	***

***- DATA MISSING

WIND DIRECTION AND SPEED DATA
DIRECTIONS 0-360 DEG. FROM TRUE NORTH, SPEEDS MPH

STATION- COROLLA LIGHT

DATE/ HOUR	1		4		7		10		13		16		19		22		MAX.		VECTOR AV.		
	S	D	S	D	S	D	S	D	S	D	S	D	S	D	S	D	S	D	S	D	
1/ 6/76	16	255	14	245	14	255	8	255	18	235	20	225	22	215	24	235	30	215	16	236	
2/ 6/76	22	245	12	235	12	235	4	275	16	65	24	65	26	75	24	65	32	55	5	74	
3/ 6/76	20	65	26	75	24	65	24	75	20	65	26	55	26	55	82	65	28	75	30	64	
4/ 6/76	26	65	26	65	32	55	32	55	32	45	32	55	36	55	34	55	42	45	31	55	
5/ 6/76	36	55	36	55	32	55	36	45	38	55	30	45	32	35	38	35	42	55	34	47	
6/ 6/76	24	35	20	35	20	35	20	35	8	65	6	85	8	165	10	165	28	35	10	50	
7/ 6/76	6	215	6	275	0	215	2	235	4	185	10	185	8	195	6	175	14	165	4	202	
8/ 6/76	6	135	8	85	16	45	20	25	20	15	14	25	4	15	8	225	26	15	8	34	
9/ 6/76	14	235	12	265	4	295	2	275	10	165	14	175	12	225	12	225	20	175	7	221	
10/ 6/76	10	235	6	215	6	205	12	165	6	185	10	205	10	205	10	215	18	165	8	203	
11/ 6/76	8	265	10	245	12	245	10	245	16	215	14	235	14	235	16	235	20	215	12	237	
12/ 6/76	10	255	12	305	12	325	4	35	4	95	16	105	20	95	22	95	30	95	4	76	
13/ 6/76	26	95	26	95	26	95	20	95	16	115	10	115	10	115	8	115	32	95	17	101	
14/ 6/76	8	115	6	135	8	105	6	125	12	135	16	165	16	175	12	205	20	155	8	152	
15/ 6/76	8	215	6	195	8	245	4	245	24	225	24	215	20	225	18	215	30	225	13	221	
16/ 6/76	12	225	16	215	20	215	16	215	30	215	32	215	30	215	26	215	34	235	22	215	
17/ 6/76	***	***	***	***	***	***	***	***	***	***	***	***	***	***	***	***	***	***	***	***	***
18/ 6/76	***	***	***	***	***	***	***	***	***	***	***	***	***	***	***	***	***	***	***	***	***
19/ 6/76	***	***	***	***	***	***	***	***	***	***	10	165	22	215	28	225	32	225	***	***	
20/ 6/76	16	235	16	215	16	205	20	175	26	205	32	215	20	215	24	205	36	235	20	208	
21/ 6/76	18	185	22	185	22	205	26	205	24	205	12	195	14	215	12	195	36	215	18	199	
22/ 6/76	24	205	16	225	6	155	18	155	10	185	14	205	8	175	4	225	26	205	11	192	
23/ 6/76	0	295	8	155	16	175	16	165	16	175	12	215	10	235	4	275	20	195	8	187	
24/ 6/76	0	95	12	155	16	155	18	215	16	215	20	225	20	235	18	235	24	195	12	210	
25/ 6/76	14	245	14	255	20	245	20	245	18	225	20	245	18	255	18	245	24	245	17	244	
26/ 6/76	16	275	8	315	14	55	12	55	4	85	6	235	2	255	2	285	28	285	2	344	
27/ 6/76	2	5	4	35	6	95	6	95	4	145	4	225	8	265	10	295	12	55	0	297	
28/ 6/76	4	325	0	185	6	105	14	155	14	175	16	225	12	49	12	255	18	155	3	185	
29/ 6/76	12	245	10	245	10	215	18	175	20	205	20	215	14	225	18	245	24	195	14	218	
30/ 6/76	16	225	20	215	20	215	24	225	36	215	30	225	26	235	20	245	46	215	23	224	

***- DATA MISSING

WIND DIRECTION AND SPEED DATA
DIRECTIONS 0-360 DEG. FROM TRUE NORTH, SPEEDS MPH

STATION- COROLLA LIGHT

DATE/	HOUR 1		4		7		10		13		16		19		22		MAX.		VECTOR AV.		
	S	D	S	D	S	D	S	D	S	D	S	D	S	D	S	D	S	D	S	D	
1/ 7/76	20	245	10	245	14	225	10	215	10	225	18	265	10	215	2	25	34	255	10	237	
2/ 7/76	4	15	10	45	8	75	10	105	10	155	12	175	12	185	10	245	14	45	4	142	
3/ 7/76	8	245	6	235	12	225	12	155	20	215	10	155	12	315	12	25	30	215	5	219	
4/ 7/76	16	5	8	5	6	335	6	55	30	65	8	45	10	15	10	5	14	35	10	29	
5/ 7/76	16	15	8	35	4	75	***	***	***	***	***	***	***	***	***	***	***	***	***	***	
6/ 7/76	***	***	***	***	***	***	***	***	***	***	***	***	***	***	***	***	***	***	***	***	
7/ 7/76	***	***	***	***	***	***	***	***	***	***	***	***	***	***	***	***	***	***	***	***	
8/ 7/76	14	245	12	255	8	255	14	235	10	225	20	205	22	235	14	235	24	215	***	***	
9/ 7/76	14	235	6	235	12	215	26	25	14	135	6	305	8	305	6	325	38	15	2	287	
10/ 7/76	16	15	8	55	8	155	12	185	16	215	16	235	20	255	16	235	26	245	6	229	
11/ 7/76	22	245	20	245	18	255	20	255	18	295	26	275	10	335	8	305	46	335	15	270	
12/ 7/76	16	285	18	285	26	245	16	25	14	5	16	5	10	355	10	305	34	245	10	315	
13/ 7/76	14	275	14	275	14	275	18	245	16	325	16	5	8	305	10	335	22	15	10	296	
14/ 7/76	12	325	0	85	10	265	12	265	12	255	12	275	8	285	10	305	14	325	8	281	
15/ 7/76	6	335	10	125	22	135	12	245	14	225	10	245	12	255	6	295	44	185	5	215	
16/ 7/76	6	305	10	165	12	235	16	255	16	255	16	285	12	315	8	335	26	325	8	270	
17/ 7/76	10	35	8	95	12	145	8	105	10	105	10	85	18	65	20	75	24	75	10	85	
18/ 7/76	18	55	20	75	16	65	12	55	10	75	10	65	12	65	10	75	22	75	13	65	
19/ 7/76	10	65	10	75	10	85	10	85	8	125	6	95	2	55	6	55	10	85	7	82	
20/ 7/76	8	65	4	125	10	145	12	205	12	225	12	245	10	245	6	265	18	245	5	212	
21/ 7/76	10	215	12	215	16	205	16	215	18	215	22	235	14	225	2	245	22	215	13	219	
22/ 7/76	***	***	***	***	***	***	***	***	***	***	***	***	***	***	***	***	***	***	***	***	***
23/ 7/76	***	***	***	***	***	***	***	***	***	***	***	***	***	***	***	***	***	***	***	***	***
24/ 7/76	***	***	***	***	***	***	***	***	***	***	***	***	***	***	***	***	***	***	***	***	***
25/ 7/76	8	355	20	35	10	45	12	65	6	245	10	215	18	265	16	335	26	285	***	***	
26/ 7/76	10	95	10	175	***	***	***	***	***	***	***	***	***	***	***	***	***	***	9	45	
27/ 7/76	***	***	***	***	***	***	***	***	***	***	***	***	***	***	***	***	***	***	***	***	***
28/ 7/76	***	***	***	***	***	***	***	***	***	***	***	***	***	***	***	***	***	***	***	***	***
29/ 7/76	***	***	***	***	***	***	***	***	***	***	***	***	***	***	***	***	***	***	***	***	***
30/ 7/76	***	***	***	***	***	***	***	***	***	***	***	***	***	***	***	***	***	***	***	***	***
31/ 7/76	***	***	***	***	***	***	***	***	***	***	***	***	***	***	***	***	***	***	***	***	***

***- DATA MISSING

WIND DIRECTION AND SPEED DATA
 DIRECTIONS 0-360 DEG. FROM TRUE NORTH, SPEEDS MPH

STATION- COROLLA LIGHT

DATE/ HOUR	1		4		7		10		13		16		19		22		MAX.		VECTOR AV.		
	S	D	S	D	S	D	S	D	S	D	S	D	S	D	S	D	S	D	S	D	
1/ 8/76	***	***	***	***	***	***	***	***	***	***	***	***	***	***	***	***	***	***	***	***	***
2/ 8/76	***	***	***	***	***	***	***	***	***	***	***	***	***	***	***	***	***	***	***	***	***
3/ 8/76	***	***	***	***	***	***	***	***	***	***	***	***	***	***	***	***	***	***	***	***	***
4/ 8/76	***	***	***	***	***	***	***	***	***	***	***	***	***	***	***	***	***	***	***	***	***
5/ 8/76	***	***	***	***	***	***	***	***	***	***	***	***	***	***	***	***	***	***	***	***	***
6/ 8/76	***	***	***	***	***	***	***	***	***	***	***	***	***	***	***	***	***	***	***	***	***
7/ 8/76	***	***	***	***	***	***	***	***	18	165	16	175	19	170	17	165	21	165	***	***	***
8/ 8/76	14	195	16	195	20	205	12	205	18	195	4	215	4	5	12	125	26	185	10	192	
9/ 8/76	11	65	14	55	23	35	40	5	45	355	40	295	22	270	12	245	70	345	16	344	
10/ 8/76	10	235	6	235	9	175	10	185	12	165	15	165	10	245	6	275	24	305	7	200	
11/ 8/76	6	35	4	35	8	35	6	25	6	55	***	***	***	***	***	***	***	***	***	***	
12/ 8/76	***	***	***	***	***	***	***	***	***	***	***	***	***	***	***	***	***	***	***	***	***
13/ 8/76	***	***	***	***	***	***	***	***	***	***	***	***	***	***	***	***	***	***	***	***	***
14/ 8/76	***	***	***	***	***	***	***	***	***	***	***	***	***	***	***	***	***	***	***	***	***
15/ 8/76	22	225	20	215	18	235	18	245	16	215	20	205	20	215	20	215	28	215	18	214	
16/ 8/76	14	265	14	325	8	295	6	25	18	35	8	55	14	45	14	65	26	245	6	13	
17/ 8/76	20	35	22	35	24	35	18	25	22	25	14	55	14	35	10	45	28	45	17	34	
18/ 8/76	10	15	10	335	10	25	22	45	28	45	28	45	26	55	30	55	36	55	19	42	
19/ 8/76	26	65	30	65	30	65	24	65	26	65	26	55	24	55	28	65	34	65	26	62	
20/ 8/76	22	75	18	85	24	75	24	85	22	75	22	75	26	75	20	95	26	75	22	79	
21/ 8/76	20	95	18	95	16	95	16	95	16	85	14	115	12	85	12	95	22	95	15	94	
22/ 8/76	8	95	10	85	8	65	6	65	6	95	8	85	6	115	8	165	12	115	6	94	
23/ 8/76	12	185	10	215	6	305	4	265	10	155	10	165	14	195	14	215	16	175	8	198	
24/ 8/76	10	225	6	265	2	305	0	335	12	55	14	75	14	95	18	95	20	105	5	90	
25/ 8/76	12	85	10	85	14	95	8	75	8	75	10	125	12	145	10	165	14	45	8	106	
26/ 8/76	12	185	6	185	6	255	2	285	5	145	14	175	18	165	14	175	22	175	8	179	
27/ 8/76	16	185	10	215	8	255	4	255	6	195	20	165	18	195	18	205	24	205	11	197	
28/ 8/76	***	***	***	***	***	***	***	***	***	***	20	165	16	185	18	215	26	215	***	***	
29/ 8/76	20	235	22	245	22	235	20	245	18	225	22	235	4	305	18	235	30	235	17	238	
30/ 8/76	16	45	30	35	36	35	26	25	24	25	20	25	18	25	18	35	38	35	23	31	
31/ 8/76	20	35	20	45	18	45	18	75	10	75	30	95	20	125	10	145	26	55	15	76	

***- DATA MISSING

WIND DIRECTION AND SPEED DATA
DIRECTIONS 0-360 DEG. FROM TRUE NORTH, SPEEDS MPH

STATION- COROLLA LIGHT

DATE/ HOUR	1		4		7		10		13		16		19		22		MAX.		VECTOR AV.	
	S	D	S	D	S	D	S	D	S	D	S	D	S	D	S	D	S	D	S	D
1/ 9/76	12	145	12	165	6	215	4	135	10	145	12	175	18	53	16	195	20	175	7	153
2/ 9/76	18	205	10	225	4	225	4	205	18	25	20	55	10	85	8	85	24	75	2	90
3/ 9/76	1	265	18	35	12	55	14	65	22	55	16	55	22	55	18	75	26	65	14	55
4/ 9/76	20	85	12	75	22	65	16	75	16	65	10	75	8	95	8	95	24	65	13	76
5/ 9/76	8	145	50	235	6	275	4	255	10	135	12	165	12	185	14	195	18	145	11	206
6/ 9/76	10	225	34	55	26	35	28	45	20	35	20	35	10	65	6	85	38	45	16	45
7/ 9/76	4	55	6	315	10	65	10	335	10	65	8	95	6	185	12	195	18	235	2	71
8/ 9/76	12	235	14	245	12	275	10	285	6	235	16	225	12	215	16	235	20	235	11	241
9/ 9/76	14	245	14	265	12	275	10	275	8	255	12	235	14	205	22	225	24	225	12	244
10/ 9/76	18	235	18	245	18	225	22	215	18	215	20	5	26	25	12	315	32	325	7	259
11/ 9/76	16	335	18	345	14	335	16	335	10	305	8	65	20	175	10	215	18	325	6	324
12/ 9/76	10	255	14	275	14	305	10	315	12	35	10	65	8	125	6	185	16	35	3	310
13/ 9/76	6	125	4	255	4	275	2	315	4	95	6	145	4	155	2	185	8	275	1	161
14/ 9/76	0	175	2	65	10	95	10	85	14	95	12	95	18	95	22	105	22	105	10	95
15/ 9/76	22	105	22	115	28	115	26	115	22	125	30	125	26	145	28	145	42	135	24	124
16/ 9/76	30	155	12	155	12	165	10	185	10	155	16	155	18	175	20	195	38	155	15	167
17/ 9/76	14	225	16	215	6	215	10	225	12	235	12	225	8	215	10	205	18	215	10	220
18/ 9/76	16	225	8	225	10	235	10	265	3	245	10	245	10	295	10	285	36	295	8	251
19/ 9/76	14	295	10	315	6	325	6	35	8	65	6	75	8	125	8	175	14	295	1	2
20/ 9/76	8	215	8	245	12	245	18	225	18	215	18	225	18	215	26	225	32	225	15	224
21/ 9/76	12	235	18	255	14	255	10	265	8	315	10	245	12	245	14	345	30	235	10	265
22/ 9/76	8	35	16	345	16	355	50	345	6	275	8	75	8	55	8	15	20	345	12	358
23/ 9/76	4	45	2	75	6	145	14	195	16	155	16	175	18	85	16	193	22	165	8	155
24/ 9/76	10	225	12	235	8	245	10	265	6	195	12	185	16	185	14	205	18	213	9	214
25/ 9/76	6	225	4	255	4	245	4	255	10	125	14	155	16	165	14	185	***	***	6	178
26/ 9/76	14	215	12	225	10	205	16	205	14	215	24	185	18	215	20	215	30	185	15	208
27/ 9/76	20	235	14	255	24	255	20	265	26	285	22	265	24	245	26	265	30	255	21	259
28/ 9/76	28	285	20	325	18	35	14	35	22	55	18	75	14	75	12	95	32	235	10	30
29/ 9/76	14	35	14	165	12	35	14	185	12	95	8	185	10	175	10	175	18	165	5	139
30/ 9/76	16	95	16	155	20	175	18	175	14	175	10	175	14	225	12	325	40	175	9	171

***- DATA MISSING

WIND DIRECTION AND SPEED DATA
DIRECTIONS 0-360 DEG. FROM TRUE NORTH, SPEEDS MPH

STATION- COROLLA LIGHT

DATE/ HOUR	1		4		7		10		13		16		19		22		MAX.		VECTOR AV.		
	S	D	S	D	S	D	S	D	S	D	S	D	S	D	S	D	S	D	S	D	
1/10/76	14	345	4	345	8	285	23	39	27	41	10	41	2	85	10	345	14	245	9	18	
2/10/76	10	5	10	235	12	15	16	245	16	225	16	295	10	305	10	265	22	225	7	278	
3/10/76	10	275	12	265	14	285	14	345	18	345	18	25	5	18	5	20	5	22	5	11 339	
4/10/76	16	55	12	85	12	85	10	5	14	45	20	85	26	40	26	65	28	85	15	59	
5/10/76	20	55	12	55	14	55	16	65	20	45	18	65	18	85	12	35	24	45	15	58	
6/10/76	10	245	10	255	6	255	4	85	6	95	10	65	14	175	10	195	18	195	3	193	
7/10/76	12	215	6	235	0	35	4	205	10	205	12	195	12	175	14	165	16	205	8	194	
8/10/76	14	185	10	175	8	181	8	175	8	275	12	155	0	165	16	215	26	215	8	190	
9/10/76	22	225	24	205	38	215	34	275	30	225	26	265	24	305	32	335	100	275	21	254	
10/10/76	26	345	20	355	18	355	16	25	14	355	10	325	14	5	8	345	24	355	15	354	
11/10/76	10	315	14	325	14	345	14	15	14	35	16	35	12	15	14	5	24	35	11	3	
12/10/76	24	35	24	65	20	65	18	55	20	35	18	25	16	55	10	55	26	35	18	48	
13/10/76	10	35	14	335	12	345	8	305	8	245	16	215	10	235	20	235	24	235	6	273	
14/10/76	26	255	22	285	12	295	10	5	14	5	16	5	8	5	6	325	32	255	10	315	
15/10/76	8	245	12	225	16	205	18	205	20	235	16	215	20	215	20	225	26	225	15	219	
16/10/76	22	245	18	235	14	245	10	345	14	35	14	55	20	85	26	75	26	75	2	50	
17/10/76	26	85	24	65	32	65	26	65	36	35	34	35	38	15	40	5	46	15	28	41	
18/10/76	26	355	36	5	22	335	20	335	28	5	20	15	16	25	14	35	44	15	21	1	
19/10/76	10	55	10	65	16	85	18	105	16	47	16	115	14	155	24	155	24	75	11	104	
20/10/76	18	155	24	145	24	145	26	145	22	175	46	155	26	185	36	265	58	145	21	168	
21/10/76	28	215	30	275	20	285	24	315	10	335	10	225	14	285	16	301	30	285	15	277	
22/10/76	12	335	12	305	16	285	16	265	20	305	18	305	12	295	8	285	28	285	13	297	
23/10/76	6	305	5	295	10	335	16	35	10	35	8	80	4	125	10	135	18	295	4	34	
24/10/76	10	155	4	205	6	215	4	295	20	135	16	155	18	185	14	215	34	135	9	174	
25/10/76	16	225	12	235	12	255	12	225	18	235	8	185	16	155	18	165	26	175	11	209	
26/10/76	22	185	30	205	18	235	30	355	40	355	30	355	22	5	28	5	44	355	12	339	
27/10/76	26	5	24	5	36	15	28	335	24	5	26	355	18	315	30	5	38	15	25	357	
28/10/76	28	15	28	15	28	5	36	5	28	25	18	5	14	355	12	345	36	15	23	8	
29/10/76	10	285	10	285	12	295	12	275	4	275	14	195	12	215	14	225	16	215	8	252	
30/10/76	12	235	12	245	12	235	10	235	***	***	***	***	***	***	***	***	***	***	***	***	***

***- DATA MISSING

WIND DIRECTION AND SPEED DATA
DIRECTIONS 0-360 DEG. FROM TRUE NORTH, SPEEDS MPH

STATION- COROLLA LIGHT

DATE/	HOUR 1		4		7		10		13		16		19		22		MAX.		VECTOR AV.	
	S	D	S	D	S	D	S	D	S	D	S	D	S	D	S	D	S	D	S	D
1/11/76	26	155	26	185	16	215	22	225	14	235	10	35	16	305	24	335	32	345	8	223
2/11/76	20	335	22	345	22	345	30	355	28	355	24	355	16	5	18	355	30	355	22	351
3/11/76	26	355	30	35	26	5	20	5	10	25	8	75	6	185	10	195	34	335	11	16
4/11/76	10	205	10	205	6	205	4	295	4	235	6	165	8	155	8	185	12	275	5	196
5/11/76	8	235	10	265	6	235	10	275	4	105	12	135	18	155	20	185	20	235	6	193
6/11/76	12	195	16	215	12	215	8	245	16	245	18	295	12	265	20	305	32	255	11	252
7/11/76	26	325	18	305	14	285	14	295	14	255	18	215	14	225	16	225	30	335	12	270
8/11/76	18	245	18	245	14	255	12	255	18	215	20	225	14	235	12	225	20	215	15	236
9/11/76	34	15	38	355	22	345	22	305	20	315	30	335	32	325	20	335	50	325	25	339
10/11/76	16	305	14	305	12	305	14	195	20	205	20	195	24	185	26	225	28	225	12	226
11/11/76	26	235	20	245	24	235	24	245	18	285	16	295	8	245	10	225	32	235	16	249
12/11/76	10	225	20	5	20	35	6	325	6	355	10	165	12	55	16	55	24	25	6	30
13/11/76	18	75	28	75	24	355	26	25	34	35	30	5	20	5	16	335	32	355	20	24
14/11/76	18	335	20	335	20	325	20	345	18	355	18	5	12	345	8	305	28	355	16	340
15/11/76	6	275	8	275	8	315	6	305	6	215	12	215	6	235	8	245	14	225	6	256
16/11/76	10	245	6	5	12	55	22	65	22	45	***	***	***	***	***	***	***	***	***	***
17/11/76	***	***	***	***	***	***	***	***	18	5	16	15	8	5	6	335	***	***	***	***
18/11/76	6	335	8	345	8	355	6	335	4	35	2	355	4	275	12	255	16	255	4	323
19/11/76	16	265	18	265	20	285	28	305	18	305	16	285	10	275	12	235	36	295	16	281
20/11/76	14	235	18	235	22	235	24	255	20	255	16	225	24	235	24	255	26	255	19	242
21/11/76	18	345	30	25	22	35	14	35	6	35	6	85	8	145	6	155	36	25	10	33
22/11/76	6	215	8	225	2	295	6	5	12	65	10	95	6	175	34	305	36	305	2	309
23/11/76	24	285	26	305	20	285	24	295	20	305	22	305	16	285	20	295	32	285	21	295
24/11/76	16	295	18	295	20	295	16	305	14	305	14	295	12	275	12	265	22	285	14	292
25/11/76	10	275	12	295	10	305	6	275	4	215	14	225	16	305	20	225	24	225	9	265
26/11/76	16	235	16	265	10	325	4	335	0	5	12	195	18	195	20	215	24	205	8	231
27/11/76	18	225	16	235	18	215	16	225	16	215	12	225	14	195	24	195	30	195	16	215
28/11/76	16	205	10	215	6	160	12	255	4	275	16	215	18	235	16	235	24	195	11	224
29/11/76	16	245	16	245	10	225	16	195	12	225	16	195	16	185	26	205	30	215	14	213
30/11/76	26	215	34	225	16	265	22	235	22	35	20	5	18	5	16	345	40	215	7	281

***- DATA MISSING

WIND DIRECTION AND SPEED DATA
DIRECTIONS 0-360 DEG. FROM TRUE NORTH, SPEEDS MPH

STATION- COROLLA LIGHT

DATE/	HOUR 1		4		7		10		13		16		19		22		MAX.		VECTOR AV.	
	S	D	S	D	S	D	S	D	S	D	S	D	S	D	S	D	S	D	S	D
1/12/76	16	355	20	5	20	5	26	5	14	15	14	5	12	5	16	265	28	5	14	357
2/12/76	0	155	14	325	14	325	12	305	6	195	12	245	14	255	22	355	34	5	8	304
3/12/76	30	15	24	15	30	5	24	35	16	35	10	35	4	35	12	355	36	5	18	18
4/12/76	8	75	8	75	10	75	4	355	8	105	2	135	8	215	6	355	12	15	3	76
5/12/76	14	25	16	35	20	55	24	35	22	35	24	35	22	55	22	55	26	35	20	41
6/12/76	24	75	22	85	24	75	28	85	22	75	22	65	14	135	28	145	32	155	20	90
7/12/76	28	175	28	165	24	275	40	195	20	235	18	325	12	345	14	15	52	195	10	218
8/12/76	18	35	26	15	30	25	26	5	26	345	28	335	22	325	16	345	38	325	22	358
9/12/76	12	285	14	275	10	315	10	325	0	315	12	205	8	215	8	215	16	285	6	265
10/12/76	2	115	2	165	2	275	4	235	2	245	12	215	18	215	16	215	20	215	6	215
11/12/76	14	235	14	305	12	295	12	305	2	65	10	105	16	135	10	165	18	225	2	239
12/12/76	10	175	6	175	6	255	6	261	10	260	10	225	14	245	20	265	26	275	8	239
13/12/76	26	305	18	325	30	5	24	15	26	35	26	25	20	25	24	45	36	15	20	9
14/12/76	20	45	16	65	14	125	10	145	8	155	8	175	12	165	16	155	22	55	8	121
15/12/76	22	175	8	35	10	75	***	***	12	105	26	55	26	55	30	55	36	55	***	***
16/12/76	26	35	28	15	20	345	18	335	16	325	8	325	10	255	20	275	30	5	13	341
17/12/76	20	305	14	275	20	301	20	275	34	265	26	235	26	245	28	5	42	265	18	279
18/12/76	30	15	20	5	12	345	12	345	20	35	4	5	6	245	6	245	30	15	10	2
19/12/76	4	175	8	215	10	225	12	205	18	205	24	215	22	215	18	215	26	215	14	211
20/12/76	14	225	16	235	18	215	22	215	24	205	20	215	30	215	22	235	36	225	20	218
21/12/76	30	335	28	305	30	305	38	305	40	295	42	305	32	305	26	305	48	265	32	306
22/12/76	26	305	20	305	18	305	10	325	8	165	18	225	20	215	18	225	30	305	11	267
23/12/76	16	235	18	245	18	245	14	285	18	255	16	245	18	245	24	275	26	265	17	253
24/12/76	14	275	24	335	26	355	22	355	26	5	10	345	4	355	4	265	34	5	14	343
25/12/76	10	195	8	235	12	215	18	215	16	235	12	185	14	185	20	175	30	215	12	203
26/12/76	10	305	12	215	22	5	22	345	30	355	20	355	8	355	16	255	42	345	12	336
27/12/76	24	255	36	325	24	315	30	325	16	325	18	295	12	195	24	195	40	335	15	294
28/12/76	32	215	40	235	10	225	26	235	26	235	16	235	16	235	18	215	30	235	22	229
29/12/76	20	235	18	265	24	325	6	245	14	345	22	295	8	355	22	285	40	285	13	292
30/12/76	18	305	22	315	22	305	16	295	8	245	20	205	24	215	22	225	36	205	13	263
31/12/76	26	235	22	235	20	305	20	315	32	5	30	5	16	355	14	5	38	15	13	324

***- DATA MISSING

APPENDIX 2.

WIND ROSE DIAGRAM PROGRAM

Appendix 2 contains a listing of the computer program which generates the wind rose diagrams illustrated in figures 4 thru 6, and 9 thru 23.

```

//VCTRPLT JOB (4891,WMVE,02,30,700,,1),'GUTMAN(VIMS)',MSGLEVEL=(1,1),
// CLASS=R,REGION=256K
/*ROUTE PRINT LOCAL
/*MESSAGE PUT IN VIMS BIN PLEASE THANK YOU
/*SETUP TAPE VS0302,RINGIN,BIN 0-029,SL
/*SETUP PLOT VS0302
// EXEC FPLOTL,TAPE=VS0302,LABEL=1
//FORT.SYSIN DD *
    DIMENSION TITL(6),X(100),IBUF(1800),A(50),R(4000),THETA(4000)
    DIMENSION XD(100),XP(100),YP(100)
    CALL PLOTS(IBUF,1800)
    CALL FACTOR(.8)
    READ(5,1)N,TITL
    1 FORMAT(I6,6X,6A4)
    READ(5,2)(R(I),THETA(I),I=1,N)
    2 FORMAT(22X,16F3.0)
    50 CONTINUE
    666 CONTINUE
    DO 210 I=1,8
    X(I)=0.0
    XD(I)=0.0
    XP(I)=0.0
    YP(I)=0.0
    210 CONTINUE
    NUMB=N
    DO 300 I=1,N
    IF(R(I).GT.150.0)GO TO 299
    CONVERTS KNOTS TO M.P.H.
    R(I)=R(I)*1.2
    R(I)=R(I)*.44704
    IF(THETA(I).LE.22.5) GO TO 51
    IF(THETA(I).LE.67.5) GO TO 52
    IF(THETA(I).LE.112.5) GO TO 53
    IF(THETA(I).LE.157.5) GO TO 54
    IF(THETA(I).LE.202.5) GO TO 55
    IF(THETA(I).LE.247.5) GO TO 56
    IF(THETA(I).LE.292.5) GO TO 57
    IF(THETA(I).LE.337.5) GO TO 58
    IF(THETA(I).LE.395.0) GO TO 51
    GO TO 300
    51 X(1)=X(1)+R(I)
    XD(1)=XD(1)+1.0
    GO TO 300
    52 X(2)=X(2)+R(I)
    XD(2)=XD(2)+1.0

```

```

      GO TO 300
53  X(3)=X(3)+R(I)
      XD(3)=XD(3)+1.0
      GO TO 300
54  X(4)=X(4)+R(I)
      XD(4)=XD(4)+1.0
      GO TO 300
55  X(5)=X(5)+R(I)
      XD(5)=XD(5)+1.0
      GO TO 300
56  X(6)=X(6)+R(I)
      XD(6)=XD(6)+1.0
      GO TO 300
57  X(7)=X(7)+R(I)
      XD(7)=XD(7)+1.0
      GO TO 300
58  X(8)=X(8)+R(I)
      XD(8)=XD(8)+1.0
      GO TO 300
299 NUMB=NUMB+(-1.0)
      GO TO 300
300 CONTINUE
      PRINT 9,NUMB
      9 FORMAT(I6)
      DO 760 I=1,8
      PRINT 7,I,X(I),XD(I)
      7 FORMAT(I6,2F12.6)
760 CONTINUE

```

```

C
C
C      COMPUTES THE AVERAGE WIND SPEED AND DURATION FOR EACH VECTOR
C
C

```

```

      DO 770 I=1,8
      X(I)={(X(I)/XD(I))-3.0}/2.0
      XD(I)={XD(I)/NUMB}*100.0
      PRINT 8,I,X(I),XD(I)
      8 FORMAT(I6,2F10.6)
      XD(I)=XD(I)/15.0
770 CONTINUE
      YN=0.0
      XNE=0.0
      YNE=0.0
      XE=0.0
      YE =0.0

```



```

XSE=0.0
YSE=0.0
XS=0.0
YS=0.0
XSW=0.0
YSW=0.0
XW=0.0
YW=0.0
XNW=0.0
YNW=0.0
YN=6.0+X(1)
XNE=(.7071*X(2))+5.7071
YNE=XNE
XE=6.0+X(3)
XSE=(.7071*X(4))+5.7071
YSE=(-.7071)*X(4)+4.2929
YS=4.0-X(5)
XSW=(-.7071)*X(6)+4.2929
YSW=XSW
XW=4.0-X(7)
XNW=(-.7071)*X(8)+4.2929
YNW=(.7071*X(8))+5.7071
XP(1)=5.0
YP(1)=6.0+XD(1)
XP(2)=(.7071*XD(2))+5.7071
YP(2)=XP(2)
XP(3)=6.0+XD(3)
YP(3)=5.0
XP(4)=(.7071*XD(4))+5.7071
YP(4)=(-.7071)*XD(4)+4.2929
XP(5)=5.0
YP(5)=4.0-XD(5)
XP(6)=(-.7071)*XD(6)+4.2929
YP(6)=XP(6)
XP(7)=4.0-XD(7)
YP(7)=5.0
XP(8)=(-.7071)*XD(8)+4.2929
YP(8)=(.7071*XD(8))+5.7071
XP(9)=XP(1)
YP(9)=YP(1)
CALL SYMBOL (0.0,1.0,0.35,'CORROLLA WIND DATA',90.0,18)
CALL PLOT (1.0,-11.0,-3)
CALL PLOT(0.0,1.5,-3)
CALL PLOT (6.0,5.0,3)
CALL CIRCL(5.0,5.0,0.0,360.0,1.0,2)

```

```

CALL PLOT(6.5,5.0,3)
CALL CIRCL(5.0,5.0,0.0,360.0,1.5,2)
CALL PLOT(7.0,5.0,3)
CALL CIRCL(5.0,5.0,0.0,360.0,2.0,2)
CALL PLOT(7.5,5.0,3)
CALL CIRCL(5.0,5.0,0.0,360.0,2.5,2)
CALL PLOT(8.0,5.0,3)
CALL CIRCL(5.0,5.0,0.0,360.0,3.0,2)
CALL PLOT(8.5,5.0,3)
CALL CIRCL(5.0,5.0,0.0,360.0,3.5,2)
CALL SYMBOL(4.7,8.7,.14,'NORTH',0.0,5)
CALL SYMBOL(18.70,4.95,.14,'EAST',0.0,4)
CALL SYMBOL(13.50,.70,.14,'INCLUDES ALL WIND SPEEDS',0.0,24)
CALL SYMBOL(4.70,1.10,.14,'SOUTH',0.0,5)
CALL SYMBOL(.90,4.95,.14,'WEST',0.0,4)
CALL SYMBOL(13.4,9.6,.21,'HATTERAS STATION',0.0,16)
CALL SYMBOL(3.3,9.2,.21,'TITL',0.0,24)
CALL SYMBOL(6.78,5.7,.14,'15%',22.5,3)
CALL SYMBOL(5.8,5.35,.14,'0%',22.5,2)
CALL SYMBOL(7.68,6.1,.14,'30%',22.5,3)
CALL SYMBOL(3.95,4.60,.14,'3.0',22.5,3)
CALL SYMBOL(3.05,4.2,.14,'5.0',22.5,3)
CALL SYMBOL(2.13,3.80,.14,'7.0',22.5,3)
CALL SYMBOL(1.49,3.55,.14,'A',22.5,1)
CALL SYMBOL(8.51,6.45,.14,'B',22.5,1)
CALL SYMBOL(4.45,5.6,.11,'AVG. WIND',0.0,9)
CALL PARROW(4.4,5.4,5.0,5.4,1)
CALL SYMBOL(5.3,5.3,.14,'A',0.0,1)
CALL SYMBOL(4.4,5.1,.11,'SPEED',0.0,5)
CALL SYMBOL(5.1,5.1,.11,'(M/S)',0.0,5)
CALL SYMBOL(4.5,4.7,.11,'DURATION',0.0,8)
CALL PLOT(4.4,4.5,3)
CALL PLOT(4.9,4.5,2)
CALL SYMBOL(4.7,4.5,.07,1,0.0,-1)
CALL SYMBOL(5.3,4.45,.14,'B',0.0,1)
CALL SYMBOL(4.45,4.25,.11,'(PERCENT)',0.0,9)
CALL PLOT(0.0,0.0,-3)
CALL BLOKNO(NNN)
PRINT 10,NNN
10 FORMAT(' THE BLOCK NO. IS ',I4)
CALL PARROW(5.0,YN,5.0,6.0,1)
CALL PARROW(XNE,YNE,5.7071,5.7071,1)
CALL PARROW(XE,5.0,6.0,5.0,1)
CALL PARROW(XSE,YSE,5.7071,4.2929,1)
CALL PARROW(5.0,YS,5.0,4.0,1)
CALL PARROW(XSW,YSW,4.2929,4.2929,1)
CALL PARROW(XW,5.0,4.0,5.0,1)
CALL PARROW(XNW,YNW,4.2929,5.7071,1)
CALL LINO(XP,YP,9,1,1,1,0.0,1.0,0.0,1.0)
CALL PLOT(15.0,0.0,-3)
CALL PLOT(20.0,-11.0,999)
STOP
END

```

APPENDIX 3.

WIND RESULTANT PROGRAM

Appendix 3 contains a listing of the computer program which generates the wind resultants illustrated in Figures 35 and 38.

```

//WINDPLT JOB (4911,MV35,01,30,300,,1),'GUTMAN(VIMS)',MSGLEVEL=(1,1),
// CLASS=R,REGION=256K
/*ROUTE PRINT LOCAL
/*MESSAGE PUT IN VIMS BIN PLEASE THANK YOU
//FORT.SYSIN DD *
    DIMENSION TITL(6),X(100),IBUF(1800),A(50),R(4000),THETA(4000)
    CALL PLOTS(IBUF,1800)
    CALL FACTOR(.5)
    DO 999 M=1,12
    READ(5,1)N,TITL
    1 FORMAT(I6,6X,6A4)
    READ(5,2,END=666)(R(I),THETA(I),I=1,N)
    2 FORMAT(22X,16F3.0)
666 CONTINUE
    DO 210 I=1,8
    X(I)=0.0
210 CONTINUE
C
    DO 300 I=1,N
    IF(R(I).GT.150.0)GO TO 300
    IF(R(I).LE.10.0) GO TO 300
    IF(THETA(I).LE.22.5) GO TO 51
    IF(THETA(I).LE.67.5) GO TO 52
    IF(THETA(I).LE.112.5) GO TO 53
    IF(THETA(I).LE.157.5) GO TO 54
    IF(THETA(I).LE.202.5) GO TO 55
    IF(THETA(I).LE.247.5) GO TO 56
    IF(THETA(I).LE.292.5) GO TO 57
    IF(THETA(I).LE.337.5) GO TO 58
    IF(THETA(I).LE.395.0) GO TO 51
    GO TO 300
51 X(1)=X(1)+(R(I)**3)
    GO TO 300
52 X(2)=X(2)+(R(I)**3)
    GO TO 300
53 X(3)=X(3)+(R(I)**3)
    GO TO 300
54 X(4)=X(4)+(R(I)**3)
    GO TO 300
55 X(5)=X(5)+(R(I)**3)
    GO TO 300
56 X(6)=X(6)+(R(I)**3)
    GO TO 300
57 X(7)=X(7)+(R(I)**3)
    GO TO 300

```

```

58 X(8)=X(8)+(R(I)**3)
   GO TO 300
300 CONTINUE
   DO 400 I=1,8
   X(I)=(X(I)*.00001)/5.0
   PRINT 8,I,X(I)
   8 FORMAT(I6,F10.6)
400 CONTINUE
   XN=5.0
   YN=0.0
   XNE=0.0
   YNE=0.0
   XE=0.0
   YE =0.0
   XSE=0.0
   YSE=0.0
   XS=0.0
   YS=0.0
   XSW=0.0
   YSW=0.0
   XW=0.0
   YW=0.0
   XNW=0.0
   YNW=0.0
   YN=5.0-(X(1))
   XNE=5.0-(.7071*X(2))
   YNE=YN-(.7071*X(2))
   XE=XNE-(X(3))
   YE=YNE
   XSE=XE-(.7071*X(4))
   YSE=YE+(.7071*X(4))
   XS=XSE
   YS=YSE+X(5)
   XSW=XS+(.7071*X(6))
   YSW=YS+(.7071*X(6))
   XW=XSW+X(7)
   YW=YSW
   XNW=XW+(.7071*X(8))
   YNW=YW-(.7071*X(8))
   CALL SYMBOL (0.0,1.0,0.35,'CORROLLA WIND DATA',90.0,18)
   CALL PLOT (1.0,-11.0,-3)
   CALL PLOT (0.0,.5,-3)
   CALL PLOT (6.0,5.0,3)
   CALL CIRCL(5.0,5.0,0.0,360.0,1.0,2)
   CALL PLOT (6.0,5.0,3)

```

```

CALL CIRCL(5.0,5.0,0.0,360.0,1.0,2)
CALL PLOT(6.5,5.0,3)
CALL CIRCL(5.0,5.0,0.0,360.0,1.5,2)
CALL PLOT(6.5,5.0,3)
CALL CIRCL(5.0,5.0,0.0,360.0,1.5,2)
CALL PLOT(7.0,5.0,3)
CALL CIRCL(5.0,5.0,0.0,360.0,2.0,2)
CALL PLOT(7.0,5.0,3)
CALL CIRCL(5.0,5.0,0.0,360.0,2.0,2)
CALL PLOT(7.5,5.0,3)
CALL CIRCL(5.0,5.0,0.0,360.0,2.5,2)
CALL PLOT(7.5,5.0,3)
CALL CIRCL(5.0,5.0,0.0,360.0,2.5,2)
CALL PLOT(8.0,5.0,3)
CALL CIRCL(5.0,5.0,0.0,360.0,3.0,2)
CALL PLOT(8.0,5.0,3)
CALL CIRCL(5.0,5.0,0.0,360.0,3.0,2)
CALL DASHLN(1.95,5.0,8.05,5.0,.2)
CALL DASHLN(5.0,1.95,5.0,8.05,.2)
CALL SYMBOL(4.7,8.2,.14,'NORTH',0.0,5)
CALL SYMBOL(8.20,4.95,.14,'EAST',0.0,4)
CALL SYMBOL(3.3,1.2,.14,'EXCLUDES WIND SPEEDS<5.0 M/S',0.0,28)
CALL SYMBOL(4.70,1.60,.14,'SOUTH',0.0,5)
CALL SYMBOL(1.40,4.95,.14,'WEST',0.0,4)
CALL PLOT(0.0,0.0,-3)
CALL BLOKNO(NNN)
PRINT 10,NNN
10 FORMAT(' THE BLOCK NO. IS',I4)
CALL SYMBOL(4.20,9.50,.21,'2/76-2/77',0.0,9)
CALL SYMBOL(3.3,9.2,.21,'HATTERAS STATION',0.0,16)
CALL SYMBOL(3.0,8.8,.21,TITL,0.0,24)
CALL PARROW(5.0,5.0,XN,YN,1)
CALL PARROW(XN,YN,XNE,YNE,1)
CALL PARROW(XNE,YNE,XE,YE,1)
CALL PARROW(XE,YE,XSE,YSE,1)
CALL PARROW(XSE,YSE,XS,YS,1)
CALL PARROW(XS,YS,XSW,YSW,1)
CALL PARROW(XSW,YSW,XW,YW,1)
CALL PARROW(XW,YW,XNW,YNW,1)
CALL PARROW(5.0,5.0,XNW,YNW,1)
CALL PLOT(15.0,0.0,-3)
999 CONTINUE
CALL PLOT(20.0,-11.0,999)
STOP
END

```

APPENDIX 4.

EOLIAN SAND TRANSPORT MODEL

Appendix 4 contains a listing of the eolian sand transport computer program.

```

C
C   MAIN PROGRAM WHICH COMPUTES SAND TRANSPORT
    DIMENSION THETA(400,10),R(400,10),PRECP(400,10),X(15),XD(15),
1  WAT(400,10),TEMP(400)
    INTEGER DATE(400)
    COMMON SHEER,THRES,WATER,RAIN,ZO,U,GRAIN,OLDWAT,TMP,WIND,DIND
    QBAG=0.0
    QHSU=0.0
    TOTQH=0.0
    TOTQB=0.0
    WAT(1,8)=0.0
    DO 210 I=1,11
    X(I)=0.0
    XD(I)=0.0
210 CONTINUE
    READ(5,1)N
    1  FORMAT(I6)
    7  FORMAT(' ',16)
    PRINT 7,N
    PRINT 60
    PRINT 61
    PRINT 62
    PRINT 64
    DO 011 K=2,N
C
C   READ WIND DATA
C
    READ(5,2,END=666) DATE(K),(R(K,I),THETA(K,I),I=1,8)
    2  FORMAT(I6,16X,16F3.0)
C
C   READ TEMP AND PRECIPITATION DATA
C
    READ(5,3,END=667) TEMP(K),(PRECP(K,I),I=1,8)
    3  FORMAT(F3.0,8F5.2)
011 CONTINUE
C
C   IF SOIL IS FROZEN SKIP TO NEXT DATA CARD
C
    DO 988 K=2,N
    IF(TEMP(K).LE.31.0)GO TO 988
    DO 111 I=1,8
    IF(R(K,I).EQ.999.)R(K,I)=0.0
    IF(I.GT.1)GO TO 40
    OLDWAT=WAT(K-1,8)
    GO TO 41
40 OLDWAT=WAT(K,I-1)
41 CONTINUE
    RAIN=PRECP(K,I)

```



```

      TMP=TEMP(K)
      WIND=R(K,I)
      DIND=THETA(K,I)
C
C   CALCULATE SOIL MOISTURE
C
      CALL MOIST
      WAT(K,I)=WATER
C
C   COMPUTE THE THRESHOLD VELOCITY FOR THIS MOISTURE REGIME
C
      IF(DIND.LT.170.0)GO TO 21
      IF(DIND.GT.350.0)GO TO 21
      ZO=5.0
      GRAIN=.025
      C=.0002
      GO TO 23
21  ZO=1.0
      GRAIN=.04
      C=.0004
23  CALL THRSH
C
C   GIVEN THRESHOLD VELOCITY COMPUTE SHEER VELOCITY
C
      U=R(K,I)*.44704
      CALL SHRVL
      IF(SHEER.LT.THRES)GO TO 111
C
C   COMPUTE SAND TRANSPORT WITH HSU EQUATION
C
      QHSU=(C*((SHEER/(SQRT(980.0*GRAIN))))**3))
C
C   COMPUTE SAND TRANSPORT WITH BAGNOLD EQUATION
C
      QBAG=((1.8*(SQRT((GRAIN*10.0)/.25)))*.00000125)*(SHEER**3)
      RAIN=RAIN*2.54
C
C   PRINT RESULTS
C
      PRINT 63,DATE(K),THETA(K,I),U,THRES,SHEER,QHSU,QBAG,
1PRECIP(K,I),WATER
60  FORMAT( 21X,38HRESULTS OF SAND TRANSPORT CALCULATIONS)
61  FORMAT('0',12X,4HWIND,8X,4HWIND,5X,6HTHRESH,6X,5HSHEER,5X,3HHSU,
17X,7HBAGNOLD)
62  FORMAT(' ',6H DATE,3X,9HDIRECTION,3X,7H SPEED,4X,8HVELOCITY,3X
18HVELOCITY,2X,9HTRANSPORT,2X,9HTRANSPORT,2X,4HRAIN,3X,7H% WATER)
63  FORMAT(' ',2X,I6,5X,F4.0,7X,F4.0,5X,F6.2,5X,F6.2,2X,F7.2,4X,F7.2
13X,F6.2,4X,F5.2)

```

```

64 FORMAT(' ',23X,5HM/SEC,5X,6HCM/SEC,5X,6HCM/SEC,2X,
18HG/CM/SEC,3X,8HG/CM/SEC,3X,2HCM)
70 FORMAT(' ',28HWIND+DIRECTION DATA FINISHED)
71 FORMAT(' ',39HTEMPERATURE+PRECIPITATION DATA FINISHED)
  QBAG=QBAG*10800.0
  QHSU=QHSU*10800.0
  IF(THETA(K,I).LE.22.5)GO TO 51
  IF(THETA(K,I).LE.67.5)GO TO 52
  IF(THETA(K,I).LE.112.5)GO TO 53
  IF(THETA(K,I).LE.157.5)GO TO 54
  IF(THETA(K,I).LE.202.5)GO TO 55
  IF(THETA(K,I).LE.247.5)GO TO 56
  IF(THETA(K,I).LE.292.5)GO TO 57
  IF(THETA(K,I).LE.337.5)GO TO 58
  IF(THETA(K,I).LE.395.0)GO TO 51
  GO TO 300
51 X(1)=X(1)+QHSU
  XD(1)=XD(1)+ QBAG
  GO TO 300
52 X(2)=X(2)+QHSU
  XD(2)=XD(2)+QBAG
  GO TO 300
53 X(3)=X(3)+QHSU
  XD(3)=XD(3)+QBAG
  GO TO 300
54 X(4)=X(4)+QHSU
  XD(4)=XD(4)+QBAG
  GO TO 300
55 X(5)=X(5)+QHSU
  XD(5)=XD(5)+QBAG
  GO TO 300
56 X(6)=X(6)+QHSU
  XD(6)=XD(6)+QBAG
  GO TO 300
57 X(7)=X(7)+QHSU
  XD(7)=XD(7)+QBAG
  GO TO 300
58 X(8)=X(8)+QHSU
  XD(8)=XD(8)+QBAG
  GO TO 300
300 CONTINUE
  IF(THETA(K,I).LT.160.0)GO TO 59
  IF(THETA(K,I).GT.360.0)GO TO 59
  X(10)=X(10)+QBAG
  XD(10)=XD(10)+QHSU
  GO TO 112
59 X(9)=X(9)+QBAG
  XD(9)=XD(9)+QHSU

```

```

112 CONTINUE
    IF(THETA(K,I).LT.100.)GO TO 600
    IF(THETA(K,I).GT.300.)GO TO 600
    GO TO 111
600 X(11)=X(11)+QBAG
    XD(11)=XD(11)+QHSU
111 CONTINUE
988 CONTINUE
    DO 977 I=1,11
    X(I)=X(I)/10.0
    XD(I)=XD(I)/10.0
977 CONTINUE
    PRINT 90
    PRINT 91
    PRINT 92
    PRINT 93
    PRINT 80,XD(1),X(1)
    PRINT 81,XD(2),X(2)
    PRINT 82,XD(3),X(3)
    PRINT 84,XD(4),X(4)
    PRINT 85,XD(5),X(5)
    PRINT 86,XD(6),X(6)
    PRINT 87,XD(7),X(7)
    PRINT 88,XD(8),X(8)
    PRINT 89
    PRINT 99,X(9),XD(9)
    PRINT 101
    PRINT 100,X(10),XD(10)
    PRINT 102
    PRINT 100,XD(11),X(11)
90 FORMAT('1',2X,9HDIRECTION,5X,18H(BAGNOLD EQUATION),8X,
114H(HSU EQUATION))
91 FORMAT(' ',16X,18HTOTAL TRANSPORT OF,6X,18HTOTAL TRANSPORT OF)
92 FORMAT(' ',18X,13HSAND FOR YEAR,12X,13HSAND FOR YEAR)
93 FORMAT(' ',20X,9HKG/M/YEAR,17X,9HKG/M/YEAR)
80 FORMAT(' ',4X,5HNORTH,10X,F9.0,16X,F9.0)
81 FORMAT(' ',4X,9HNORTHEAST,6X,F9.0,16X,F9.0)
82 FORMAT(' ',4X,4HEAST,11X,F9.0,16X,F9.0)
84 FORMAT(' ',4X,9HSOUTHEAST,6X,F9.0,16X,F9.0)
85 FORMAT(' ',4X,5HSOUTH,10X,F9.0,16X,F9.0)
86 FORMAT(' ',4X,9HSOUTHWEST,6X,F9.0,16X,F9.0)
87 FORMAT(' ',4X,4HWEST,11X,F9.0,16X,F9.0)
88 FORMAT(' ',4X,9HNORTHWEST,6X,F9.0,16X,F9.0)
89 FORMAT('0',5X,38HONSHORE TRANSPORT (180-340 DEGREES AZ))
99 FORMAT(' ',19X,F9.0,16X,F9.0)
101 FORMAT('0',5X,37HOFFSHORE TRANSPORT (0-160 DEGREES AZ))
100 FORMAT(' ',19X,F9.0,16X,F9.0)
102 FORMAT('0',3X,46HTRANSPORT ACROSS SLIPFACE (300-100 DEGREES AZ))

```

SUBROUTINE MOIST

```

C
C
C   CALCULATES SOIL MOISTURE FROM PRECIPITATION, WIND AND TEMPERATURE DATA
COMMON SHEER, THRES, WATER, RAIN, ZO, U, GRAIN, OLDWAT, TMP, WIND, DIND
IF(RAIN.GT.0.0)GO TO 1
XWAT=.532*((TMP*WIND)/(-100.0))
GO TO 2
1  XWAT=11.5 + (40.*RAIN)+((-0.097)*TMP) + ((-0.46)*WIND)
   WATER=XWAT
   GO TO 3
2  WATER=OLDWAT+XWAT
3  IF(DIND.LT.170.0)GO TO 5
   IF(DIND.GT.350.0)GO TO 5
   WATER=WATER*1.2
5  IF(WATER.GT.0.0)GO TO 6
   WATER =.000001
6  CONTINUE
   RETURN
   END

```

SUBROUTINE THRSH

```

C
C
C   USES EQUATION OF KADIB
COMMON SHEER, THRES, WATER, RAIN, ZO, U, GRAIN, OLDWAT, TMP, WIND, DIND
C   CALCULATE PERCENT WATER FROM PRECIP DATA
IF(WATER.GT..10)GO TO 15
THRES=28.0
GO TO 20
15  THRES=(.1*(1.8+(.6*(ALOG10(WATER)))))*(SQRT(2359929.1*GRAIN))
20  CONTINUE
   RETURN
   END

```

SUBROUTINE SHRVL

```

C
C
C   USES EQUATION OF HSU TO COMPUTE SHEER VELOCITY AT THE SURFACE
FROM CORROLA STATION ANEMOMETER
COMMON SHEER, THRES, WATER, RAIN, ZO, U, GRAIN, OLDWAT, TMP, WIND, DIND
SHEER=((U-4.0)/(ALOG(3000.0*ZO)))*40.0
RETURN
END

```

VITA

Andrew L. Gutman

Born in Scarsdale, New York, 9 June 1953. Graduated from Scarsdale High School, June 1971. B.S., Natural Resources from University of Michigan, 1974. M.A., Marine Science, College of William and Mary, Williamsburg, Virginia, 1978.